Imperial College

School of Public Health

Department of Infectious Disease Epidemiology

The transmission dynamics of Middle East Respiratory Syndrome Coronavirus in dromedary camels: implications for vaccination

Amy Dighe

Supervised by Dr Thibaut Jombart and Professor Neil Ferguson

Submitted in part fulfilment of the requirements for the degree of Doctor of Philosophy of Imperial College London, April 2022

Statement of Originality

I declare that all the work presented in this thesis is my own, produced under the supervision of Neil Ferguson and Thibaut Jombart, and with guidance from Maria Van Kerkhove. All sources of data and methodology used in this thesis have been cited appropriately.

Chapter 2 was published as the following article

> Dighe, A., Jombart, T., Van Kerkhove, M. D., & Ferguson, N. (2019). A systematic review of MERS-CoV seroprevalence and RNA prevalence in dromedary camels: Implications for animal vaccination. *Epidemics*, *29*, 100350.

I conducted the analyses and wrote the first draft of the manuscript.

Copyright

The copyright of this thesis rests with the author. Unless otherwise indicated, its contents are licensed under a Creative Commons Attribution-Non Commercial 4.0 International Licence (CC BY-NC). Under this licence, you may copy and redistribute the material in any medium or format. You may also create and distribute modified versions of the work. This is on the condition that: you credit the author and do not use it, or any derivative works, for a commercial purpose. When reusing or sharing this work, ensure you make the licence terms clear to others by naming the licence and linking to the licence text. Where a work has been adapted, you should indicate that the work has been changed and describe those changes. Please seek permission from the copyright holder for uses of this work that are not included in this licence or permitted under UK Copyright Law.

Acknowledgements

Firstly, thank you to my supervisors, Neil Ferguson, and Thibaut Jombart, for your expert guidance and for the many engaging discussions throughout the past four years. Thank you for giving me the opportunity to pursue so many exciting things right from the beginning. I have learnt so much from you both, not only about how to approach problems and conduct robust epidemiological research, but also about how I want to conduct myself as a scientist and team member, for which I will be forever grateful.

I would also like to thank Maria Van Kerkhove at WHO for offering her invaluable insights to this project, and for allowing me the opportunity to engage with and learn from the wider community of public health practitioners, veterinarians, policy makers and scientists working to tackle MERS-CoV. These wider perspectives strengthened the outcomes of this work considerably.

I would like to express my appreciation to my PhD assessors Nick Grassly and Eve Miguel for their encouragement, constructive feedback, and contributions to shaping this project. Thanks especially to Eve for hosting me at MIVEGEC despite my horrible French, and to Nick for the Early Stage Assessment camel trophy which has lifted my mood on multiple occasions.

Thank you Rich Fitzjohn and team for developing odin and odin.dust which were key to the computation of the results in this thesis, and thanks Rich for being so patient whilst supporting my use of them. I also benefited greatly from discussions with Anne Cori about model selection, Zulma Cucunubá, Natsuko Imai and Matt Dixon about catalytic models, Ben Lambert and Charlie Whittaker about MCMC, Joe Challenger about viral load, Clare McCormack about metapopulation models, and Katy Gaythorpe about modelling vaccination strategies.

I will always be thankful for the members of the department who strive to make DIDE an inclusive and collaborative environment in which to pursue a PhD. Thank you Natsuko Imai, Hannah Slater, Sangeeta Bhatia and Katy Gaythorpe for being fantastic mentors and role models for me. Sree, Conni, and Saskia, you have been a dream cohort to be on this rollercoaster with.

I am endlessly grateful to Julie Middleton who has supported us through so many formative parts of the PhD including first international conferences, assessments, and the early stages of the COVID-19 pandemic, all of which would have been a lot more daunting without your patience and practicality. Thanks also to the Wellcome Trust for my funding, and for being flexible during the pandemic, allowing me to work with the COVID-19 response team.

Thanks Lily, OJ, Joel, James, Julia, Finlay, Izzy, Will and Charlie for being fantastic friends, for facilitating work breaks of increasingly detrimental frequency and length, and for some of the most iconic, if occasionally scarring, lunch time conversations I've ever had. And thank you, Grace for being my day one epidemiologist ride-or-die.

Thanks to my family and friends, for always asking "how are the camels", and for making me the proud owner of a significant stash of dromedary memorabilia. Special thanks to Yasmeen, Grace, Abi, Enrico, Clara, Lucy, Marissa, Ed, Liz, Emma, Mel, Sammy, George, Angela and Grantley who have taken turns to make London such a fantastic place to live for the last 5 years.

Finally, thank you to Maggie. You never asked to know so much about dromedaries or mathematical modelling, but as it is you could probably pass my viva and for that I am sorry! Thank you for being such a source of happiness throughout everything.

Abstract

Middle East Respiratory Syndrome Coronavirus (MERS-CoV) causes severe disease in humans – with a reported case fatality ratio of 35% – and is capable of causing explosive nosocomial outbreaks. Sporadic outbreaks in the Arabian Peninsula are driven by recurring zoonotic spillover from dromedary camels (*Camelus dromedarius*), leading to demand for a dromedary vaccine to avert human cases. With two vaccine candidates shown to reduce viral shedding, there is an urgent need to assess the potential impact of dromedary vaccination. This is hindered, however, by poor understanding of the transmission of MERS-CoV in dromedaries and a lack of mathematical models of transmission dynamics.

In this thesis, I use mathematical models to better characterise the dynamics of MERS-CoV in dromedary populations and to simulate the potential impact of vaccination. In Chapter 2, published measures of MERS-CoV infection prevalence and seroprevalence in dromedaries are systematically reviewed. In Chapter 3, age-stratified seroprevalence data from dromedary populations across Africa, the Middle East and South Asia are used to fit catalytic models of seroconversion, producing estimates of transmissibility and the rate of waning of maternally acquired antibodies. In Chapter 4, a stochastic, age-structured, dynamic transmission model of MERS-CoV in dromedaries is developed. The model is used to estimate key, epidemiological quantities including R_0 and the critical community size, that give an insight into how controllable MERS-CoV is in different dromedary populations. Seasonal calving is also explored as a potential driver of peaks of infection. Finally, in Chapter 5, the dynamic model is extended to simulate vaccination under different efficacy scenarios. The potential impact of vaccination on transmission in dromedaries is evaluated, as well as the optimal age for vaccination. Alongside empirical studies, insights from dynamic models such as those developed in this thesis could contribute to informing an effective response to the zoonotic transmission of MERS-CoV.

Contents

Statement of Originality 2
Copyright 2
Acknowledgements 3
Abstract 4
List of tables 9
List of figures 10
Abbreviations 12
Chapter 1: Introduction 14
Thesis Motivation 15
Background 17
MERS-CoV is a Zoonotic Coronavirus 17
MERS-CoV in humans 21
Evidence that Dromedary camels are the key zoonotic reservoir of MERS-CoV 25
Characteristics of the global dromedary camel population 27
The epidemiology of MERS-CoV in dromedaries 34
Vaccination of dromedaries 38
Mathematical modelling as a tool to inform public health decisions around MERS-CoV 39
Thesis overview 43
Chapter 2: A systematic review of MERS-CoV seroprevalence and RNA prevalence in dromedary camels 44
Introduction 45
Methods 47
Results 49
Seroprevalence – cross-sectional studies 49
Prevalence of active MERS-CoV infection – cross-sectional studies 56
Evidence of infection and immunity from longitudinal studies 59
Discussion 60
Conclusions 64
Chapter 3: Estimating the transmissibility of MERS-CoV in dromedaries using age-stratified seroprevalence data 66
Introduction 67
Methods 68
Data extraction 68
Interpretation and cleaning of the data 69
Estimating the FoI 72

Model-fitting 75
Model selection 77
Model validation 78
Results 78
Model Validation 78
Model selection 78
Rates of antibody waning 82
The Force of Infection, λ 83
Overdispersion 87
Parameter correlation 87
Discussion 87
The Force of Infection of MERS-CoV in dromedary populations 87
Seroreversion and test sensitivity 91
Maternally-acquired antibodies (mAbs) 93
Overdispersion 94
Conclusions 94
Chapter 4: A dynamic model of MERS-CoV transmission in dromedary camels 95
Introduction 96
Methods 99
Modelling infection and immunity 101
Implementing stochastic movement between disease states 103
Modelling dromedary demography 104
Model initialisation 106
Estimation of R_0 107
Persistence 108
Periodicity 110
Results 111
Estimating R_0 for MERS-CoV in dromedary populations 111
Persistence and Critical Community Size (CCS) 114
Endemic periodicity 119
Discussion 122
The basic reproduction number, R_0 122
CCS 124
Endemic periodicity 125
Conclusion 127
Chapter 5: Evaluating the potential impact of dromedary vaccination 129
Introduction 130

Dromedary vaccination as potential tool to avert human MERS cases 130
Modelling vaccination 130
Relevant knowledge gaps 131
Methods 133
Representing vaccination of dromedaries in the dynamic transmission model 133
Modelling the effects of the vaccine: three different scenarios 134
Parameterising vaccine-induced reductions in infectiousness and susceptibility 135
Results 136
Optimal target age for vaccination 136
A shift in the age distribution of first infections 139
The feasibility of preventing sustained transmission 142
Target Product Profile for the MERS-CoV dromedary vaccine 149
Discussion 151
Age optimisation 152
Vaccine impact on persistence and incidence 153
Limitations 154
Conclusions 155
Chapter 6: Discussion 157
Summary of the contributions made by this thesis 158
Limitations 162
Future extensions to the work in this thesis 163
1) Tailoring the generalised dynamic model to specific dromedary populations 163
2) Integrating genetic data streams into the dynamic model 164
3) Relating reductions in dromedary infectiousness to reductions in zoonotic spillover 164
Conclusions 165
Bibliography 167
Appendix Chapter 2 184
A2.1. Search Terms 185
A2.2. PRISMA 2009 Flow Diagram 187
A2.3. PRISMA 2009 Checklist 188
Appendix Chapter 3 190
A3.1 – Rules followed for interpreting age classes in serological studies 191
A3.2 – Catalytic model solutions 192
A3.3 – Model validation – recovery of true parameters when fitting to simulated data 200
A3.4 – Model validation – Influence of each individual dataset 204
A3.5 – DIC models when alternative fixed test-specific sensitivity and specificity is used 210

A3.6 – Catalytic model fits for all models....211
Appendix Chapter 4....222
A4.1 R_0 estimates across all scenarios....223
A4.2 Mean R_e values are close to unity at endemic equilibrium....223
A4.3. Choosing representative R_0 values....224
A4.4 Persistence of transmission in homogeneous and structured populations....225
A4.5 CCS estimates as determined using different cut-offs for defining persistence....226
A4.6 Periodicity when births are moderately seasonal....227
Appendix Chapter 5....228
A5.1 The effect of target age of vaccination on incidence of infection when mAbs last 6 months....229
A5.2. The percentage of stochastic model runs in which a patch experienced infection when infectiousness was proportional to the log(viral shedding)....230
Appendix 6....232
A6.1 Assuming a constant mortality rate, μ_0, for camels <2 years, and μ for camels ≥2 years rather than a uniform age distribution within each class....232

List of tables

Main Thesis

1.1 Zoonotic coronaviruses that cause severe disease in humans 18
1.2 Demography of dromedary populations by farm type in the Kingdom of Saudi Arabia... 33

2.1 Cross-sectional surveys of MERS-CoV seroprevalence and RNA prevalence in camels.... 50
2.2 Studies reporting seroprevalence stratified by age 54

3.1 Age-stratified seroprevalence used in fitting catalytic models of infection 71
3.2 Model selection using the Deviance Information Criterion 79
3.3 Parameter values estimated using the best fitting models 82

4.1 Dynamic model parameters 100
4.2 Study population specific R_0 estimates for MERS-CoV in dromedaries 112
4.3 The Critical Community Size of MERS-CoV in different transmission settings 115

5.1 Parameters used to model vaccination 135
5.2 The vaccine coverage needed to interrupt transmission 142

Appendices

A3.5.1 Comparison of the fit of the four catalytic models, using alternative fixed values of test-type specific sensitivity and specificity 209

A3.6.1 Parameter estimates for core catalytic models 217

A3.6.2 Parameter estimates for the four catalytic models, using alternative fixed values of test-type specific sensitivity and specificity 218

A4.1.1 R_0 estimates across all scenarios. See separate file "A4.1.xlsx" 222

A4.2.1 Mean R_e values are close to unity at endemic equilibrium 222

A6.1.1 Comparing FoI estimates when individuals are assumed to be distributed uniformly versus exponentially 236

A6.2.1 Comparing R_0 estimates when individuals are assumed to be distributed uniformly versus exponentially 237

List of figures

Main Thesis

1.1 Summary of the nature of MERS-CoV transmission 20
1.2 Confirmed global MERS-CoV cases reported to the World Health Organisation 24

2.1 Systematic review strategy 48
2.2 Map of MERS-CoV seroprevalence in dromedary camels 52
2.3 Map of the prevalence of active MERS-CoV in dromedary camels 57

3.1 Four catalytic models of MERS-CoV seroconversion in dromedary populations 73
3.2 Predicted seroprevalence and FoI estimates using Model 4b 81
3.3 The posterior distributions of each parameter estimated in Model 4b 85
3.4 Hamiltonian Monte Carlo traces for each parameter estimated in Model 4b 86

4.1 A dynamic model of MERS-CoV transmission in dromedaries 99
4.2 The seasonality of dromedary births throughout the year 105
4.3 A structured population 109
4.4 R_e oscillates overtime with annual periodicity 114
4.5 Persistence of MERS-CoV transmission in dromedary populations of different sizes 116
4.6 The Critical Community Size in populations with differing levels of structure 118
4.7 The periodicity of endemic transmission 120

5.1 The extension of the dynamic model to incorporate vaccination 132
5.2 A breakdown of the different vaccine efficacy scenarios modelled 133
5.3 The incidence of infection following vaccination of different target age groups 136
5.4 The age distribution of first infection and reinfection in the absence of vaccination 137
5.5 The average change in annual infectious-state-weighted incidence in dromedaries older than 18 months 140
5.6 The percentage of stochastic model runs in which an average patch experienced infection in scenario 1 146
5.7 The percentage of stochastic model runs in which an average patch experienced infection in scenario 2 147
5.8 The percentage change in cumulative incidence over the ten years following vaccine introduction 149

Appendices

A3.3.1 Comparison of true FoI values used in binomially distributed data simulation and recovered estimates for all four catalytic models of infection 199

A3.3.2 Comparison of true FoI values used in overdispersed data simulation and recovered estimates for all four catalytic models of infection 200

A3.3.3 Comparison of true and recovered estimates for the rate of waning of mAbs, ω 201

A3.3.4 Comparison of true and recovered estimates for the rate of waning of Abs following infection, σ 201

A3.3.5 Comparison of true and recovered estimates for the overdispersion parameter, *k*..... 202

A3.4.1 Comparison of the DIC across models when each dataset is left out in turn..... 204

A3.4.2 Comparison of the model 1 estimate of the overdispersion parameter, *k,* when each dataset is left out in turn..... 205

A3.4.3 Comparison of the model 2 estimates of the overdispersion parameter, *k*, and the rate of waning of mAbs, ω, when each dataset is left out in turn..... 206

A3.4.4 Comparison of the model 3 estimates of the overdispersion parameter, *k*, and the rate of waning of Abs following infection, σ, when each dataset is left out in turn..... 207

A3.4.5 Comparison of the model 4 estimates of the overdispersion parameter, *k*, the rate of waning of mAbs, ω, and the rate of waning of Abs following infection, σ, when when each dataset is left out in turn..... 208

A3.6.1 Predicted seroprevalence and FoI estimates using Model 1a (binomial)..... 210

A3.6.2 Predicted seroprevalence and FoI estimates using Model 1b (overdispersed)..... 211

A3.6.3 Predicted seroprevalence and FoI estimates using Model 2a (binomial)..... 212

A3.6.4 Predicted seroprevalence and FoI estimates using Model 2b (overdispersed)..... 213

A3.6.5 Predicted seroprevalence and FoI estimates using Model 3a (binomial)..... 214

A3.6.6 Predicted seroprevalence and FoI estimates using Model 3b (overdispersed)..... 215

A3.6.7 Predicted seroprevalence and FoI estimates using Model 4a (binomial)..... 216

A3.7.1 Correlation between posterior samples when seroprevalence is assumed to be overdispersed..... 219

A3.7.2 Correlation between posterior samples when seroprevalence is assumed to be binomially distributed..... 220

A4.3.1 Choosing representative R_0 values..... 223

A4.4.1 Persistence of transmission in homogeneous and structured populations..... 224

A4.5.1 CCS estimates as determined using different cut-offs for defining persistence..... 225

A4.6.1 Periodicity when births are moderately seasonal ($\delta = 0.5$)..... 226

A5.1.1 The effect of target age on incidence of infection in the ten years following vaccine introduction, when mAbs were assumed to last six months..... 228

A5.2.1 The percentage of stochastic model runs in which a patch experienced infection in scenario 1, when infectiousness was proportional to the log(viral RNA shedding)..... 229

A5.2.2 The percentage of stochastic model runs in which a patch experienced infection in scenario 2, when infectiousness was proportional to the log(viral RNA shedding)..... 230

Abbreviations

Ab – Antibodies

ACF – Autocorrelation coefficient

ACE2 – angiotensin converting enzyme 2

AIC – Akaike Information Criterion

AUC – Area Under Curve

BIC – Bayesian Information Criterion

CFR – Case Fatality Ratio

CrIs – Bayesian Credible Intervals

DIC – Deviance Information Criterion

DPP4 – Dipeptidyl peptidase 4

ELISA – Enzyme-Linked Immunosorbent Assay

FAO – Food and Agricultural Organisation of the United Nations

FoI – Force of Infection

GHA – Greater Horn of Africa

HCWs – Health Care Workers

HMC – Hamiltonian Monte Carlo

IFR – Infection Fatality Ratio

IgG – Immunoglobulin G

KSA – Kingdom of Saudi Arabia

LOO-CV – Leave One Out Cross Validation

mAbs – Maternally acquired Antibodies

MCMC – Markov Chain Monte Carlo

MERS – Middle East Respiratory Syndrome

MERS-CoV – Middle East Respiratory Syndrome Coronavirus

MVA – Modified Vaccinia Ankara

NT – Neutralisation Test

PM – Protein Microarray

PPE – Personal Protective Equipment

ppNT – pseudoparticle Neutralisation Test

R_0 – Basic Reproduction Number

R_e – effective Reproduction Number

RNA – Ribonucleic acid

RT-PCR – Reverse Transcription Polymerase Chain Reaction

UAE – United Arab Emirates

WAIC – Watanabe Akaike Information Criterion/Widely Applicable Information Criterion

WHO – World Health Organisation

Chapter 1: Introduction

Thesis Motivation

Middle East Respiratory Syndrome Coronavirus (MERS-CoV) is a zoonotic coronavirus which poses a significant threat to public health. MERS-CoV infection causes severe respiratory and renal disease in humans and has a high reported case fatality ratio of approximately 35.5% [1]. The World Health Organisation (WHO) classifies MERS-CoV as a priority pathogen based on its pandemic potential and the lack of effective therapeutics or vaccines against the disease caused by the virus. The severity of the disease and the role of dromedary camels (*Camelus dromedarius*) as the zoonotic drivers of recurring human infection [2]–[4] has led decision-makers to strive to accelerate availability of a vaccine to target dromedaries as part of the plan to prevent human cases [5].

For vaccination of dromedaries to successfully avert human infections, it is necessary to: a) develop an efficacious vaccine and; b) deploy an effective implementation strategy for targeting vaccination within dromedary populations. Progress on vaccine development is being made with two candidate vaccines shown to reduce viral shedding by dromedaries following infection [6]–[8]. The design of an informed vaccine implementation strategy, however, is hindered by insufficient understanding of the transmission of MERS-CoV in dromedary populations, and the lack of a dynamic transmission model within which to assess the potential impact of vaccination.

It is evident that MERS-CoV is endemic in dromedary camel populations across much of the globe, but knowledge gaps around the transmissibility of the virus, and the nature of immunity persist. A lack of estimates for how fast the virus spreads in dromedary populations and a lack of understanding of how dromedary demographic factors (such as seasonal calving, and population structure) affect transmission, have prevented quantitative evaluation of the vaccine efficacy and vaccine coverage needed to prevent circulation. Knowledge gaps pertaining to the nature and duration of immunity afforded by maternally acquired antibodies (mAbs) or past

infection with MERS-CoV also make it difficult to identify the target populations and define optimal dose schedules needed for an effective vaccination strategy.

Data driven mathematical models of transmission are often used to simulate and compare the potential impact of vaccine strategies [9]–[14]. They can be key to informing vaccine strategy design and are especially useful for optimising vaccine use in the face of finite resources, but no suitable model of MERS-CoV transmission in dromedaries has yet been developed. This makes it difficult for decision makers to weigh up the potential epidemiological impact of vaccination strategies and to consult with stakeholders on vaccine implementation. However, data sources have gradually become available, and can be used to parameterise models in order to estimate some of these unknowns.

Models of transmission must be driven by data describing infection within dromedary populations. Whilst dromedaries do not usually show symptoms of MERS-CoV infection – making case-based surveillance unfeasible – there is a growing wealth of studies that have collected age-stratified serological and infection prevalence data from dromedary populations in a wide range of settings. By fitting mathematical models of infection to this prevalence data we can estimate key parameters that describe the dynamics of how an infectious disease spreads in a population. These data sources have not previously been utilised in this way.

This thesis aims to address the gaps in understanding about the transmission of MERS-CoV in dromedary populations. It does this by, first, estimating the transmissibility of MERS-CoV in dromedaries and the rates of antibody waning by fitting models of infection to published seroprevalence data. These estimated parameters – along with dromedary demographical data from the literature – are then used to develop a dynamic model of MERS-CoV transmission in dromedaries. The dynamic model provides a framework in which to simulate different potential vaccination strategies, evaluate their possible impact using efficacy data from field trials, and highlight remaining data gaps to direct future study.

In combination with a greater understanding of the dynamics of MERS-CoV transmission in dromedaries and how they vary globally, the dynamic transmission model provides a way to simulate and evaluate potential dromedary vaccination strategies that is currently lacking. This could be informative for policy-making around dromedary vaccination and wider interventions at the dromedary-human interface. Developing a sound understanding of the dynamics of MERS-CoV in dromedaries is an essential component of tackling MERS. Beyond this, however, it could also provide an important case study for broadening our general understanding of novel coronaviruses in their animal hosts and ameliorating the threats they pose.

Note that throughout this thesis I use the terms "dromedary demography", "epidemic" and "endemic", despite referring to a non-human animal population. I made this choice as the meanings of these three, human centred terms are widely and immediately recognised by a larger readership compared to their corresponding, animal-centred terms – that is, "zoography", "epizootic" and "enzootic".

Background

MERS-CoV is a Zoonotic Coronavirus

Coronaviruses, so called for their crown-like appearance under the electron microscope, are a family of single stranded RNA (Ribonucleic acid) viruses which were first discovered in the 1960s as a cause of common cold symptoms. [15]–[17]. Since then, four coronavirus species have been found to be endemic in human populations – HCoV-NL63, HCoV-229E, HCoV-OC43 and HCoV-HKU1. Together, the seasonal circulation of these four endemic coronaviruses is estimated to cause 1-29% of cases of the common cold [18]–[22]. Although first discovered in humans, coronaviruses are known to infect a wide range of vertebrates [23]. Transmission of coronaviruses from non-human animals to humans – known as zoonotic transmission – has caused three major public health incidents in the past 20 years. The movement of coronaviruses between different host species continues to pose a significant threat to public health, animal health and the livestock industry.

Before the 21st century, coronaviruses had only been seen to cause mild disease in immunocompetent people. Since 2002, however, three novel zoonotic coronaviruses have emerged that cause severe and potentially fatal disease in humans. The first was Severe Acute Respiratory Syndrome Coronavirus (SARS-CoV) which emerged from wildlife brought together at animal markets in Guangdong province in southern China in 2002 [24]. SARS-CoV spread globally through air travel networks but was ultimately contained in July 2003 after around 8000 reported cases [25]. Sporadic SARS-CoV cases were detected following a further spillover event from palm civets in Guangzhou in late 2003 [26] as well as after lab-related infections in Singapore, Taiwan and Beijing, but no further cases have been reported since 2004. MERS-CoV was the second zoonotic coronaviruses to emerge, with the first cases detected in 2012 in Kingdom of Saudi Arabia (KSA) and Jordan. Unlike SARS-CoV, MERS-CoV continues to cause small outbreaks of severe disease in human populations in the Arabian Peninsula. Finally, the third zoonotic coronavirus to emerge and cause severe disease in humans is SARS-CoV-2 – the cause of the ongoing COVID-19 pandemic. Since emerging in Wuhan, China, in late 2019, SARS-CoV-2 has had a devastating impact on public health and wider aspects of society all over the world. More details on these three high consequence zoonotic coronaviruses are available in ***Table 1.1***.

Table 1.1 *Zoonotic coronaviruses that cause severe disease in humans.*

	SARS-CoV	*MERS-CoV*	*SARS-CoV-2*
Year of emergence	2002	2012	2019
Human-to-human transmissibility	Efficient (R_0~3).	Inefficient (average R_0<1 with significant heterogeneity)	Very efficient (R_0 of 2-6 for the "wild type" variant[a], and higher for recent dominant variants[b])
Disease severity	CFR*~ 11% globally	CFR*~35%	CFR* highly variable due to reporting and resources IFR**0.001-8% depending on age[d] , or 1% overall for "wild type" pre-vaccines[d].
Reservoir	Horseshoe bat → palm civets (*Paguma larvata*)	Dromedary camels (*Camelus dromedarius*)	Likely horseshoe bat[e] → unknown intermediate host
Role of reservoir	Initial infection of first human cases	Continued infection of humans	Initial infection of first human cases
Status in human population	Eradicated after ~8000 reported cases	Recurring small outbreaks. ~2,600 reported cases to date.	Ongoing pandemic driven by human-to-human transmission.
Sources	[25]	[1], [27]	a. [28], b. [29], c. [30], d. [31], e. [32]

**Case Fatality Ratio – the proportion of reported cases that are fatal (note that mild cases are often underreported so CFR measures are usually an inflation of the underlying Infection Fatality Ratio).*

*** Infection Fatality Ratio – the proportion of infections that are fatal*

Of the three zoonotic coronaviruses MERS-CoV has the highest case fatality ratio but is the least transmissible with an $R_0 < 1$ (***Table 1.1***). MERS-CoV host cell entry is facilitated by binding of the viral spike protein to host DPP4 (dipeptidyl peptidase 4) receptors [33], whereas the SARS-CoV and SARS-CoV-2 use ACE2 (angiotensin converting enzyme 2) [34], [35]. Receptor usage is linked to a virus' ability to infect specific tissues – known as tissue tropism – which may contribute, along with other aspects affecting host-virus interactions, to the differences in severity associated with the three viruses.

Although the precise zoonotic origin of SARS-CoV-2 remains under investigation, phylogenetic evidence confirms that all three high-consequence zoonotic coronaviruses likely originated in bats before infecting humans via an intermediate zoonotic host [32], [36]–[40]. Despite this common paradigm, however, the role the zoonotic host plays in ongoing transmission of MERS-CoV presents a very different public health challenge to that of SARS-CoV and SARS-CoV-2. In the cases of both SARS-CoV 2002-2003 outbreak and the SARS-CoV-2 pandemic, the role played by the animal reservoir was limited to the initial introductions of the virus into the human population [41]. Thereafter, the spread of the virus was driven by efficient human-to-human transmission, demanding a response focused on preventing human-to-human infection. In contrast, following historical spillover from bats into dromedaries, recurrent outbreaks of MERS-CoV in human populations continue to be driven by repeated introduction of the virus into the human population from dromedary camels in which the virus is now endemic, whilst human-to-human transmission remains too inefficient to sustain circulation [2]. See ***Figure 1.1*** for a schematic summary of MERS-CoV transmission.

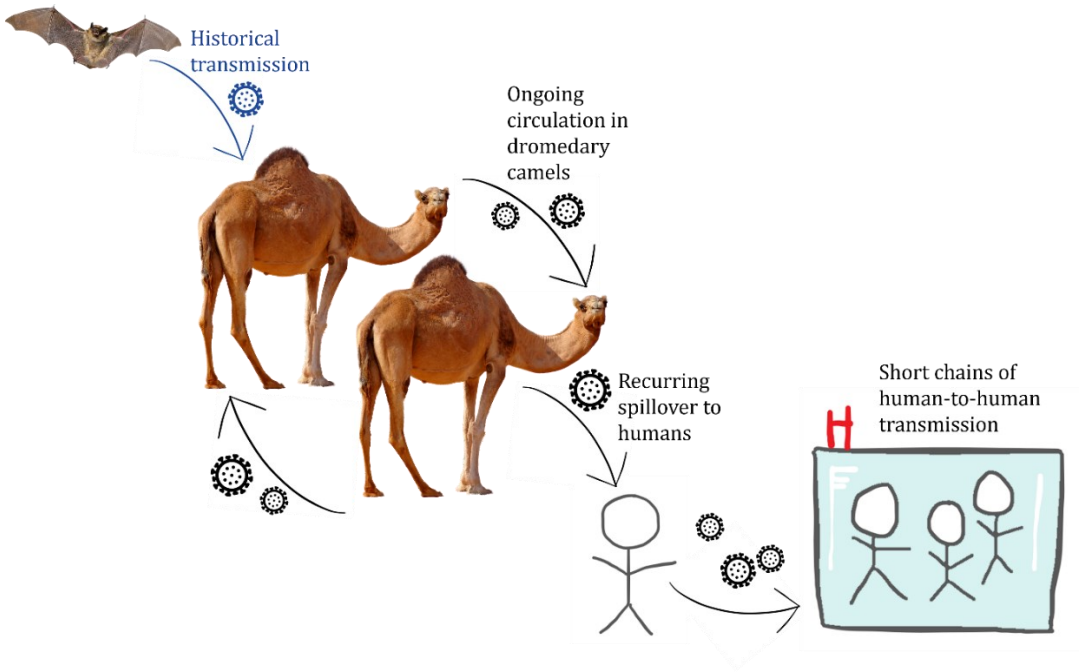


Figure 1.1. Summary of the nature of MERS-CoV transmission*. Historical transmission occurred from bats to dromedary camels in which the virus now circulates widely. Recurring dromedary-to-human transmission leads to recurring small epidemics, largely confined to nosocomial environments such as hospitals (H). Dromedary and bat vector image sources: pngimg.com (license: Creative Commons 4.0 BY-NC).*

The nature of the zoonotic reservoir of MERS-CoV is also very different to that of SARS-CoV. This also has implications for control. Firstly, the size and reach of the reservoirs are different. MERS-CoV is endemic in dromedaries globally and is likely to have been circulating in the animals for decades before the first human case was detected [42]. In contrast, SARS-CoV is not thought to have been endemic in palm civets (*Paguma larvata*) which evidence suggests were the immediate source of human SARS-CoV infection [24], [26]. Rather, the virus is thought to have spilled over from Horseshoe bats (*Rhinolophus* spp) into palm civets – and potentially other wildlife species – which then acted as amplifying intermediate hosts and infected humans via live animals markets [24], [26], [39]. Secondly, the levels of interaction between humans and the reservoirs for SARS-CoV and MERS-CoV are very different. Unlike wild civets, dromedaries are highly domesticated, and their presence is deeply embedded in the livelihoods and societies of millions of people globally. Whilst interaction with the SARS-CoV reservoir could be temporarily limited through closure of wild animal markets in Southern China, it is not possible to restrict the extensive human interaction with dromedaries in the same way. Taken together,

the role and nature of the MERS-CoV reservoir means that preventing zoonotic transmission is critical to prevent ongoing human infection.

Evidence suggests that MERS-CoV originated in bats –likely in Africa – and adapted to circulate widely in dromedary camel populations long before spillover into humans was first detected in 2012 [36]–[38]. Retrospective analysis of serum samples confirms that camels in Sudan and Somalia had MERS-CoV specific antibodies as far back as 1983 [42]. There is no substantial evidence that direct transmission of MERS-CoV from bats to humans has ever occurred, and the MERS-CoVs currently infecting humans and camels has not been found in bats. Whilst a virus isolated from an Egyptian tomb bat (*T. perforates)* in the local area of a MERS-CoV index case was found to be 100% identical to the patient's virus, but the fragment was only 190 nucleotides in length and thus led to an inconclusive result [43]. However, several MERS-CoV-related viruses have been found in bats. The phylogenetic tree of MERS-CoV is currently rooted by NeoCoV – a MERS-related-CoV discovered in South African *Neoromicia capensis* bats with 85% sequence identity to MERS-CoV [38]. Several *Neoromicia* species are prevalent in the Horn of Africa where camel populations are very dense. Differences in the sequence encoding the spike protein which MERS-CoV uses to enter host cells suggest that recombination of MERS-related-CoVs occurred in bats before widespread amplification of MERS-CoV in dromedary camels [38].

MERS-CoV in humans

Transmission

Understanding the nature of MERS-CoV transmission in humans was initially complicated by the fact that only the most severe cases are detected [44]. However, phylogenetic analyses and serosurveys have since confirmed that, unlike SARS-CoV and SARS-CoV-2 which are characterised by efficient human-to-human transmission following initial zoonotic spillover events, MERS-CoV infection in humans is driven by recurring spillover from dromedary camels, with humans essentially representing a terminal host [2].

It was estimated that 12% of the MERS-CoV cases in KSA (Kingdom of Saudi Arabia) between January 2013 and July 2014 were due to zoonotic transmission, with the remainder a result of subsequent human-to-human transmission [45]. Human-to-human transmission is relatively inefficient, limited to a few generations of infection and largely restricted to close, unprotected contact environments such as hospitals and, to a lesser extent, households [46]–[50]. Like the SARS-CoVs, transmissibility of MERS-CoV is highly heterogeneous. Although on average an individual with MERS-CoV will infect less than one other person, the reproduction number for MERS-CoV is extremely variable, giving rise to occasional super-spreading events where tens of MERS cases have been infected by a single infected individual [49], [51]. The repeated zoonotic transmission of MERS-CoV continues to pose a threat to public health globally through its potential to cause explosive, nosocomial outbreaks.

Global distribution of cases

MERS-CoV was first identified in sputum from a patient with pneumonia and renal failure in the KSA in September 2012 [52], with retrospective analysis showing that a cluster of MERS cases had occurred prior to this in a group of Health Care Workers (HCWs) in Jordan in April 2012 [53]. Since its discovery, 2,583 laboratory confirmed MERS cases and 889 associated deaths have been reported globally as of December 2021, 84% of which have been reported in KSA [27]. Laboratory confirmed MERS cases detected in countries outside of the Middle East have all been traced back to importation of cases from the Arabian Peninsula. Onward transmission following importation has been very limited, except for a 2015 outbreak in South Korea in which 186 known cases arose from nosocomial super-spreading events following a single imported case [49], [54]. Autochthonous cases (resulting from transmission from a camel or a person with camel contact within the local community, as opposed to from an imported case) have only been reported in countries within the Arabian Peninsula and Iran, and not in Africa or South Asia, despite widespread circulation of the virus in those camel populations. Recent studies, however, have found evidence of MERS-CoV specific immunity in some at-risk

populations with camel contact in Kenya, Nigeria, Morocco, Egypt and Pakistan, suggesting undetected camel-to-human transmission has likely occurred in these locations [55]–[59].

Extent of infection and spectrum of symptoms

MERS-CoV infection in humans can be asymptomatic or lead to mild respiratory symptoms but, in most reported cases, infection is associated with severe respiratory and renal disease. This has resulted in a high reported CFR of approximately 35.5% [1]. This is likely to be an overestimation of the infection fatality rate (IFR) as infections resulting in mild or no symptoms are more likely to go unreported. Currently, no study has attempted to estimate the underlying IFR. Older people with co-morbidities (especially men) are overrepresented in reported cases – particularly in primary cases [60]. When comparing reporting of primary and secondary cases, there is likely to be a bias towards reporting of severe primary cases over mild primary cases. This is because primary case reporting relies almost exclusively on healthcare seeking behaviour, whereas secondary cases are also found through active contact tracing which may pick up milder disease. Elevated bias towards severe cases in primary case reporting may explain the overrepresentation of older people with co-morbidities as these co-morbidities are risk factors for severe disease. Whether the risk of zoonotic transmission is also higher in older men has not been elucidated.

Serological surveys conducted in KSA suggest a large number of undiagnosed, asymptomatic and mild MERS-CoV infections [4], [61]. A nationwide serological survey in 2013 found that 0.15% of the general population had neutralising antibodies against the MERS-CoV spike protein [42]. Samples taken from healthy blood donors in Western region of Saudi Arabia between 2011 and 2016 found that 0.23% of donors aged 15-44 had neutralising antibodies against the MERS-CoV spike protein, with a significant increase in seropositivity over the study period [61]. Both studies made extrapolations assuming their sample was representative of the population of KSA, respectively estimating that 45,000 people >15 years old in KSA had been infected with MERS-CoV as of 2013 and that, as of 2016, 19,000 people had been infected in the

Western region alone. This is compared to ~2,600 laboratory confirmed cases globally. Neutralising antibody tests are highly specific to the MERS-CoV spike protein. As such, these are likely to be conservative estimates.

Distribution of cases over time

Sporadic cases and small outbreaks of MERS cases have been detected since the virus emerged in 2012 (***Figure 1.2***). Due to the severity of MERS-CoV, many countries that experienced outbreaks between 2012 and 2015 have since implemented interventions to improve the control of nosocomial and zoonotic transmission. This coincides with a reduction in both the reported number of primary cases (cases assumed by WHO to be due to camel-to-human transmission) and secondary cases since 2016 [62], although recurring transmission events from dromedary camels do continue to drive outbreaks in the human population in the Arabian Peninsula. There have been less cases reported during 2020 and 2021 (visually assessed from ***Figure 1.2***) which overlaps with the COVID-19 pandemic.

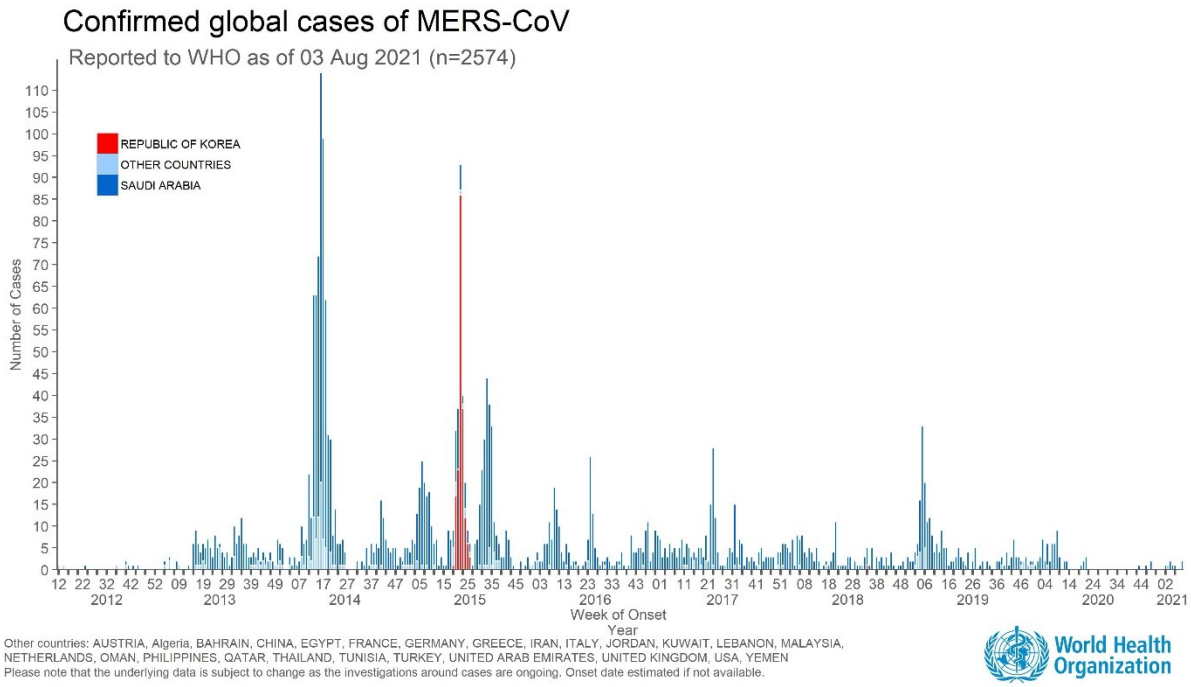


Figure 1.2 *Confirmed global cases of MERS-CoV reported to WHO. Up to date as of 3rd August 2021. Source: Reproduced from the WHO MERS-CoV situation update [Accessed 26/03/2022] https://www.who.int/health-topics/middle-east-respiratory-syndrome-coronavirus-mers#tab=tab_1. © Copyright World Health Organization (WHO), 2021. All Rights Reserved.*

Evidence that Dromedary camels are the key zoonotic reservoir of MERS-CoV

Outbreak investigations, phylogenetic analyses and large epidemiological studies all point to dromedary camels as the key zoonotic source of recurring human MERS-CoV infection. The different types of evidence supporting this are outlined below.

MERS-CoV infection is widespread in dromedaries

RT-PCRs surveys and isolation of whole viruses have found MERS-CoV circulating in dromedary populations across the Middle East [63]–[66], Africa [63], [67], [68], and Pakistan [69]. Serological surveys have found that most dromedaries have been infected with MERS-CoV by the time they reach adulthood [63], [69]–[74]. MERS-CoV specific neutralising antibodies have also been found in Bactrian camels and Bactrian-Dromedary hybrids, alpacas and llamas living in close quarters with dromedaries in the Middle East, although the virus itself has not been isolated from these animals [75], [76]. Despite many studies testing non-camelid species in the Middle East and wider areas, neutralising antibodies have not been found in any other livestock species.

Viral sequences from linked dromedaries and humans are found to be identical

Outbreak investigations have found active infection in dromedaries coinciding with infection in their human contacts. One study found the full genome of the MERS-CoV virus isolated from a camel to be genetically identical to that isolated from its owner who had been caring for the camel shortly before showing symptoms of MERS-CoV infection [3]. Serology showed that the antibody response to MERS-CoV in the dromedary preceded that of the owner, indicating the direction of transmission was from dromedary to human. An identical virus to that found in the camel and the patient was also found in the air in the camel barn [77]. A virus isolated from a dromedary in Qatar was found to be 99.9% identical to a virus isolated from a patient who had travelled from Qatar to England and developed MERS [78]. Similarly, an outbreak investigation on a farm connected to two human cases in Qatar found that, given the mutation rate of MERS-

CoV, the sequences of the Open Reading Frame 1a (ORF1a) region of the MERS-CoV RNA detected in camels were very similar to that in the two human patients [79].

Camel contact is a risk factor for evidence of MERS-CoV infection in humans

Studies conducted in KSA have found camel contact to be a risk factor for MERS-CoV infection in humans [80] and being seropositive for MERS-CoV [81]. A nationwide serological survey also found that those in professions involving interaction with camels had a higher seroprevalence than the general population – shepherds had 15-fold higher seroprevalence and slaughterhouse workers had a 23-fold higher seroprevalence than the general population [4]. A survey of ~500 people, including almost 300 people with regular camel contact and 200 without, found neutralising antibodies only in those with camel contact [82]. A study comparing abattoir workers who had dromedary contact with abattoir workers without contact, non-abattoir workers in Nigeria, and a control group from Guangzhou China, found no one to be seropositive, but did find MERS-CoV specific T-cell response in 30% of abattoir workers who had contact with dromedaries, and 0% in the other groups [56]. A study of animal market and slaughterhouse workers in Abu Dhabi found high seroprevalence in camel workers (6-19% across rounds) – this was especially high amongst camel salesmen (with almost 50% seropositivity) and those transporting camels and their waste (22% seroprevalence) [83]. Camel traders in Egypt were found to be 25% seropositive, as determined by IgG ELISAs, but neutralising antibodies – the gold standard for measuring MERS-CoV seropositivity in humans – were not tested for in this case [57].

Despite clear evidence for the key role of dromedaries in transmission, serological studies in camel workers scarcely find seropositivity – even, in some cases, where the virus was documented to be circulating in the animals. This suggests that transmission to humans is a relatively rare occurrence [84]–[88]. In Pakistan, Zohaib found 0% seroprevalence in humans including camel handlers [69], but Zheng found 12% neutralising Abs in 100 camel workers and members of their families [58].

WHO records MERS cases as primary cases if they cannot be linked to another known human case or outbreak. Of these primary cases, just over half have had contact with camels, compared with around 1% of secondary cases [89] but this is not the case for the remaining primary cases. There may be undetected mild human index cases responsible for these cases, or another animal species. Evidence does not currently support another zoonotic reservoir, however.

Phylogenetic evidence of recurring zoonotic transmission

One of the most important pieces of evidence that confirm the ongoing role of dromedaries in human infection came from a phylogenetic study of the publicly available MERS-CoV genomes isolated from humans and dromedaries [2]. The study found that long-term viral evolution occurs in dromedaries, whilst humans are essentially terminal hosts. The authors showed that recurring introductions from the dromedary population into the human population drive the recurring clusters of human cases. This dynamic is supported by epidemiological evidence suggesting inefficient human-to-human transmission in the community characterised by short transmission chains [46].

Characteristics of the global dromedary camel population

The importance of dromedary camels to the livelihoods and cultures of hundreds of millions of people globally provides opportunities for continued zoonotic transmission of MERS-CoV. Dromedaries are a domesticated species used for milk, meat, and transport, as well as for entertainment through the flourishing racing and pageant industries. Despite the wide circulation of MERS-CoV in dromedaries, zoonotic transmission from an infected camel seems to be a relatively rare event. The route(s) of dromedary-to-human transmission of MERS-CoV have not been fully elucidated, but evidence strongly suggests that the virus can spread directly from live infected dromedaries, for example through contact with nasal secretions and exhaled droplets, or indirectly through fomites [3], [77], [90]. It is also plausible that exposure could occur through unpasteurised milk contaminated by calves sometimes used to stimulate milk

production [91]. Around 95% of the world's camels are dromedary camels, the remainder belong to the two-humped Bactrian species (*Camelus bactrianus*) of Central Asia [92]. Although serological data suggests MERS-CoV may occasionally spill over from dromedaries into co-housed Bactrian camels, and small camelids [75], [76], dromedaries are the major zoonotic reservoir of MERS-CoV.

This section shall therefore focus on the characteristics of the global dromedary population that are necessary for understanding the challenge posed by MERS-CoV, including the global distribution and movement of dromedary camels, and the heterogeneity in dromedary husbandry practices globally.

Global distribution and movement of dromedary camels

There were estimated to be approximately 40 million camels globally in 2020 [93]. This is likely to be an underestimation of the true population size as censuses are not frequently conducted, in part due to the mobility of dromedary populations and the absence of obligatory vaccination [94]. FAO databases do not currently distinguish between dromedary and Bactrian camels, however dromedary camels are estimated to make up 95% of the world's large camelids [92]. Since the 1960s, the dromedary population is estimated to have grown almost 3-fold. Dromedary husbandry is growing in many regions of Africa in response to desertification, where dromedary adaptation to arid conditions makes them more robust to droughts than cattle [94]. Populations are also growing exponentially in many Middle Eastern countries with growing urbanisation increasing the demand for camel meat, changing farming practices, and the role of dromedaries as livestock and companion animals in urban life [60], [94], [95].

According to FAO databases 87% of the global dromedary population is in Africa [93]. The Greater Horn of Africa (GHA: Somalia, Ethiopia, Kenya, Sudan, South Sudan, Eritrea and Djibouti) is the most densely populated region, alone harbouring 60% of the world's dromedary population [96], with more than one camel for every two people in Somalia [60]. Despite well documented widespread circulation of MERS-CoV in the dromedary camel populations in Africa

[63], [72], [97]–[99], all reported MERS cases in humans have been linked back to countries within the Arabian Peninsula or Iran. Countries of the Arabian Peninsula are the key importers of live dromedaries globally and have considerable dromedary populations. The remainder of the global dromedary population is distributed across South Asia, with small but increasing numbers of dromedaries in Europe and North America (where they are mainly used for tourism and incidental milk production) and a large feral population in Australia that descended from dromedaries brought over during the establishment of the penal colonies [100], [101]. MERS-CoV has been detected in dromedaries in South Asia, but not Europe, the Americas or Australia [69], [102]–[104].

Mobility underpins the mixing of populations and so is very important for understanding animal disease transmission and control opportunities [105]. Dromedary mobility, however, is difficult to assess. With the exception of annual estimates of numbers of camels formally traded internationally, there is little data available on the movement of dromedary herds and their contact with other dromedary populations. A large proportion of transboundary movements (crossing borders between countries or areas) consist of informal trade or occur through porous borders in desert areas and so are not recorded in databases. It is estimated that only 10% of the trade of dromedaries from major exporter Somalia occurs through formal channels [106].

Most international trade of live dromedaries occurs unidirectionally from countries within the GHA to countries in the Arabian Peninsula (KSA, Yemen, UAE, Qatar, and Bahrain), and to Egypt and Libya in Northern Africa [107] where the imported animals are largely used to meet the demand for camel meat [106]. Somalia and Sudan are the major exporters of dromedaries globally. Other countries within the Sahelian region of Africa, such as Mauritania, Mali, Niger and Chad also export camels to Northern Africa [106]. In Western Africa, the major trade occurs from Mauritania to Morocco, Algeria and other Northern African countries.

Despite the unidirectional trade from GHA to the Arabian Peninsula, MERS-CoV displays region-dependent genomic diversity. MERS-CoV viruses belonging to Clade C (describing the genetic similarities of virus sequences isolated from dromedaries in Africa) are not found in local or imported dromedaries in the Arabian Peninsula [108]. Analysis of replication of viruses from different clades in human lung tissue and in mice expressing human DPP4 receptors suggests that Clade A and B viruses (widely circulating in the Arabian Peninsula) may have a replicative advantage in dromedaries compared to Clade C, which may explain this separation in the face of huge unidirectional trade [109]. Clade C viruses isolated in Western Africa also exhibit differences from those in Eastern Africa, with several mutations rendering Western African viruses less able to reproduce in lung tissue *in vivo* [68]. The lack of major East-West trade in Africa may contribute to this genomic separation.

Large dromedary markets act as hubs for movement and trade both in Africa and in the Middle East. Egypt has the largest camel market in Africa and in addition to the GHA receives considerable numbers of dromedaries from Kenya and Chad, via Ethiopia [107]. In countries of the Arabian Peninsula importation is often followed by a prolonged period on a fattening farm rather than immediate slaughtering as conducted in Northern Africa. Markets and holding farms are known drivers of the transmission of other zoonotic diseases such as avian influenza [110]. Annual entertainment events are also known to affect dromedary movement in some countries with large numbers of animals being brought together for competitions and for trading.

Other than trade, dromedary mobility is also tied to transhumance and nomadism of pastoralists. Transhumance involves seasonal migration of pastoralist camel farmers between areas and is documented to characterise annual dromedary movement in Central Africa for example [106]. Despite the growing number of intensive farms and sedentary herds, a considerable proportion of dromedaries in KSA are part of Bedouin husbandry systems practising nomadism [111]. Gikonyo *et al.* (2018) produced a very detailed mapping of dromedary migrations and points of mixing in Kenya which describes large annual variations in

seasonal trade at the major markets, and examples of seasonal movements such as drought driven migration of pastoralists for dry season grazing [112]. More quantitative data describing the numbers of dromedaries moving and mixing due to trade, annual migrations, and events, is important for understanding the dynamics of MERS-CoV spread and opportunities for implementing optimal interventions to reduce transmission.

Dromedary demography – herd size, structure, births, and mortality

Herd size has been found to be a risk factor for MERS-CoV infection [98]. The size of dromedary herds varies hugely both within and between countries. For example, in a study conducted across Burkina Faso, Ethiopia and Morocco, all herds sampled in Burkina Faso were comprised of ≤50 camels whereas herd size ranged from ≤50 up to 300 camels in Ethiopia and Morocco [98]. In KSA herd sizes can be larger still, with three main types defined by Abbas *et al.* (2000) with mean sizes of 14, 86, and 1,260. Abdallah and Faye (2013) measured populations to range from a single individual to more than 800 individuals in a herd, with a mean of 66-100 across the 8 herd types identified across KSA.

Female dromedaries make up the majority of herds, with males removed at a young age in both the Arabian Peninsula and camel exporting countries such as Ethiopia and Somalia [95], [113]–[115]. Although dromedaries can live as long as 40 years, most farmed dromedaries have an expected life span of closer to 20 years. A recent systematic review of camel husbandry practices in Ethiopia found the maximum life expectancy to be between 22 years for males and 29 years for females [113], and in the large study of farm types in Qassim KSA, the majority of animals were <14 years of age [114]. Herds in Somalia report that around 25% of the herd is <2 years old although this varies by season [115]. Little qualitative or quantitative data is available describing herd structure in terms of camel contact patterns, other than that calves tend to be separated from their mothers after 12 months in the Arabian peninsula [116].

Camel calving is highly seasonal [114], [117]–[121]. Mating occurs in winter, and the duration of camel pregnancy is 12-13 months [114]. Most calves are born between October and March in

KSA. Reports of dromedary calving in African countries reported similar calving seasons with births peaking between October and April in Egypt [121], and October to December in Nigeria [119]. Quantitative data on calving throughout the year was only found for KSA where 83% of births were measured to occur during the high season [114].

Like most livestock, mortality is highest in young calves and new-born mortality of up to 50% has been measured in eastern Africa [115]. Mortality is widely reported to be higher in the first two years of life compared to in adult dromedaries. In KSA total mortality is reported to range between 10-26% and was dependent on husbandry practices and farm type [95].

Heterogeneity in camel husbandry globally

There is a lot of variability in how camels are raised and used globally. Husbandry has the potential to impact the epidemiology of MERS-CoV in dromedaries due to differences in herd turn-over, degree of isolation, movement, and density, all of which impact mixing of susceptible and infectious animals. Traditionally, dromedaries have been farmed in extensive systems with low input and high mobility. Over the past 60 years, however, urbanisation and economic growth have driven dramatic intensification of husbandry practices in the Arabian Peninsula – particularly in KSA which holds 78% of the peninsula's dromedaries [60]. As well as Bedouin herds under traditional nomadic management systems, there are growing numbers of sedentary herds near to big cities. Increasing numbers of dromedaries are imported from the GHA for meat, and several large commercial camel dairy farms now operate in KSA and UAE to meet the growing demand for commercial dromedary products. Dromedary herds have also been integrated into the social fabric of urban life with owners farming dromedaries as a leisure pursuit rather than out of necessity or for purely commercial reasons [95]. On the other hand, dromedary husbandry practices remain largely extensive and pastoralist-led in the major dromedary exporting countries in Africa, [107], with some intensification and growing number of sedentary dairy herds being farmed in peri-urban areas in Kenya and Djibouti [122]. Large

scale shifts in dromedary husbandry practices has been hypothesised as one potential causal factor in the emergence of MERS-CoV in the human population in the Arabian Peninsula [60].

As well as heterogeneity in husbandry practices globally, different types of herd management exist within countries. For example, several studies have classified different farm types in KSA. A study conducted by Abbas *et al* in the Qassim region in 2000 characterised four farm types: Commercial dairies, prestige herders, pastoralists or agropastoralist herders, and peri-urban feedlots [114]. Young calf mortality rates were highest in the commercial dairies, which also kept the largest camel populations by far, with an average of 1,260 animals. Herds kept by pastoralists and in urban feedlots were on average small with lower mortality rates (***Table 1.2***). It is not clear from this study how integrated these farms were into markets or other larger networks of camels.

Table 1.2 *– Demography of dromedary populations by farm type in KSA*

Farm Type	**Mortality (%)[1]**					**Fecundity (%)[2]**	**N[3]**	**Reference**
	0-1	**1-2**	**2-3**	**3-4**	**4+**			
Commercial Dairies	12	2	9	5	3	68 over all	1260	[114]
Prestige Herders	11	2	3	5	4		86	
Pastoralist/agropastoralist herders	9	1	3	1	2		14	
Peri-urban Feedlots	4	1	3	NA	1	NA	17	
Type 1a *	18					41	100	[95]
Type 1b *	15					45	66	
Type 2a *	23					30	72	
Type 2b *	14					37	56	
Type 3a *	17					44	66	
Type 3b *	26					47	73	
Type 4a *	10					42	60	
Type 4b *	14					53	63	

1. *Mortality was measured as the percentage of animals dying annually*
2. *Fecundity was measured as the percentage of*
3. *Mean herd size*

**Farm Types 1a-4b were defined using automatic classification in* [95] *and are explained in the text on page 34*

A more recent typology was derived using automatic classification of camel farms in Northern, Eastern and Central regions of Saudi Arabia, and identified four major farm types, each of which

was split further into two, based on status of the farmers, herd composition, farming practices, and degree of integration into markets [95]. The types identified are slightly less intuitive than the Abbas *et al.* (2000) classification but not reliant on *a priori* assumptions:

1. Farms with big herds run by pure camel farmers either
    a. living in the desert and using traditional farming practices, or
    b. moving herds made up of only one breed, using more modernised farming practices and higher market integration.
2. Camel farms run by retired people either
    a. as a hobby, or
    b. for market activity
3. Small herds well integrated into markets either
    a. run by pure farmers living in the desert and moving, or
    b. multi-active farmers working in security, using traditional management.
4. Farms run by multi-active farmers living in cities either
    a. purely as a hobby, or
    b. with commercial interests and higher productivity.

Mortality and fecundity rates are calculated for each of these types (***Table 1.2***). However, these parameters do not vary greatly between farm types, rather herd turnover through buying and selling is the main differentiator. The differences in dromedary herd structures, movements and demography might suggest we should expect MERS-CoV dynamics to be regionally heterogeneous too.

The epidemiology of MERS-CoV in dromedaries

This section will summarise what is currently known and what remains to be addressed about the dynamics of MERS-CoV in dromedary populations including the disease presentation, transmissibility, the nature of immunity, and risk factors for infection.

Disease presentation

Although MERS-CoV infection can cause severe disease in humans, infection in dromedaries is largely asymptomatic making assessing the epidemiology of the virus in the zoonotic reservoir even more challenging. The expression of the MERS-CoV cell entry receptor DPP4 on human cells in the lower respiratory tract and the renal system, as opposed to in the upper respiratory tract in dromedary camels, may partly explain the difference in severity of disease experienced by these two host species [123]. Most dromedaries show no outward signs of infection, with some calves showing very mild symptoms such as the presence of nasal discharge [124].

Global distribution of infection

Neutralising antibodies specific to MERS-CoV have been found by multiple studies in dromedaries across Africa, the Middle East, and South Asia [63], [69]–[74], [125]. Almost every country in which RT-PCR testing has been conducted within these three regions has also found a proportion of dromedaries to be shedding viral RNA indicative of active infection, with the exception of single studies conducted in Bangladesh, Uganda and Israel [63], [76], [125]. High levels of seroprevalence and active infection suggests wide ongoing circulation of MERS-CoV in the Africa and parts of South Asia as well as in the Middle East where human cases are reported. This raises the question of whether transmission dynamics are different in dromedary populations outside of the Middle East, or whether other factors such as surveillance or human contact with dromedaries play a part in the lack of locally acquired MERS cases reported in camel dense areas of Africa. On the other hand, there is no evidence of past or active MERS-CoV infection in dromedaries in Europe,[1] North America, South America, Japan or notably, the large feral population in Australia. With so many cross-sectional studies now available, a systematic review of prevalence studies is needed to draw out further patterns in the global distribution extent of MERS-CoV infection in dromedary camels.

[1] excluding the Canary Islands where there is evidence of limited past infection possibly following importation from Morocco [165], [179]

Transmissibility

Quantifying the transmissibility of an infectious disease is critical to understanding how best to control spread and to modelling the potential impact of interventions. Literature searches suggest that excluding estimates based on weekly human cases, there is only one estimate of transmissibility of MERS-CoV in dromedaries available. The study used age-stratified seroprevalence data from dromedary herds in Kenya to estimate the Force of Infection (FoI) – defined as the rate at which susceptible animals become infected over time [126]. The annual FoI was estimated to be ~0.5 overall but ranged from 0.1-1 for pastoral herds using the best fitting age-dependent quadratic model, with some negative FoI estimates for ranching herds as seroprevalence decreased slightly with age. This could perhaps be explained either by the model assumption of endemic transmission not being met in ranching herds, or that there is waning of antibodies over time which is not considered by the model.

R_0 – the average number of secondary infections produced by a single infection introduced into an entirely susceptible population – is perhaps a more intuitive measure of transmissibility than the FoI. It also has the advantage of being more widely used and therefore easier to compare across different diseases. However, estimates of R_0 for MERS-CoV in dromedaries have only been made available by two studies which based them on human weekly case data, giving estimates ranging from 1 to 3 under different model assumptions [127], [128].

Other insights into the transmissibility of MERS-CoV have mainly come from incidental observations in longitudinal studies. For example, following infection, RT-PCR tests have measured dromedaries to shed detectable levels of MERS-CoV RNA for around 14 days [6], [116], [129]. The duration of shedding of infectious virus particles has not been measured following natural infection, but in experimental settings infectious viruses could be isolated for the first 7 days following infection [130]. In a vaccine field study, it was documented that infection transmitted from a pen housing infectious dromedaries to dromedaries that were part of a different aspect of the study in a pen 200 metres away. The authors assessed CCTV footage

which confirmed all protocols to avoid mechanical transmission were followed correctly, meaning this could suggest a high level of airborne transmission is possible between dromedaries [6].

Immunity

Calves born to seropositive mothers may acquire MERS-CoV antibodies through colostrum [116], [131]. Longitudinal studies have observed a wave of infection sweeping through calf populations after mAbs have waned over the first few months of life, suggesting they initially offer protection from infection [116], [131].

Seroconversion commonly follows first MERS-CoV infection, and population levels of seropositivity have been measured to be very high especially in adult dromedaries [73], [88], [116]. However, cases of reinfection of seropositive animals suggest seropositivity is not a proxy for complete immunity to MERS-CoV, and the level of protection conferred by past infection is unclear. Rapid reinfection of animals has been documented in high transmission settings such as markets and pens containing many infectious dromedaries [6], [65], [129]. Reinfected animals have been measured to have a lower viral load and are likely to be less infectious than first-time infected animals [6]. The exact relationship between this reduction in viral load and the reduction in infectiousness has not been fully elucidated.

Risk factors for infection

Several cross-sectional surveys have measured increasing seroprevalence with age, and RT-PCR studies have found active infection to be more common in calves compared to adults. This suggests first infection with MERS-CoV may occur in the first two years of life in some study populations, with most animals becoming infected before adulthood. Other potential risk factors for MERS-CoV infection or seropositivity include the geographical region sampled. Multiple studies have measured sub-national regional differences in seroprevalence and infection prevalence [67], [88], [132]. Herd characteristics such as size, density and husbandry management system have also been significantly associated with differences in seroprevalence

in some studies, but the direction of association is not always consistent. For example, large herd size was a risk factor for seroprevalence in western Africa, but not in Kenya [98], [133]. The type of site sampled and the camel function have also been seen to influence prevalence measures, for example higher prevalence has been found at abattoirs and wholesale markets compared to farms [98], [134], [135]. In a study conducted across Morocco, Burkina Faso and Ethiopia, camels raised for milk and meat were measured to have significantly higher seroprevalence than those used for transport [98]

Vaccination of dromedaries

Owing to the severity of MERS-CoV infection in humans, and its potential to cause explosive nosocomial outbreaks, there is a demand for interventions to avert the camel-to-human transmission events driving ongoing cases. Several non-pharmaceutical interventions are already in place including guidance around use of Personal Protective Equipment (PPE) when interacting with dromedaries, and advice to vulnerable individuals to avoid dromedaries when possible. Although restrictions have been discussed at various points, currently there is no evidence that preventing the trade of MERS-CoV positive animals would reduce the risk of human infections in the Arabian Peninsula [107]. MERS-CoV has established long-standing widespread circulation in major camel importing countries, meaning infection would likely occur in holding pens or fattening farms once imported. Such restrictions would also likely be economically devastating to major exporters. Other suggestions have included delaying weaning and reducing human contact with calves as they are more likely to be infectious than adult dromedaries [116].

In addition to non-pharmaceutical interventions, there is clear call from decision makers to implement dromedary vaccination to avert human cases [5]. Multiple vaccine candidates have been developed across a diverse range of platforms with three having reached the stage of being tested in dromedaries. These include a synthetic consensus DNA vaccine [136], an MVA-based (Modified Vaccinia Ankara) vaccine, and the adenovirus vectored ChAdOx1 MERS vaccine [6]

that formed the starting point for the Oxford–AstraZeneca COVID-19 vaccine. All three candidates target the MERS-CoV Spike protein known to facilitate cell entry by binding to DPP4 host cell receptors and known to be key to developing immunogenicity against MERS-CoV [33], [137]. The synthetic consensus DNA vaccine was measured to produce a strong humoral immune response in the three immunised dromedaries but its efficacy against infection has not yet been measured in the animals. Both the MVA-based vaccine and ChAdOx1 MERS, however, have been shown to reduce viral shedding in dromedaries following infection when compared with controls [6], [8].

Implementing MERS-CoV vaccination in dromedaries will be challenging. As MERS-CoV infection does not cause significant disease in camels, a dromedary vaccine will be implemented solely for the purpose of preventing human infections. While there are several examples of vaccinating animals to protect humans from infection [138] (including low pathogenic avian influenza [139], [140], Hendra virus [141] and rabies [142]), overcoming concerns of camel owners and the camel industry will require consultation with owners, industry and political leaders in countries with high dromedary density. It is critical that any animal vaccine implementation will not harm the livelihoods of animal owners and those involved in the selling, trading, or recreational use of the animals. Further discussion of these wider challenges of implementing a MERS-CoV vaccine in dromedaries, would benefit from being informed by a clearer picture of what an epidemiologically optimal vaccination strategy would involve and the likely impact it would have on transmission in dromedaries.

Mathematical modelling as a tool to inform public health decisions around MERS-CoV

Mathematical modelling has been widely used to evaluate the impact of interventions on infectious disease transmission and has supported the development and implementation of many vaccination programs including the response to the 2009 Influenza pandemic [14], [143], Ebola [12], [13], and most recently COVID-19 [10], [144].

Modelling involves describing the behaviour of a system – in this case, the spread of infectious disease in a population – using mathematical concepts. When decisions are made about how to intervene in infectious disease transmission – be that by members of the public or policy makers – those involved in decision-making processes make choices based on their current understanding of how the disease spreads. Their decision might involve the assumption that infected individuals become infectious after symptom onset, that infection takes two weeks to clear, that transmission is higher indoors, or that previously infected individuals are immune to reinfection, for example. In so doing, they are, knowingly or unknowingly, making use of a simple model.

Mathematical models can add value to these decision-making processes in a number of ways. Firstly, in the process of developing mathematical models that quantitatively represent the spread of infectious agents, assumptions can be explicitly acknowledged and formalised. This is important to ensure that assumptions are made transparent, more open to scrutiny, and better able to be interrogated against data describing infections. Secondly, comparing the fit of different potential models of transmission to epidemiological data can allow us to infer which model presents the most likely scenario, given the data available. Thirdly, for new and emerging pathogens, where data are limited, modelling can be especially important to assess the likely impact of the outbreak early on. Finally, although mathematical models will always be a simplification of the true spread of infectious disease, they can – where there is confidence that models produce reasonably accurate representations of true dynamics – be used to infer the likely impact of interventions and optimise implementation strategies through simulation. As long as model limitations and uncertainties are recognised and communicated effectively [145], these four benefits make mathematical models very useful as part of the research informing public health response to infectious disease epidemics.

Mathematics was first applied to infectious disease by Bernoulli in the 18th Century to predict the effect of smallpox inoculation on life span [146]. In the early 20th Century, Hamer

conceptualised the importance of the number of susceptible individuals and infectious individuals for disease spread, and several physicians developed the first models of disease spread that assigned individuals to compartments (e.g., Susceptible, Infectious, and Recovered in the SIR model) [147]. Ross pioneered the used compartmental models to assess the likely impact of interventions in his work on malaria transmission [148]. This, along with important concepts such as the Reproduction number, R_0, first introduced by MacDonald in 1957, have paved the way for the use of mathematical modelling in epidemiology today [149]. More recently, extensions of deterministic compartmental modelling to include stochasticity, along with the development of forms of modelling such as agent-based modelling (in which individuals are modelled rather than compartments) and network modelling where the contacts between susceptible individuals and infectious individuals can be modelled explicitly [150], have broadened the toolkit available to infer and simulate infectious disease dynamics.

Modelling was gradually integrated into the public health response to infectious disease outbreaks during the 21st century as it was used to inform the response to key emergence events such as Foot and Mouth [151], [152], SARS-CoV [153], [154], influenza H1N1 [143], Ebola [12], [13] and COVID-19 [144]. Modelling transmission dynamics is also increasingly recognised as critical to cost-effective intervention planning in the field of health economics. Vaccination programs in response to the 2009 influenza pandemic, Ebola, and most recently COVID-19 have all made use of data-driven mathematical models of the transmission dynamics to simulate different vaccination strategies, This has supported decision making by ensure finite numbers of vaccines are targeted most effectively within a population, as well as evaluating the expected impact. [10], [12]–[14], [155].

With two vaccine candidates now shown to reduce shedding in dromedaries, there is an urgent need for an appropriate mathematical model of MERS-CoV transmission with which to assess potential impact of animal vaccination. Models of MERS-CoV have tended to focus on human-to-human transmission, and there is no appropriate dynamic model of MERS-CoV transmission in

dromedaries available for assessing the potential impact of animal vaccination. Descriptions of three deterministic models of MERS-CoV transmission were found in the published literature. The first model fitted camel-to-camel transmission rates to incidence of reported human MERS cases whilst assuming a constant fixed proportion of weekly human cases were a result of zoonotic transmission [128]. Inferring dynamics in dromedaries using reported human MERS cases is a challenging approach to take as primary zoonotic cases are under-reported, and the dynamics of zoonotic spillover are poorly understood. It is likely to be problematic to assume a fixed proportion of reported human MERS cases are zoonotic during a period with several large nosocomial outbreaks. A second dynamic model was published in 2021 however this was designed as a purely theoretical model focused on deriving expressions of R_0 with no data used to parameterise transmission between camels [156]. A third model was published in 2022, describing the transmission of MERS-CoV in KSA, in human and dromedary populations, however it is unclear how the dromedary transmission model was parameterised [127]. Weekly numbers of reported human cases were again used to parameterise the human-to-human and dromedary-to-human transmission parameters, but no source of data pertaining to dromedary camels is referenced until the discussion and it is not clear how it was used. No stochastic or age-structured models are currently available. Disease transmission is a stochastic process, and the inclusion of stochasticity within transmission models can be important as it reflects the uncertainty in measured processes as sampled from a larger statistical population. Random variations in processes such as transmission, births, and recoveries affect epidemic trajectories, particularly when populations or numbers of infectious individuals are small. Phenomena such as epidemic fadeout – defined as the elimination of infection due to stochastic fluctuation during a trough in the number of infectious individuals – can only be captured using stochastic models. The inclusion of age-structure of the dromedary population is also important as interventions are likely to be age targeted.

Modelling MERS-CoV in dromedaries has been limited by the challenges of surveying infection in an asymptomatic animal population. However, there is now a wealth of stratified data

describing seroprevalence and active infection data for MERS in camels that has so far been under-utilised for inferring dynamics of transmission.

Thesis overview

This thesis focuses on better characterising the transmission of MERS-CoV in dromedary populations and developing a dynamic model of transmission that can be used to evaluate potential animal vaccination strategies. Firstly, in Chapter 2, the literature reporting seroprevalence and RNA prevalence of MERS-CoV in dromedary populations is systematically reviewed. In Chapter 3, a series of catalytic models are fit to age-stratified seroprevalence data collated in Chapter 2, to estimate the transmissibility of MERS-CoV in dromedaries in the form of the Force of Infection (FoI). Taken together with viral shedding data extracted from a published vaccination trial, and dromedary demography data, the FoI estimates are used to parameterise a stochastic, age-structured dynamic model of MERS-CoV transmission in Chapter 4. In Chapter 5 the dynamic transmission model is used to simulate vaccination of strategies and multiple vaccine efficacy scenarios are explored. Finally, the overarching contributions, limitations, and implications of these findings of Chapter 2-5 are discussed in Chapter 6.

Chapter 2:

A systematic review of MERS-CoV seroprevalence and RNA prevalence in dromedary camels

The work described in this chapter was published in the following peer reviewed publication: Dighe, A., Jombart, T., Van Kerkhove, M. D., & Ferguson, N. (2019). A systematic review of MERS-CoV seroprevalence and RNA prevalence in dromedary camels: Implications for animal vaccination. *Epidemics*, *29*, 100350.

Author contributions are as follows. A. Dighe designed and conducted the literature search with supervision from N. Ferguson, T. Jombart and M.D. Van Kerkhove. A. Dighe extracted and analysed the data. A. Dighe wrote the manuscript with editing by N. Ferguson, T. Jombart and M.D. Van Kerkhove.

Introduction

The primary aim of this thesis is to address the gaps in understanding about MERS-CoV transmission in dromedary populations that are currently hindering animal vaccination strategies. This chapter takes the first step towards closing these gaps through collating the available data on MERS-CoV infection amongst dromedaries and examining patterns in the distribution of infection – geographically, temporally and by dromedary demographic factors such as age.

There are two main types of data that are commonly relied upon as indicators of viral infection in epidemiological analyses. Firstly, there is serological data which describes the presence of antibodies specific to the virus of interest in an individual's blood. Production of these proteins by the host's adaptive immune system is triggered by their ability to bind specifically to the virus infecting the host [157]. Certain antibody isotypes continue to be detectable in the blood for some time after infection has cleared [157]. The specificity and longevity of antibodies mean that seropositivity (the presence of antibodies in the blood above a chosen threshold metric) can be used to test for past infection. Increases in antibody titres can also be used to determine infection within a particular window when sequential measures are available.

The prevalence of seropositivity can be used to estimate what proportion of a population has been infected with a particular pathogen. When broken down by age class, seroprevalence can tell us when most individuals encounter the infection for the first time and can be used to infer the rate at which susceptible individuals become infected. This rate is known as the Force of Infection (FoI) [158]. Age-stratified seroprevalence data has been used to estimate the FoI for many infectious diseases including measles, dengue and chagas disease [159]–[161].

Serological tests for detecting MERS-CoV specific antibodies were developed rapidly following the virus' emergence. They include ELISAs (Enzyme Linked Immunosorbent Assays), a protein microarray [162] and viral neutralisation tests, including some pseudo-particle or pseudo-virus based assays that do not require high level biosafety facilities [163], [164]. Serosurveys of

animal populations have played a major role in the discovery of dromedaries as the key zoonotic reservoir of MERS-CoV [73], [165]. Published measures of MERS-CoV seroprevalence are available for dromedary populations across Africa, the Middle East, and South Asia, and for small camel populations in Europe, North America, and South America, but have not previously been systematically reviewed.

The second main type of data used as an indicator of a specific viral infection within a population is the detection of the virus itself within the host. This usually involves detection and amplification of the virus' specific genetic material from a host sample using the Polymerase Chain Reaction (PCR) [166], [167]. PCR relies on the specific binding and subsequent extension of short genetic sequences (known as primers), to target nucleic acid sequences within the genome of the virus of interest. With quantitative or "real-time" PCR it is also possible to estimate the initial concentration of nucleic acid, allowing the measurement and comparison of viral load [168]. Many viruses, including MERS-CoV, have an RNA genome so the viral genetic material must first be reverse transcribed into DNA, using a combinative process known as RT-PCR (Reverse Transcription Polymerase Chain Reaction) [169]. A protocol for detection of MERS-CoV using real-time RT-PCR was developed rapidly in response to the emergence of the virus and is used to diagnose active MERS-CoV infection in humans and dromedaries [170]–[172].

Published measures of MERS-CoV seroprevalence in dromedary populations are available for populations across a wide geographical area. There are also a growing number of published studies measuring the prevalence of RNA detection through real-time RT-PCR of nasal swabs taken from dromedaries. Like seroprevalence, RNA prevalence in dromedaries has not previously been systematically reviewed. This makes it challenging to establish the global picture of MERS-CoV in dromedaries, to address gaps and to identify opportunities to maximise the use of the available data to better understand transmission dynamics.

In this chapter, I systematically review published studies that measure MERS-CoV antibody seroprevalence in dromedaries and/or detection of viral RNA in dromedaries. The results provide a comprehensive database of the measured seroprevalence and prevalence of active MERS-CoV infection in dromedaries. By conducting a qualitative synthesis of the study findings, considering reported heterogeneities, and summarising the results of longitudinal studies of infection and immunity, I assess the extent of current understanding of MERS-CoV epidemiology in dromedaries, implications for control, and gaps to be addressed going forward.

I note that a similar systematic review of the literature up until May 2018 was unknowingly carried out in parallel to this one [173], with no discussion between the two groups. Here, I validate and update the results of the parallel review, discussing the results in the context of potential animal vaccination and implications for developing a mathematical model of MERS-CoV transmission in dromedary camels.

Methods

Studies published prior to 31st December 2018 reporting measures of seroprevalence or presence of MERS-CoV RNA in dromedary populations were systematically reviewed. EMBASE [174], MEDLINE [175] and Web of Science [176] were searched using the strategy in ***Figure 2.1***. The search and the data extraction were conducted by a single author and no publication date restrictions were imposed. The previous name of MERS-CoV "hCoV-EMC" was included in the searches for completeness. For a full list of search terms used, corresponding PRISMA flowchart and checklist see ***Appendix Chapter 2: A2.1, A2.2*** and ***A2.3***, respectively.

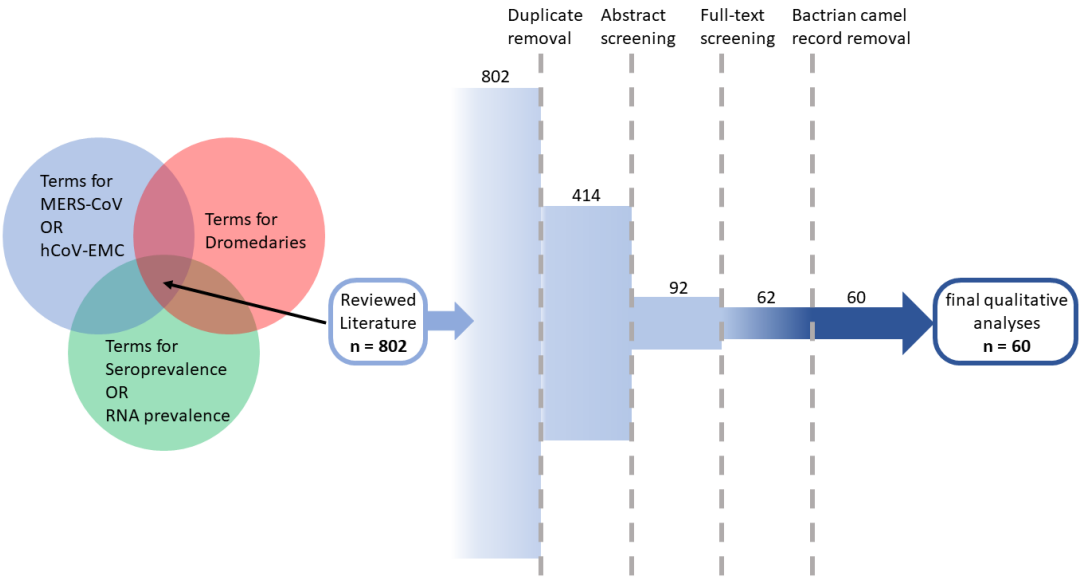


Figure 2.1. Systematic review strategy*. Published studies found with all three of the selected search term groups were then assessed against the exclusion criteria resulting in a final selection of 60 publications.*

Records were excluded if they met the following criteria established prior to the search: opinion pieces, or reviews reporting no new data; studies investigating an aspect of MERS-CoV or another pathogen that did not involve dromedary samples or involved experimentally infecting dromedaries with MERS-CoV; and studies not available in English. Remaining studies were categorised as longitudinal or cross-sectional for qualitative synthesis. To address potential bias, I consider studies investigating dromedary populations epidemiologically linked to human MERS-CoV infection separately from those that aimed for random or opportunistic sampling.

When available, I took the results of neutralisation-based testing over methods that determined seropositivity based on antibody screening tests alone. Neutralising antibody tests are highly specific and are the World Organisation for Animal Health (OIE) recommended method for confirming MERS-CoV seropositivity in dromedaries [171].

I extracted RNA prevalence values determined by RT-PCR of nasal swabs, ignoring any additional samples taken. Use of RT-PCR to test for the presence of at least two of the established genomic regions unique to MERS-CoV is the OIE standard for detection of active MERS-CoV infection in dromedaries [171] and viral RNA is most frequently and abundantly

present in nasal swabs compared to other non-invasive samples [177].Throughout this chapter, 'calf' is used to refer to animals under one-year-old, 'juvenile' ≤2 years old, and 'adult' to mean >2 years old.

Results

The search retrieved 802 publications. Duplicates were detected and removed in EndNote X8.2 [178], leaving 414 unique publications. A further 322 records were excluded during abstract screening using the criteria established prior to the search (see Methods). Of the remaining 92, full text screening proved that a further 30 records met the exclusion criteria. Two records sampled Bactrian camels,[2] leaving 60 records pertaining to MERS-CoV seropositivity and/or RNA positivity in dromedaries (***Figure 2.1***). Of the 60 remaining records, 55 described cross-sectional studies of dromedary populations, sampling each animal at a single time-point only (40 measured seroprevalence and 32 measured RNA prevalence). Six studies were designed to investigate groups of dromedaries that had been epidemiologically linked to human cases of MERS-CoV infection rather than conducting a systematic/random survey. Longitudinal studies that measured seropositivity and viral RNA shedding in the same animals at multiple time-points featured in 11 publications.

Seroprevalence – cross-sectional studies

Studies either conducted dedicated MERS-CoV sero-surveys, opportunistically tested samples taken for other means, tested stored sera or sampled dromedaries during human outbreak investigations. Not all studies used neutralisation-based testing to determine or confirm seropositivity, and, between those that did, cut-off positivity titres varied.

[2] Largely geographically separated from dromedaries, Bactrian camels are mostly restricted to Central Asia where there is no indication of active infection with with MERS-CoV. More recently, antibody reactivity has been found by ELISAs in some Mongolian Bactrians but these antibodies are not able to neutralise MERS-COV [241]. Bactrian camels do not make a key contribution to the zoonotic reservoir of MERS-CoV at the time of review. [188], [202], [203]

Table 2.1. Cross-sectional surveys of MERS-CoV seroprevalence and RNA prevalence in camels

Ref	*Country*	*Year*	*Seroprevalence*			*RNA prevalence*			
			%	n[a]	Range[b]	%	n[a]	Range[b]	*stratifications*
[104]	Australia	2013-14	0%	307	-	-	-	-	-
[71]		2014	0%	25	-	-	-	-	-
[125]	Bangladesh	2015	31%	55	-	0%	55	-	age, site type, origin, sex, body condition
[98]	Burkina Faso	2015	80%[d]	525	73-85%	5%[d]	525	0-12%	Region. Further factors assessed in GLMM
[165]	Canary Islands	2012-13	9%	105	-	-	-	-	origin
[179]		2015	4%	170	-	-	-	-	origin
[42]	Egypt	1997	79%	43	-	-	-	-	-
[180]		2013	92%	52	-	4%	110	3-30%	sex
[164]		2013	94%	110	-	-	-	-	-
[71]		2014	100%	8	-	-	-	-	-
[72]		2014-16	71%	2541	59-95%[e]	15%	2825	1-36%[e]	age, origin, site type, sex, month
[181]		2015-16	85%	1031	77-96%[e]	4%	1078	1-9%[e]	age, origin, site type, sex
[99]	Ethiopia	2010-11	96%[d]	188	95-100%	-	-	-	age, region
[182]		2013	96%	66	-	-	-	-	-
[98]		2015	96%[d]	632	85-99%	10%[d]	632	0-16%	region. Further factors assessed in GLMM
[183]	Iraq	2014-15	85%	180	85-86%	-	-	-	age, region, sex
[184]		2015-16	-	-	-	15%	100	0-35%	age, region, month
[76]	Israel	2012-17	62%	411	-	0%	540	-	-
[185]		2013	72%	71	-	-	-	-	sex
[186]	Japan	<2015	0%	5	-	0%	4	-	-
[187]	Jordan	2013	100%	11	-	-	-	-	
[124]		2016	82%[d]	45	77-87%	62%	45	48-77%	age, region, lifestyle
[188]	Kazakhstan	2015	0%	455	-	-	-	-	-
[189]	Kenya	1992-2013	30%[f]	228	0-100%	-	-	-	region, year
[133]		2013	47%[d]	335	14-83%	-	-	-	age, herd, lifestyle, isolation
[88]		2013	90%	NA	-	-	-	-	age, region, sex
[190]		2016-17	-	-	-	0.35%[d]	1421	0-1.2%[d]	region,
[67]		2016-18	68%	1163	17-87%	0.95%[d]	1163	-	age, region, sex
[73]	KSA[k]	1992-2010	87%[d]	264	77-100%	-	-	-	age, region, year
[73]		2013	74%	150	66-100%	25%	202	0-66%	age, region
[191]		2015-16	-	-	-	14%	44	0-23%	year[g]
[192]		2016	84%	171	-	-	-	-	age, sex
[71]		1993	90%	131	73-96%	-	-	-	region
[193]		2012-13	90%	310	85-94%	-	-	-	age, region
[66]		2015-17	-	-	-	56%	698	5-85%	region, site-type, month, year
[194]		2013-14	-	-	-	29%	96	-	age, site, month
[135]		2014-15	-	-	-	0.12%	1309	-	-
[132]	Mali	2009-10	88%	562	0-91%	-	-	-	region
[98]	Morocco	2015	77%[d]	343	48-100%	2%[d]	343	0-8%	region. Further factors assessed in GLMM
[195]	Nigeria	2015	96%	131	-	11%	132	-	-
[99]		2010-11	94%	358	82-96%	-	-	-	region
[84]		2016	-	-	-	3%[d]	2529	0-8.4%[h]	age, week tested
[196]	Oman	2013	-	-	-	7%	76	-	-
[165]		2013	100%	50	-	-	-	-	-
[102]	Pakistan	2012-15	40%	565	0-83%	-	-	-	age, region
[69]		2015-18	76%	1050	72-80%	3%[d]	776	-	age, region, sex, lifestyle

[177]	Qatar	2014	-	-	-	79%	53	67-92%	-
[91]		2014	100%	33	-	21%[d]	33	0-58%	region
[78]		2014	-	-	-	2%	53	-	-
[42]	Somalia	1983-4	81%[d]	86	-	-	-	-	year
[42]	Sudan	1984	82%	60	-	-	-	-	year
[99]*a*	Tunisia	2009	49%[d]	204	36-100%	-	-	-	age, region
[74]	UAE[l]	2003 + 13	97%	651	-	-	-	-	year
[103]		2005	82%	11	0-100%[e]	-	-	-	site
[116]		2014	93%	853	-	5%	871	-	age
[197]		<2015	95%	254	-	0%	254	-	age
[134]		2014	-	-	-	1.6%	7803	-	site-type
[65], [198]		2015	-	-	-	29%[i]	376[i]	-	-
[103]	USA[m] & Canada	2000-1	0%	6	-	-	-	-	-
Studies investigating dromedary camel populations linked to human MERS-CoV infection									
[129]	UAE	2012	-	-	-	4%	1113		farm
[199]	UAE	2014	-	-	-	100%[j]	6[j]	-	-
[200]	UAE	2015	100%	8	-	100%	8	-	-
[70]	KSA	2014-16	71%	595	37-100%	13%	584	0-56%	region, age, sex
[79]	Qatar	2013	100%	14	-	21%	14	-	-
[201]	Qatar	2014	97%	103	-	59%	105	-	-
Bactrian camels									
[202]	Mongolia	2014	0%	190	-	0%	190		-
[203]	Mongolia	2015	0%	200	-	0%	200		-
[188]	Kazakhstan	2015	0%	95	-	-	-		-

a. total number of camels sampled
b. range across sub-national locations surveyed
c. cut off titre to determine positivity if neutralisation test used
d. we calculated this value from disaggregated values presented by the authors
e. range given is across site types rather than geographical locations
f. neutralisation at dilution >1:80 gave 15% seropositivity but regional range only available for ELISA (Enzyme Linked Immunosorbent Assay) results – reported accordingly
g. study also tested different site-types but measured RNA in serum sample rather than nasal swab, so this was not included
h. range is across weeks rather than regions
i. both [198] and [65] report RNA prevalence from the same study
j. unclear whether study found negative camels – it only mentions that 6 camels were tested, found positive and viral genomes were isolated
k. Kingdom of Saudi Arabia
l. United Arab Emirates
m. United States of America
•neutralisation test limited to a subset of samples or only used to detect presence of high titres
** No positivity cut-off titre given but all samples had extremely high titres and were able to neutralise at dilution >1:1280

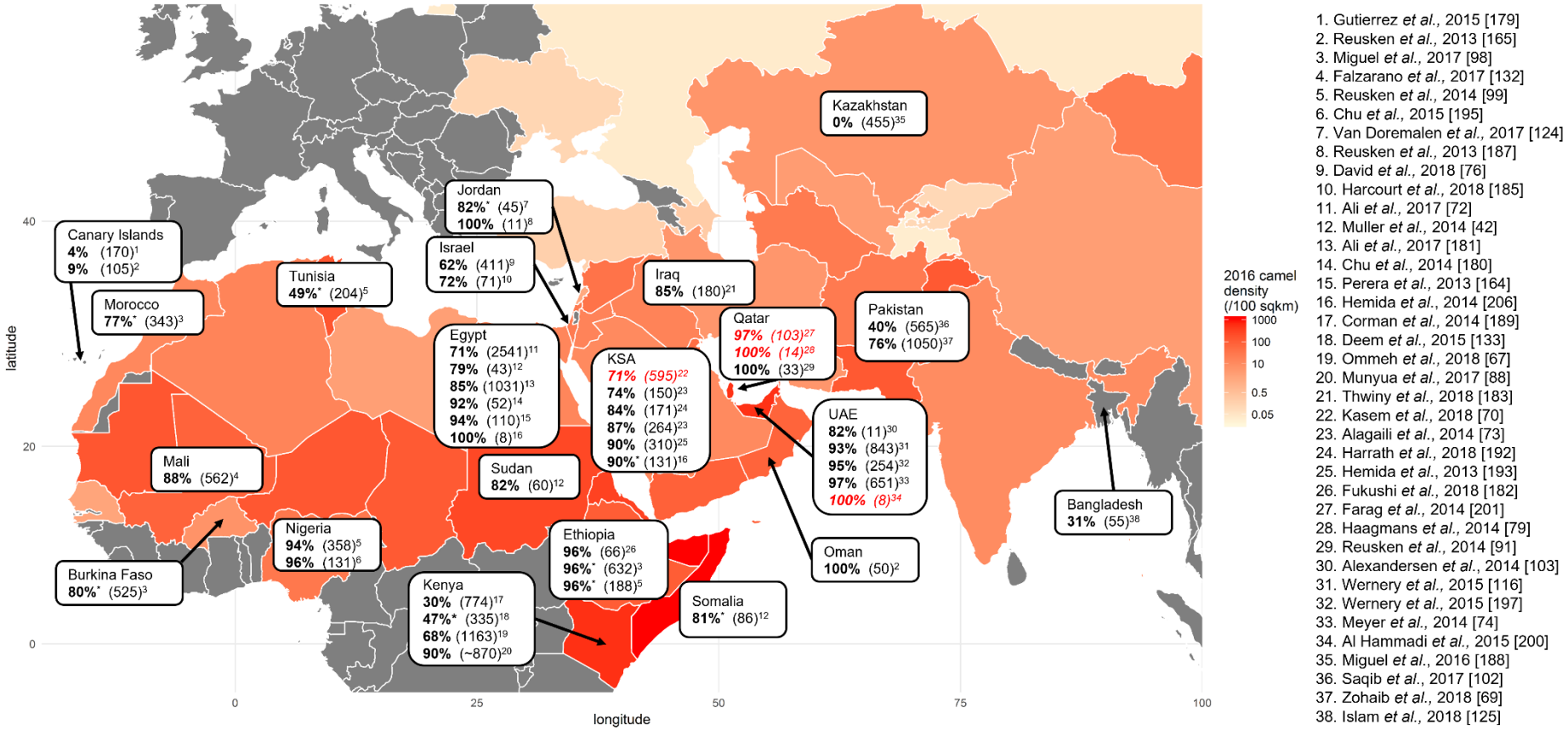


Figure 2.2. Map of MERS-CoV seroprevalence in dromedary camels. *Measures of MERS-CoV seroprevalence in dromedaries, aggregated at the country level. Total sample size tested is given in parenthesis. Camel density is calculated using FAOSTAT country-level camel population data* [204] *and World Bank data on country surface area* [205]. ** denotes values calculated from disaggregated sub-national measures of seroprevalence. Red text highlights studies conducted in dromedary populations in response to an epidemiologically linked human MERS-CoV infection.*

Seropositive dromedaries have been found in 20 of the 24 countries studied. See ***Table 2.1*** and ***Figure 2.2*** for a geographical map of seropositivity. MERS-CoV seroprevalence was between 70-100% in most country-level, age-aggregated study populations across West, North and East Africa and the Middle East. Exceptions included 62% seroprevalence measured in one of the two studies in Israel, and measures of 4-49% in Bangladesh, one study in Pakistan, the Canary Islands, Tunisia and two of the studies in Kenya. Samples taken from the large, feral camel population in Australia were seronegative, along with dromedaries in Kazakhstan and in zoos in Japan and North America [71], [103], [104], [186], [188]. No other species tested alongside dromedaries had neutralising antibodies, except a small number of alpacas and llamas living in close quarters with dromedaries in Israel [76] and one sheep in Egypt [181]. Seroprevalence was >70% in all 4 studies conducted in dromedary populations epidemiologically linked with human MERS-CoV infection.

Factors effecting seroprevalence

Age

MERS-CoV seroprevalence was found to increase with dromedary age in 13 studies (***Table 2.2***). Whilst seroprevalence was 80-100% in adult dromedaries in most populations across the Middle East and the GHA, juveniles in the same populations were repeatedly found to have lower and more variable seroprevalence (~40-90%). One study conducted in UAE disaggregated calf age through the first year of life. In this setting, calves had high seroprevalence, increasing with age to 90% in 7-12-month-olds [197].

Table 2.2 Studies reporting seroprevalence stratified by age

Country	*Stratified seroprevalence*	*Reported trend*	*Reported significance*	*Ref.*
Bangladesh	<2yrs 9% (n = 11) ≥2yrs 36% (n = 44)	Higher in camels >2yrs	Not significant	[125]
Burkina Faso, Ethiopia and Morocco	Generalised Linear Mixed Model (n = 1500)	Increase with age	**p = 0.032**	[98]
Egypt	<2yrs 52% (n = 81) ≥2yrs 87% (n = 950)	Higher in camels >2yrs	**p < 0.0001**	[181]
Egypt	<2yrs 37% (n = 595) ≥ 2yrs 82% (n = 1946)	Higher in camels >2yrs	**p < 0.0001**	[72]
Ethiopia	1- ≤2yrs 93% (n = 31) 2-13yrs 97% (n = 157)	None	Not significant	[99]
Iraq	<2yrs 89% (n = 44) >2yrs 84% (n = 136) 2-4yrs 81% (n = 58) >4yrs 86% (n = 78)	Lower in camels 2-4yrs compared with <2yrs	Not significant	[183]
Jordan	≤2yrs 74%[a] (n = 31[a]) >2yrs 100%[a] (n = 14[a])	ELISA ratio higher in camels >3yrs	Significant p = NA	[124]
Kenya	<2yrs 29%[a] (n = 141[a]) >2yrs 61% (n = 194) <6m 39% (n = 61) 6m-2yrs 21% (n = 80)	Higher in camels >2yrs than <6m	**p < 0.05**	[133]
Kenya	1-4yrs 73% (n = 285) 4-6yrs 98% (n = 116) 6yrs 98% (n = 476)	Higher in camels >4yrs	**p < 0.05**	[88]
Kenya	<4yrs 36% (n = 319) >4<7yrs 59% (n = 70) >7yrs 82% (n = 760)	Higher in camels >7yrs	**p < 0.001**	[67]
KSA	≤2yrs 55% (n = 104) >2yrs 95% (n = 98)	Higher in camels >2yrs	**p < 0.0001**	[73]
KSA	≤2yrs 73% (n = 77) >2yrs 93% (n = 187)	Higher in older animals	Not presented	[73]
KSA	1-2yrs 93% (n = 71) 3-5yrs 78% (n = 100)	Lower in camels >2yrs	**p = 0.03**	[192]
KSA	<1yr 72% (n = 65) >1yr 95%[a] (n = 245) 1-3yrs 95% (n = 106) 4-5yrs 97% (n = 76) >5yrs 92% (n = 63)	Higher in camels >1yr	**p < 0.01**	[193]
Mali	<2yrs 83% (n = NA[b]) 3-8yrs 91% (n = NA[b]) 9-16yrs 88% (n = NA[b])	None	Not significant	[132]
Pakistan	≤3yrs 58% (n = 177) 3.1-10yrs 79% (n = 712) >10yrs 81% (n = 161)	Lower in animals ≤3yrs	**p < 0.001**	[69]

Pakistan	≤2yrs 29% (n = 89) 2.1-5yrs 30% (n = 208) 5.1-10yrs 51% (n =180) >10yrs 49% (n = 88)	Higher in older animals	**p < 0.001**	[102]
Tunisia	<2yrs **30%** (n = 46) ≤2yrs **54%** (n = 158)	Not reported	Not tested	[99]
UAE	<1yr **85%** (n = 108) >1yr **96%**[a] (n = 650) 2-4yrs 97% (n = 340) >4yrs 96% (n = 310)	Lower in calves <1yr	**p < 0.05**	[116]
UAE	<1yrs **84%** (n = 121) >1yrs **99%** (n = 133) 0-3m 75% n = 32) 4m 79% (n = 14) 5-6m 89% (n = 46) 7-12 90% (n = 29)	Increase with age	Not tested	[197]
Studies investigating dromedary camel populations linked to human MRS-CoV infection				
KSA	*≤2yrs **58%** (n = 25)* *>2yrs **81%** (n = 344)* *2.1-4yrs 77%[c] (n = 156)* *4.1-6yrs 81%[c] (n = 98)* *>6yrs 87%[c] (n = 90)*	*Higher in camels >2yrs*	***p = 0.003***	[70]

a. age-stratified results were calculated by us, using disaggregated results presented by authors
b. number of animals in each age class not supplied

Geographic location

Although MERS-CoV seroprevalence is consistently high across West, North and East Africa and the Middle East at country level, some studies measured considerable within-country variation in seroprevalence, particularly in Africa. In Kenya, all three studies that presented sub-nationally disaggregated results showed seroprevalence to vary greatly by province. Tunisia, Morocco, and Mali also showed considerable regional seroprevalence variation. Less regional variation in seroprevalence was observed within Middle Eastern countries.

Sample population characteristics

Several studies found imported animals to have significantly higher seroprevalence than their locally bred counterparts [72], [125], [179], [181]. Dromedaries sampled at markets, abattoirs and quarantine sites had higher seroprevalence than those in farms, villages, and research facilities [72], [124], [125], [181]. In some cases, dromedary origin varied with the type of site sampled suggesting confounding.

In a study conducted across Burkina Faso, Morocco and Ethiopia, dromedaries used for milk and meat had higher seroprevalence than those used for transport [98]. In most studies that stratified by sex, little difference was seen but, in Kenya, female dromedaries had statistically significantly higher seroprevalence than males – 93% vs. 81% in one study [88], and 74% vs. 54% in another [67]. In Egypt and KSA, males had significantly higher seroprevalence – (72% and 84% in males vs. 66% in females) [70], [72]. Large and medium herd-size was a risk factor for seropositivity across Burkina Faso, Morocco, and Ethiopia [98]. Conversely, in Kenya there was a non-statistically significant trend for smaller herds to have higher seroprevalence [133]. Across Burkina Faso, Morocco, and Ethiopia, both nomadic and sedentary husbandry systems were risk factors for seropositivity when compared with a mixed lifestyle [98]. Two studies in Kenya showed higher seroprevalence in nomadic herds compared with those kept on ranches or those with agro-pastoralist management. However, ranches were in a different region from nomadic herds and the sample size for agro-pastoralist management was small [88], [189].

Prevalence of active MERS-CoV infection – cross-sectional studies

Dromedary populations in 16 countries have been tested for MERS-CoV RNA, 13 of which report positive results. These include: KSA (0.12-56%) [66], [70], [73], [135], [191], [194], UAE (0-29% or 0-100% if dromedaries epidemiologically linked to human MERS-CoV cases are included) [65], [116], [129], [134], [197]–[200], Qatar (22-79%) [79], [91], [177], [201], Oman (7%) [196], Iraq (15%) [184] and Jordan (62%) [124], as well as Egypt (4-15%) [72], [180], [181], Ethiopia (10%) [98], Kenya (0.35-0.95%) [67], [190], Nigeria (3-11%) [84], [195], Burkina Faso (5%) [98], Morocco (2%) [98] and Pakistan (3%) [69]. See ***Figure 2.3*** for a map of RNA prevalence, and ***Table 2.1***. Despite moderate seropositivity, surveys have not detected active MERS-CoV infection in the dromedary populations of Bangladesh or Israel [76], [125]. RNA prevalence in dromedary populations linked to human cases was similar to more randomly sampled populations in the same country, with the exception of two small outbreak studies in the UAE which found 100% dromedaries to be infected [199], [200].

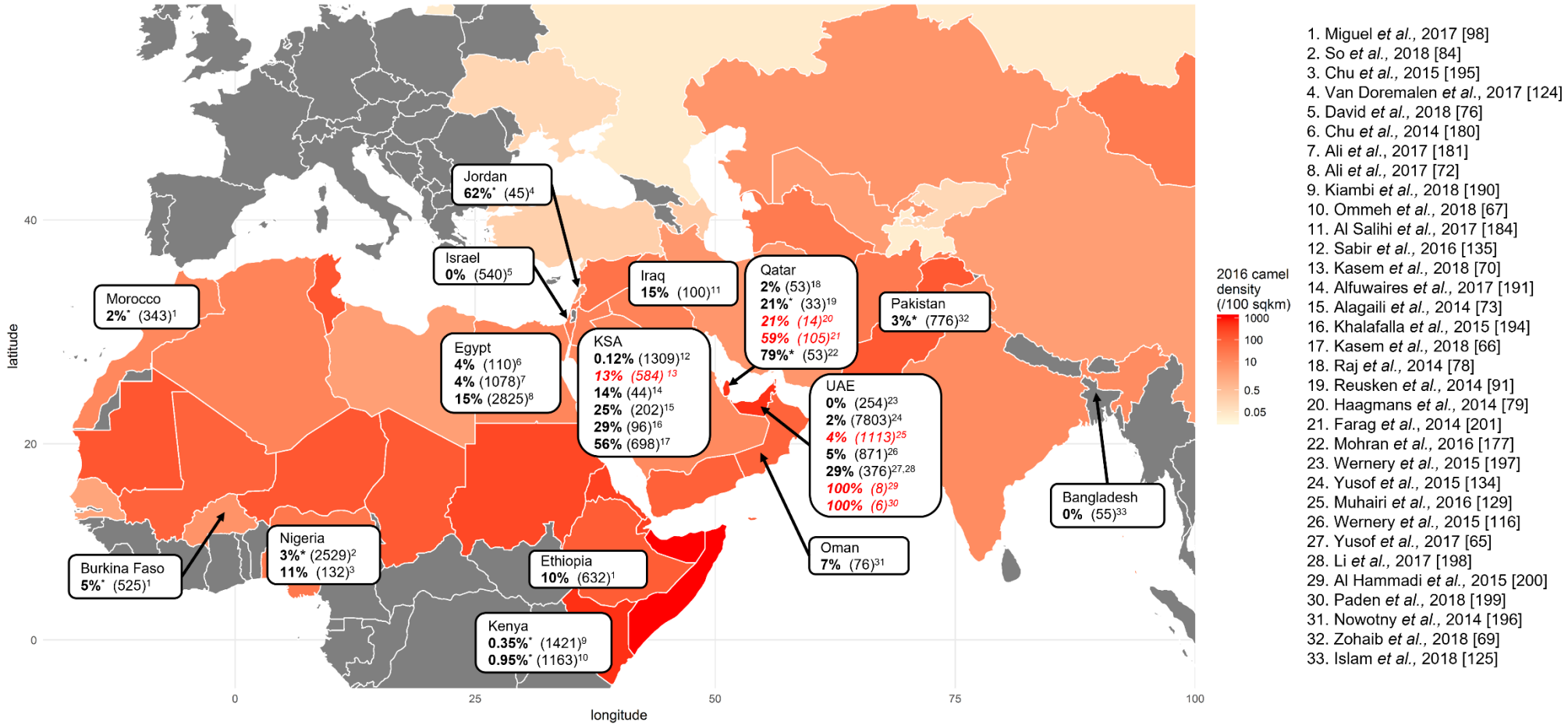


Figure 2.3. Map of the prevalence of active MERS-CoV infection in dromedary camels*. Measures of MERS-CoV RNA prevalence in dromedaries, aggregated at the country level. Total sample size tested is given in parenthesis. Camel density is calculated using FAOSTAT country-level camel population data* [204] *and World Bank data on country surface area* [205]*. * denotes values calculated from disaggregated sub-national measures of seroprevalence. Red text highlights studies conducted in dromedary populations in response to an epidemiologically linked human MERS-CoV infection.*

Factors affecting prevalence of infection

Age

Age-stratified studies in KSA and Jordan found that juveniles had a higher RNA-positivity than adults [70], [73], [124]. RNA-positivity also had an inverse association with age in dromedaries across Morocco, Burkina Faso and Ethiopia [98]. Two studies in Egypt measured similar positivity rates between juveniles and adults [72], [181].

Sample population characteristics

Whilst higher prevalence of RNA shedding was found in imported animals by three studies in Egypt, site-type is a potential confounder, with local camels being sampled from farms and villages, whilst imported animals were sampled in markets, quarantine centres and abattoirs [72], [180], [181]. A study in KSA which sampled both local and imported dromedaries within live animal markets found that locally reared animals had significantly higher prevalence of viral shedding [135]. Overall, three studies reported abattoirs and one reported wholesale markets to be associated with an increase in measured prevalence of shedding compared to villages, farms and quarantines [98], [134], [135], [191]. Much like seroprevalence, RNA positivity was significantly higher in dromedaries bred for meat or milk compared with those used as transport in Burkina Faso, Morocco and Ethiopia, and shedding was higher amongst females, albeit sex and function were highly correlated [98].

Potential temporal trends

Five studies measured RNA prevalence at a defined site at multiple points in time, although animals were not themselves sampled longitudinally. Three studies in Egypt and KSA showed a peak in prevalence of viral RNA shedding in the winter months (December to May) [66], [72], [194]. The fourth, conducted in wholesale markets in KSA, saw lower rates of infection during July and August, and higher positivity in December [135]. At an abattoir in Nigeria, no infection was seen from October to mid-January, with prevalence of infection peaking in February after which no more samples were taken [84].

Evidence of infection and immunity from longitudinal studies

Ten longitudinal studies were found describing nine outbreaks of natural infection on farms and in quarantine facilities – one in Egypt [72], four in KSA [77], [206]–[208], five in UAE [65], [116], [129], [131], [200], and one study taking monthly samples of 430 dromedaries in Kenya [190].

Duration of viral shedding

Four studies of natural infection measured viral shedding in dromedaries at approximately weekly intervals. The maximum time window in which all consecutive nasal samples taken were positive for MERS-CoV RNA ranged from 7-45 days across published studies, with most positive animals becoming negative within two weeks [65], [116], [129], [200]. All available studies followed animals that were found to be MERS-CoV RNA positive at the first instance of sampling, with the duration of shedding prior to sampling unknown. Further to this, intermittent RNA shedding, and evidence of potential rapid reinfection/coinfection has been observed [65], [129].

Evidence of Reinfection

Three studies found dromedaries to be shedding MERS-CoV RNA despite having high antibody titres months or weeks prior to detectable infection. Both older animals whose antibodies reflect past exposure [72], [131], [208] and young calves whose high antibody titres were maternally-acquired immediately post-partum, became infected [131].

One study directly observed reinfection amongst a herd of dromedaries in Egypt, with four animals shedding 1-3 months prior to a herd-wide epidemic in which they tested RNA-positive once more [72]. Sequenced MERS-CoV isolates from a market in UAE showed lineage switching from week to week, which is also supportive of rapid reinfection or coinfection in calves [65].

Longitudinal studies also indicated that mAbs may offer some protection. In both studies of calf-mother-pairs conducted in UAE, MERS-CoV infection became highly prevalent in calves between 4-6 months of age when assumedly mAbs had waned [116], [131]. Samples from reinfected

animals have been found to have lower viral loads, suggesting that past infection may ameliorate future infections [208]. Viral load and probability of isolating infectious virus were greater when sampling calves, than adults [67], [131].

Discussion

A wealth of cross-sectional studies were found measuring MERS-CoV seroprevalence and prevalence of viral shedding in dromedary populations. This allowed the identification of trends that were common to multiple studies such as the association between prevalence and age. There were, however, very few studies that collected longitudinal data describing prevalence or incidence of infection or seropositivity or seroconversion over time, making it challenging to pick out any seasonal trends. The lack of longitudinal data also meant the duration of antibody mediated immunity could not be established without further analyses beyond the scope of the systematic review. This is addressed further in ***Chapter 3*** of this thesis.

The results of this systematic review show that MERS-CoV circulates widely in dromedaries across the Middle East and Africa but suggests that transmission dynamics vary spatially and perhaps temporally. The sub-national range of MERS-CoV seroprevalence appears to be larger in countries outside of the Arabian Peninsula. Within-country variation in seroprevalence is potentially indicative of differences in transmission dynamics, meaning vaccine strategy evaluation and mathematical modelling will need to be conducted at a sub-national resolution where data allows.

The rise of MERS-CoV seroprevalence from 40-90% in juveniles to 80-100% in adult dromedaries across much of West, North and East Africa and the Middle East, is characteristic of an endemic disease where the probability of infection increases with time. High seroprevalence in calves <1-year-old in some populations in UAE and KSA suggests high transmission intensity in the Arabian Peninsula, with most dromedaries becoming infected during the first year of life, although mAbs may contribute to seropositivity in young calves [116], [193], [197]. The age-dependent seroprevalence values synthesised here should be used to fit models of MERS-CoV

transmission in dromedaries and elucidate the likely transmission intensity of the virus in the Middle East and in Africa – a key parameter for estimating vaccination impact. Reporting finer age-stratification of young dromedaries would allow a better comparison of transmission intensity in different regions through fitting models of seroconversion.

Age-dependent seroprevalence patterns suggest that the higher prevalence of viral shedding in juveniles compared with adults is likely due to immunological naivety. The age-distribution of reported infections synthesised here suggests that contact with juveniles may pose greater risks of human transmission than adults, making them potential targets for vaccination. Frequency of human contact with dromedaries may also be animal-age-dependent, however [116]. Calf-focused vaccination may reduce the overall number of dromedary infections, but the reduced risk of exposure could mean that any remaining infections would likely occur at an older age than in the absence of vaccination. It will therefore be important to investigate the age-dependency of human-dromedary contact patterns and the way in which these vary across different countries and husbandry systems. Vaccination strategies should be evaluated not only on their likely impact on prevalence of active infection in dromedaries, but also on the age-distribution of infections.

Both live markets and abattoirs had higher prevalence of RNA shedding compared to other site-types in multiple studies and are key locations for animal mixing [98], [134], [135], [164]. Mixing underpins the interaction between infectious and susceptible individuals and, therefore, the dynamics of MERS-CoV transmission. A role for markets as drivers of disease dissemination is characteristic of other zoonotic diseases such as avian influenza [110], [209]. Mapping the movement and mixing of dromedaries is necessary to understand the underlying spatial transmission dynamics of MERS-CoV. If available, quantitative data describing the movement and trading patterns of dromedary populations could inform spatial models of transmission and help to assess the potential impact of vaccination at different points in the camel value chain.

More evidence is needed to establish whether MERS-CoV in dromedaries is seasonal. The limited number of long-term longitudinal studies in this review observed higher prevalence of active infection between December and May [66], [72], [84], [135], [194]. These studies were conducted in Egypt and KSA where dromedary calving occurs between October and April [117], [118], [120], [121], and Nigeria which has a similar calving season peaking between October and December [119]. In order to establish whether MERS-CoV is seasonal, the incidence of infection needs to be tracked over multiple years. If seasonal calving is driving the trend and calves become susceptible between 4-6 months [116], [131], we might expect the number of susceptible dromedaries to be higher between January and May – which is close to the observed peaks in animal infection in the long-term longitudinal studies available.

As well as calving times, seasonal environmental factors have also been hypothesised to effect transmission dynamics, with lower temperatures and humidity found to be associated with higher numbers of reported primary human MERS cases in KSA [210]. Phylogenetic analysis of MERS-CoV genomes isolated from humans and dromedaries has estimated that a seasonal period of elevated risk of dromedary-to-human transmission exists between April and July [2]. However, a study did not find a seasonal pattern in the numbers of primary human MERS-CoV cases reported to the World Health Organisation between 2013 and 2017 [211]. More longitudinal studies and mechanistic models of possible seasonal drivers are needed to further investigate potential seasonal trends and whether they affect the risk of zoonotic transmission throughout the year.

The results of longitudinal studies included in this review demonstrate re-infection of dromedaries despite high titres of MERS-CoV specific antibodies being present in their sera. Unfortunately, the degree and duration of protection afforded by mAbs and those acquired from infection is unclear. Fitting models of seroconversion and reversion to the age-stratified data available could help elucidate the rates at which these antibodies wane. Informative surveys of a

better proxy for protective immunity in dromedaries would improve the accuracy of models of reinfection and the likely effects of vaccination.

The maximum duration of RNA shedding is found to range from 7-45 days across longitudinal studies in this systematic review. These studies were not designed to measure the duration of viral shedding, however, and suffered infrequent sampling and left censoring due to unknown onset of infection. Evidence of intermittent shedding or rapid reinfection coupled with the infrequent sampling also complicated interpretation of the measured duration of shedding. After this systematic review was finalised, a study measuring MERS-CoV shedding in vaccinated and control groups of dromedaries overcame these caveats. The investigators captured the onset of infection and made daily measurements of viral shedding in naturally infected non-vaccinated dromedaries in a controlled environment where reinfection with a different MERS-CoV virus was unlikely. They found shedding to reduce over 14 days post infection and be below the level of detection in all of the animals by day 14, giving a much better idea of temporal dynamics of viral shedding (Alharbi et al 2019). No studies of natural infection have attempted to measure the duration of shedding of infectious virus (as opposed to viral RNA). A controlled challenge study in four dromedaries performed daily sampling and saw that infectious virus (as determined by plaque assay) was isolatable for the first seven days [130]. However, the biological relevance of the challenge dose is not known.

Limitations of the work described in this chapter include that a single author completed the systematic search and data extraction and that only published literature was included, thereby introducing potential publication bias. The available studies exhibit differences in study design, criteria for seropositivity, sample-site type and sample population characteristics. Some studies report that the latter two variables are associated with statistically significant differences in seroprevalence or prevalence of infection within individual studies [72], [98], [124], [134], [135], [181], [189]. These heterogeneities made quantitative pooling inappropriate.

Available published studies do not include results from camel dense regions of northern Africa, Rajasthan in India or Yemen. In addition to the countries included in this systematic review of the published literature, OIE has received reports of RNA positive camels in Iran and Kuwait in 2014 [212]. Together with their country counterparts, members at WHO and the Food and Agriculture Organisation of the United Nations (FAO) are planning and/or implementing further RNA testing studies in several countries in Africa (including Ethiopia, Kenya, Egypt, Somalia, Sudan, Algeria and Morocco), the Middle East (including. Jordan), and South Asia (including Pakistan) (personal communication, Maria D. Van Kerkhove). Since this systematic review was conducted and published, a study also surveyed seroprevalence and RNA prevalence in 7 countries including Senegal and Uganda where dromedary populations had not previously been tested. Dromedaries were found to be seropositive in both countries and evidence of active infection was found in dromedaries in Senegal [63].

Conclusions

The findings of this systematic review provide strong evidence that MERS-CoV is endemic in dromedary populations across much of West, North and East Africa, South Asia, and the Middle East.

In addition, the results highlight several epidemiological characteristics of MERS-CoV in dromedaries that should be explored further in mechanistic transmission models to inform the design of MERS-CoV animal vaccination strategies. These characteristics are as follows:

1. calves are likely to play a central role in sustaining circulation of MERS-CoV;
2. sites where dromedaries mix may also play a role in driving transmission; and
3. the transmission dynamics of MERS-CoV in dromedary populations are likely to vary both between regions and more finely at the subnational level.

The results also emphasise several gaps that must be addressed including: the transmissibility of MERS-CoV in dromedaries and how contextual factors affect this; the nature of immunity

following infection or acquisition of mAbs; and whether transmission occurs seasonally and, if so, what mechanism drives temporal peaks in population infectiousness.

Finally, an important product of this review is the comprehensive dataset describing age-stratified seroprevalence in dromedaries across three continents. This dataset is used to fit models of seroconversion and infer key parameters describing transmission dynamics in ***Chapter 3***.

Chapter 3: Estimating the transmissibility of MERS-CoV in dromedaries using age-stratified seroprevalence data

Introduction

In this chapter I aim to address a key gap in understanding MERS-CoV in dromedaries by estimating the transmissibility of the virus using age-stratified seroprevalence data. Quantifying transmissibility is important for planning interventions to control or reduce infectious disease spread. Currently, estimates of the transmissibility of MERS-CoV in dromedaries are limited to a single study which estimated the Force of Infection (FoI – defined as the rate at which susceptible individuals become infected over time), under one set of immunity assumptions, in dromedaries in Kenya [126]. Without a better idea of the transmissibility and how it varies by geographical/husbandry context, it is not possible to predict what vaccination coverage and vaccine efficacy would be required to prevent the circulation of MERS-CoV in a herd, nor to establish how factors such as herd size or population structure are likely to affect transmission dynamics.

Transmissibility is often described in terms of the R_0 (defined on page 36) or the FoI. Transmissibility is best estimated from longitudinal incidence data describing the daily numbers of new infections (also known as epidemic curves). Unfortunately, it can be very difficult to reliably measure incidence, especially when dealing with a broadly asymptomatic infection in an animal population. Whilst a small number of longitudinal studies measuring MERS-CoV infection in dromedaries have provided valuable insight into reinfection and duration of shedding [72], [116], [131], [208], these studies cannot be used to infer transmissibility due to constraints on time scales and frequency of sampling.

Whilst there is a lack of longitudinal data describing MERS-CoV incidence in dromedaries, there are multiple studies which have measured age-stratified seroprevalence. Due to the temporal dimension introduced by age-stratification, cross-sectional seroprevalence survey data can be used to estimate the rate at which susceptible animals acquire infection – the FoI. This approach to estimating transmissibility, originally conceptualized by Muench (Muench 1934), has been

used to better understand the dynamics of many infectious diseases such as measles, dengue and Chagas disease [159]–[161].

In this chapter, I use publicly available age-stratified seroprevalence data (extracted during the systematic review described in Chapter 2) to estimate the Force of Infection of MERS-CoV in dromedary populations across Africa, the Middle East and South Asia. By comparing the fit of different models of antibody waning to the age-stratified seroprevalence data, I investigate the potential contribution of maternally acquired antibodies (mAbs) and estimate the rate of waning of antibodies (seroreversion) following infection.

Methods

Data extraction

The FoI of MERS-CoV in dromedary camels was estimated by fitting catalytic models of infection to age-stratified seroprevalence data. The data was extracted through a systematic review of the peer reviewed literature describing MERS-CoV seroprevalence in dromedary populations published prior to January 1st, 2019, which included 19 studies across 10 countries that stratified seroprevalence by dromedary age (please see ***Chapter 2*** of this thesis for more details of the systematic review process and exclusion criteria). The studies were conducted in South Asia (Bangladesh [125] and Pakistan [69], [102]), Africa (Tunisia & Ethiopia [99], Kenya [67], [88], [133], and Egypt [72], [181]), and the Middle East (Kingdom of Saudi Arabia (KSA) [70], [73], [192], [193], United Arab Emirates (UAE) [116], [197], Jordan [124], and Iraq [183]). In total, three studies that were included in the systematic review were excluded from the analysis in this chapter. Two of these studies were excluded as their sampling strategies were not appropriate for FoI estimates which assumes a random cross-sectional sample of seroprevalence. The first sampled dromedaries with epidemiological connection to human cases [70], and the second sampled camels in response to finding a dromedary which tested positive

for MERS-CoV during what turned out to be the height of an outbreak [197]. Finally, the third study was excluded because it was not possible to determine whether the sample population [181] overlapped with another larger study conducted in the same area that was included [72]. To make the geographical range of the FoI estimates as comprehensive as possible, seroprevalence measures from one additional study published after the systematic review were also included. This further study measured seroprevalence in camel populations in Senegal and Uganda - two additional countries not represented in the literature previously [63].

Interpretation and cleaning of the data

Age class boundary estimation

If the study gave no lower age bound for the lowest age class and an age range was not given in the text, the lower bound is assumed to be zero. If the study gave no upper age bound of the highest age class, this is assumed to be 20 years. The maximum life expectancy of farmed or working camels has been reported to be between 14 and 29 years [113], [114], and, of the studies in the systematic review that reported maximum ages, no individual was reported to be older than 16 years of age. One study [124] supplied individual ages for each camel. In this case I grouped the camels into roughly equally sized age classes that followed common classifications by other studies, when possible, whilst preserving finer divisions of younger age classes. In this way, all datasets could be analysed simultaneously using the same likelihood function. For more detailed rules of how reported age class bounds were interpreted, please see ***Appendix Chapter 3, A3.1***. The results presented in this chapter assume a uniform distribution of ages in each reported age classes, however, this analysis was repeated assuming that the sampled populations in each age class perfectly represent the larger population structure assumed by the later dynamic modelling chapter with a constant mortality rate of μ_0 for individuals under two years old and a lower rate μ for individuals over two years old. Detailed descriptions of these alternative model solutions and associated results are given in ***Appendix 6.1.***

Seropositivity

Studies used different methods to test for seropositivity (***Table 3.1***) including commercially available EUROIMMUN AG IgG ELISAs (Immunoglobulin G Enzyme Linked Immunosorbent Assays), in-house IgG ELISAs, PM (Protein Microarrays) [162], [165] or neutralisation tests including MN (Micro Neutralisation Tests) [42] and ppNTs (pseudoparticle Neutralisation Tests) [164].

The MN test and ppNT, which require the antibodies in the sample to neutralise MERS-CoV activity, are highly specific to MERS-CoV antibodies [42], [171]. There is no indication of cross-reactivity with other coronaviruses infecting dromedaries such as Bovine coronavirus (BCoV) when using MN, ppNT, or PM [74], [165], [185], [193]. Measures of specificity are not readily available for ELISAs, however the ELISA assays as used by Saqib *et al.,* (2017) and others have been measured to be 99% specific when correlated with MN tests [42], [102]. In general, ELISAs are considered more sensitive to MERS-CoV antibodies as they can pick up non-neutralising antibodies that are not detected by neutralisation tests [171]. The seroprevalence measured by studies using neutralisation tests often approaches or reaches 100% in adult dromedaries suggesting that – assuming they are indeed highly specific – they must also have a fairly high sensitivity. In the core analyses presented in this Chapter I have therefore assumed 100% assay specificity and 99% sensitivity across test types, but to explore how potential differences in assays used may impact results, the analysis was also repeated assuming that neutralisation tests are less sensitive than PMs and ELISAs, and that ELISAs are less specific than MNs, ppNT and PM tests. One study, [135], used sequential testing and, in this case, the predicted observed seroprevalence, p_{obs}, was defined as:

$$p_{obs} = sensitivity * p_{true} + (1 - specificity) * (1 - p_{true}) \quad 3.1$$

where p_{true} is the predicted true seroprevalence, and *sensitivity* is defined as:

$$sensitivity = sensitivity_{test1} * sensitivity_{test2} \quad 3.2$$

whilst *specificity* is defined as:

$$specificity = 1 - (1 - specificity_{test1})(1 - specificity_{test2}) \quad 3.3$$

Table 3.2. Age-stratified seroprevalence used in fitting catalytic models of infection

Country	*Stratified seroprevalence*	*Test type*	*Ref.*
Bangladesh	<2yrs 9% (n = 11) ≥2yrs 36% (n = 44)	ppNT	[125]
Egypt	<2yrs 37% (n = 595) ≥ 2yrs 82% (n = 1946)	MN	[72]
Egypt	<2yrs 16% (n = 447) ≥2yrs 84% (n = 1586)	MN	[63]
Ethiopia	1- ≤2yrs 93% (n = 31) 2-13yrs 97% (n = 157)	PM	[99]
Iraq	<2yrs 33% (n = 6) ≥2yrs 57% (n = 21)	MN	[63]
Iraq	<2yrs 89% (n = 44) 2-4yrs 81% (n = 58) >4yrs 86% (n = 78)	ELISA	[183]
Jordan	<2yrs 50% (n = 82) ≥2yrs 92% (n = 222)	MN	[63]
Jordan	≤2yrs 74%[a] (n = 31[a]) >2yrs 100%[a] (n = 14[a])	ELISA	[124]
Kenya	<6m 39% (n = 61) 6m-2yrs 21% (n = 80) >2yrs 61% (n = 194)	PM	[133]
Kenya	1-4yrs 73% (n = 285) 4-6yrs 98% (n = 116) 6yrs 98% (n = 476)	ELISA	[88]
Kenya	<4yrs 36% (n = 319) >4<7yrs 59% (n = 70) >7yrs 82% (n = 760)	ELISA	[67]
KSA	≤2yrs 55% (n = 104) >2yrs 95% (n = 98)	ELISA	[73]
KSA	≤2yrs 73% (n = 77) >2yrs 93% (n = 187)	ELISA	[73]
KSA	1-2yrs 93% (n = 71) 3-5yrs 78% (n = 100)	ELISA	[192]
KSA	<1yr 72% (n = 65) 1-3yrs 95% (n = 106) 4-5yrs 97% (n = 76) >5yrs 92% (n = 63)	ppNT	[193]
KSA	<2yrs 82% (n = 11)	MN	[63]

	≥2yrs 82 % (n = 211)		
Pakistan	≤3yrs 58% (n = 177) 3.1-10yrs 79% (n = 712) >10yrs 81% (n = 161)	ELISA, followed by MN	[69]
Pakistan	≤2yrs 29% (n = 89) 2.1-5yrs 30% (n = 208) 5.1-10yrs 51% (n =180) >10yrs 49% (n = 88)	ELISA	[102]
Senegal	<2yrs 29% (n = 17) ≥2yrs 69% (n = 181)	MN	[63]
Tunisia	<2yrs 100% (n = 28) ≥2yrs 87% (n = 754)	MN	[63]
Tunisia	<2yrs 30% (n = 46) ≥2yrs 54% (n = 158)	PM	[99]
UAE	≤1yr 85% (n = 108) 2-4yrs 97% (n = 340) >4yrs 96% (n = 310)	ELISA	[116]
Uganda	<2yrs 52% (n = 150) ≥2yrs 66% (n = 350)	MN	[63]

a. age-stratified results were calculated by me, using disaggregated results presented by authors

Estimating the FoI

The Force of Infection (FoI) is defined as the annual rate of MERS-CoV infection per susceptible animal. Assuming the FoI is constant over time and with age, one would expect the proportion of animals that have been infected (the seroprevalence) to increase monotonically with age, where age acts as a proxy for time spent in the at-risk population, as originally conceptualised by Muench [158], [213]. We can therefore use the age-stratified seroprevalence to estimate the FoI by fitting a model of seroconversion to the data. These models were called "catalytic models" by Muench due to their similarity to models of catalysed chemical reactions.

Catalytic models assume that seropositivity exclusively follows infection and is lifelong. For MERS-CoV in dromedaries, however, these assumptions may not hold true. In many disease systems, individuals can passively acquire antibodies from their mother during pregnancy and through suckling following birth. These are known as maternally-acquired antibodies (mAbs). There is evidence that dromedary calves born to MERS-CoV seropositive dams acquire MERS-

CoV specific mAbs through colostrum [116], [131]. One study observed young animals to be shedding MERS-CoV despite high antibody titres but both studies observed an outbreak of infection and re-seroconversion following waning of what were assumed to be mAbs, suggesting that these may provide some protection against infection [116], [131]. The simplest catalytic models also ignore the possibility that antibodies and their protection may wane over time. To probe different potential immunity scenarios for MERS-CoV in dromedaries, I used four catalytic models of seroconversion (***Figure 3.1***, and ***Equations 3.1-3.4***).

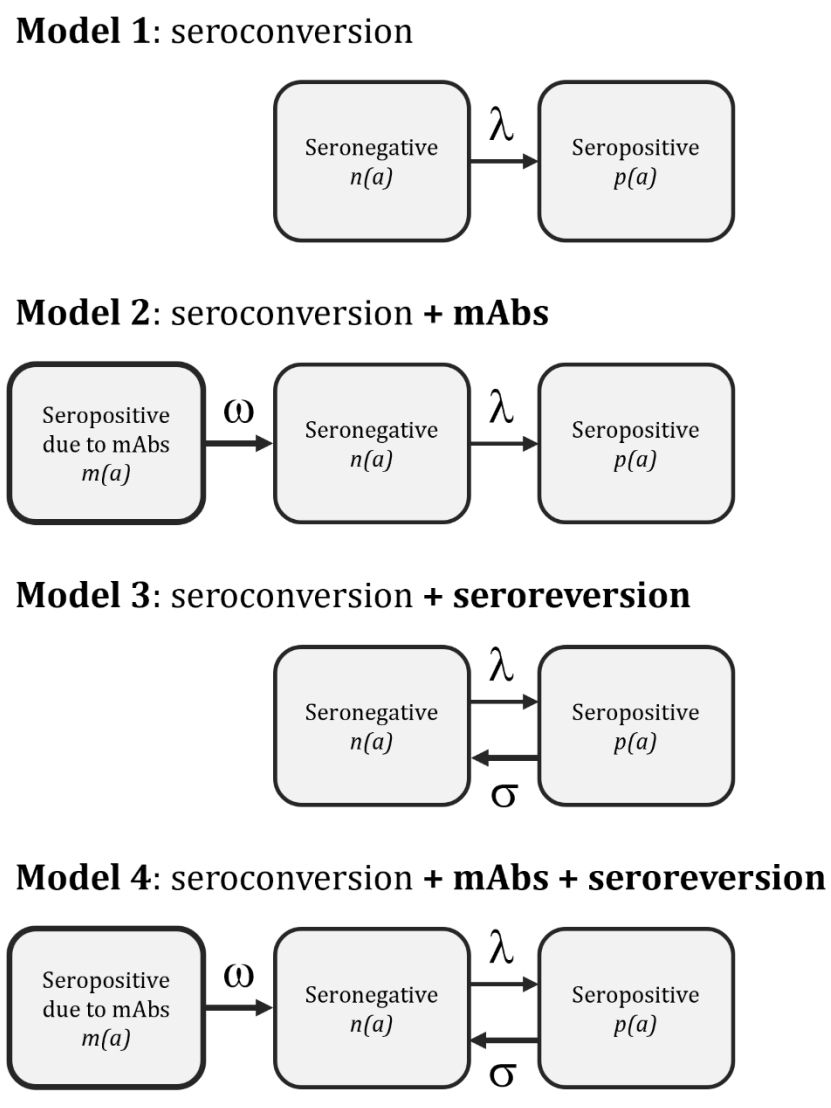


Figure 3.1 Four catalytic models of MERS-CoV seroconversion in dromedary populations*, where λ is the force of infection, ω is the rate of waning of mAbs, and σ is the rate of waning of antibodies following infection.*

In Model 1, all animals are initially seronegative, becoming irreversibly seropositive at rate λ (the FoI) as described by Muench:

$$p(a) = 1 - e^{-\lambda a} \quad 3.1$$

Where $p(a)$ is the expected proportion of animals that are seropositive at age a.

I then considered the possible contribution of mAbs in Model 2 as described formally in ***Equation 3.2*** where m_0 is the proportion of calves born with mAbs, which then wane at rate ω. I estimated m_0 by solving the equivalent model in the absence of mAbs to find the proportion of adults of reproductive age that are predicted to be seropositive and therefore pass their antibodies onto their calves.

$$p(a) = 1 - e^{-\lambda a} - m_0\left(\frac{\lambda}{\lambda - \omega}\left(e^{-\omega a} - e^{-\lambda a}\right)\right) \quad 3.2$$

Model 3 (formally described by ***Equation 3.3***) allows for possible seroreversion - the waning of protective antibodies acquired through natural infection at rate σ. Formulation of Model 3 was informed by catalytic models of seroconversion described and used to estimate the FoI of dengue by Imai *et al.,* [159]. Model 4 brings mAbs and seroreversion together (as described by ***Equation 3.4***).

$$p(a) = \frac{\lambda}{\lambda + \sigma}\left(1 - e^{-(\lambda+\sigma)a}\right) \quad 3.3$$

$$p(a) = \frac{\lambda}{\lambda + \sigma}\left(1 - e^{-(\lambda+\sigma)a}\right) - m_0\,\frac{\lambda}{\lambda + \sigma - \omega}\left(e^{-\omega a} - e^{-(\lambda+\sigma)a}\right) \quad 3.4$$

Equations 3.1-3.4 show the derived solutions for the proportion of the population seropositive at age 'a'. To make the model more robust to potential predicted trends in seroprevalence especially within the wider age classes in the data, the predicted mean seroprevalence in an age class in the data was calculated explicitly by integrating the predicted seroprevalence across the age class, rather than approximating it by calculating the predicted seroprevalence at the mean age of the age class. Please see ***Appendix Chapter 3, A3.2*** for the full details of how the model solutions were reached.

Model-fitting

The models were fit to the age-stratified seroprevalence data within a Bayesian framework to quantify uncertainty about the unknown parameters, and to incorporate prior information on their plausible ranges. Initially, I assumed that the number of camels testing seropositive in each age-stratification was binomially distributed as described formally below:

$$X_i \sim Binomial(N_i, p_i) \quad 3.5$$

Where X_i is the number of camels testing seropositive, N_i is the number of camels in age class i, and p_i is the probability of testing seropositive.

However, the MERS-CoV seroprevalence studies were conducted across a range of camel populations in different locations and herd management systems and used different assays to determine seropositivity. This could mean that the data has higher variance than is expected when I assume it is binomially distributed. To account for this potential overdispersion I assume that the binomial parameter p_i is itself beta distributed, so that X_i follows a beta-binomial distribution defined as:

$$X_i \sim BetaBinomial(N_i, p_i, k) \quad 3.6$$

where k represents the amount of overdispersion in the data.

The likelihood of the beta-binomial model is defined by the probability mass function of the beta-binomial distribution:

$$L(p_i) = \binom{N_i}{X_i} \frac{B(X_i + \alpha,\ N_i - X_i + \beta)}{B(\alpha, \beta)} \quad 3.7$$

where α and β are the standard parameters of the beta distribution and are both >0:

However, for my purposes it was useful to re-parameterise the beta-binomial distribution in terms of the mean probability of being seropositive, *p*, and an overdispersion parameter, *k*.

$$p = \frac{\alpha}{\alpha + \beta} \quad 3.8$$

$$k = \frac{n - 1}{\alpha + \beta + 1} \quad 3.9$$

The parameter $k > 0$, and a *k* approaching zero would indicate negligible overdispersion. With this reparameterisation, the variance of the beta-binomial distribution becomes:

$$var[X] = np(1 - p)\{1 + k\} \quad 3.10$$

Note that the first term in ***3.10***, $np(1 - p)$, is equal to the variance of binomially distributed observations meaning the reparameterization results in a quasi-binomial parameterisation for the beta binomial, in which binomial variance is scaled by a fixed constant *1 + k*. This gives a weaker overdispersion than the more standard reparameterisation of the beta-binomial [214] in which overdispersion scales with n^2, and so offers better control of overdispersion through the use of priors. A normal distribution with a mean of zero and a standard deviation of 0.5, restricted to positive values (a "half-normal" distribution), was used as the prior for the overdispersion parameter. Priors for *k* with greater standard deviations up to 2 were also used to test whether the results were robust to the choice of prior.

Analysis was conducted in R (V 4.0.3) [215]. The Stan programming language and rstan package [216], [217] were used to implement Hamiltonian Monte Carlo (HMC) algorithm to compare the likelihood of different model iterations and to infer the posterior distribution of the estimated model parameters. HMC is a Markov Chain Monte Carlo (MCMC) method for sampling from a probability distribution (in this case the distribution of each of the model parameters). HMC can

be more efficient than other MCMC methods as it uses Hamiltonian dynamics when proposing a new set of parameter values, meaning greater distance between proposals and more time spent exploring areas of the parameter space with high posterior probability density [218]–[220]. Uniform prior distributions between 0 and 10 were used for the rate of waning of mAbs and the annual FoI. An FoI >10 was deemed implausible as this would mean animals getting infected >10 times per year on average. A uniform prior and between 0 to 1 for the annual rate of seroreversion following infection. For each simulation 4 chains were run for 10,000 iterations with a discarded burn-in period of 3,000 iterations chosen to be conservative after visually assessing convergence. Chains were not thinned as it is not largely required or advised to thin HMC chains as the nature of the algorithm reduces autocorrelation within chains, increasing sampling efficiency as compared to algorithms that exhibit random walk behaviour [218], [221]. Autocorrelation was assessed using the bayesplot package [222], [223] and found to be approximately zero even at a lag of 1 iteration for the FoI parameters and for the overdispersion parameter. Autocorrelation was also low for σ and ω, declining to zero at a lag of 5 iterations.

Whilst the FoI was estimated per data set to account for potential true differences between the FoI across husbandry systems, I assumed that the rate at which antibodies wane does not vary by location. As such, I estimated a global value for ω and σ across all the datasets.

Model selection

In order to evaluate which of the models was best supported by the data, their fit was compared using Deviance Information Criterion as described by [224]. DIC was the preferred method of comparison since analysis was conducted in a Bayesian framework, and since it penalises model complexity. LOO-CV (Leave One Out Cross Validation) and WAIC (Watanabe Akaike / Widely Applicable Information Criterion) were problematic for small data sets where leaving out a single dataset would mean study specific FoI could no longer be estimated.

Model validation

Simulations

Each of the four models was used to simulate 23 different age-stratified seroprevalence data sets with the same age class divisions as the real data, each containing 500 animals. Three different values were used for each global parameter, and three sets of study specific FoI values were drawn randomly from a uniform distribution roughly representing the range of values estimated for the real data. The models were then fitted to the sets simulated data for model validation.

Evaluating the influence of each dataset on the results

To check the influence of each real data set on the global parameters, each data set was removed in turn and the parameters were re-estimated.

Results

Model Validation

When the models were fit to simulated data, the true FoI values were recovered well by all models, as were the rates of waning of mAbs, ω, and Abs following infection, σ (***Appendix Chapter 3, A3.3, Figures A3.3.1-4***). The true overdispersion parameter, k, used in data simulation was recovered well when the true value was 1.0, but was often overestimated when the true value was 0.01 or 0.1 (***Figure A3.3.5***). This did not affect the models' ability to recover the epidemiological parameter values, however.

Model selection

When the fits of the four catalytic models were compared using Deviance Information Criterion (DIC), the age-stratified seroprevalence data best supported model 4 which incorporated both mAbs and antibody waning following infection (***Table 3.2***). This was robust to exclusion of each dataset from the analysis (see ***Appendix Chapter 3, A3.4, Figure A3.4.1)*** for a complete breakdown of parameter estimates when each study is excluded). The addition of either mAbs

or seroreversion alone improved the model fit considerably as compared to the simplest model. The addition of seroreversion provided the greatest improvement in fit, but this depended on the inclusion of the dataset collected in Egypt by Kandeil *et al.* (2019)[63]. When this dataset was excluded, and data was assumed to be binomially distributed, there was negligible difference in the improvement in fit provided by seroreversion and that afforded by including mAbs, and when data was assumed to be over dispersed, the inclusion of mAbs provided a greater improvement in model fit than the addition of seroreversion. The over dispersed models (denoted with suffix "b" in ***Table 3.2***) fit the data better compared to the binomial distribution across all four models.

Table 3.2. *Model selection using DIC*

		DIC	*Effective number of parameters*
Binomial	Model 1a: seroconversion	1384	17
	Model 2a: seroconversion + mAbs	848	18
	Model 3a: seroconversion + seroreversion	766	18
	Model 4a: seroconversion + mAbs + seroreversion	668	21
Over-dispersed	Model 1b: seroconversion	615	18
	Model 2b: seroconversion + mAbs	528	21
	Model 3b: seroconversion + seroreversion	513	22
	Model 4b: seroconversion + mAbs + seroreversion	496	21

Model selection was not affected by use of alternative test specific fixed values of sensitivity and specificity. Regardless of whether global test sensitivity was 99% and specificity 100%, or whether sensitivity of neutralisation tests and specificity of ELISAs were reduced to 85%, model 4b provided the best fit to the data. However, the reduction in DIC values between Model 3b and the best fitting Model 4b was smaller when sensitivity and specificity were lower – likely because reduced test sensitivity could explain more of the data so seroreversion wasn't as

necessary to improve fit. DIC values when alternative fixed test-specific sensitivity and specificity are available in ***Appendix Chapter 3, A3.5, Table A3.5***.

The seroprevalence predicted by model 4b fit the data well, overlapping with age-stratified seroprevalence data in most cases with a few exceptions (***Figure 3.2A***). The very high levels of seroprevalence measured by Kandeil *et al.,* (2019) in young calves in Tunisia and KSA [63] were underestimated, and the model struggled to reproduce the data collected in one study in KSA where seroprevalence was very high in calves and dropped considerably in adults [192]. The predicted seroprevalence and FoI estimates from the models that fit less well are available in ***Appendix Chapter 3, A3.6, Figures A3.5.1-7***

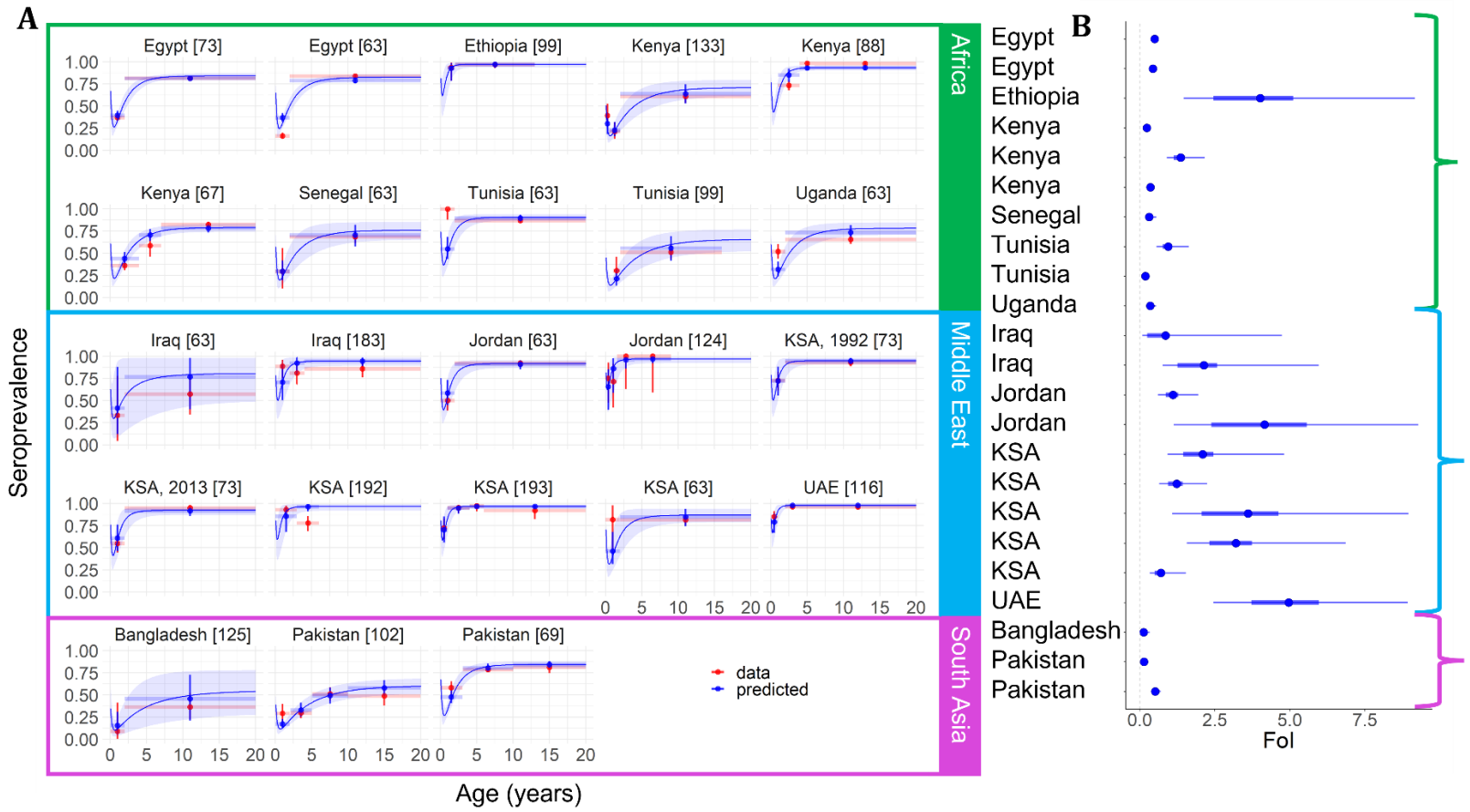


***Figure 3.2 Predicted seroprevalence and FoI estimates using Model 4b**: **A**. Predicted seroprevalence by age (blue) with vertical 95% credible intervals, fitted to age-stratified seroprevalence shown with vertical 95% confidence intervals (red). Horizontal bars show age class width **B.** Posterior estimates for the FoI for each study, where the point represents the mean, the thicker line represents the 25th-75th percentiles and the thinner line represents the range of samples falling between the 2.5th and 97.5th percentiles*

Rates of antibody waning

Maternally acquired antibodies (mAbs)

The best fitting model (4b) estimated that mAbs wane over the first 3-6 months of life. When all datasets were included, the average rate of waning of mAbs, ω, was 4.42 yr^{-1} corresponding to approximately 3 months (95% CrI 1.3-5.5 months) of protection. This parameter, however, was considerably affected by the exclusion of the dataset collected in Egypt by Kandeil *et al.,* [63] after which mAbs were estimated to last for 6 months. (***Table 3.3***). Estimates from the models that fit less well are presented in ***Appendix Chapter 3, A3.5, Table A3.5.1***.

Table 3.3. *Estimated parameter values from the best fitting models*

	Dataset	*Model 4b: All datasets mean (95% CrI)*	*Model 4b: Omitting Egypt mean (95% CrI)*
FoI, λ	***Africa***		
	Egypt [72]	0.49 (0.37, 0.65)	0.50 (0.37, 0.70)
	Egypt [63]	0.44 (0.34, 0.57)	NA
	Ethiopia [99]	4.08 (1.44, 9.13)	4.83 (1.78, 9.44)
	Kenya [133]	0.24 (0.14, 0.37)	0.22 (0.14, 0.36)
	Kenya [88]	1.36 (0.91, 2.17)	1.59 (1.03, 2.68)
	Kenya [67]	0.36 (0.26, 0.49)	0.37 (0.26, 0.55)
	Senegal [63]	0.32 (0.17, 0.56)	0.33 (0.18, 0.60)
	Tunisia [63]	0.95 (0.56, 1.64)	1.00 (0.59, 1.74)
	Tunisia [99]	0.19 (0.11, 0.31)	0.20 (0.11, 0.32)
	Uganda [63]	0.35 (0.22, 0.55)	0.34 (0.22, 0.55)
	Middle East		
	Iraq [63]	0.84 (0.10, 4.63)	0.67 (0.09, 3.35)
	Iraq [183]	2.17 (0.76, 6.20)	1.92 (0.76, 5.22)
	Jordan [63]	1.11 (0.61, 2.00)	1.11 (0.61, 1.98)
	Jordan [124]	4.18 (1.12, 9.29)	4.10 (1.05, 9.24)
	KSA, 1992-2010 [73]	2.09 (0.93, 4.70)	1.99 (0.91, 4.23)
	KSA, 2013 [73]	1.24 (0.64, 2.28)	1.18 (0.61, 2.13)
	KSA [192]	3.57 (1.13, 8.84)	3.17 (0.99, 8.36)
	KSA [193]	3.19 (1.59, 6.56)	3.25 (1.63, 6.56)
	KSA [63]	0.71 (0.33, 1.58)	0.73 (0.35, 1.54)
	UAE [116]	4.94 (2.43, 8.95)	4.50 (2.35, 8,36)
	Asia		
	Bangladesh [125]	0.13 (0.04, 0.34)	0.12 (0.04, 0.30)
	Pakistan [102]	0.14 (0.10, 0.20)	0.15 (0.11, 0.21)
	Pakistan [69]	0.52 (0.38, 0.71)	0.54 (0.39, 0.77)
	Global		
rate of waning of mAbs, ω	Across all datasets	4.42 (2.17, 8.96)	2.04 (1.24, 3.99)
rate of waning of Abs, ω σ	Across all datasets	0.09 (0.06, 0.13)	0.10 (0.06, 0.17)
overdispersion, k	Across all datasets	2.61 (2.03, 3.23)	2.04 (1.46,2.68)

Seroreversion following infection

The seroreversion rate following infection was estimated to be low at 0.09 yr^{-1} (95% CrI 0.06-0.13) in model 4b, corresponding to an average duration of seropositivity of 11 years (95% CrI 7.7 – 16.7 years). This estimate was relatively robust to exclusion of individual datasets (***Appendix Chapter 3, A3.4, Figure A3.4.5***), but decreased to 0.03 yr^{-1} (95% CrI 0.01-0.05) corresponding to an average duration of seropositivity of 33 years when the fixed sensitivity of neutralisation tests was reduced to 85%. When the lifespan of dromedaries is considered, this rate of seroreversion is negligible. The complete set of estimates using alternative fixed values of test sensitivity and specificity are available in ***Appendix Chapter 3, A3.4, Table A3.6.2***.

The Force of Infection, λ

Estimates for the FoI varied between countries and between different datasets within countries. The FoI estimates for each study population are shown in ***Figure 3.2B***, and in ***Table 3.3***. Annual FoI estimates are highest within the Middle East, especially in Jordan and the UAE, with variable estimates across datasets collected in the KSA. The FoI estimates are lower for datasets collected from South Asia and Africa except for the study of the population sampled in Ethiopia [99]. There was high variability between the Kenyan datasets, with the heterogeneity corresponding to the different regions sampled.

For some studies in which age-class specific seroprevalence is measured to be close to 100% the FoI is estimated to be very high (for example an annual FoI of 4.0 corresponds to a mean of 4 infections per animal per year). Once FoI passes the threshold at which it predicts maximum seroprevalence, further increases in FoI would all predict similar levels of seroprevalence of around the maximum and would therefore all fit the data similarly well. This is reflected in some of the posterior distributions for the FoI presented in ***Figure 3.3***. For example, the posterior distributions of the FoI in Ethiopia, (Reusken *et al.,* 2014), Jordan, (Van Doremalen *et al.,* 2017), KSA (Harrath *et al.,* 2018), and UAE (Wernery *et al.,* 2015) are fairly flat with long tails. The corresponding HMC traces for these estimates are shown in ***Figure 3.4***. When

alternative test specific sensitivity and specificity values were assumed, including lower sensitivity of neutralisation tests, some of these high FoI estimates became even greater. This is likely to be because the lower test sensitivity reduced the theoretical maximum seroprevalence.

When, rather than being assumed to be uniform, the age distribution of individuals in each sampled age class was assumed to reflect a constant mortality rate of μ_0 for calves <2 years old and μ for animals ≥2 years old, the FoI was estimated to be slightly higher in most populations (see ***Appendix 6.1***). The increase was very small and did not meaningfully affect the overall range of transmissibility. Transmissibility was still generally highest in the Middle East.

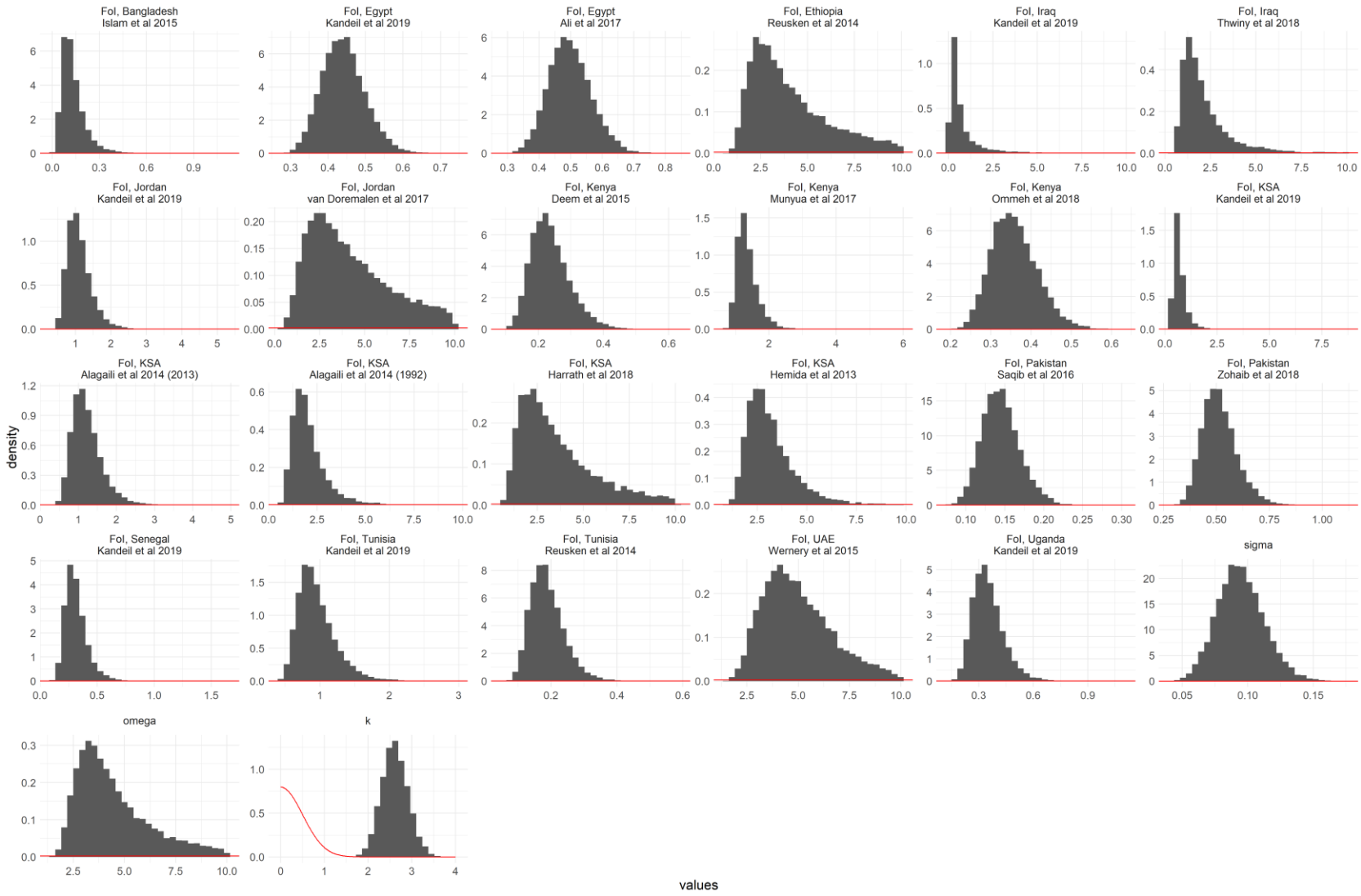


Figure 3.3 The posterior distributions of each of the parameters estimated in Model 4b, *assuming overdispersion (grey histograms), overlaid with the prior distributions (red). When the prior extended much wider than the posterior, only the range of the posterior is presented.*

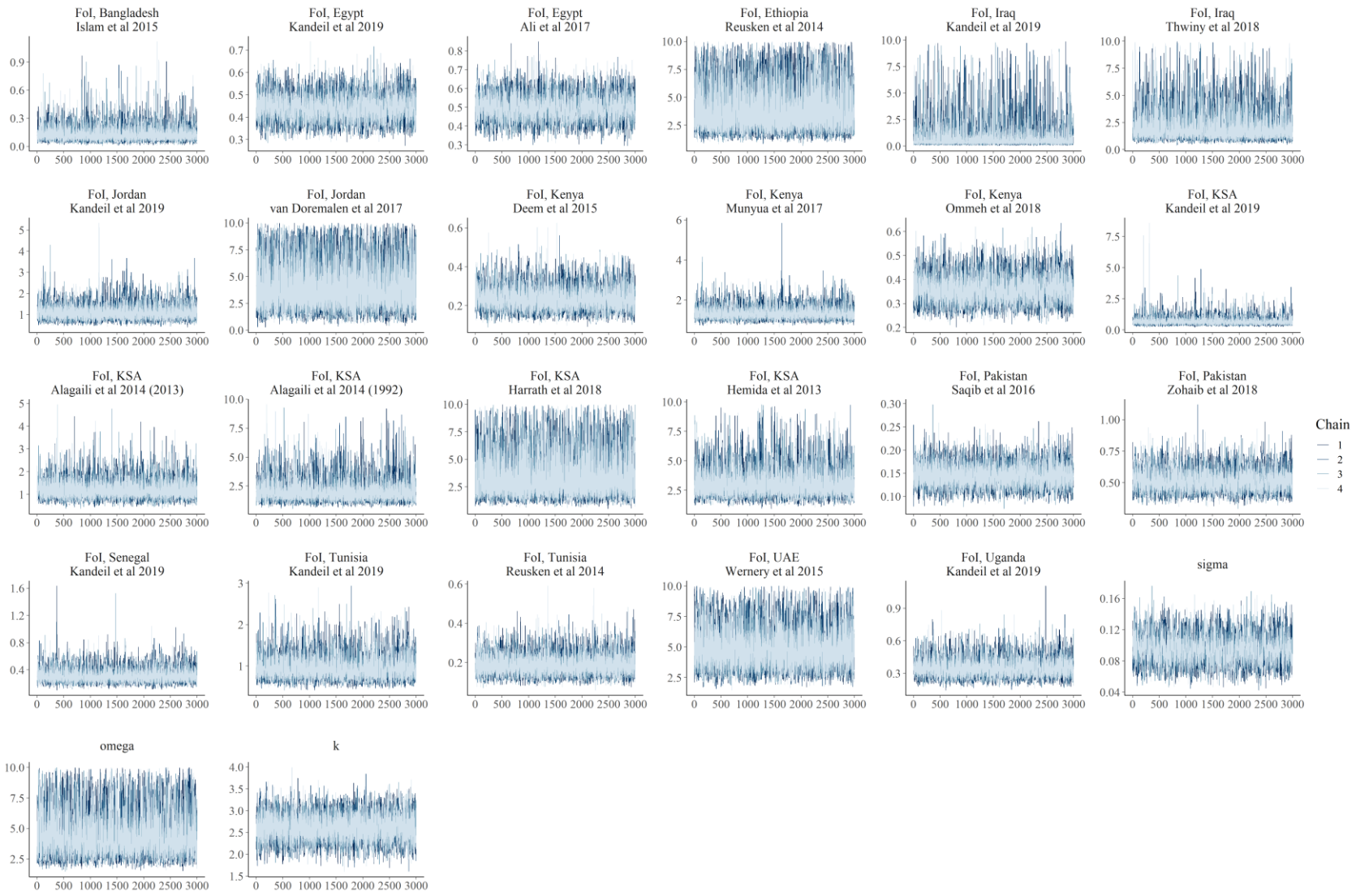


Figure 3.4. Hamiltonian Monte Carlo traces for each of the model parameters estimated for model 4b.

Overdispersion

When the prior on the overdispersion parameter, *k*, was a normal distribution with a mean of zero and a standard deviation of 0.5, restricted to positive values, *k* was estimated to be around 2.0-2.6 meaning the variance of the data was estimated to be around 3.0-3.6 times greater than what would be expected if the data were binomially distributed. This value for *k* is very high in the context of the prior (the prior density (red) is overlayed onto the posterior (black) in ***Figure 3.3***). When larger standard deviations were used in the prior, overdispersion was estimated to be extremely high. The high level of overdispersion could account for the patterns in the data and so the likelihood was very similar across different sets of epidemiological parameters making them unidentifiable. The prior with a standard deviation of 0.5 was used for all core results to constrain the overdispersion to values that I believed were more plausible.

Parameter correlation

The rate of seroreversion, σ, was strongly positively correlated with the FoI in the posterior samples (a correlation matrix is presented in ***Appendix Chapter 3, A3.7, Figure A3.7***). The study specific FoI estimates were also positively correlated with each other but only when seroreversion was included in the model. This suggests that the correlation between FoIs is due to their respective correlations with the rate of seroreversion rather than due to a causal relationship between them which would not be expected since they are fitted independently. The rate of waning of mAbs, ω, had a weaker positive correlation with other parameters.

Discussion

The Force of Infection of MERS-CoV in dromedary populations

Results across all models suggest that the annual FoI of MERS-CoV is generally higher in dromedary populations in the Middle East (between 1-4 for most study populations) compared to those sampled in South Asia and Africa (mostly <1). The notable exception is the high annual FoI of ~4 estimated within the dromedary population sampled in Ethiopia. Two of the main

factors affecting the FoI of a disease are: a) intrinsic properties of the pathogen and; b) contact patterns between susceptible and infectious individuals. Both of these could have contributed to the difference in FoI estimates between the regions in this analysis. All viruses sampled from dromedaries in western, northern and eastern Africa can be grouped together by their genetic similarities into Clade C. Strikingly, despite the large number of live dromedaries imported from Africa, all viruses isolated from dromedaries and humans in the Arabian Peninsula have belonged to genetically distinct clade A and B viruses. A study at an abattoir in KSA found that both local and newly imported dromedaries from Sudan and Somalia were infected with clade B viruses suggesting imported animals were infected in KSA [108]. The absence of clade C in the Arabian Peninsula – even in newly imported animals – coupled with results from a recent study that found clade C to have a reproductive disadvantage compared with clade A and B in human lung tissue [109], suggests that the clade C viruses prevalent in Africa may be less transmissible. The lower FoI estimates for Africa found here would be expected if the reduced ability of clade C viruses to infect human *ex vivo* lung tissue extends to reduced infectiousness within populations of live animals. It is not clear what clade circulates in South Asia, so it is not known if intrinsic viral differences could explain the FoI estimates for Bangladesh and Pakistan.

The variation in global camel husbandry practices could also potentially explain differences in FoI. In the Arabian Peninsula, dromedary farming has become increasingly intensive and urban in the past 60 years, whilst remaining largely extensive pastoralist techniques elsewhere [60]. These differences may impact the type and frequency of contact between animals which could impact the FoI. Studies have found prevalence of MERS-CoV infection to be higher at sites where different populations mix [63], [98], [134], [164]. The characteristics of the population sampled in Ethiopia were not stated, however, if animals were sampled at markets this could potentially explain the higher FoI estimates estimated compared to other locations across Africa. It could be that both intrinsic viral properties and contact patterns are contributing to the difference in FoI observed in the Middle East compared to Africa and South Asia.

Differences in the transmissibility of MERS-CoV would have implications for control in the different regions. If clade-specific intrinsic viral properties are contributing it will be important to find out and avoid seeding clade B into African dromedary populations. If it were possible to collect clade type and seroprevalence data and estimate the Force of Infection of MERS-CoV in the dromedary populations of Somalia and Sudan – the major exporters of live dromedaries to the Arabian Peninsula – this could provide greater insight into intercontinental transmission dynamics. I did not find any measures of age-stratified seroprevalence data from Somalia or Sudan, however. Although genetically distinct, viruses from different clades and sub-clades have been found to be antigenically similar and therefore there is unlikely to be a need for clade specific considerations during vaccine design [68].

As well as varying between countries, estimates of the Force of Infection varied within countries. For example, in Kenya, FoI was higher for Munyua *et al.*'s 2017 survey of Marsabit county compared to in Deem et al.'s 2015 data from Laikipia county and Ommeh *et al*.'s 2018 countrywide survey [67], [88], [133]. The disaggregated seroprevalence per county for the countrywide survey, Laikipia county was measured to have very low seroprevalence consistent with Deem et al.'s results, and Marsabit county had the highest seroprevalence of any county consistent with Munyua et al.'s findings. This consistency suggests the variability in FoI for Kenya may reflect true regional differences perhaps associated with population contact patterns. Of note, the FoI estimates for Kenya are within the range of the FoI estimated for populations in Kenya by Gardner et al [126]. The estimates of FoI also varied a lot across KSA. The regions surveyed are not comparable between most datasets.

Further investigation of what is driving perceived differences between transmission intensities will be important for devising context-specific vaccination or other control strategies. The dromedary population is highly heterogeneous in terms of husbandry practice even at the local scale [98], [114]. Prevalence has also been found to differ with herd size, life-style and camel function [98]. Differences in these factors by region could be creating true regional variability in

transmission intensity. Estimating the FoI for populations with differing herd characteristics could help elucidate how differences in husbandry practices affect transmission and therefore the potential impact of vaccination.

Several limitations could have also contributed to some of the differences in estimates of FoI. Firstly, the studies used different tests to determine seropositivity, including ELISAs, Protein Microarrays and two types of neutralisation tests. It is probable that there are some differences in sensitivity and specificity across these tests. Whilst neutralisation tests are known to be highly specific, ELISAs are potentially more sensitive as they also detect non-neutralising MERS-CoV specific antibodies. Since the FoI is calculated using relative differences in seroprevalence within a single study where a single test type was used, these estimates should not be greatly affected except when seroprevalence is very high (as it may approach the limit of sensitivity). To test the influence of differences in test sensitivity and specificity across test types, models 1b-4b were re-fit to the data whilst assuming reduced specificity of ELISAs and reduced sensitivity of neutralisation tests. The general pattern remained with FoI estimated being generally higher in the Middle East and lower in Africa and South Asia. Several FoI estimates for studies with very high seroprevalences increased when these alternative fixed values for test specific sensitivity and specificity were used. This is likely to be because with lower sensitivity of neutralisation tests, the maximum seroprevalence is lower and so is reached or indeed exceeded by some studies. In these cases, once the FoI reaches the minimum rate required to predict maximum seroprevalence, further increases in the FoI will no longer change the predicted seroprevalence making the likelihood fairly flat and the mean FoI higher. This saturation of the maximum seroprevalence may even be affecting some of the FoI estimates in the core analysis where sensitivity is high since seroprevalence reaches 100% in some studies. The wide credible intervals and relatively long tails seen in posterior FoI estimates in ***Figure 3.3*** may be signatures of this effect. The possible overestimation of FoI when seroprevalence is maximal is a limitation of this analysis. Finally, it is possible that if the intrinsic assumption of endemic equilibrium and a constant FoI over time is invalid for some datasets, this could affect

the estimation of FoI. If transmission was changing over time, for example if infections were seasonal, and a population had just experienced a large outbreak, the seroprevalence would likely be higher than on average in that population and could lead to overestimation of the mean FoI. In addition to infection changing over time, dromedary herd composition is likely to be dynamic which could also affect FoI estimates. For example, if young animals are bought into the herd at a common age, from a population with higher seroprevalence this could give a false impression of a higher FoI within the studied herd.

The dromedary populations reflected in the FoI estimates are based on age stratified seroprevalence surveys and are likely to be affected by several biases including potential publication bias towards extreme seroprevalence measures, and bias towards countries with sufficient resources to detect human cases and to study MERS-CoV in their dromedary populations. This means that not all relevant dromedary populations are represented in the FoI estimates. For example, it was not possible to estimate the FoI of MERS-CoV in Somalia and Sudan – the most camel dense areas in the world – due to a lack of age stratified seroprevalence data for these populations. Further studies of the seroprevalence patterns within these populations will be important for better understanding transmission dynamics in these major dromedary producing countries.

Seroreversion and test sensitivity

Despite the importance of seroreversion for improving model fit according to DIC, the estimated rate of seroreversion was low, and heavily dependent on the assumed sensitivity of the seropositivity tests used. The duration of antibodies was 11 years when test sensitivity was high across all tests, but this increased to 33 years when sensitivity of neutralisation tests and specificity of ELISAs were reduced. 33 years is longer than the mean life expectancy of dromedaries in the model and so is essentially a negligible rate of seroreversion suggesting life-long protection. The relative contributions made by test sensitivity and seroreversion cannot be

fully disentangled, but even when test sensitivity was assumed to be very high, the rate of seroreversion was relatively low.

Given the low estimated rate of seroreversion, I wanted to see if the improved fit afforded by the inclusion of seroreversion could be attained by fitting a global test sensitivity instead, as reduced test sensitivity could produce a similar signal to seroreversion in the data. When I inferred test sensitivity rather than including seroreversion, test sensitivity was estimated to be 92% and this model fit the data slightly better than model 4b according to DIC, but the estimates for FoI were implausibly high for studies with seroprevalence >92%, with many only constrained by the upper limit on the uniform distribution set by my prior belief that an annual FoI >10 would be implausible. Again, the issue of maximal seroprevalence being measured by studies is potentially made worse by reduced test sensitivity in the face of high specificity. Since lower test sensitivity and higher FoI could produce similar predicted seroprevalence measures to lower FoI and higher test sensitivity, there is also likely to be an identifiability issue when trying to estimate test sensitivity and FoI simultaneously.

Another factor to consider when interpreting the role of seroreversion in dynamics from these results is that the improved fit afforded by the inclusion of seroreversion could be partially because the implicit assumptions of catalytic models, namely that transmission is at endemic equilibrium and the FoI is constant over time, might not be being met in all locations. An albeit low rate of seroreversion gives the model greater flexibility to fit datasets in which there were small decreases in seroprevalence with age, or unexpectedly small increases between some age classes. The occasional decrease with age could in fact be due to fluctuations in the force of infection over time as a result of other factors underpinning the dynamics of transmission such as depletion of susceptible individuals.

Finally, the approach I have used did not allow for the distinction between constant boosting of antibody levels by repeated infection, and long-lasting antibodies following a single infection. In addition, longitudinal studies have observed several instances of infection of adult animals that

were seropositive, suggesting seropositivity may not be a good proxy for protection and so inferences about the duration of antibodies cannot be translated into inference about protective immunity [72], [131], [208].

Maternally-acquired antibodies (mAbs)

The results presented in this chapter support the existence of protective mAbs against MERS-CoV. The best fitting model estimated the average duration of seropositivity from mAbs to be approximately three months, but this depended on the inclusion of the dataset collected by Kandeil et al dataset in Egypt [63], without which it increased to six months. These estimates are comparable to the five months suggested by calf-dam pair studies in UAE [116], [131]. The duration of maternally-acquired protection could be very important for optimising the timing of potential calf vaccination, for example, if mAbs interfered with vaccine immunogenicity, administration would ideally need to occur after mAbs wane below protective levels. However, the ChAdOx1 MERS vaccine candidate for use in dromedaries does not express the MERS-CoV spike protein on its surface and so is thought to be unaffected by circulating antibodies [6].

The ability to estimate the rate of waning of mAbs was limited by the number of datasets which stratified young calves by age. Only two of the included studies – conducted in Jordan [124] and Kenya [133] – divided the first year of life into finer age classes. Accurate reporting of the age of calves, and the inclusion of very young animals, will be needed in future cross-sectional studies to better estimate the rate of waning of mAbs.

I chose to fit the rate of mAbs waning as a global parameter, assuming that if mAbs contributed to the dynamics of MERS-CoV transmission in dromedaries, they would do so in every location. To my knowledge, there is no existing literature on factors affecting the rate of waning of mAbs in calves, although it is conceivable that variables such as mother and calf health or incidence of cross-reactive infections could lead to some variation in the effective rate of mAbs waning by location which could be a limitation of my approach and would mean that 3-6 months might not be representative of the rate of waning in every location.

Overdispersion

Across all models, assuming the seroprevalence data was over-dispersed provided a better fit than assuming it was binomially distributed. The estimated overdispersion parameter, *k*, decreased with model complexity, which is to be expected, as more of the heterogeneity in the seroprevalence data can be accounted for by complex models. It should be noted that during model fitting, the estimate of *k* was not robust to the choice of prior, with more relaxed priors leading to extremely high estimates of the overdispersion, and difficulties estimating the epidemiological parameters. During model validation, values for *k* were overestimated, but epidemiological parameter recovery was not adversely affected.

Conclusions

The FoI of MERS-CoV was higher in the Middle East than in Africa and South Asia. Estimates were found to vary between and within countries. This variation may be explained by a combination of differences in husbandry practices underpinning dromedary contact patterns, and intrinsic virological differences between clades. Further investigation into what factors underpin this heterogeneity in FoI will be important for devising vaccination strategies to target the widely connected and diverse dromedary population.

Age-stratified seroprevalence data supports the existence of protective mAbs in dromedaries. When fitted across the 23 datasets at my disposal, this protection is estimated to last for the first 3-6 months of life. More seroprevalence data broken down over the first year of life would likely improve the reliability of this estimate.

Chapter 4:

A dynamic model of MERS-CoV transmission in dromedary camels

Introduction

This chapter focuses on the development of a dynamic model of MERS-CoV transmission in dromedary camel populations. In ***Chapter 3***, catalytic models of infection were fitted to age-stratified seroprevalence data. This approach provided estimates of the population-specific FoI and the rate of waning of MERS-CoV specific maternally acquired antibodies (mAbs) in dromedaries. However, since catalytic models assume a constant FoI, they cannot easily be used to explore the dynamics of disease transmission over time, or to simulate change-inducing interventions. Dynamic models, on the other hand, are defined by their explicit inclusion of the mechanistic transmission process in which the FoI experienced by susceptible individuals depends on the time-varying number or proportion of infectious individuals in the population, making them well-suited to both purposes. If we are to model the likely impact of vaccinating dromedaries against MERS-CoV, a dynamic model of transmission is needed.

Despite their potential usefulness, and the growing amount of data describing MERS-CoV in dromedary populations, there is a lack of dynamic models of MERS-CoV transmission in the zoonotic reservoir. Although three deterministic models have been published, one was intended as a theoretical exercise focused on expressing R_0 [156], and the other two have faced challenges parameterising transmission within and from the zoonotic reservoir using weekly reported human MERS case data [127], [128]. No stochastic models are available, and the published data on seroprevalence in dromedaries has not previously been utilised in model development.

In this chapter, I present a stochastic, age-structured dynamic model of MERS-CoV transmission in dromedary camel populations. The risk that a susceptible camel becomes infected is parameterised using the FoI estimates inferred from age-stratified seroprevalence data in ***Chapter 3***. Published viral load data from longitudinal field studies are used to estimate the infectious period and the relative infectiousness of primary infections and reinfections [6], and the level of protection offered by past infection is explored through several alternative

scenarios. The dynamic transmission model is then used to investigate three key knowledge gaps in MERS-CoV transmission in the zoonotic reservoir.

Firstly, the dynamic model is used to estimate R_0 for MERS-CoV in dromedary populations. Measures of transmission intensity are important for intervention planning. By calibrating the dynamic model to the FoI estimates from ***Chapter 3***, I estimate the corresponding R_0 values, which are often a more intuitive measure of transmission intensity than the FoI. There are two existing estimates of R_0. Lin *et al.* (2018) estimated R_0 to be approaching 4 in dromedary camels in KSA, however this is based on fitting a model of MERS-CoV transmission in dromedaries to weekly human cases whilst assuming a fixed proportion of weekly cases are due to zoonotic transmission [128]. Rui *et al.* (2022) estimated an R_0 of 1.04 in dromedaries in KSA using a next generation matrix approach, but it is unclear how data collected from dromedaries were used [127]. The discussion cites the study by Khalafalla *et al.,* (2015) which sampled animals at two sites at eight time points between 2013-14 [194], as a source of data but there is no indication of whether this was directly used to estimate R_0 and if so under what assumptions. It will be important for intervention planning to see how R_0 estimates vary between study populations and geographically, given the patterns observed in FoI estimates in ***Chapter 3***.

The stochastic nature of the dynamic model allows the estimation of a second useful quantity - the critical community size (CCS) of MERS-CoV in dromedaries. The CCS is the closed population size in which transmission is as likely to go extinct as it is to persist [225]. In a population smaller than the CCS, stochastic fluctuations are likely to lead to epidemic fadeout – the extinction of infections when numbers are low following a peak. First conceptualised in the mid-20th century in the context of measles, the CCS has since proven very extremely useful in determining the vaccination coverage needed to interrupt transmission of infectious diseases and in deducing the level of intervention and intervention efficacy needed to control transmission [226]–[228]. Applied to MERS-CoV in camels, the CCS has implications for the feasibility of controlling the disease in the animal population using vaccination. For example, if

the CCS is relatively small, high levels of vaccine coverage would be needed to interrupt transmission in a population. The CCS can be measured empirically, [225], but this has not been possible for MERS-CoV in dromedaries as it requires measuring epidemic fadeout which relies very strong surveillance data – which would be very challenging to collect for an asymptomatic animal disease. Inference from age-stratified seroprevalence data suggests that the FoI tends to be higher in dromedary populations sampled in the Middle East compared to most populations in Africa and South Asia (***Chapter 3***). The potential implications of these differences in transmissibility on the CCS are explored.

Thirdly, the dynamic model is used to investigate the expected time between peaks of transmission. Periodicity and its driving factors can give insight into potential seasonality and the times of year when spillover risk may be higher. Assessing the potential seasonality of MERS-CoV in dromedaries is a priority outlined by the FAO-OIE-WHO working group on MERS-CoV (2018) [5], and ultimately relies on resource intensive longitudinal studies of the prevalence of infection in dromedaries over many years. By simulating transmission using what we know about the FoI, and dromedary demography, however, dynamic models can be used to explore whether we should expect seasonality under different immunity scenarios and, if so, what periodicity we would see between peaks in infection in different populations.

Several gaps remain around understanding the level of protection from reinfection afforded dromedaries by past MERS-CoV infection. Modelling different potential scenarios and assessing the sensitivity of simulations to assumptions can indicate which knowledge gaps it is most important to address and provide an insight into the kind of data it is most important to collect to better inform decision-making.

Methods

Based on what we know about dromedary demography from the literature and the FoI estimates inferred in ***Chapter 3***, a stochastic, age-structured model of MERS-CoV transmission in dromedary camels was developed. Whilst the inference from age-stratified seroprevalence in ***Chapter 3*** suggested that antibodies are long-lasting following infection, documented reinfection of seropositive animals [6], [65], [129] indicates that MERS-CoV seropositivity is not a good proxy for protective immunity in dromedaries and so multiple, potential immunity scenarios have been included. The model was formulated in R [215], using the package odin [229] and stochastic iterations were run using odin.dust [230], [231].

The structure of the dynamic transmission model is represented schematically in ***Figure 4.1,*** with a single age class shown for clarity, and in deterministic form by the ordinary differential equations ***4.1-4.6***. All symbols used are defined in ***Table 4.1*** alongside the parameter values and their sources.

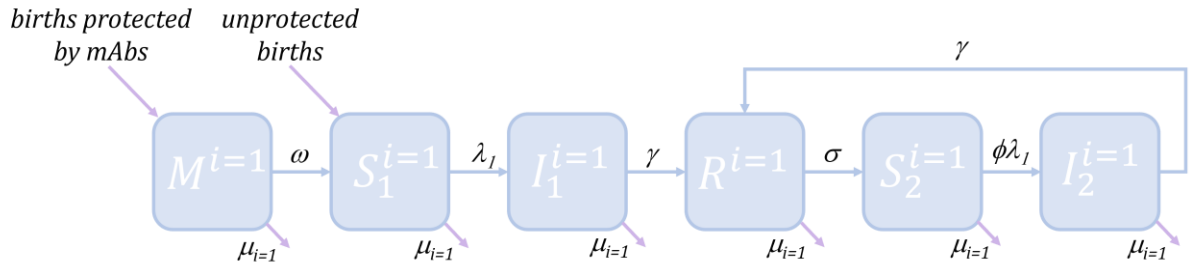


Figure 4.1. ***A dynamic model of MERS-CoV transmission in dromedary populations*** *shown for the youngest of i age classes (i = 1). This is repeated for each of the further 48 age classes. Calves are either born into state M with maternally acquired antibody protection, or into state S_1 in which they are entirely susceptible to infection. Entirely susceptible animals become infected at a rate λ_1 and infectious in state I_1, before recovering at a rate γ into state R in which they are temporarily completely immune to further infection. Complete immunity wanes at a rate σ with animals becoming partially susceptible again in S_2. Animals in S_2 become reinfected at a rate $\phi\lambda_1$ where $\phi<1$ reflecting the reduced susceptibility of previously infected animals compared to animals in S_1. Reinfected animals in state I_2 recover back into state R at rate γ.*

$$\frac{dM}{dt} = -(\mu + \omega)M + mAb\ protected\ births \quad 4.1$$

$$\frac{dS_1}{dt} = \omega M - \beta \frac{I_1 + rI_2}{N} S_1 - \mu S_1 + unprotected\ births \quad 4.2$$

$$\frac{dI_1}{dt} = \beta \frac{I_1 + rI_2}{N} S_1 - (\mu + \gamma) I_1 \quad 4.3$$

$$\frac{dR}{dt} = \gamma(I_1 + I_2) - (\mu + \sigma)R \quad 4.4$$

$$\frac{dS_2}{dt} = \sigma R - \phi\beta \frac{I_1 + rI_2}{N} S_2 - \mu S_2 \quad 4.5$$

$$\frac{dI_2}{dt} = \phi\beta \frac{I_1 + rI_2}{N} S_2 - (\mu + \gamma) I_2 \quad 4.6$$

Table 4.1. Model parameters

Symbol	*Description*	*Core value(s)*	*Source*
N_0	Initial population size	varied (50 – 10,000,000)	NA
α	Birth rate	Varied annually around a mean of 0.000565 camel^{-1} day^{-1} based on initial population size.	Fecundity data and herd composition data from [95], [114].
β	Effective contact rate	0.1-1.5 camel^{-1} day^{-1}	Calibrated using FoI estimates inferred in ***Chapter 3*** of this thesis
γ	Rate of recovery from infectiousness	1/14 days	[6], [8], [116], [129]
δ	Strength of seasonality of births ($0 \leq \delta \leq 1$)	1 (0, 0.5 also considered)	[114] see methods section "Modelling dromedary demography" for implementation
σ	Rate of waning complete immunity	1/30 days, 1/90 days (scenario with no complete immunity also considered)	NA
ω	Rate of waning of mAbs	1/3 months (1/6 months also considered)	***Chapter 3*** of this thesis
μ_1	Daily mortality rate of camels ≤2yrs	0.0011 camel^{-1} day^{-1}	Within the ranges described in [95] but exact value set to balance mean birth-rate

μ_2	Daily mortality rate of camels aged >2yrs	0.00036 camel^{-1} day^{-1}	Within the ranges described in [95] but exact value set to balance mean birth-rate
ϕ	Susceptibility to reinfection relative to first infection ($0<\phi<1$)	0.75 (0-1 considered)	NA
r	Infectiousness of reinfections relative to first infections ($0<r<1$)	0.01, 0.25, 0.5	[6]

Modelling infection and immunity

Infection

Camels are born either entirely susceptible to MERS-CoV infection (state S_1) or with complete protection by mAbs (state M) which wanes at a rate ω with calves becoming susceptible after an exponentially distributed period of time with a mean of 3 months (or 6 months as a sensitivity analysis), as estimated from age-stratified seroprevalence data in ***Chapter 3***. The proportion of calves born in state M is dictated by the proportion of animals of reproductive age (>4 years) which have been previously infected. Animals in S_1 become infected and transition to state I_1 in a frequency dependent manner – with the FoI, λ_1, defined as the product of the effective contact rate, β, and the proportion of individuals in the population which are infectious:

$$\lambda_1 = \beta \frac{I_1 + rI_2}{N} \tag{4.7}$$

Where I_2 is the number of reinfected individuals, $r<1$ and represents the relative infectiousness of reinfections compared to first infections, and β is varied to calibrate λ_1 to the FoI estimates in ***Chapter 3***. Modelling transmission as density dependent was deemed less appropriate as dynamics are compared across populations of extremely different sizes (varying from 50-10,000,000) and density dependent transmission would have implicitly assumed that each of these populations was inhabiting an area of the same size.

No data is available on the potential latent period following MERS-CoV infection in dromedaries. Infected animals are assumed to be instantaneously infectious. The period spent in state I_1 is exponentially distributed around a mean of 14 days in agreement with the duration of shedding reported in longitudinal studies [6], [116], [129].

Immunity and reinfection

Infectious individuals recover into state *R* in which they are not infectious and are completely immune to further infection. Longitudinal studies have observed rapid reinfection of dromedaries in environments where transmission intensity is likely to be high, such as markets and natural challenge studies [6], [65]. Therefore, following a short period in state *R* which is exponentially distributed around a mean of 1-90 days depending on the scenario, individuals become susceptible to reinfection in state S_2. Most animals found to be shedding MERS-CoV in field surveys are calves and naïve animals, suggesting there is some long-term protection offered by past infection [70], [73], [98], [124]. To reflect this, the degree of susceptibility in state S_2 is modelled to be less than that experienced by individuals in state S_1, meaning individuals in state S_2 experience a reduced FoI, λ_2. A scenario in which individuals in S_2 are just as susceptible to infection as a naïve animal is explored as a sensitivity analysis.

Parameterising the relative infectiousness of reinfected individuals

When animals in S_2 become reinfected they enter the I_2 state. The individuals in I_2 are modelled to be less infectious than individuals in I_1 experiencing their first infection. This is based on daily measures of viral load collected by Alharbi *et al.,* (2019) as part of a vaccination field study [6]. The viral load data were digitally extracted from Figure 4A in Alharbi *et al*'s paper using PlotDigitizer version 2.2 [232]. I extracted the daily mean viral load on a linear scale for seronegative calves (which I assumed to be infected for the first time during the study) and seropositive calves (which I assumed to be reinfected during the study) in the unvaccinated control group. I then calculated the difference between the area under the viral load curve for each of the two groups. Reinfected animals were approximately 1% as infectious as first-time

infected animals when assuming a linear relationship between viral load and infectiousness and 50% as infectious when assuming that infectiousness is proportional to the logarithm of the viral load. The relationship between infectiousness and MERS-CoV RNA shedding is not well defined. A trial of the MVA-based vaccine candidate in dromedaries measured a similar or slightly greater decreases in a measure of infectious viral particles compared to a measure of viral RNA shedding following vaccination of four calves [8], suggesting infectiousness may be closer to being proportional to viral load than the logarithm of viral load. However, the study was not designed to have the power to reliably define the relationship between shedding and infectiousness. Therefore, the two extremes of 1% and 50% – as well as a middle value where reinfected animals are 25% as infectious as first-time infected animals – were chosen to represent three, potential scenarios of infectiousness of reinfected individuals.

Implementing stochastic movement between disease states

The model is described as a set of ordinary differential equations ***4.1-4.6*** for simplicity but is implemented stochastically with a discrete time step of one day. To represent the transmission of MERS-CoV in camels more accurately – particularly in smaller populations where disease dynamics are more sensitive to stochasticity – the daily number of each type of transition or 'disease event' is treated as random variables following binomial distributions. Probabilities of an event v (denoted P_v) are defined from the rate of that event, t_v:

$$P_v = 1 - e^{-t_v} \qquad 4.8$$

For example, the number of individuals in state S_1 that become infected on a particular day is determined in the following two steps. Firstly, the total number of individuals leaving S_1 for all reasons (death or infection, in this case) is determined by randomly sampling from a binomial distribution where the mean joint probability of death or infection happening to any one individual is $1 - e^{-(\lambda_I + \mu)}$ and the number of 'draws' is the number of camels in S_1 at that time.

Then, out of the number of individuals determined to be leaving S_1, the number of individuals that became infected is determined by sampling from a second binomial distribution where the mean probability of infection is:

$$\frac{1 - e^{-\lambda 1}}{1 - e^{-(\lambda 1 + \mu)}} \qquad 4.9$$

and the number of draws is the number of individuals that are already known to be leaving S_1.

Modelling dromedary demography

Births

Dromedary calving is reported to be strongly seasonal [114], [117]–[121]. Studies in KSA report most calves being born between October and March, with one study quantifying this at 83% during the high season [114]. The calving season is very similar in Egypt where it is reported between October and April [121] and in Nigeria where surveyed pastoralists identified the calving peak to occur in the early dry season between October to December [119]. To capture this seasonality, the number of births per day is drawn from a Poisson distribution with a mean of αN_0 where α varies annually as a function of cosine (***Equations 4.10-11***, ***Figure 4.2***) and N_0 is the initial population size. Using N_0 rather than having a dynamic birth rate based on the time-varying number of individuals in the population gives the model more stability. The strength of seasonality can be weakened by setting $\delta < 1$ during sensitivity analyses. However, when $\delta = 1$, 82% of births fall between October and March which is in line with the 83% reported for dromedary births in Qassim, KSA [114]. The mean birth rate $\bar{\alpha}$ is set to be 5.65e-04 births per camel per day. This is based on estimates of 45.2% annual fecundity rates from surveys conducted across KSA [95] and taken together with assumptions that 90% of the population are female (based on high male calf removal rates [114]) and that 50% of the female population are of reproductive age [114].

$$births \sim Pois(\alpha(t)N_0) \quad 4.10$$

$$\alpha(t) = \bar{\alpha}\left\{1 + \delta \cos\left(\frac{2\pi t}{360}\right)\right\} \quad 4.11$$

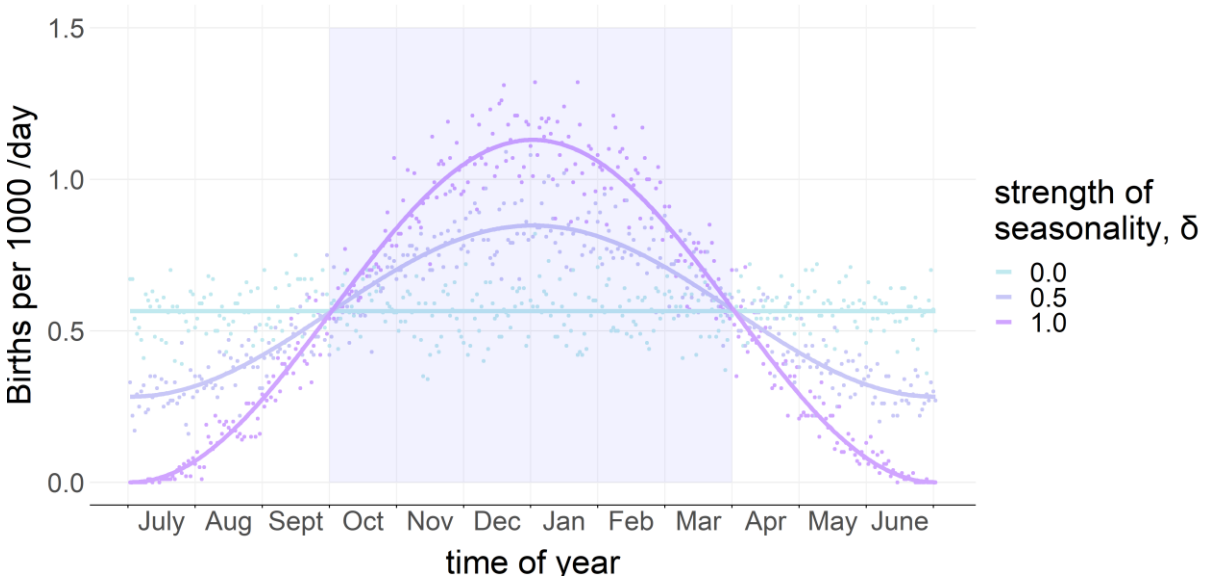


Figure 4.2. The seasonality of dromedary births throughout the year *when the strength of seasonality, δ, is varied from 1.0 (bright purple - full strength) to 0.0 (light blue - no seasonality). Points represent the stochastic number of births per day per thousand animals and lines represent the non-dynamic daily birth rate per thousand. The calving season commonly reported in the literature is shaded in grey.*

Mortality and removal

Since MERS-CoV causes very mild disease in dromedaries, infection is modelled to have no bearing on mortality. Dromedaries die off from each disease state compartment at the same age-dependent average rate μ_i, with the mean number of deaths per day being equal to the size of the compartment multiplied by $1 - e^{-\mu_i}$. The model assumes a higher probability of calf death in the first two years of life than in adulthood, as reported in KSA [95], [114]. The modelled mortality rates are calibrated to the birth rate to give a stable population size and are equivalent to ~40% mortality for <2yrs and ~13% for >2yrs. This is representative of overall mortality estimates for populations in KSA which are described in the literature as 10-26%, depending on herd type [95].

Age structure

Inclusion of age structure is vital given the strong dependence of infection status and seroprevalence on age, as well as for simulating age targeted interventions. For this reason, the model is stratified into month-wide classes, with camels moving to the next age-strata every 30 days in a 360-day year. From the 48th month wide class, camels enter a class aged >4 years where they remain until death. Having fine age classes up until the age of four years enables accurate representation of age within the window where first infections are happening and allows for accurate, age-targeted intervention modelling. Adult dromedaries over the age of four years are rarely stratified into further age groups in the MERS-CoV literature. Interventions are not likely to require fine age targeting within the adult population, making it reasonable to have a wide final compartment once dromedaries reach maturity.

Model initialisation

The model is initialised at demographic equilibrium – with the population distributed across the age classes reflecting the expected age distribution once the model stabilises. The expected proportion of the population in each age class at equilibrium is estimated using the seasonal birth rate, the age-dependent mortality rate, and the time spent in each age class. For the final, open-ended age class, the time spent in the compartment is estimated using the mortality rate. The initial number of animals in each age class is then sampled from a Poisson distribution where the mean count is the expected proportion of the population in the age class at equilibrium, multiplied by the overall target population size.

Infection is introduced through the addition of 25 infectious individuals on day one of the simulation, combined with a background FoI of 1.5e-05 (equivalent to an average of ~5 infections per thousand animals per year) for the first ten years of the model run. After the first ten years are up, background FoI is set to zero meaning all transmission occurs as a result of infections within a closed population. It is important to have no external sources of infection for

assessing endemic persistence but, as the model will not start at endemic equilibrium, having an initial background FoI helps to reduce the risk of early epidemic fade-out.

Estimation of R_0

R_0 is often a more intuitive parameter than the FoI when representing transmission intensity. In this chapter, the dynamic model is used to estimate an R_0 value for each of the studies for which FoI was inferred in ***Chapter 3***. The mean annual FoI in the dynamic model is calibrated by varying β. For each immunity scenario, the model was run over many beta values. Linear interpolation was then used to pick out the beta value needed to produce the FoI inferred for each study in ***Chapter 3***. Once the beta values were calibrated, R_0 was approximated using ***Equation 4.12***. The one-to-one relationship between beta and FoI means that the credible intervals (CrIs) around the FoI can be used to take forward the uncertainty into the R_0 estimates.

$$R_0 \cong \frac{\beta}{\gamma} \qquad 4.12$$

As birth rate and removal rate are balanced, the population size is at equilibrium when infection is introduced, and demography does not need to be considered in R_0 approximation. Model complexities such as multiple infectious states can sometimes complicate estimation of R_0. There are two levels of infectiousness in the model (states I_1 and I_2). However, as I_2 pertains to reinfections, these differing levels of infectiousness can be ignored in the calculation of R_0. This is because R_0 relates to an entirely susceptible population in which, by definition, all infections will be first-time infections. Although there is no need to consider multiple infectious states in the calculation of R_0, assumptions about the infectiousness of reinfections will affect the estimates of R_0 made from simulations of endemic transmission. This necessitates the consideration of several immunity scenarios.

In addition to R_0, the effective reproduction number, R_e, is estimated. This is defined as the mean number of secondary cases expected from each primary case (not contingent on the entire

population being susceptible). R_e would be expected to oscillate around ~1 during endemic transmission. Ordinarily, in the absence of a second infectious class, R_e is simply the product of the basic reproduction number and the proportion of the population that are susceptible to infection. However, to estimate R_e, both the relative reduction in susceptibility of the S_2 class, ϕ, and the relative reduction in infectiousness of the I_2 class, r, must be considered. R_e is therefore the proportion of infections that are in state I_1, p_{I1}, multiplied by the average expected number of infections caused by individuals in I_1, R_{I1}, plus the proportion of infectious individuals in I_2 , p_{I2}, multiplied by the average expected number of infections caused by individuals in I_2, R_{I2}. As described formally in ***Equations 4.13-4.17*** below.

$$p_{I1} = \frac{S_1}{S_1 + \phi S_2} \quad 4.13$$

$$p_{I2} = \frac{\phi S_2}{S_1 + \phi S_2} \quad 4.14$$

$$R_{I1} = R_0 \frac{S_1 + \phi S_2}{N} \quad 4.15$$

$$R_{I2} = r R_0 \frac{S_1 + \phi S_2}{N} \quad 4.16$$

$$R_e = p_{I1} R_{I1} + p_{I2} R_{I2}$$
$$= R_0 \frac{S_1 + r\phi S_2}{N} \quad 4.17$$

Persistence

To evaluate the CCS of MERS-CoV in dromedary populations, I estimated the size of the population required for transmission to be sustained for 25 years in a closed population with no external sources of infection. The CCS was defined as the window of population sizes between which transmission began to be sustained in at least 50% of stochastic model runs.

For large populations, it becomes unrealistic to assume populations are well mixed. For example, in the population of ~10,000 dromedary camels in Laikipia county, Kenya [112], an individual camel is far more likely to have contact with individuals in its own herd or grazing area than with animals in other areas of the county. Population structure also has a bearing on

transmission dynamics, including persistence [150], [233]–[235]. The movements and interactions between herds of dromedaries are not well documented. In order to explore the effect population structure has on dynamics, I developed a rudimentary structured population model where sub-populations or patches are arranged over a grid (***Figure 4.3***). Individuals are most likely to be in contact with other individuals in the same patch, less likely to meet individuals in neighbouring patches, and do not meet individuals in distant patches.

A representation of the structured population model is shown in ***Figure 4.3.*** Patches experience different degrees of connection depending on whether they are in a corner, on edge or within the middle of the grid. In reality, herds will also have varying levels of connection to other herds or larger sub-populations. Until better data on population structure allows a more accurate representation of networks and movements of dromedaries within a region, the grid serves as a naïve representation of this reality.

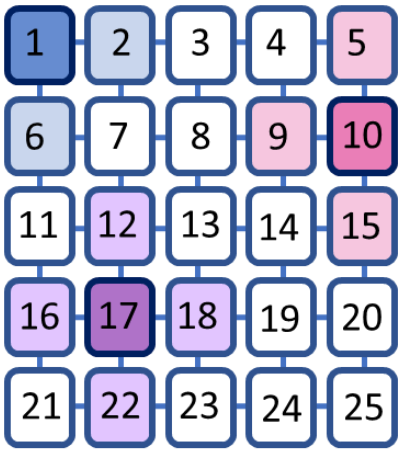


Figure 4.3. A structured population*. A grid of 5x5 patches is used to represent herds or larger sub-populations connected to their nearest neighbours. Individuals in herds in the corners such as in herd 1 (in dark blue) have contact with individuals in 2 neighbouring herds (light blue). Individuals in herds on grid edges such as herd 10 (dark pink) have contact with individuals in 3 neighbouring herds (light pink), and individuals in internal herds such as herd 17 (dark purple) have contact with individuals in 4 neighbouring herds (light purple).*

The connections between neighbouring patches are modelled as external contributions to the FoI experienced by susceptible individuals in each patch. For example, if for simplicity we ignore reinfections and assume a single infectious state I, then the FoI, λ^i, experienced by a completely susceptible individual in herd i in ***Figure 4.3*** is as follows:

For herd 1 – a corner connected to two neighbouring patches:

$$\lambda^1 = (1-2\upsilon)\frac{\beta I^1}{N^1} + \upsilon\left(\frac{\beta I^2}{N^2} + \frac{\beta I^6}{N^6}\right) \quad 4.18$$

For herd 10 – on an edge with three neighbouring patches:

$$\lambda^{10} = (1-3\upsilon)\frac{\beta I^{10}}{N^{10}} + \upsilon\left(\frac{\beta I^5}{N^5} + \frac{\beta I^9}{N^9} + \frac{\beta I^{15}}{N^{15}}\right) \quad 4.19$$

For herd 17 – within the middle of the grid with four neighbouring patches:

$$\lambda^{17} = (1-4\upsilon)\frac{\beta I^{17}}{N^{17}} + \upsilon\left(\frac{\beta I^{12}}{N^{12}} + \frac{\beta I^{16}}{N^{16}} + \frac{\beta I^{18}}{N^{18}} + \frac{\beta I^{22}}{N^{22}}\right) \quad 4.20$$

Where β is the effective contact rate, I^i is the number of infectious individuals in herd i, N^i is the total number of individuals in herd i, and υ represents the strength of connection between neighbouring herds. If υ = 0.01, this means that 1% of a dromedary's contacts are from each of their neighbouring herds and the remainder of their contacts are within their own herd. So, for example a total of 2% of the contacts of a dromedary in herd 1 are with dromedaries from neighbouring herds and 98% are with other dromedaries within herd 1.

Periodicity

To determine the average time between peaks in infections, the autocorrelation between each simulated time series of infections and lagged versions of itself was measured, using Pearson's correlation test, implemented through the acf function in the R "stats" package [215]. The lag that maximised the autocorrelation coefficient (ACF) was used as the estimate of the periodicity (excluding the very short lags <100 days and any ACF deemed to be below the significance level according to 95% confidence intervals). This analysis was conducted in the context of strongly

seasonal and moderately seasonal births for four different R_0 values representing the span of transmissibility inferred from the 23 studies of age-stratified seroprevalence. Three different immune scenarios were included where past infection reduces the infectiousness of reinfections to either 1%, 25% or 50% of the infectiousness of a first-time infection.

Results

Estimating R_0 for MERS-CoV in dromedary populations

The dynamic model was used to estimate the reproduction number R_0 associated with each of the study specific FoI estimates inferred using model 4b in ***Chapter 3***. Much like the FoI, the highest R_0 estimates were generally found in the Middle East, with lower R_0 values for dromedary populations in Africa and South Asia (***Table 4.2***). The R_0 estimates depended on model assumptions about the nature of immunity – in particular, the relative infectiousness of reinfected individuals. When relative infectiousness was assumed to be 1% in reinfected animals, central estimates of R_0 ranged from 5.3-25.8 in the Middle East, 2.3-21.9 in Africa (2.3-8.7 when the single study in Ethiopia is excluded) and 1.9-4.3 in South Asia. At the other extreme, when infectiousness was expected to be only halved in reinfections, R_0 ranged from 2.3-5.0 in the Middle East, 1.6-4.5 in Africa and 1.4-2.1 in South Asia. R_0 estimates for studies with very high FoI estimates were most sensitive to assumptions about immunity as, in these populations, a higher proportion of infections at endemic equilibrium are reinfections and are therefore affected by reduced susceptibility and infectiousness parameters.

Table 4.2 *R_0 estimates for each study population*

	Study	FoI (annual)	R_0 relative infectiousness of reinfections 1%	25%	50%
Africa	Egypt [63]	0.44 (0.34, 0.57)	3.8 (3.2, 4.6)	2.6 (2.4, 2.9)	2.0 (1.9, 2.2)
	Egypt [72]	0.49 (0.37, 0.65)	4.2 (3.4, 5.0)	2.8 (2.5, 3.1)	2.1 (1.9, 2.3)
	Ethiopia [99]	4.08 (1.44, 9.13)	21.9 (9.1, 44.9)	7.6 (4.4, 12.7)	4.5 (2.9, 7.3)
	Kenya [133]	0.24 (0.14, 0.37)	2.6 (2.0, 3.4)	2.0 (1.7, 2.5)	1.7 (1.5, 1.9)
	Kenya [88]	1.36 (0.91, 2.17)	8.7 (6.4, 12.8)	4.3 (3.6, 5.4)	2.8 (2.5, 3.4)
	Kenya [67]	0.36 (0.26, 0.49)	3.4 (2.7, 4.1)	2.4 (2.1, 2.8)	1.9 (1.7, 2.1)
	Senegal [63]	0.32 (0.17, 0.56)	3.1 (2.2, 4.5)	2.3 (1.8, 2.9)	1.8 (1.5, 2.2)
	Tunisia [63]	0.95 (0.56, 1.64)	6.6 (4.5, 10.1)	3.7 (2.9, 4.7)	2.5 (2.2, 3.0)
	Tunisia [99]	0.19 (0.11, 0.31)	2.3 (1.7, 3.1)	1.9 (1.5, 2.3)	1.6 (1.4, 1.8)
	Uganda [63]	0.35 (0.22, 0.55)	3.3 (2.5, 4.5)	2.4 (2.0, 2.9)	1.9 (1.7, 2.1)
Middle East	Iraq [63]	0.84 (0.10, 4.63)	6.0 (1.7, 24.4)	3.5 (1.5, 8.2)	2.4 (1.3, 4.8)
	Iraq [183]	2.17 (0.76, 6.20)	12.8 (5.6, 31.6)	5.4 (3.3, 9.8)	3.4 (2.3, 5.7)
	Jordan [63]	1.11 (0.61, 2.00)	7.4 (4.8, 11.8)	3.9 (3.0, 5.2)	2.6 (2.2, 3.2)
	Jordan [124]	4.18 (1.12, 9.29)	22.3 (7.5, 45.6)	7.7 (4.0, 12.9)	4.5 (2.7, 7.4)
	KSA [63]	0.71 (0.33, 1.58)	5.3 (3.2, 9.8)	3.2 (2.4, 4.6)	2.3 (1.9, 3.0)
	KSA 2013 [73]	1.24 (0.64, 2.28)	8.1 (4.9, 13.4)	4.1 (3.1, 5.5)	2.7 (2.2, 3.4)
	KSA 1992 [73]	2.09 (0.93, 4.70)	12.4 (6.5, 24.7)	5.3 (3.6, 8.2)	3.3 (2.5, 4.8)
	KSA [192]	3.57 (1.13, 8.84)	19.5 (7.5, 43.6)	7.0 (4.0, 12.5)	4.2 (2.7, 7.1)
	KSA [193]	3.19 (1.59, 6.56)	17.7 (9.9, 33.2)	6.6 (4.7, 10.2)	4.0 (3.0, 5.9)
	UAE [116]	4.94 (2.43, 8.95)	25.8 (14.2, 44.1)	8.5 (5.7, 12.6)	5.0 (3.5, 7.2)
South Asia	Bangladesh [125]	0.13 (0.04, 0.34)	1.9 (1.3, 3.2)	1.6 (1.2, 2.4)	1.4 (1.1, 1.9)
	Pakistan [102]	0.14 (0.10, 0.20)	2.0 (1.7, 2.3)	1.7 (1.5, 1.9)	1.5 (1.4, 1.6)
	Pakistan [69]	0.52 (0.38, 0.71)	4.3 (3.5, 5.3)	2.8 (2.5, 3.3)	2.1 (1.9, 2.3)

Varying the duration of complete immunity following infection from 30-90 days did not have a considerable effect on R_0 estimates. A full table of results across all scenarios is available in ***Appendix Chapter 4, A4.1, Table A4.1 (separate .xlsx file)***. Increasing the relative susceptibility of recovered individuals following the waning of complete immunity from 75% to 100% also had little effect on the R_0 estimates (***Table A4.1***). Decreasing the relative susceptibility to 25% led to an increase in R_0 when relative infectiousness of reinfections was >1% as the susceptible pool was more depleted. However, the reinfection seen in seropositive calves in the ChAdOx1 MERS vaccine study suggests relative susceptibility of previously infected individuals is greater than 25% [6]. The estimates shown in ***Table 4.2*** assume that individuals experience a mean of 90 days of complete immunity before having a relative susceptibility of 75% to further infection. Increasing the duration of mAbs from 3 months (presented in ***Table***

4.2) to 6 months led to a small increase in the estimates of R_0 across the studies, with the size of the increase roughly proportional to the size of the estimate (***Table A4.1***). For example, comparing the R_0 estimates when relative infectiousness was 1%, the central estimate for the population in Egypt sampled by Kandeil *et al*. (2019), increased from 3.8 to 4.1 when duration of mAbs was increased to 6 months, and the central estimate for Kenya (dataset: Munyua *et al*., 2017) went from 8.7 to 9.4. Larger increases were seen for higher R_0 estimates for example the estimate for KSA (dataset: Harrath *et al*., 2018) went from 19.5 to 21.1.

The effective reproduction number R_e was also estimated for endemic equilibrium in each population. At endemic equilibrium, the mean R_e is approximately one – as would be expected. A table of mean R_e values are available in ***Appendix Chapter 4, A4.2, Table A4.2***. Over time, R_e oscillates around one, with the amplitude of oscillations increasing with transmission intensity and decreasing with relative infectiousness of reinfections. When relative infectiousness of reinfections is low, births are the only source of highly infectious (first-time infected) animals so larger annual oscillations are seen. ***Figure 4.4*** provides an illustration of how R_e varies over time for different levels of relative infectiousness of reinfections and for different transmission settings using the following examples – low (Pakistan), moderate (Tunisia), high (Iraq) and very high R_0 values (Jordan).

When relative infectiousness of reinfections is only 1%, R_e oscillates between approximately 0.5-1.6 when calibrated to the high transmissibility estimated for populations sampled in Jordan, compared to 0.98-1.01 when calibrated to the low transmissibility estimated for populations sampled in Pakistan. The phase relationship of R_e with the calving season also changes with transmissibility. R_e lags the height of the calving season by a longer time period when transmissibility is lower as it takes longer for the wave of new, susceptible individuals to start to become infected and increases the proportion of infectious individuals that are highly infectious first-time infections (***Figure 4.4***).

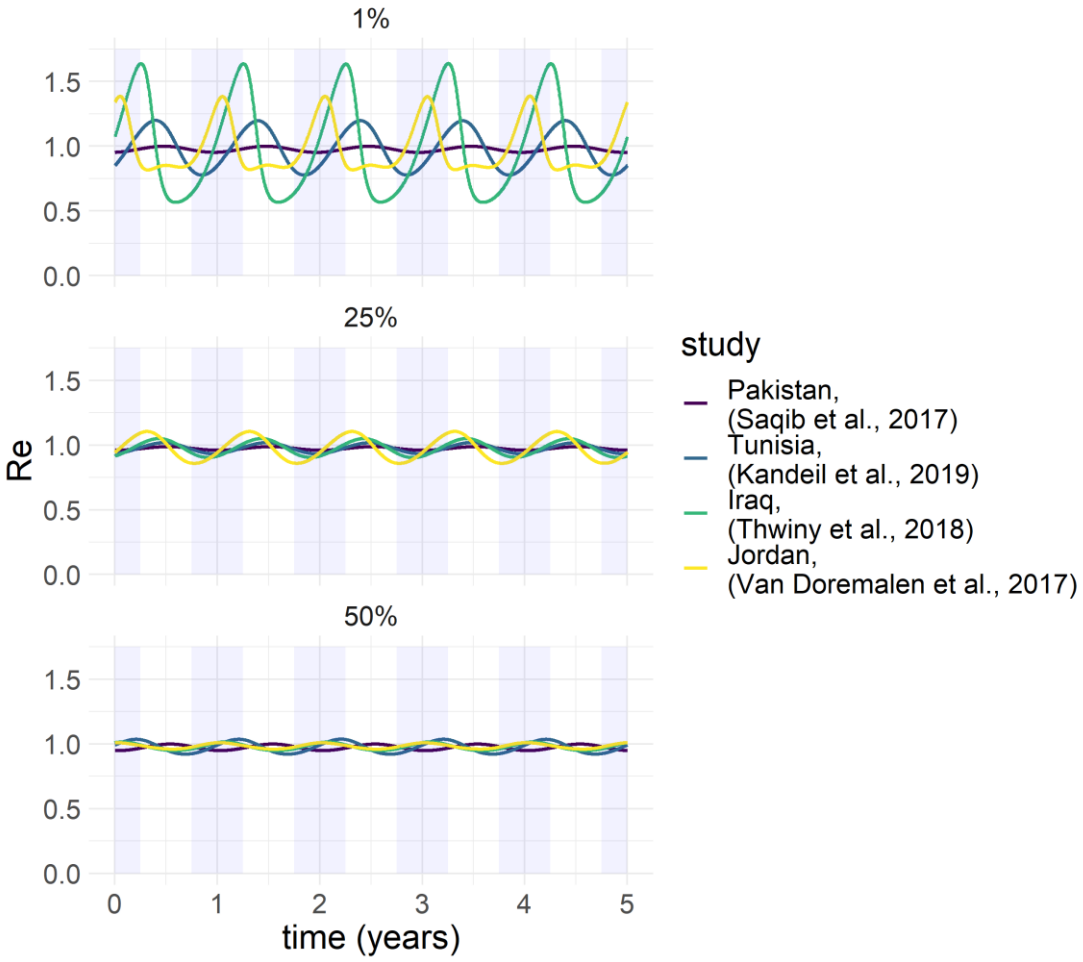


Figure 4.4. R_e oscillates over time with an annual periodicity*. The amplitude of oscillation increases as relative infectiousness of reinfections increases from 1% to 50% (panels from top to bottom). Light blue shading shows the modelled calving season.*

Persistence and Critical Community Size (CCS)

To estimate the CCS, I assessed the persistence of transmission in closed populations of different sizes 25 years after background FoI was switched off. The persistence analysis was repeated for four R_0 values, spanning the R_0 estimates corresponding to the 23 studies of age-stratified seroprevalence. This was done for two different strengths of seasonality of births and for each of the three different infectiousness scenarios (with reinfected individuals either 1%, 25% or 50% as infectious as first-time infected animals). The assumed infectiousness of reinfection alters the R_0 estimate corresponding to each inferred FoI. With this in mind, the low, moderate, high, and very high R_0 values are scenario specific to ensure they represent those

estimated for the study populations in each scenario. More details on the choice of representative R_0 values are available in ***Appendix Chapter A4, A4.3***.

Estimates of the CCS for MERS-CoV in dromedaries

When R_0 is relatively low, representing the transmissibility inferred for populations in South Asia and much of Africa, the CCS for MERS-CoV in dromedaries ranges from 10,000-75,000, depending on assumptions about immunity and population structure (***Table 4.3, Figure 4.5***). When R_0 is moderate, representing transmissibility inferred for multiple studies in the Middle East and two of the four studies in Kenya, the CCS is estimated to be in the range of 2,500-50,000. For high and very high R_0 values, representing the remainder of studies in the Middle East and the study in Ethiopia, the CCS is estimated to be 1,000-50,000, and 500-50,000 respectively.

Table 4.3*. The Critical Community Size (CCS) in different transmission settings, under different assumptions regarding infectiousness of reinfections, strength of seasonal forcing of births, and population structure. The interval represents the modelled population sizes between which transmission first persists >50% of the time.*

		Full strength seasonality of births (δ = 1)		Moderate strength seasonality of births (δ = 0.5)	
Infectiousness of reinfections	R_0	CCS homogeneous population	CCS structured population	CCS homogeneous population	CCS structured population
1%	3.50	25,000-50,000	50,000-75,000	25,000-50,000	50,000-75,000
	7.00	10,000-25,000	25,000-50,000	10,000-25,000	25,000-50,000
	14.00	50,000-75,000	25,000-50,000	10,000-25,000	10,000-25,000
	21.00	10,000-25,000	25,000-50,000	5,000-7,500	10,000-25,000
25%	2.50	10,000-25,000	25,000-50,000	10,000-25,000	25,000-50,000
	4.00	2,500-5,000	7,500-10,000	2,500-5,000	7,500-10,000
	5.50	1,000-2,500	2,500-5,000	1,000-2,500	2,500-5,000
	7.50	750-1,000	2,500-5,000	750-1,000	2,500-5,000
50%	1.75	10,000-25,000	25,000-50,000	10,000-25,000	25,000-50,000
	2.50	2,500-5,000	7,500-10,000	2,500-5,000	7,500-10,000
	3.50	1,000-2,500	2,500-5,000	1,000-2,500	2,500-5,000
	4.50	500-750	1,000-2,500	500-750	1,000-2,500

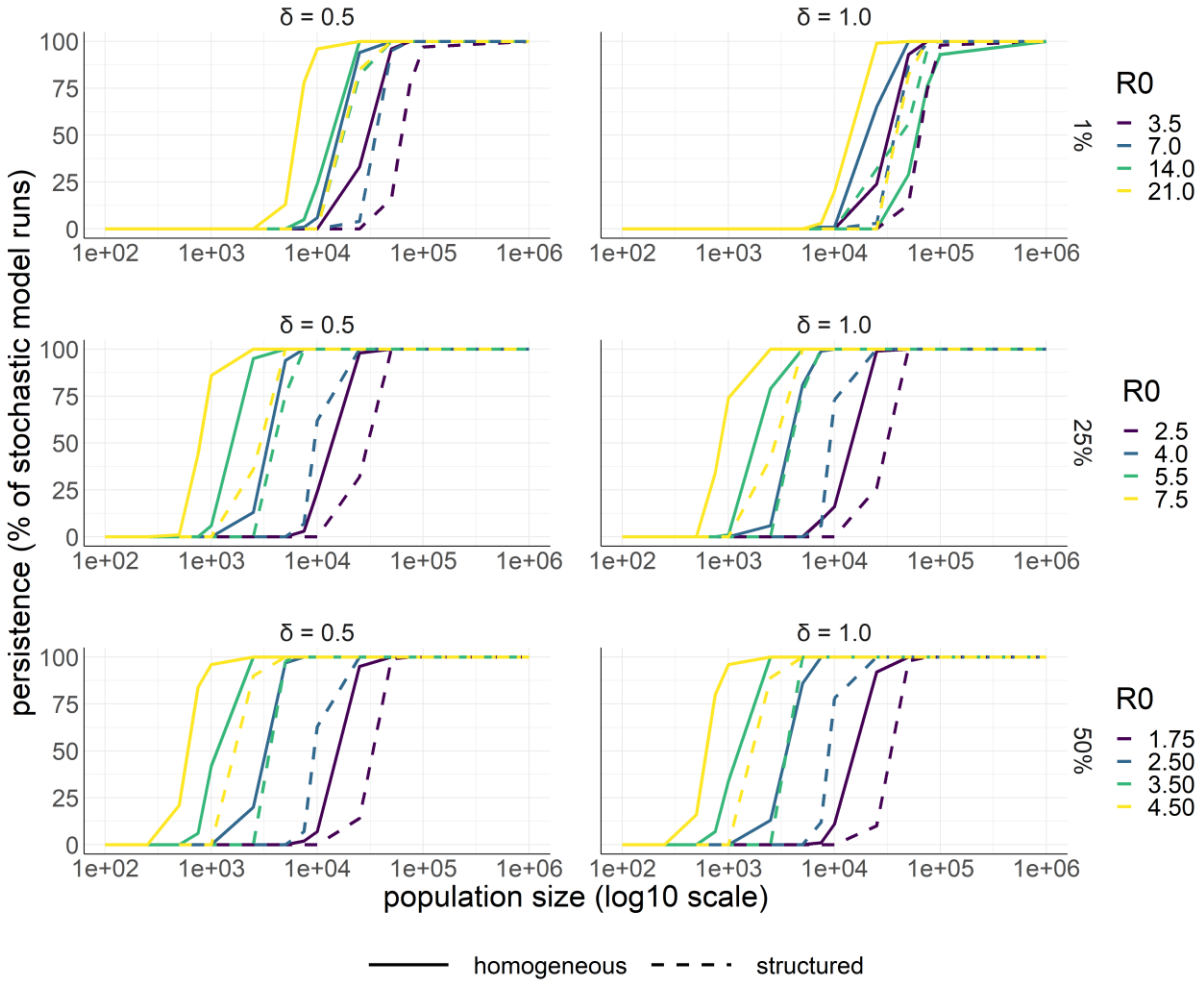


Figure 4.5 Persistence of transmission in populations of different sizes. *Persistence as the percentage of stochastic model runs where transmission is sustained for 25 years after background FoI is switched off, plotted against population size. Results for the homogeneous population are shown as solid lines. Results for the structured population with connectivity of 0.01 are dashed lines. Results are shown for weakened seasonal forcing of births (δ = 0.5 left panels) and full-strength seasonal forcing of births (δ = 1.0 right panels). Three different assumptions regarding the relative infectiousness of reinfections are displayed (from top to bottom).*

The effect of the transmission setting on the CCS

Across almost all scenarios, the CCS is smaller when R_0 is greater (***Table 4.3***, ***Figure 4.5***). The exception is the scenario in which seasonal forcing of births is at full strength, infectiousness of a reinfected individual is only 1% of the infectiousness of a first-time infection and the population is modelled as homogeneous. In this case, high transmissibility results in a larger CCS (between 50,000-75,000) than low or medium transmissibility (between 25,000-50,000 and 10,000-25,000, respectively). As with other scenarios, the CCS is still smallest when R_0 is

very high (***Table 4.3***, ***Figure 4.5***). This likely represents a complex interaction between seasonality, transmissibility, and accumulation of susceptible individuals.

The effect of the relative infectiousness of reinfections on the CCS

As the relative infectiousness of reinfections increases, the CCS decreases. For example, when births are highly seasonal and R_0 is very high, the CCS decreases from 10,000-25,000 when relative infectiousness is assumed to be 1%, to only 500-750 when relative infectiousness is assumed to be 50%. This is to be expected as first-time infections are less important for sustaining transmission as infectiousness of reinfections increases.

The effect of the strength of seasonal forcing of births on the CCS

The strength of seasonality of births does not affect the CCS estimates, except in one scenario – when the relative infectiousness of reinfections is low, and transmissibility is high. In this case, when seasonality of births is weaker (meaning births are less concentrated around one point of the year), transmission can be sustained in smaller populations. This exception is seen both when the population is assumed to be homogeneous and when structured into connected subpopulations.

The effect of population structure on the CCS

In general, the estimated CCS is larger when the population is assumed to be structured than when it is assumed to be homogeneous. The increase in CCS with population structure is summarised in ***Figure 4.6*** and ***Table 4.3***, and the persistence is presented in greater detail in ***Appendix Chapter 4, A4.4, Figure A4.4.*** The stronger the connection between the subpopulations, the smaller the CCS gets as it approaches the estimate for the homogeneous population. Again, there is an exception when births are strongly seasonal, relative infectiousness of reinfections is low at 1% and transmissibility is high (***Figure 4.6***, left panel). In this scenario, transmission can persist in smaller populations if they are structured with moderate connectivity, with larger homogeneous populations needed to see the same level of

persistence. The increased persistence in structured populations with moderate connectivity in this scenario is likely to be because of the so-called "rescue effect", whereby, when the epidemic fades out in a local sub-population, infection may be reseeded from neighbouring sub-populations with asynchronous epidemics, and take off again locally once enough time has passed for susceptible individuals to re-accumulate [236].

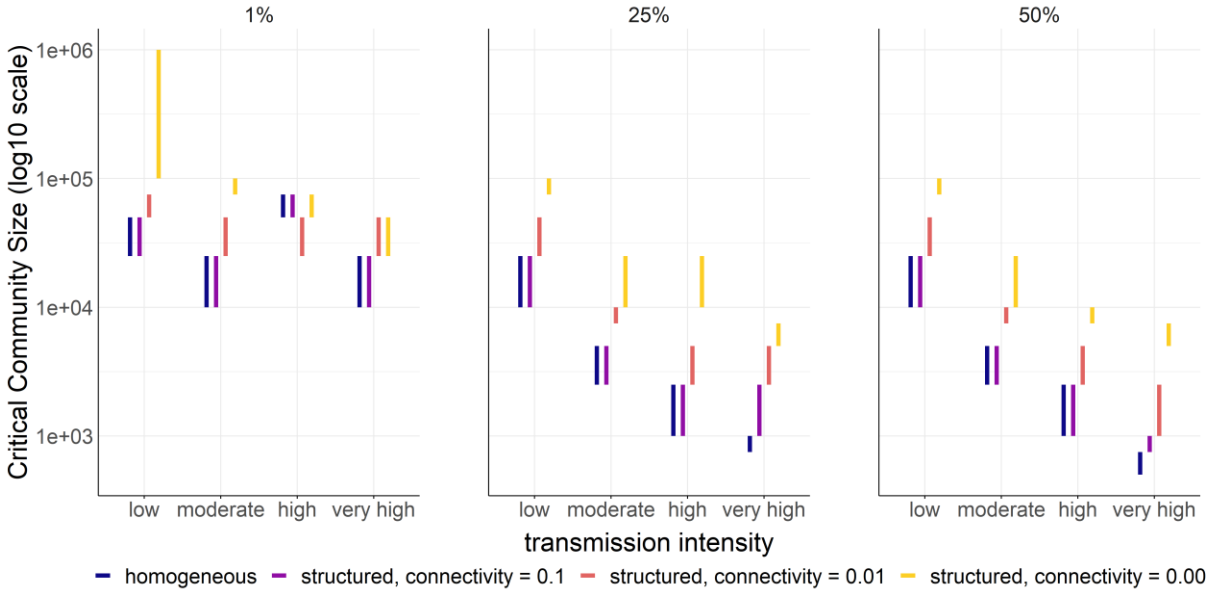


Figure 4.6 The Critical Community Size (CCS) in populations with differing levels of structure *(colours), in different transmission settings (x axis). Homogeneous population is assumed to be perfectly mixed whilst structured populations split the same number of animals into sub-populations connected to their nearest neighbours with a strength of 0.001-0.1.*

When the strength of connection between sub-populations is very weak the rescue effect is not seen in any scenario. This suggests a trade-off where separation into partially connected sub-populations can allow for re-seeding but very weak connections can increase the chance of fade-out at the population level as reseeding from neighbouring patches becomes very unlikely. When connectivity between neighbouring herds or sub-populations is 0.1, the estimated CCS is almost always the same as when homogeneous mixing is assumed (compare dark blue and purple CCS measures in ***Figure 4.6***).

Sensitivity to the cut-off used to define persistence

During this analysis, I noticed signs that the rate of epidemic fade-out was higher within the first few years after the background FoI was switched off compared to in the years that followed. To ensure that the CCS estimates were robust to my chosen measure of persistence, I compared CCS estimates using different temporal cut-offs for persistence. When the CCS was calculated based on transmission persisting five years after the background FoI was switched off, the CCS estimates were smaller than when a 15-year threshold was used in most scenarios. In contrast, there was commonly none or very little difference in the CCS calculated at 15 years versus at 25 years after external FoI was switched off. This suggests a lower rate of fade-outs over time (CCS estimates using different thresholds are plotted in ***Figure A.4.5*** in ***Appendix Chapter 4, A4.5***, for interest). Dynamics around the establishment of transmission, rather than around sustaining transmission, may be inflating the initial rate of fade-outs. To ascertain how much establishment dynamics in the first 5 years following external FoI switch-off contribute to CCS estimates, an alternative measure of CCS was calculated based on persistence for 25 years *given* that transmission was established. Establishment was defined as persisting for 5 years after the external FoI was switched off. The CCS estimates were robust to this change in calculation so, for the results presented in this Chapter, persistence was simply defined as sustained transmission for 25 consecutive years in a closed population.

Endemic periodicity

When births are seasonal, the number of infections over time has an annual periodicity in large populations, with peaks of a similar size occurring each year (***Figure 4.7.A***). In small populations, or when transmissibility is low, biennial, triennial, and quadrennial periodicities - with a larger annual peak in infections occurring every 2, 3, or 4 years respectively – are observed in a proportion of stochastic iterations. Examples of the autocorrelation coefficients for time series with supra-annual periodicities, and examples of the time series themselves are shown in ***Figure 4.7.B***. No seasonality in infections is observed when the birth rate is constant.

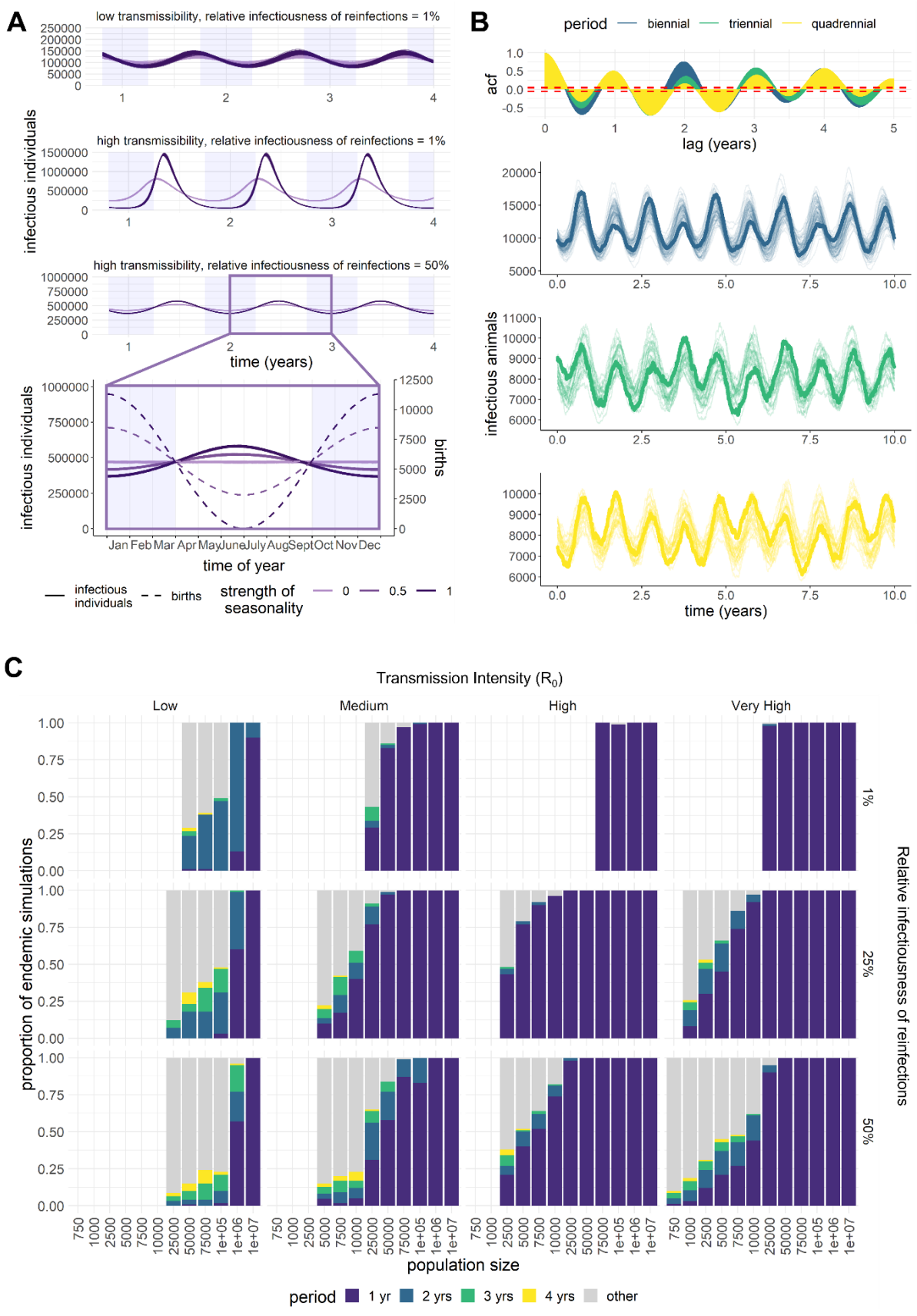


Figure 4.7. The periodicity of endemic transmission. A. *Examples of time series under three sets of conditions in which infections peak annually when births are strongly seasonal (dark purple)*

and moderately seasonal (lighter purple). A large population size was modelled for clarity. The peak of the calving season is shown by blue shading. ***B.*** *Example of the ACF for different lags of time series with biennial (blue), triennial (green) and quadrennial (yellow) periodicity in panel one. Examples of stochastic time series with biennial, triennial and quadrennial periodicity, with a single time series of each type highlighted in the remaining three panels.* ***C.*** *The proportion of stochastic simulations of persistent transmission in which periodicity was annual (purple), biennial (blue), triennial (green), quadrennial (yellow) and other (grey) for increasing population sizes along the x-axis. Each panel shows the results for a particular transmission intensity (columns) and for different assumed level of infectiousness of reinfected animals relative to first-time infections (rows).*

The relationship between peak in infections and peak in calving

The phase relationship between the annual peak of infections and the height of the calving season varies with transmission intensity and with relative infectiousness of reinfections. For example, considered in the context of the year (where calving season occurs between October and March) in a high transmission setting, infections peak between April and May if relative infectiousness of reinfections is 1% and between June and July if relative infectiousness is 50%. In a low transmission setting, infections do not peak until just before the next calving season begins. (***Figure 4.7A***).

The effect of transmissibility and the relative infectiousness of reinfections on the periodicity

Figure 4.7C shows how transmission intensity (panel columns) and relative infectiousness of reinfections (panel rows) affects the periodicity measured for 100 stochastic iterations for each population size when births are seasonal ($\delta = 1$). Annual periodicity (purple) dominates in most scenarios. This is also the case when $\delta = 0.5$ meaning seasonality of births is not as strong (***Appendix Chapter 4, A4.6, Figure A4.6***). Generally, as transmissibility increases from low to high, the proportion of stochastic iterations with annual periodicity increases, with very few supra-annual periodicities measured in high transmission settings, even in relatively small populations. Once transmission is very high there is a reversal in this trend, with supra-annual periodicities measured a slightly more often. Similarly, as relative infectiousness of reinfection increases from 1% to 25% transmission with an annual periodicity make up a higher proportion

of stochastic iterations, including in smaller population sizes. However, the CCS is larger when infectiousness is 1% meaning the periodicity of endemic transmission in smaller populations cannot be assessed. When the relative infectiousness is increased again from 25% to 50%, we see a smaller proportion of time series experiencing annual epidemics and a larger proportion with unstable or absent seasonality (***Figure 4.7.C***).

When the population is small, and either the transmissibility or relative infectiousness of reinfections is low, there is sometimes no clear periodicity to the timeseries (coloured grey and labelled "other" in ***Figure 4.7.C***). In these cases, the lag that gives the maximum ACF is either very variable with no similar periods across stochastic iterations, or is the shortest lag assessed (the time series tends towards the maximum correlation seen with its unlagged self), or the ACF is below the level of significance.

Discussion

Models of MERS-CoV transmission have previously focused on human-to-human transmission. However, as recurring dromedary-to-human transmission drives human cases there was a growing need for a model of transmission in the zoonotic reservoir. The dynamic model presented in this chapter brings together what is currently known about MERS-CoV transmission in the zoonotic reservoir, including: transmissibility estimates inferred from age-stratified seroprevalence data; viral shedding data from vaccine field trials; and dromedary demographic data from the wider literature. The resultant mathematical representation of MERS-CoV transmission in the dromedary populations permitted the estimation of R_0, the CCS, and the exploration of calving seasonality as a potential driver of seasonal infection.

The basic reproduction number, R_0

This chapter provides the first estimates of R_0 for MERS-CoV in dromedary populations outside of KSA. Estimates varied by population but overall suggest that – unlike in human populations

where on average R_0 <1 – MERS-CoV is very efficiently transmitted between dromedaries. This finding was to be expected given the young age of first infection observed [131], [197] and the high levels of MERS-CoV seroprevalence in adult dromedaries [70]–[74]. Much like the FoI, R_0 estimates tended to be highest for populations sampled in the Middle East but were still relatively high outside of the region.

The R_0 estimates were very sensitive to model assumptions pertaining to relative infectiousness of reinfections, ranging from 2-5 across studies when relative infectiousness was 50% based on infectiousness proportional to the log of the viral load and 2-26 when relative infectiousness was only 1% based on a linear relationship between viral RNA shedding and infectiousness. Such differences in R_0 have large implications for the CCS and control of transmission in dromedary populations. Visual comparison of titres for infectious virus and viral RNA shed by four dromedaries following vaccination [8] suggest the changes in infectiousness are more closely related to the change in viral load than the logarithm of the change in viral load. Taken together with the results in this chapter, this would suggest that R_0 can be very high in some settings, but more data describing the relative infectiousness of reinfections compared to first-time infections will be important to narrow down the estimates R_0 reliably. An R_0 above 20 is likely implausible, although other livestock diseases are known to have very high transmissibility in intensive farming settings with high population density [237], [238]. Such high R_0 estimates could also be a consequence of FoI overestimation in ***Chapter 3*** – for example due to maximum seroprevalence being reached in young age groups, or as a result of study populations experiencing an epidemic rather than transmission being at endemic equilibrium. The existing published estimate of R_0 for MERS-CoV (based on weekly reported human MERS cases and a fixed rate of zoonotic spillover) is around 4 for dromedaries in KSA which is comparable to the estimates for KSA in this chapter in scenarios when relative infectiousness of reinfection is ≥25%, and lower than estimates when relative infectiousness is 1%.

CCS

Much like R_0, the estimated CCS for MERS-CoV was highly sensitive to the relative infectiousness of reinfections. In high transmission settings, if relative infectiousness of reinfections was ≥25%, the CCS (which was reached at some point between 500-2,500 for homogeneous and 1,000-5,000 for structured populations) was comparable to the size of large, commercial herds in KSA and UAE [114]. However, if infectiousness is proportional to viral load, relative infectiousness of reinfections is likely to be lower than 25% and, in these scenarios, the CCS was between 25,000 and 75,000. Although this is quite high, it is comparable to only 1% of the FAO estimated dromedary population of Kenya in 2020 and 10% of that estimated for KSA [93], [112]. When sub-national dromedary population sizes are considered, it is realistic that this population threshold is exceeded in many locations. For example, county-level dromedary populations in Kenya reach 800,000 in traditional camel keeping regions and are likely to be highly connected through markets and shared grazing lands [112]. These CCS estimates suggest that MERS-CoV could not persist in individual herds in most settings, where herd sizes tend to be well under 1,000 animals [98], [113], [114]. This underscores the importance of connections between herds – through trade, travel, and shared grazing land – to sustained circulation of the virus. Vaccination prior to trade could offer an opportunity to reduce transmission between herds.

The decrease in the CCS in settings with increased transmissibility and increased connectivity is to be expected as MERS-CoV is not an immunising disease in dromedaries, meaning higher transmissibility and higher connectivity within the population make transmission less likely to go extinct following a peak in infections. When relative infectiousness of reinfected individuals was assumed to be low, this trend was reversed with an increase in the CCS as transmission increased from moderate to high, and as the population become more connected. This reversal is likely to be because more susceptible individuals are needed to sustain transmission at a high intensity in this scenario, as first-time infections are the main source of onward transmission, making fadeout more likely when transmission is high, and when there is no metapopulation rescue effect. The dependence of CCS on R_0, taken together with the difference in R_0 estimates

across populations, suggests that MERS-CoV will be harder to control in dromedary populations in some areas than others. In settings in the Middle East where MERS-CoV is estimated to have a high R_0, the virus may be able to persist in a population 2-20 times smaller (depending on the relative infectiousness of reinfections) than in a setting with a low R_0, such as those sampled in South Asia. The relatively small CCS estimates for high transmission scenarios suggest that a high vaccination coverage would be needed to control transmission in some settings.

Endemic periodicity

The results of the simulations suggest that seasonality of births can be expected to drive annual, seasonal peaks in infection in large populations when transmission intensity is comparable to the high R_0 estimates for MERS-CoV in populations in parts of the Middle East, and Ethiopia. Whilst infections tended to peak outside of the calving season, the lag between the simulated peak in births and annual peak in infection depended on R_0. This suggests that even if calving drives annual peaks in infection, we might not expect the peak to occur at the same time of year across disparate transmission settings.

When closed population sizes were relatively small (<10,000), biennial, triennial, and quadrennial patterns of infection often developed. This was more common when transmissibility was low (comparable to R_0 values estimated in populations in South Asia, as well as some parts of Africa). The difference between the size of the peaks in sequential years is not as large as, for example, in measles where biennial transmission is very intense. The dominance of annual periodicity at large population sizes suggests that, in a deterministic model, the periodicity would be annual and that deviation from this is a product of stochastic intermittency at smaller population sizes and lower transmissibility contexts.

If MERS-CoV infections peak annually in some settings as these simulations suggest, there may be seasons in which risk of zoonotic transmission is elevated. Better understanding of when peaks occur would provide opportunities to mitigate risk and avert human cases. One limitation of this analyses is that calving was the only factor included in the dynamic model which could

drive seasonality. In reality, however, other factors that were not considered such as annual migrations and seasonal events that affect dromedary mixing could also affect the transmission dynamics of MERS-CoV in the zoonotic reservoir. Ultimately, it is necessary to undertake long-term surveillance of dromedary populations over several years to better ascertain the seasonality of MERS-CoV in dromedaries, and how risk of zoonotic transmission can be further mitigated.

Limitations

The process of model development highlighted remaining gaps in knowledge around the nature of immunity which necessitated simulation of several alternative scenarios for: a) the duration of complete immunity; b) the relative susceptibility of previously infected animals; and c) the relative infectiousness of reinfected animals. As has been discussed, transmission dynamics were most sensitive to the relative infectiousness of reinfections, highlighting this as a priority area to address in order to improve the picture we have of MERS-CoV transmission in dromedaries. Developing a better understanding of the infectiousness of reinfections will be an important part of improving the accuracy of this current model of MERS-CoV transmission in dromedaries before the potential impact of vaccinations can be assessed with confidence.

Transmissibility estimates in ***Chapter 3*** have revealed the likely heterogeneity in MERS-CoV dynamics in different dromedary populations. The dynamic model was run for different transmission intensities – from those reflective of estimates for high transmission settings (such as populations in the Middle East and Ethiopia) to those representative of lower transmission settings (such as sampled populations in Pakistan and Bangladesh). A weakness of the model in its current state, however, is that the parameters describing mortality rates and birth rates are mostly based on generalised populations in KSA. To tailor the model more explicitly to different farm types or other regions, dromedary demographical parameters should reflect population turnover in the particular setting of interest.

The effect of population structure on the CCS estimates emphasises that more data on location-specific dromedary population size, structure and movement would also be needed if this model were to be relied upon for accurate prediction of intervention impact in a particular setting. The way structure was modelled here as a simple grid is a rudimentary representation of the true dromedary population structure. A grid was chosen, over other commonly used meta-population structures such as the torus, due to the grid's edges and corners that could be used to represent the likely reality that some sub-populations are connected to fewer neighbouring sub-populations than others. Choosing a different structure to represent the population, such as a donut shaped torus structure with no edges, or a random network, could potentially change transmission persistence dynamics across the population as a whole. Varying transmissibility and population size across patches within the meta-population model could also affect persistence and CCS estimates. It will be very important to collect better data on dromedary population structure and movement and consider representing this more accurately whilst assessing the impact of vaccination or other interventions in particular populations.

Conclusion

The dynamic model presented in this chapter is, to the best of my knowledge, the first available stochastic model of MERS-CoV transmission in dromedaries. It is also the first to use parameters inferred from dromedary seroprevalence data, rather than weekly human cases, to provide an up-to-date representation of MERS-CoV transmission in the zoonotic reservoir as we currently understand it. Model estimates of R_0 suggest that MERS-CoV is transmitted efficiently between dromedaries in parts of Africa, and South Asia but estimates were especially high in populations sampled in the Middle East. Taken together with the CCS estimates, this suggests that in the Arabian Peninsula and potentially parts of East Africa, MERS-CoV may persist in a population 2-20 times smaller than in lower transmission settings, meaning high vaccine coverage and efficacy is likely to be needed to interrupt transmission in some regions. The CCS is unlikely to be comparable to individual herd sizes unless reinfections are >25% as infectious as first-time

infections in which case very large commercial herds found in the Arabian Peninsula could potentially see sustained transmission. This highlights the importance of connections between herds, such as markets, as a target for interrupting transmission. Finally, Seasonal calving was sufficient to drive annual peaks in infection in moderate population sizes, suggesting there is potential for seasonal elevations in risk of zoonotic transmission of MERS-CoV, and the need for multi-year longitudinal studies.

Simulated dynamics were very sensitive to the assumed relative infectiousness of reinfected animals, indicating that better quantification of this should be a priority for improving model accuracy. Population structure also had a large effect on persistence of transmission, highlighting the need to collect data describing dromedary networks and incorporate this into future evaluations of the potential impact of interventions.

Chapter 5:

Evaluating the potential impact of dromedary vaccination

Introduction

Dromedary vaccination as potential tool to avert human MERS cases

The continued development of sporadic clusters of MERS in humans is driven by recurring zoonotic transmission from the dromedary camel population [2]. The role dromedaries play in driving ongoing human disease, coupled with the lack of effective therapeutics for people, has led to interest in dromedary vaccination as part of a package of interventions to avert human infection and MERS associated deaths [5]. One unique benefit of dromedary vaccination when compared with interventions that aim to reduce human-to-human transmission is that dromedary vaccination would tackle transmission at the source. Reducing the risk of zoonotic transmission to humans through dromedary vaccination would therefore complement the current mainstay of MERS-CoV control – infection control in nosocomial environments.

Two vaccine candidates have been shown to significantly reduce viral shedding compared to placebos when tested in dromedaries – an MVA (Modified Vaccinia Ankara) based vaccine [8] and the adenovirus vectored ChAdOx1 MERS vaccine [6]. With at least two promising candidates in the pipeline, it is becoming increasingly vital to model the likely impact of vaccinating dromedaries and to compare the expected reduction in transmission across different implementation strategies – for example, strategies targeting different age groups. Assessments of the expected epidemiological impact of different dromedary vaccination strategies will be important to present and compare with other intervention packages when consulting camel owners, government organisations and other stakeholders prior to potential vaccine implementation.

Modelling vaccination

The simulation of vaccination within transmission models has been widely used to inform vaccination programs against infectious diseases including measles, influenza, dengue, Ebola, and COVID-19 [10], [12]–[14], [155]. Previously, there has been a lack of appropriate dynamics

models of MERS-CoV in dromedaries within which to simulate vaccination. Together with viral load data from MERS-CoV dromedary vaccination studies and dromedary demographic data from the wider literature on camel husbandry, estimates of transmissibility inferred from data describing age-stratified MERS-CoV seroprevalence in dromedaries in ***Chapter 3*** enabled the development of the stochastic, age structured, dynamic model of transmission in dromedaries described previously in ***Chapter 4***. In this chapter, the dynamic transmission model is extended to simulate animal vaccination.

Relevant knowledge gaps

The dynamic model reflects current knowledge of the transmission of MERS-CoV in dromedaries, including the transmissibility estimates from ***Chapter 3***. However, key uncertainties about immunity do remain. In particular, the relative infectiousness of reinfections is parameterised using viral RNA shedding data collected for naïve and previously infected animals in the control group of the ChAdOx1 MERS efficacy trial and could be between 1% and 50%, depending on whether infectiousness is proportional to viral RNA shedding or the log of the viral RNA shedding. The simulated transmission dynamics are sensitive to this uncertainty around the relative infectiousness of reinfected animals which necessitates modelling both extremes – where infectiousness is proportional to viral shedding or the log of viral shedding – to assess the potential impact of vaccination.

There are also two main uncertainties relating to the epidemiological characteristics of the MERS-CoV vaccine candidates. Firstly, there is uncertainty around the vaccines' effects on susceptibility to infection. In the MVA study, all four vaccinated animals became infected but the challenge dose – administered directly into the nasal cavity – may be high compared to natural infection. The ChAdOx1 MERS study – which administered the challenge by adding one, naturally-occurring infectious animal per two vaccinated or control animals in the pen – also saw all previously seronegative vaccinated animals become infected. However, one of the five vaccinated and previously seropositive, dromedaries did not become infected at all, despite very

high levels of infection in the pen. This suggests that whilst vaccine is not likely to be protective against infection in naïve animals in high transmission environments, there may be some level of vaccine-induced reduction in susceptibility for previously infected animals. It is not possible to ascertain whether the vaccine would offer any reduction in susceptibility to infection in an environment with a lower transmission intensity.

There is also uncertainty around the vaccine candidates' efficacy in dromedaries that have never been infected with MERS-CoV, compared to those that have previously been infected. The MVA-based vaccine has only been tested in seronegative dromedaries (assumed to have never been infected) and was shown to significantly reduce shedding [8]. On the other hand, the ChAdOx1 vaccine was tested in both naïve and previously infected animal and, whilst it reduced shedding considerably in seropositive individuals, it had poor efficacy in the five seronegative animals [6]. Authors suggested this could be because these animals were very young (all 6-12 months old) but they were a comparable age to the seronegative animals in the MVA study (all 6-8 months old). This leaves uncertainty around the efficacy of the vaccine when targeting animals that are naive to MERS-CoV infection. Both vaccine candidates use a vector to deliver the RNA encoding the MERS-CoV spike protein and do not display the spike protein on their surface so are unlikely to be affected by antibodies from past infection [6], [8].

In this chapter, the extended dynamic transmission model is used to explore the potential impact of vaccination under multiple vaccine efficacy scenarios to reflect the uncertainties described above. The optimal target age for routine vaccination is evaluated based on the transmission dynamics and the feasibility of using vaccination to interrupt transmission in dromedary populations is assessed in different transmission settings, reflecting the inferred transmissibility of MERS-CoV in populations across Africa, South Asia and the Middle East in ***Chapter 3 & 4***.

Methods

Representing vaccination of dromedaries in the dynamic transmission model

The dynamic transmission model that forms the focus of ***Chapter 4*** is extended to simulate vaccination by duplicating the set of disease states to create a parallel set of vaccinated states shown collapsed into a single age class in ***Figure 5.1***. Vaccination is implemented in an age dependent manner. Ageing is modelled as in ***Chapter 4***, with 48 month-wide age classes where dromedaries are shifted into the next age class every 30 days until reaching the final 49th age class (>4 years old) where they remain until death. Vaccination occurs immediately at the point at which dromedaries reach the age being targeted for vaccination. For example, vaccination of 80% of animals at six months is simulated as animals transition from the 6th to the 7th month-wide age class as follows. For each unvaccinated disease state, a number of animals from the 6th age class is sampled from a Poisson distribution with a mean of 0.8 multiplied by the number of animals in the class. These animals then shift into the 7th age class of the vaccinated equivalent to their disease state, with the remainder shifting into the 7th age class whilst remaining unvaccinated.

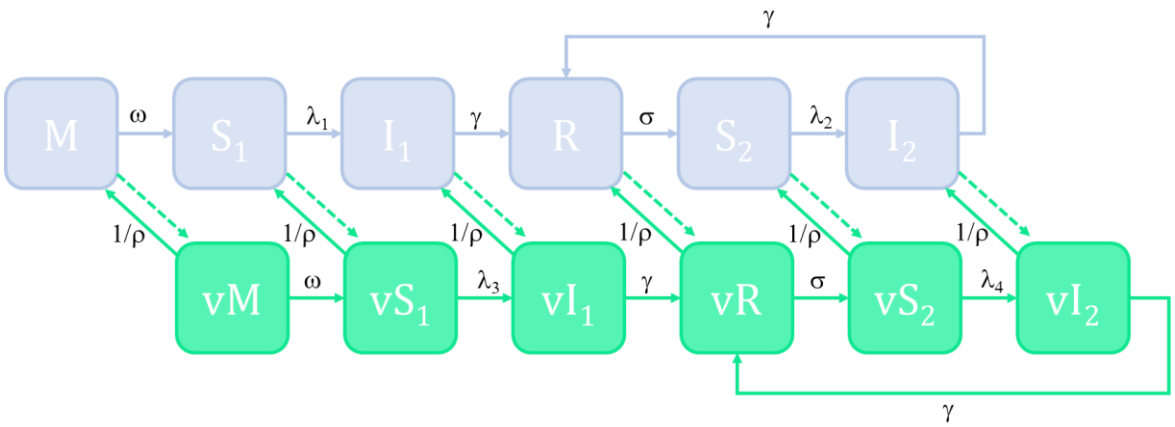


Figure 5.1. The extension of the dynamic model to incorporate vaccination*. Demographic transitions including births, deaths and ageing are not shown for simplicity. Unvaccinated individuals transition between the original M, S_1, I_1, R, S_2 and I_2 states (in blue), whilst vaccinated individuals transition between the equivalent states denoted by v prefixes (in green). Unvaccinated individuals are vaccinated in an age dependent manner (dotted arrows). Vaccinated individuals transition back to unvaccinated set of states at a constant rate $1/\rho$.*

Modelling the effects of the vaccine: three different scenarios

Due to the uncertainties surrounding aspects of the vaccine candidates' effect on susceptibility and potential differences in efficacy in naïve versus previously infected animals, three main scenarios are modelled: 1) the vaccine reduces both susceptibility to infection and infectiousness for all vaccinated animals regardless of their infection history; 2) the vaccine reduces infectiousness alone for all vaccinated animals; and 3) the vaccine reduces both susceptibility and infectiousness but only in animals that have been previously infected. See ***Figure 5.2*** for a summary of the different scenarios modelled.

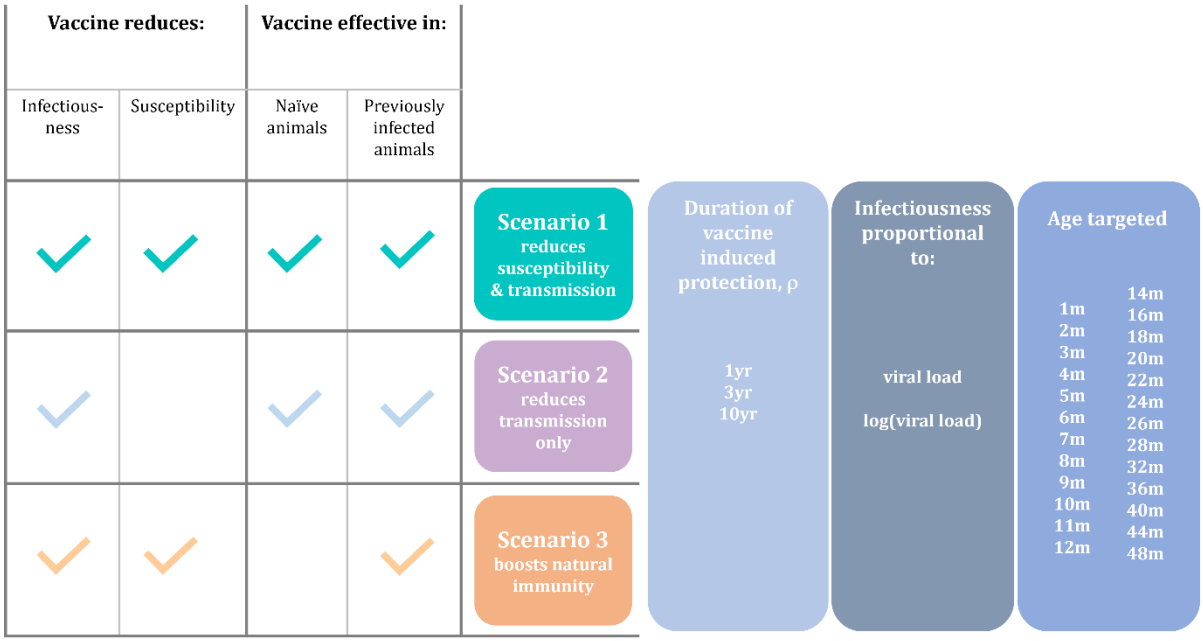


Figure 5.2. A breakdown of the different vaccine efficacy scenarios modelled*. Each of the three main scenarios described in the table is run for three further sub-scenarios, assuming different durations of vaccine induced protection. Finally, each sub-scenario is run assuming that infectiousness is either proportional to viral load (viral RNA shedding by real time RTPCR) or the log of viral load. This gives a total of 18 sub-scenarios which are each run for a range of target age classes for vaccination.*

Due to the scope of the efficacy studies, it is not possible to estimate the rate of waning of vaccine-induced effects, $1/\rho$. Instead, for each main scenario, three options are explored with effects lasting one, three and ten years (***Figure 5.2***), resulting in nine sub-scenarios. Across all sub-scenarios, the relative infectiousness of vaccinated infected animals and of vaccinated reinfected animals compared to unvaccinated naïve animals was parameterised using viral RNA

shedding data from Alharbi *et al.,* (2019) [6], assuming that infectiousness is either proportional to viral RNA shedding or to the log of viral RNA shedding. The target age group was then varied from one month old to four years old for each sub-scenario. The vaccine efficacy was not modelled to vary with age.

Parameterising vaccine-induced reductions in infectiousness and susceptibility

In scenarios 1 and 2 vaccination was assumed to reduce the relative infectiousness of first-time infected animals (r_v) by the same amount as natural infection reduces the infectiousness of reinfected individuals (down to 1% when infectiousness is assumed proportional to viral RNA shedding and 50% when proportional to the log of viral RNA shedding). The relative infectiousness of reinfected vaccinated individuals (r_{inf_v}) was fixed as 0.15% when a linear relationship between infectiousness and viral RNA shedding was assumed, and 33% when infectiousness was assumed to be proportional to the log of viral RNA shedding based on data from the ChAdOx1 MERS vaccine trial [6]. See ***Table 5.1*** for the complete set of parameters used to model the effect of vaccination.

In scenario 1, in which the vaccine is assumed to reduce susceptibility as well as infectiousness for all animals regardless of vaccination history, the vaccine is modelled to offer naïve animals the same reduction in susceptibility as natural infection, giving them a relative susceptibility, ϕ_v, of 75%. Previously infected vaccinated animals are assumed to have a susceptibility of 50% in scenario 1 and 3 (***Figure 5.1***, ***Table 5.1***).

Table 5.1. Parameters used to model vaccination

	Description	*Value(s)*	*Source*
r_v	Relative infectiousness of vaccinated animals	**1%** or **50%** dependent on relationship between viral load and infectiousness (or **100%** in scenario 3)	[6]
r_{inf_v}	Relative infectiousness of vaccinated previously infected animals	**0.15%**, or **33%** dependent on relationship between viral load and infectiousness	[6]
ϕ_v	Relative susceptibility of vaccinated animals	**75%** (or **100%** in scenario 2)	NA. Larger reduction in susceptibility unlikely given all vaccinated previously seronegative animals were infected in [6] and [8]
ϕ_{inf_v}	Relative susceptibility of vaccinated previously infected animals	**50%** (or **75%** in scenario 2)	NA. Indication of reduced susceptibility in [6] but unable to reliably quantify in small population
$1/\rho$	The rate of waning of vaccine-induced effects	**1**, **3**, or **10** years^{-1}	NA

Results

Optimal target age for vaccination

The optimal target age for vaccination was assessed in a large, homogeneous population of 1 million dromedaries. When vaccines were assumed to reduce infectiousness in naïve as well as previously infected animals, vaccinating calves within their first few months of life led to the greatest reduction in incidence of MERS-CoV infection (S1 and S2 columns in ***Figure 5.3***). In the absence of vaccination, most animals are first infected when they are <1 year old – as shown in ***Figure 5.*** In targeting younger calves, vaccination precedes first infection in a greater number of individuals and reducing their subsequent infectiousness. Since first infections are more infectious than reinfections, early vaccination indirectly reduces incidence to a greater extent. The only scenario where this pattern was not seen was scenario 3 in which the vaccine is not effective in naïve animals and only acts as a booster to natural immunity. In this scenario, the reduction in incidence was more consistent across strategies targeting different age classes, but a slightly greater reduction in incidence is seen when calves are vaccinated later in life, beginning at 9-18 months depending on transmissibility (***Figure 5.3***, column S3). This just precedes the age that the majority of reinfections start to take place (seen in purple in ***Figure 5.4***).

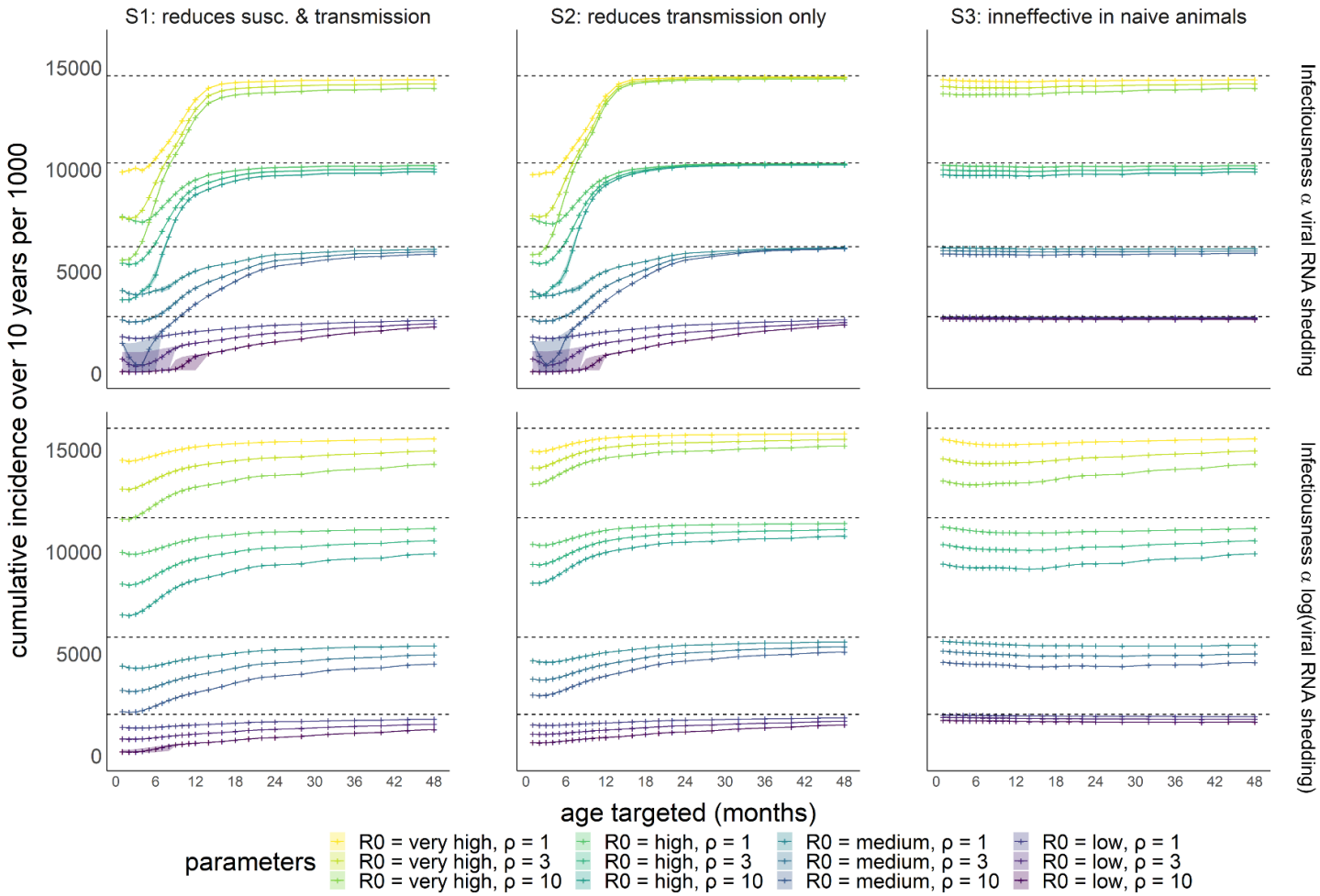


Figure 5.3 The incidence of infection following vaccination of different target age groups. *Incidence is calculated as cumulative incidence of infection per 1,000 animals in the 10 years following vaccine introduction, under different vaccine efficacy scenarios (columns) and different assumptions about the relationship between infectiousness and viral RNA shedding (rows). Colours indicate different combinations of R_0 and duration of vaccine-induced effects, ρ. Dotted lines show the incidence per 1000 in the absence of vaccination for each R_0 value. Points show mean values over 100 stochastic runs and transparent ribbons represent 95% quantiles.*

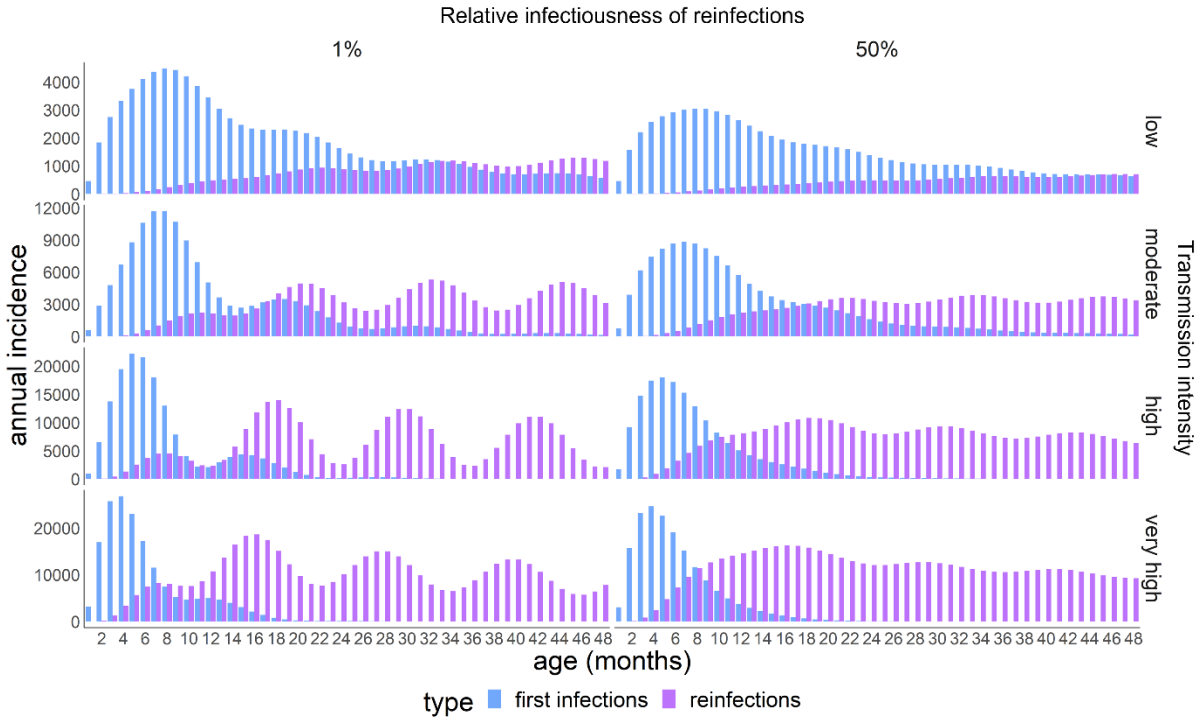


Figure 5.4 The age distribution of first infection and reinfection in the absence of vaccination*. Annual incidence of first infections (blue) and reinfections (purple) is presented in the first four years of life for a population of 1 million dromedaries. Distributions are shown for four settings with increasing transmission intensity from low to very high (rows) and for two different assumptions in which reinfections are either 1% or 50% as infectious as first infections (columns).*

The effect of vaccine-induced reduction to susceptibility on optimal target age for vaccination

Vaccinating animals at a younger age led to greater reductions in incidence, regardless of whether the vaccine reduced both infectiousness and susceptibility of vaccinated animals (scenario 1) or just reduced infectiousness (scenario 2). The reduction in incidence was slightly greater across all ages targeted in scenario 1. When infectiousness is proportional to viral RNA shedding (***Figure 5.3.*** top row), vaccinating older age groups after first infections have occurred has almost no effect on incidence in scenario 2, whereas a slight reduction is still achieved by reducing the susceptibility of the older animals to reinfection in scenario 1.

Additional factors influencing the effect of target age on the reduction in incidence

The additional reduction in incidence achieved by vaccinating animals at a younger age in scenarios 1 & 2 was particularly large when infectiousness was assumed to be proportional to viral RNA shedding (see in in the top row of panels in ***Figure 5.3***). This is expected as, under this

assumption, the drop in infectiousness of reinfections and infected vaccinated individuals compared to first-time infected naïve individuals is greater than when infectiousness is assumed to be proportional to the log of viral RNA shedding. The reduction in incidence afforded by targeting younger animals was also larger in higher transmission settings where first infections occur earlier, with reductions in incidence diminishing quicker as the target age class is increased compared to in lower transmission settings. When R_0 was low or moderate, early vaccination sometimes led to stochastic fadeout, particularly when the effects of the vaccine were long-lasting. In these cases, the difference in incidence between stochastic runs was often large (the 2.5% and 97.5% quantiles are represented by transparent ribbons in ***Figure 5.3***).

In some scenarios, most notably when R_0 was moderate and ρ was 10 years, the mean incidence dips to its lowest when vaccination targets 3–4 month olds – as opposed to simply increasing with age from 1 month. This appeared to be because, in these scenarios, vaccinating 1–2 month olds led to increases in incidence in adult dromedaries and is likely linked to the protection offered by maternally acquired antibodies to calves under three months of age. When sensitivity analysis was conducted with maternally acquired antibodies lasting an average of six months, this dip at 3-4 months was not seen – instead, incidence increased as age targeted increased. Other than this, the pattern in incidence reduction was very similar to when maternally acquired antibodies were assumed to last for an average of three months, although stochastic variation was greater, with more instances of fadeout or large drops in incidence when the vaccine targeted very young calves (see ***Figure A5.1*** in **Appendix Chapter 5, A5.1**).

A shift in the age distribution of first infections

Although vaccination reduced the total incidence of MERS-CoV infection, vaccination of calves led to an increase in incidence in older animals in some scenarios, due to a shift in the age distribution of infections. Since reinfections and infected vaccinated animals are modelled to be less infectious than infected naïve animals based on viral RNA shedding data, not all incident

infections pose equal risk of zoonotic transmission. In order to better ascertain the potential implications of the increased incidence in older age classes, the incidence of reinfections and infections in vaccinated animals were down-weighted by their infectiousness relative to first time infections to give the infectious-state-weighted incidence. Increases in the age specific infectious-state-weighted incidence occurred in calves between 5-8 months old and animals over 18 months old. ***Figure 5.5*** shows the vaccine-induced change in infectious-state-weighted incidence in >18-month-olds for different scenarios.

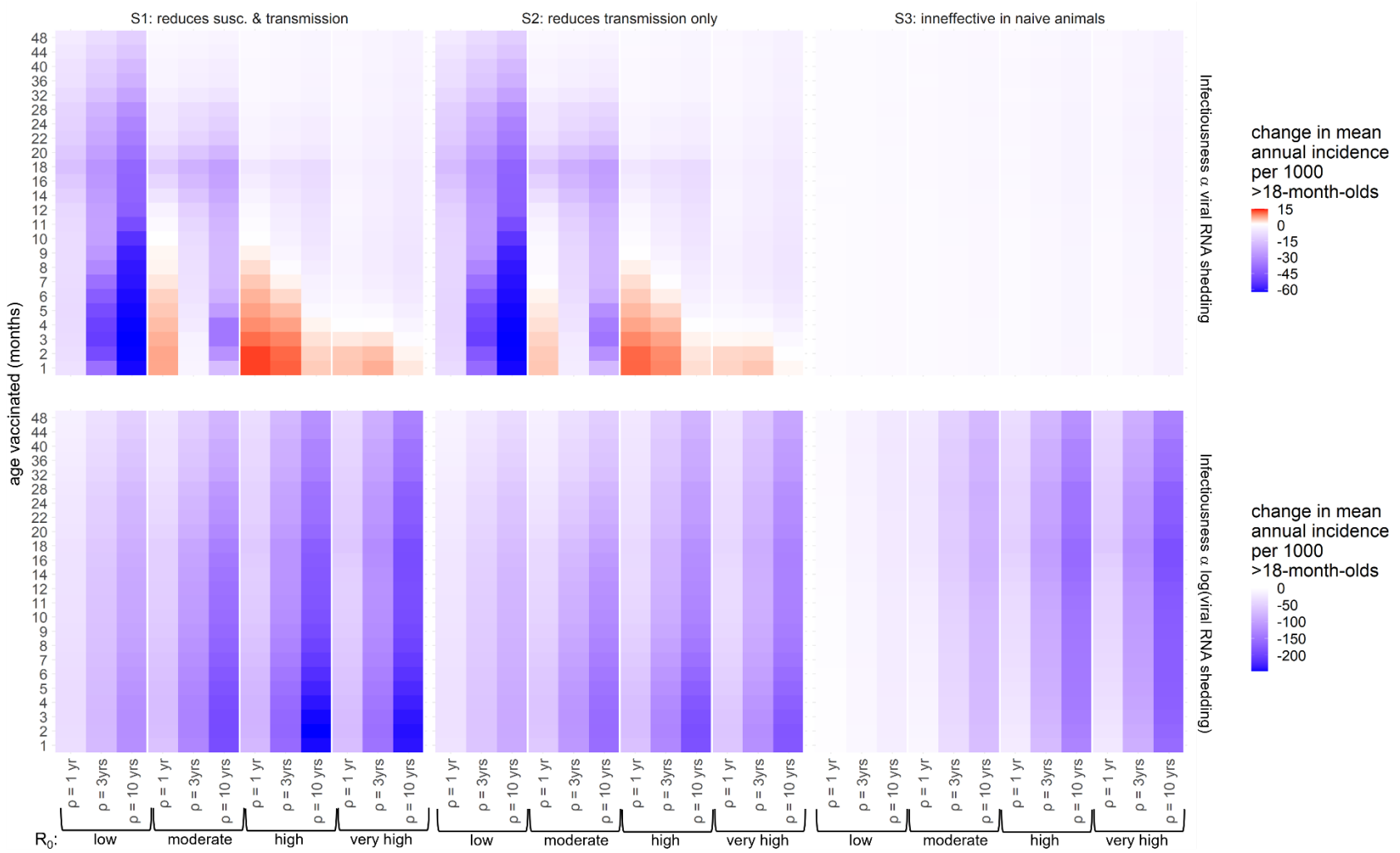


Figure 5.5 The average change in annual infectious-state-weighted incidence in dromedaries older than 18 months *per 1,000 animals in the ten years following vaccine introduction compared to in the absence of vaccination. Red denotes increases and blue denotes decreases. Results are shown for efficacy scenarios 1-3 (columns) and under different assumptions about the relationship between infectiousness and viral RNA shedding (rows).*

The increases in infectious-state-weighted incidence (shown in red in ***Figure 5.5***), were seen when vaccination targeted calves <10 months old. Increases were only seen when infectiousness was assumed to be proportional to viral RNA shedding (that is, when vaccination and/or previous infection leads to the greatest reduction in infectiousness) and were largely limited to efficacy scenarios 1 and 2 in which the vaccine is effective in both naïve and previously infected animals. In scenario 3, the largest increase in mean annual infectious-state-weighted incidence in dromedaries aged >18 months was only ~0.06 per 1,000 over the ten years following vaccine introduction in a population of 1 million dromedaries, compared to ~10-15 per 1,000 in scenarios 1 and 2. Maximum increases were seen in cases when calves were vaccinated in the first three months of life, when transmissibility was high and when duration of vaccine-induced effects was relatively short. Some level of increase was seen regardless of the duration of vaccine induced effects, ρ, when transmissibility was high but, when transmissibility was moderate, increases were only seen when vaccine induced effects were short-lived. Increases were never seen when transmissibility was low.

When vaccination targeted animals aged between 6-12 months, weighted incidence also increased in 5-8 month olds as first infections shifted from very young calves into slightly older calves following the vaccine-induced reduction of the FoI. However, there was still a considerable net decrease in the weighted incidence in calves <12 months.

The feasibility of preventing sustained transmission

The metapopulation model described in ***Chapter 4*** was used to evaluate the persistence of transmission when dromedary calves were vaccinated at six months of age. The feasibility of interrupting transmission was assessed under the different vaccine efficacy scenarios and in different transmission settings. Two different total population sizes were considered: 75,000 – roughly the size of a dromedary population in an emerging dromedary farming county in Kenya [112]; and 500,000 – the size of the dromedary population in KSA, according to the most recent FAO estimates [93]. Persistence was explored at the patch level and the population level.

Transmission was said to have been interrupted at the patch level if vaccination made an average patch more likely to be MERS-CoV free than to have experienced infections during the 10th year post introduction (that is, when on average each patch experienced infection in <50% of stochastic runs). Interruption of transmission at the population level was defined as when infection was more likely to have gone extinct than to be persisting in the population as a whole at the end of the 10th year following vaccination.

When the vaccine was only effective in previously infected animals (scenario 3), vaccination was not able to interrupt transmission under any circumstances. The coverage needed to interrupt transmission in scenarios 1 and 2 is detailed below in ***Table 5.2***.

Table 5.2 The vaccine coverage needed to interrupt transmission *under different efficacy scenarios and in varying transmission settings*

	Scenario	Duration of vaccine-induced effects, ρ (years)	R_0	Vaccine coverage (%) required to interrupt transmission			
				at the patch level*		at the population level†	
				N = 500,000	N = 75,000	N = 500,000	N = 75,000
infectiousness α to viral RNA shedding	*S1 vaccine reduces infectiousness and susceptibility in both naïve and previously infected animals*	*1*	*low*	NA	40	NA	40
			moderate	NA	80	NA	80
			high	NA	90	NA	90
			very high	NA	80	NA	80
		3	*low*	80	40	80	40
			moderate	90	70	90	70
			high	NA	80	NA	70
			very high	100	60	100	60
		10	*low*	70	40	70	40
			moderate	80	60	80	60
			high	100	80	100	80
			very high	90	50	100	40
	S2 vaccine reduces infectiousness only, in both naïve and previously infected animals	*1*	*low*	NA	50	NA	50
			moderate	NA	80	NA	80
			high	NA	90	NA	90
			very high	NA	70	NA	70
		3	*low*	80	40	80	40
			moderate	90	70	90	70
			high	NA	70	NA	70
			very high	100	60	100	60
		10	*low*	70	40	70	40
			moderate	80	60	80	60
			high	90	60	90	60
			very high	90	60	90	50

infectiousness α to log(viral RNA shedding)	*S1 vaccine reduces infectiousness and susceptibility in both naïve and previously infected animals*	*1*	*low*	NA	NA	NA	NA
			moderate	NA	NA	NA	NA
			high	NA	NA	NA	NA
			very high	NA	NA	NA	NA
		3	*low*	NA	70	NA	80
			moderate	NA	NA	NA	NA
			high	NA	NA	NA	NA
			very high	NA	NA	NA	NA
		10	*low*	80	60	0.8	0.6
			moderate	NA	NA	NA	NA
			high	NA	NA	NA	NA
			very high	NA	NA	NA	NA
	S2 vaccine reduces infectiousness only, in both naïve and previously infected animals	*1*	*low*	NA	NA	NA	NA
			moderate	NA	NA	NA	NA
			high	NA	NA	NA	NA
			very high	NA	NA	NA	NA
		3	*low*	NA	90	NA	90
			moderate	NA	NA	NA	NA
			high	NA	NA	NA	NA
			very high	NA	NA	NA	NA
		10	*low*	100	60	100	60
			moderate	NA	NA	NA	NA
			high	NA	NA	NA	NA
			very high	NA	NA	NA	NA

*meaning an average patch experienced infection during the 10th year following vaccine introduction in <50% of stochastic model runs

†meaning there was no infection in the whole population by the end of the 10th year following vaccine introduction

Persistence at the population level when infectiousness was proportional to viral RNA shedding

In a population of 500,000, with no external sources of infection, vaccination could interrupt transmission in low, moderate, and very high transmission settings as long as vaccine induced effects lasted at least 3 years and coverage was high (between 70-100% depending on transmissibility). To interrupt transmission when transmissibility was high, ρ had to be 10 years and coverage had to be 90% if the vaccine reduced both susceptibility and infectiousness, and 100% if the vaccine only reduced infectiousness.

In a population of 75,000, vaccination of six month olds was capable of interrupting transmission, regardless of the transmissibility and even when the vaccine-induced effects only

last for one year. The coverage required varied from 40-90% depending on transmissibility and the duration of vaccine induced effects. When ρ was 10 years, a coverage of ≤40 to 60% depending on transmissibility is needed in scenario 2, and from ≤40% to 80% in scenario 1. Interrupting transmission when transmissibility was high required higher coverage than when transmissibility was very high. This is likely to be because of a complex interaction between transmissibility, seasonality, and the availability of susceptible individuals. In high transmission settings, a slightly higher vaccine coverage was needed to interrupt transmission at the population level when the vaccine reduced infectiousness and susceptibility (scenario 1), compared to when it reduced infectiousness alone (scenario 2).

Persistence at the population level when infectiousness was proportional log (viral RNA shedding)

When infectiousness was proportional to the log of viral RNA shedding, vaccination was only able to interrupt transmission in low transmission settings. To interrupt transmission at the patch-level in a population of 500,000 in a low transmission setting, vaccine-induced effects needed to last ten years and vaccine coverage had to be very high – reaching 80% when the vaccine reduced susceptibility and 100% when the vaccine only reduced infectiousness. In a population of 75,000, a three year duration of vaccine-induced effects was sufficient for vaccination to interrupt transmission at the population level when coverage was 80% in scenario 1 and 90% in scenario 2. When vaccine-induced effects lasted ten years, the coverage required to interrupt transmission dropped to 60%.

Persistence at the patch level

Comparing the coverage required to interrupt transmission at the patch versus population level in ***Table 5.2*** shows that, in some cases, the coverage needed for patches to experience infection <50% of the time in the 10th year following vaccine introduction was slightly lower than that needed to see population level fadeout <50% of the time by the end of year ten. This suggests that vaccination restricted transmission to a smaller number of patches in these cases. Most of the time, however, the coverage needed to interrupt transmission at the population level was

the same as that needed to interrupt it at the patch level, suggesting that, in this particular structure, fadeout generally occurred across the population rather than transmission being sustained by a few patches consistently. It is conceivable that this result is dependent on the assumption of consistent transmissibility and population size across patches, and that if these two variables were instead varied across the population transmission could potentially persist more easily in some patches than others. The four incidences in ***Table 5.2*** where the coverage needed for infection to be experienced <50% of the time in year ten at the patch level was greater than that needed to interrupt transmission at the population level by the end of year ten arise due to fadeouts occurring *during* the tenth year. By definition, if transmission has been interrupted at the population level at a particular time-point, it has also been interrupted at the patch-level.

Persistence at the patch level over time since vaccine introduction

The percentage of stochastic runs in which a patch experienced infection is presented for each year from 1-10 years after vaccine introduction in ***Figure 5.6*** (scenario 1) and ***Figure 5.7*** (scenario 2), under the assumption that infectiousness is proportional to viral RNA shedding. The equivalent figures when infectiousness is assumed proportional to the log of viral RNA shedding are not included here as vaccination only impacts persistence in low transmission settings, but they can be found in ***Appendix Chapter 5, A5.2 Figures A5.2.1-2*** for interest.

Generally, for both population sizes and scenarios, the average patch was less and less likely to experience an infection the longer vaccination had been in place. When transmissibility was low and ρ was small, however, patches were least likely to experience an infection during the years around the 5th year following vaccine introduction, with the percentage of model runs in which an infection was experienced increasing slightly in the following years before stabilising.

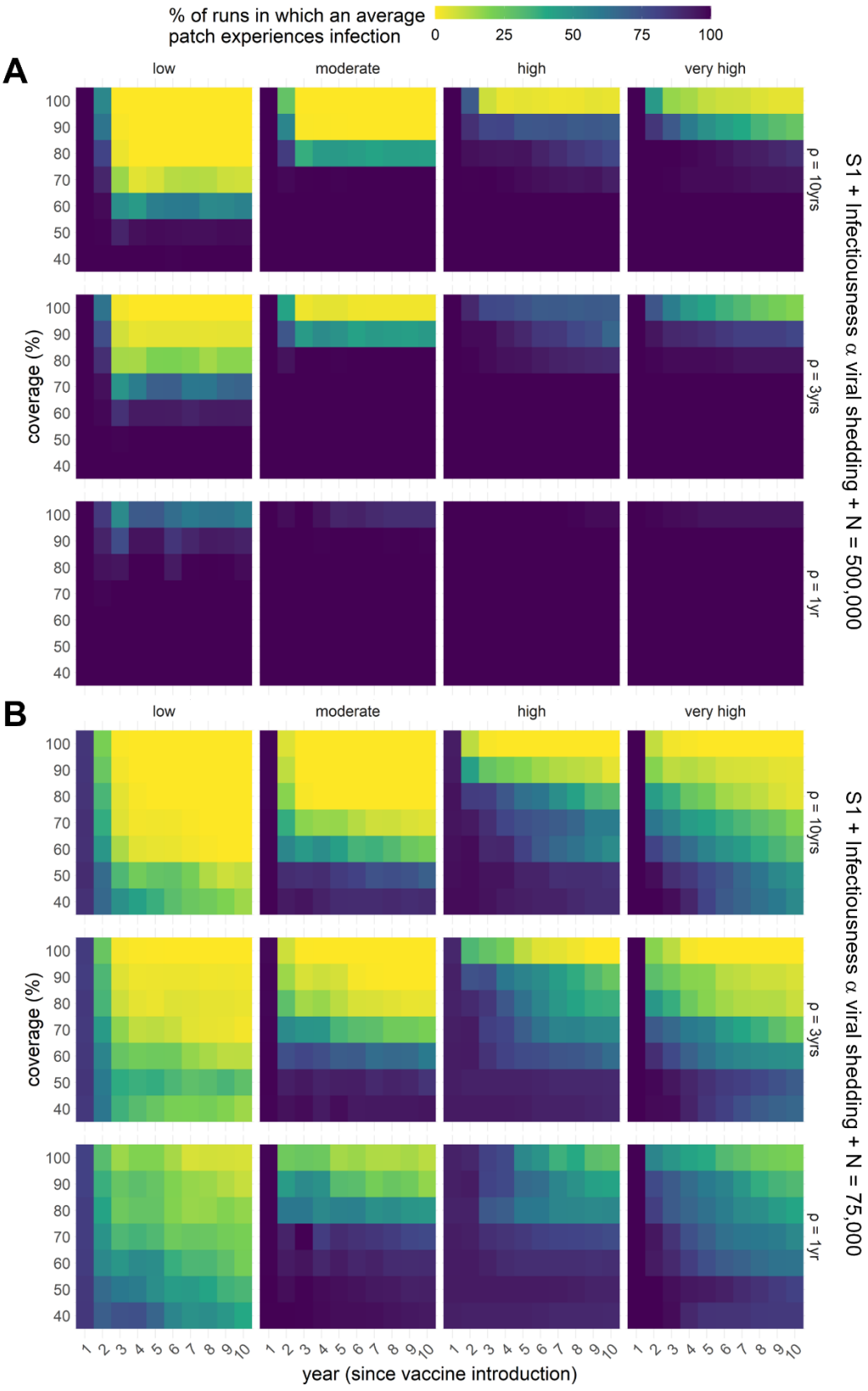


Figure 5.6 The percentage of stochastic model runs in which a patch experienced infection in scenario 1 *for each year following vaccine introduction. Results are shown in different transmission settings (columns) and for different durations of vaccine induced effects (rows) for* ***A****. a population of 500,000 dromedaries and* ***B****. a population of 75,000 dromedaries.*

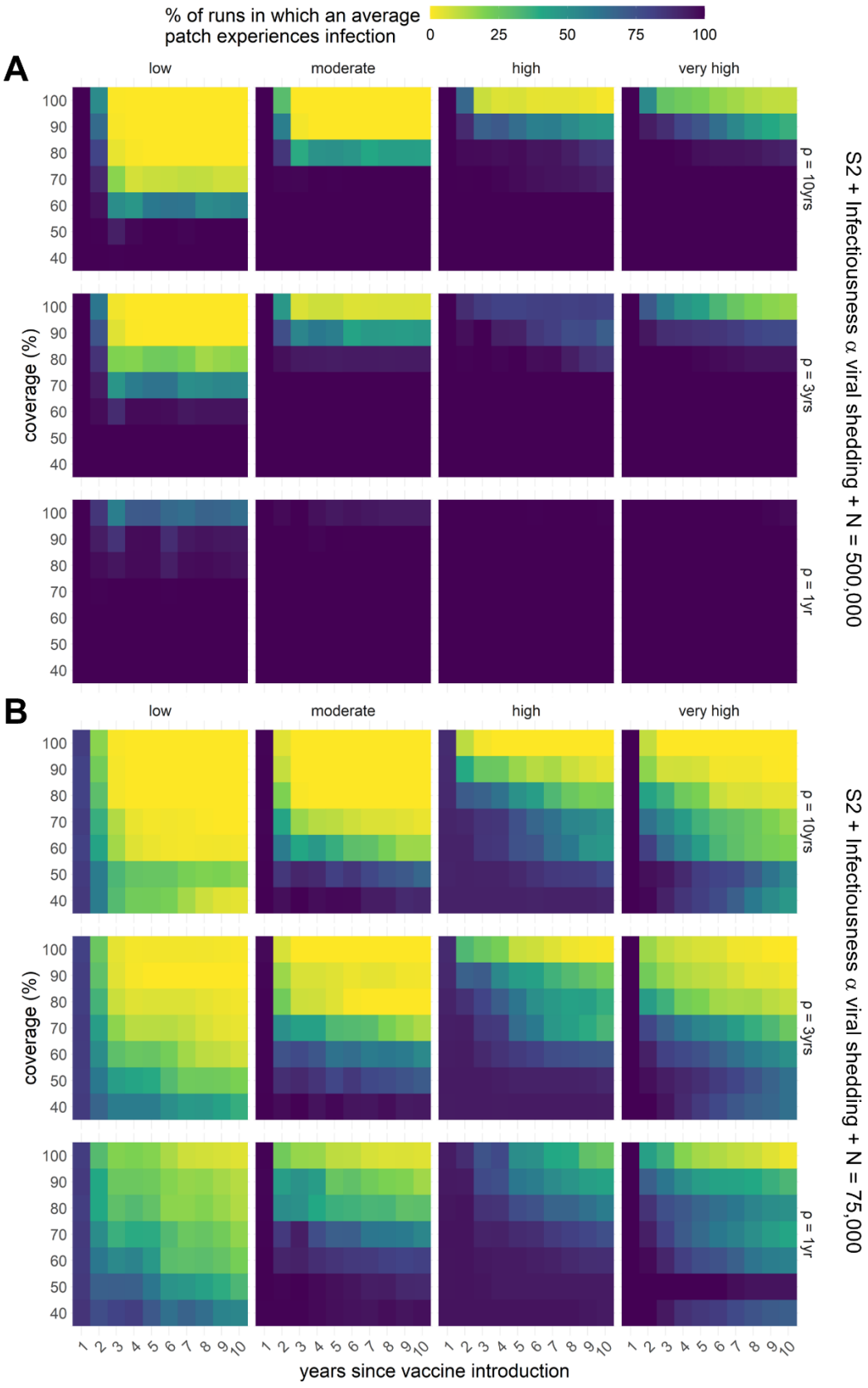


Figure 5.7 The percentage of stochastic model runs in which a patch experienced infection in scenario 2 *for each year following vaccine introduction. Results are shown in different transmission settings (columns) and for different durations of vaccine induced effects (rows) for* ***A****. a population of 500,000 dromedaries and* ***B****. a population of 75,000 dromedaries.*

Stochastic variation

When the population is 500,000 it can be seen in ***Figures 5.6.A*** and ***5.7.A*** that patches either experience infection in close to 100% of stochastic runs or 0% of stochastic runs once vaccine coverage passes a threshold – the value of which depends on transmissibility and duration of vaccine-induced effects, ρ. There is a relatively small coverage window in which stochastic fluctuations occur. This is not the case for the smaller population of 75,000 in which there is a lot more stochastic variation, over a wider window of coverage.

Perverse effects of small increases in low coverage

When the population is 75,000 and transmissibility is either low or very high, patch-level fadeouts are sometimes less likely when vaccine coverage is 50%, compared to when coverage is lower at 40% (***Figures 5.6.B*** and ***5.7.B***). In scenario 1, this occurs when vaccine-induced effects are short-lived. In scenario 2, the effect is seen in low transmission settings when ρ is 10 years and is seen in very high transmission settings regardless of ρ but seen most strongly when ρ is 1 year. This is likely to be due to an interaction between a coverage-dependent vaccine-induced shift in age at first infection and the timing of seasonal births. Such an interaction could affect the relative timing of the peak in infections and the availability of susceptible individuals, making stochastic fadeout less likely despite a slightly higher coverage.

Target Product Profile for the MERS-CoV dromedary vaccine

In order to ascertain the characteristics that the MERS-CoV vaccine would need to have to achieve considerable reductions in infection in a dromedary population the size of that of KSA, the percentage reduction in incidence over ten years post vaccine introduction was assessed under the different vaccine efficacy scenarios. This is presented in ***Figure 5.8***. The reduction in the infectious-state-weighted incidence was not notably different to the reduction in incidence.

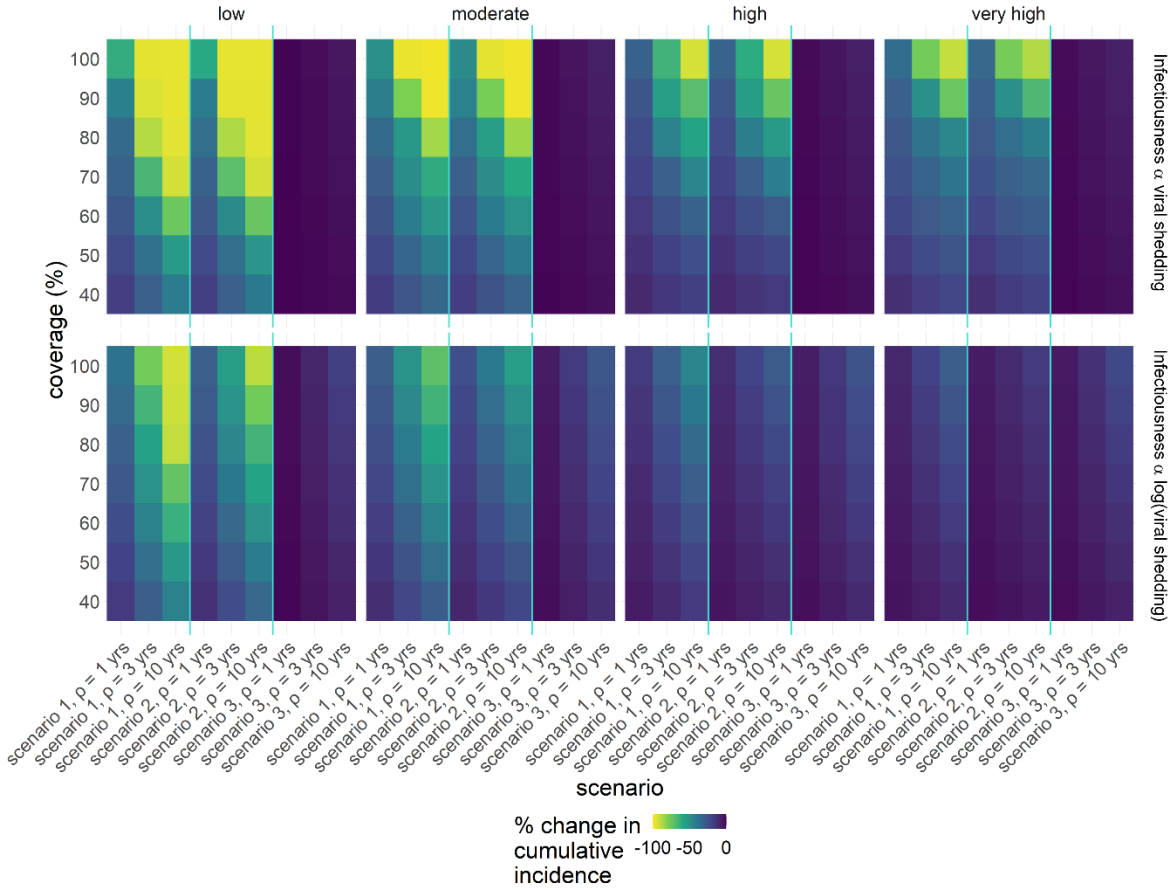


Figure 5.8. The percentage change in cumulative incidence over the ten years following vaccine introduction *in different transmission settings (columns) under different assumptions about the relationship between infectiousness and viral RNA shedding (rows). The percentage change presented is averaged across stochastic model runs.*

When infectiousness was proportional to viral RNA shedding (top row, ***Figure 5.8****):*

When the vaccine candidate was modelled to only be effective in previously infected animals (scenario 3), vaccination had a negligible effect on incidence, with decreases of 0-5%. In contrast, when vaccine candidates were modelled to be effective in both naïve and previously infected animals in scenarios 1 and 2, vaccine-induced reductions in incidence reached >75%. Such reductions were achieved in both scenarios – that is, even if the vaccine only reduced infectiousness and did not reduce susceptibility of vaccinated animals.

In ***Chapters 3*** and ***4*** of this thesis, the transmissibility of MERS-CoV was estimated to fall into high or very high for the majority of the six populations sampled in KSA, with moderate transmissibility estimated for two studies. When ρ was 10, the coverage required to achieve a

75% reduction in incidence in a moderate transmission setting was 80%, rising to >90% in high or very high transmission settings. When ρ was lower at 3 years, coverage of 90% is required to achieve the same reduction in moderate settings. The same reduction was no longer achievable in high transmission settings and required coverage of 100% in very high transmission settings.

In a low transmission setting representative of the populations sampled in South Asia and most of those sampled in Africa, a vaccine coverage of 60% was sufficient to see reductions in incidence decrease by more than 75% over the ten years following vaccine introduction, when ρ was 10 years. When ρ was 3 years, 80% of coverage was required to see the same reduction in incidence. When vaccine induced effects lasted only one year, the greatest reduction achieved was 60%, but this required 100% coverage. At a more achievable coverage of 70%, the greatest reduction in incidence achieved was 30%.

*When infectiousness was proportional to the log of viral RNA shedding (bottom row, **Figure 5.8**):*

The reductions in incidence afforded by vaccination in efficacy scenario 3 were slightly greater when infectiousness was proportional to the log of the viral RNA shedding than when this relationship was assumed to be linear but were still fairly low overall, ranging from 0-25%. Even when the vaccine candidates were assumed to be effective in both naïve and previously infected animals (scenarios 1 and 2), considerable reductions in incidence were only seen in low and moderate transmission settings when the duration of vaccine-induced effects was ten years and coverage was high.

Discussion

In this chapter, a dynamic transmission model was used to simulate the vaccination of young calves against MERS-CoV under different vaccine efficacy scenarios. The results suggest that, if the vaccine candidate is able to reduce infectiousness in both naïve and previously infected dromedaries, large reductions in incidence are possible, even if the vaccine does not reduce

susceptibility of individuals to infection. However, these large reductions require high vaccine coverage, especially in high transmission settings in which transmissibility was representative of that experienced by most dromedary populations studied in the Middle East.

Age optimisation

Vaccination led to the greatest reduction in incidence when calves were targeted in the first few months of life. However, vaccination of very young calves did lead to small increases in annual incidence in animals over the age of 18 months when infectiousness was proportional to viral RNA shedding and transmissibility was moderate, high, or very high (representative of transmissibility in the Middle East and some sampled populations in Africa). Data describing the age-dependent contact patterns between dromedaries and humans is lacking but contact is likely to be higher once calves have been weaned [116]. The age of weaning varies but has been reported to be around 12 months in UAE [116] and between 6-12 months in Eastern Africa [113]. There was still a net increase in annual incidence in animals >12 months when vaccination targeted calves under 5 months, reaching a maximum of 6.4 per 1000 annually on average in ten years following vaccination when transmissibility was high – around half the net increase seen in >18-month-olds. In most settings, it may be optimal to target calves at six months of age to balance the overall reduction in incidence with preventing incidence increases in dromedaries that have more contact with humans.

Whilst scenarios were simulated in which the vaccine was not effective in seronegative animals, it was assumed that the vaccine efficacy was not affected by age itself. During the field trial of the ChAdOx1 MERS vaccine in dromedaries, however, authors hypothesised that the poor efficacy measured in seronegative calves could be due to the age of the calves rather than their serostatus as the seronegative animals were, on average, younger than the seropositive animals [6]. If further field trials support reduced efficacy of the ChAdOx1 MERS vaccine in younger animals, this will need to be accounted for in the estimation of the optimal age of vaccination with ChAdOx1 MERS specifically.

Vaccine impact on persistence and incidence

If a MERS-CoV vaccine candidate is able to reduce infectiousness in naïve and previously infected dromedaries, simulations from the dynamic model indicated that large reductions in incidence are possible if a high proportion of six month old calves are vaccinated. Although the ChAdOx1 MERS vaccine had poor efficacy in naïve animals, potentially due to their age, the MVA vaccine is efficacious in naïve animals.

When infectiousness was assumed to be proportional to viral RNA shedding, vaccination was able to interrupt transmission in a population of 500,000 when vaccine-induced effects lasted three or ten years and provided that coverage was >70% in six month olds. In high transmission settings, coverage needed to be 90-100%. This suggests that, under model assumptions about population structure and vaccine efficacy, it would be difficult to entirely interrupt transmission in some Middle Eastern settings by using vaccination alone, but that incidence could still be greatly reduced. If infectiousness is proportional to the log of viral RNA shedding and vaccination leads to a much smaller decrease in infectiousness, then large reductions in incidence are only likely to be possible in low and moderate transmission settings when coverage is high and vaccine-induced effects are long lasting. Achieving high coverage of MERS-CoV vaccination would be demanding and would require effective engagement with camel owners and other stakeholders. Since dromedaries do not experience significant disease following MERS-CoV infection, there is no veterinary incentive – dromedary vaccination is purely to avert human cases. However, the MVA-based vaccine has been shown to induce a protective immune response to the virus that causes camel pox – a disease which can lead to high levels of mortality in calves and may make vaccination more attractive to owners as a multi-purpose intervention.

It is not clear how long the effects of the MVA-based vaccine or the ChAdOx1 MERS vaccines last in dromedaries. If they last less than three years, the results presented in this chapter suggest that targeting a single age group may not be sufficient to see large reductions in incidence and

that repeat vaccination may need to be considered in future evaluations of expected vaccine impact.

Limitations

There are several limitations to the estimates of vaccine impact provided in this chapter. Firstly, there are limitations pertaining to the representation of dromedary populations. The expected vaccine impact on persistence and on incidence were evaluated in a closed population of 75,000 (intended to represent a small county-level population of dromedaries) and 500,000 (intended to be comparable to the size of the dromedary population of KSA). There is, however, uncertainty about the true number of dromedaries in KSA, with some sources suggesting that 500,000 may be a considerable underestimate[94]. In addition, the population of dromedaries in KSA is not closed – importation of infectious dromedaries likely occurs through international trade from the GHA. However, studies have found that African clade C MERS-CoV viruses do not circulate in KSA, meaning that modelling a closed population in terms of infection sources may be an acceptable simplification. It is likely to be unrealistic, however, to assume no external sources of infection for a small, county-level population of 75,000. With importation of infections, a higher vaccine coverage than is estimated here may be required to interrupt transmission in a small, county-level dromedary population. A third potential limitation of the way populations have been modelled arises from the scarcity of data describing the structure of populations. Whilst the modelled, rudimentary grid of connected sub-populations introduces a level of structure that is more realistic than modelling an entirely homogeneous population, it is unlikely to capture the true structure of dromedary populations. When the population of 75,000 was divided into 25 connected patches of 3,000 dromedaries, for example, this grid is likely to be an oversimplification of true patterns of connectivity between subpopulations as, in reality, herds are smaller than this.

The uncertainty around relative infectiousness of previously infected and vaccinated animals, stemming from the undefined relationship between viral RNA shedding and infectiousness, was

another limitation of the analysis presented in this chapter. The expected vaccine impact was sensitive to the assumed relative infectiousness. The expected reductions in incidence when infectiousness was assumed to be proportional to viral RNA shedding were much greater than when infectiousness was assumed proportional to the log of viral RNA shedding, with very different implications for the feasibility of achieving large reduction in MERS-CoV incidence in dromedaries through vaccination.

Further to these limitations, there are two main ways in which vaccine simulation could be extended. Firstly, heterogeneity in vaccine coverage and transmissibility in neighbouring patches could be incorporated. In ***Chapter 3***, transmissibility was estimated to vary sub-nationally as well as internationally, and it is plausible that higher vaccination coverage could be achieved in certain populations and husbandry systems than others. Secondly, a variety of repeat dosing regimens could be considered in addition to the strategies targeting a single age-group that were simulated in this analysis.

Conclusions

Uncertainties remain about the efficacy of MERS-CoV vaccine candidates in dromedaries but simulating vaccination within a dynamic transmission model under different efficacy scenarios suggested that large reductions in incidence are possible if the vaccine is able to reduce infectiousness of naïve animals as well as previously infected animals.

Large reductions are possible even if the vaccine candidate does not reduce susceptibility to infection, provided coverage in calves is high. Calves should be targeted at around six months old to balance achieving large overall reductions in incidence with avoiding increases in incidence in older animals that may have more contact with humans.

Coverage will need to be high to achieve large reductions in transmission, especially in high transmission settings. Ideally vaccine-induced effects would last longer than three years to see impact at levels of coverage that may be feasible to achieve. Once more is known about vaccine

efficacy and duration of protection, future evaluations of potential vaccine impact could consider repeated vaccination regimens.

Chapter 6:

Discussion

The motivation of this thesis was to better characterise the transmission dynamics of MERS-CoV in dromedary camels and to provide a quantitative mechanistic model of transmission with which to simulate potential vaccination strategies. Using a combination of catalytic and mechanistic modelling methods, the publicly available data on MERS-CoV in dromedaries was harnessed in ways it has not been previously: to estimate transmissibility of the virus in populations across Africa, the Middle East, and South Asia, and to develop a mathematical model of MERS-CoV transmission in the zoonotic reservoir. Together, these approaches have contributed to a greater understanding of and better quantified the transmissibility of MERS-CoV, including: providing the first data-driven estimates of R_0 and the Critical Community Size (CCS) in dromedaries; allowing for simulation of vaccination strategies; and highlighting the importance of addressing remaining uncertainties around immunity, vaccine efficacy and population structure. The contributions this research has made to our understanding of MERS-CoV transmission in dromedaries are discussed in this final chapter, as well as the limitations of this thesis and potential directions for future work.

Summary of the contributions made by this thesis

My research started with a systematic review of MERS-CoV seroprevalence and RNA prevalence in dromedary populations presented in Chapter 2. This review clarified the state of current knowledge and helped to shape the chapters that followed it in several important ways. Firstly, the consistent increase in seroprevalence with age and high prevalence of infection in calves painted a clear picture of MERS-CoV as an endemic disease in dromedary populations across much of Africa and South Asia and the Middle East, despite all reports of human MERS-CoV infection being traced to the Arabian Peninsula or Iran. These indications of widespread circulation informed the assumption of endemicity underpinning the use of catalytic models to estimate transmissibility in Chapter 3. Secondly, the systematic review in Chapter 2 highlighted that rapid reinfection was documented in seropositive animals in multiple longitudinal studies.

This formed the basis for including reinfection in the dynamic transmission model in Chapter 4 and indicated that antibodies are not a proxy for complete immunity. Thirdly, as is the case for other zoonotic diseases such as avian influenza [110], the review found that multiple studies measured prevalence to be higher at sites like markets where different populations of dromedaries mix, stressing the importance of contact networks and movement in MERS-CoV transmission dynamics. Finally, the age-stratified seroprevalence data collated during the review allowed the estimation of MERS-CoV transmissibility in dromedaries using catalytic modelling approaches.

In Chapter 3, catalytic models of infection were fit to age-stratified seroprevalence data to produce Force of Infection (FoI) estimates for MERS-CoV in dromedaries. The FoI was generally estimated to be higher in populations sampled in the Middle East, compared to populations sampled in Africa and South Asia. The variability of the FoI across populations emphasised the importance of simulating vaccination in different transmission settings and suggested that higher vaccine coverage is likely to be required to control transmission in some regions than others. Comparison of different catalytic models of seroconversion supported the presence of protective maternally acquired antibodies (mAbs) against MERS-CoV in calves. The mAbs were estimated to wane over the first few months of life, in line with previous findings from two small, longitudinal studies[116], [131]. The two most advanced vaccine candidates for dromedaries do not express MERS-CoV spike protein on their surface so are unlikely to be inhibited by mAbs [6], [8] but, if other vaccine platforms more susceptible to inhibition are considered, this work suggests that calves should be targeted after 6 months of age.

In Chapter 4, the first stochastic, dynamic, model of MERS-CoV transmission in dromedary camel populations was developed. R_0 was estimated by calibrating the dynamic model to the FoI estimates inferred in Chapter 3. Dynamics were sensitive to uncertainty around the relative infectiousness of reinfections which was varied from 1-50% depending on whether infectiousness was assumed to be proportional to either the viral RNA shedding or the log viral

RNA shedding collected in vaccination field trials by Alharbi *et al.,* (2019) [6]. When infectiousness was proportional to the log of viral RNA shedding, most R_0 estimates were between 1.4-2.8 outside of the Middle East (excluding one population sampled in Ethiopia where R_0 was 4.5) and 2.3-5.0 for populations sampled within the Middle East. When infectiousness was proportional to viral RNA shedding instead, R_0 estimates were between 1.9-8.7 for most populations outside of the Middle East (21.9 for the Ethiopian population) and between 5.3-25.8 within the Middle East. The higher transmissibility in dromedary populations in the Middle East estimated in this thesis – coupled with work by Zhou *et al.,* (2021) showing Middle Eastern clade B viruses to have a reproductive advantage over African clade C viruses in *ex vivo* lung tissue [109] – suggests that viral genetic differences could affect the population-level transmissibility of MERS-CoV in dromedaries. Understanding the relative contributions of clade genetics to the higher transmissibility in the Middle East over other factors such as the intensification of farming practices will be crucial to assess if more active measures need to be put in place to prevent introduction of clade B into African dromedary populations.

Having estimated R_0, the dynamic model was then used to estimate the CCS and the mean period between peaks in infections for different transmission settings. When relative infectiousness of reinfections was low, CCS estimates ranged between 25,000-75,000 and between 500-2,500 when it was high. In all scenarios, the CCS was estimated to be larger than most reported herd sizes, emphasising the importance of focusing interventions on reducing inter-herd infections for interrupting transmission. The CCS also depended on transmissibility which, together with the difference in R_0 across populations, suggested that MERS-CoV may be able to persist in a population 2-20 times smaller in high transmission settings found in the Arabian Peninsula, compared to lower transmission settings. This means that vaccine coverage would likely need to be much higher to interrupt transmission in the Arabian Peninsula. Finally, it was shown that seasonal calving was sufficient to drive annual peaks in infection in moderately sized populations, indicating that there could be a higher risk of zoonotic spillover at certain times of the year in some regions. The time in which infection peaked relative to the calving season was

dependent on transmissibility and the assumed infectiousness of reinfected animals. Seasonality of zoonotic transmission has previously been suggested by phylogenetic analysis [2]. Longitudinal, empirical studies of the timing of seasonal peaks could help better direct resources to prevent seasonal spillover.

In Chapter 5, the dynamic model of MERS-CoV transmission was extended to simulate dromedary vaccination and provided the first estimates of the potential impact of vaccines against MERS-CoV in dromedary camels under several alternative efficacy scenarios. When the vaccine was effective in naïve and previously infected animals, vaccination of calves in the first few months of life led to the greatest reduction in incidence. However, in high transmission settings, when infectiousness was assumed to be proportional to viral RNA shedding, vaccinating very young calves led to a small increase in incidence in dromedaries over the age of 12 months – animals which humans may have more contact with. Depending on the level of additional contact humans have with older animals, in high transmission environments where infection is not likely to be totally interrupted it may be beneficial to slightly delay vaccination until calves are 6 months old or, repeat vaccination in adult dromedaries. This chapter provided the first estimates of the potential impact of vaccines against MERS-CoV in dromedary camels. The impact was very dependent on assumptions about relative infectiousness. When infectiousness was proportional to viral shedding, results suggested that large reductions in incidence are possible if the vaccine is able to reduce infectiousness of naïve animals as well as previously infected animals, even if the vaccine does not reduce susceptibility to infection, provided coverage in calves is high. When infectiousness was proportional to the log of viral RNA shedding, meaning vaccination led to a much smaller reduction in infectiousness, large reductions in incidence were only possible in low transmission settings. Although reductions in infectious viral particles were comparable to reductions in viral RNA shedding in four vaccinated calves in MVA-based vaccine trial, larger empirical studies of the relative infectiousness of vaccinated and reinfected dromedaries are critical to narrow down impact estimates.

Limitations

The main limitations of this body of work arose from both data scarcity and shortcomings of the model frameworks. In the catalytic modelling work, one primary limitation was the potential for overestimation of the transmissibility of MERS-CoV if populations had very high seroprevalence approaching the assumed test sensitivity threshold in young age classes, or if the assumption of endemic equilibrium was invalid and seroprevalence reflected the height of an outbreak. If the FoI was overestimated in these cases, the dynamics simulated at a very high transmissibility would not be representative of true transmission settings. The second main limitation was that the rate of seroreversion could not be reliably identified due to uncertainty around test sensitivity and challenges distinguishing long-lasting antibodies from repeated boosting of antibodies following recurring infection in the catalytic model framework. Documented reinfection of seropositive animals shows that antibodies are not a proxy for complete immunity to MERS-CoV. With this in mind, the rate of seroreversion estimated in Chapter 3 did not inform parameterisation of waning immunity in the transmission model, meaning this limitation did not impinge on the dynamic modelling work.

The main limitations of the dynamic modelling chapters centred around three main data gaps which necessitated modelling transmission and vaccination under a series of different assumptions. Firstly, the undefined relationship between viral RNA shedding data and infectiousness led to uncertainty in the relative infectiousness of reinfected animals and infected vaccinated animals. This, in turn, led to differences in estimates of R_0, the CCS and vaccine impact. Better quantifying the relative infectiousness of reinfected and vaccinated animals should be a priority for establishing a clearer picture of the dynamics of MERS-CoV in dromedaries. Secondly, there was a lack of data describing dromedary population structures. Population structure was shown to affect dynamics around persistence of transmission but, as it was not possible to base metapopulation model structures on true populations, a rudimentary grid of connected sub-populations was used to approximate the structuring of the population into herds or patches. Finally, the effect of vaccination on susceptibility and vaccine

effectiveness in naïve animals were not clear from current field trials so a range of scenarios were included. As these three aspects influencing MERS-CoV transmission in dromedaries become clearer, it will be possible to improve mathematical models of MERS-CoV transmission and become increasingly confident that they accurately represent transmission in the zoonotic reservoir.

Future extensions to the work in this thesis

The work in this thesis lays the ground for further research to support the prevention of zoonotic MERS-CoV infections in a number of ways. Three potential extensions are outlined below.

1) Tailoring the generalised dynamic model to specific dromedary populations

The generalised dynamic model developed in this thesis could be tailored to specific dromedary populations of interest to decision makers. Whilst the effect of population-specific transmissibility on dynamics and vaccine impact has been assessed in this thesis, other population-specific variables found to be important – such as population structure and connection between herds – could be adapted to better represent dromedaries in a particular region. Dromedary network data would need to be collected to facilitate this. For example, quantifying dromedary movement along routes such as those mapped by Gikonyo *et al*. (2018) for Kenya [112] to provide the size and timing of flows of dromedaries from different herds or areas into common grazing land or markets would provide greater clarity about the mixing of dromedaries and opportunities to control transmission in a particular area. A comprehensive system to track dromedary movements nationwide using microchips was approved in 2018 by the Ministry of Environment, Water and Agriculture in KSA [239] and has been applied to dromedaries involved in racing and shows [240]. Due to the potential sensitivities around tracking dromedaries, consultation with owners alongside the nationwide rollout of this scheme may make it more acceptable to those impacted and result in a more sustainable source of data. If successful, this could provide a rich mobility data stream and an opportunity to better

simulate realistic transmission of MERS-CoV in dromedaries in the country that bears the brunt of the MERS burden. This would allow vaccine impacts to be assessed with more confidence.

2) Integrating genetic data streams into the dynamic model

Despite extensive unidirectional trade from the Greater Horn of Africa to the Arabian Peninsula, MERS-CoV exhibits region-specific genetic diversity, with all viruses sampled from dromedaries and people in the Middle East falling into clades A (historically) and B (contemporary), and all samples from dromedaries in Africa falling into clade C [68], [108]. Studies have shown differences in reproductive fitness of the clades in *ex vivo* tissue [109], however different clades were not considered in the models developed in this thesis. Integration of MERS-CoV genetic data into the dynamic model framework could enable the dynamics of the different MERS-CoV clades to be investigated. This would be particularly illuminating at sites such as fattening pens in KSA where imported dromedaries mix with local dromedaries. A recent study at an abattoir in KSA found only clade B viruses to be circulating in both imported and local animals [108]. Further studies identifying clade types as well as measures of incidence in imported populations could be used to fit clade-specific transmission parameters within the dynamic model and better understand the potential threat clade B viruses pose internationally.

3) Relating reductions in dromedary infectiousness to reductions in zoonotic spillover

The research described in this thesis has provided a framework for simulating expected vaccine-induced reductions in the incidence of MERS-CoV infection in dromedary populations. Future research to better define the relationship between the number of infectious dromedaries and the risk of zoonotic spillover events would allow this expected reduction in infection in the animal reservoir to be translated into the expected number of human cases averted. Defining the relationship between infection in the reservoir and zoonotic spillover risk is likely to be challenging as evidence suggests that dromedary-to-human MERS-CoV infection is a relatively rare event and often goes unreported. It would likely require heightened surveillance in a large group of individuals from high-risk populations (such as camel owners and traders) in order to

identify zoonotic spillover events, alongside collection of qualitative data describing the individuals' interactions with dromedaries. Although demanding, this type of study could form a crucial bridge between reducing infection in dromedaries and reducing spillover events. Extending the dynamic model to include zoonotic spillover would permit health economists to evaluate the cost-effectiveness of dromedary vaccination as an intervention against MERS-CoV. Relating dromedary infection to zoonotic spillover may also inform vaccine distribution. If humans have more contact with dromedaries of a certain age or in certain settings, for example, incorporating this into simulations may shift the optimal target population for vaccination.

Conclusions

Understanding the transmission dynamics of MERS-CoV in dromedary camels is vital to evaluating the potential public health impacts of animal vaccination but has been hindered by the scarcity of data describing what is a largely asymptomatic infection in this species. By using age-stratified seroprevalence and viral load data extracted from published studies, however, I have developed a dynamic model of MERS-CoV transmission in dromedaries, allowing for the first evaluations of the potential impact of dromedary vaccination on transmission. Whilst uncertainties around immunity and aspects of vaccine efficacy remain, five key conclusions about the transmission dynamics of MERS-CoV in dromedary populations can be drawn from this thesis. They are as follows:

1) MERS-CoV can be highly transmissible in dromedaries in populations in Africa and South Asia, but transmissibility is generally highest amongst populations in the Middle East. This geographical variation in dynamics demands setting-specific adaptation of vaccination strategies.
2) The CCS for MERS-CoV in dromedaries is relatively small – especially when reinfected animals are assumed to still be considerably infectious – but still larger than the size of

most individual herds. Interrupting transmission between herds is key to seeing large reductions in transmission.

3) The highly seasonal calving of dromedaries is likely to be sufficient to drive annual peaks in endemic infection in moderately sized populations. If empirical studies of infection over time confirm this seasonality, interventions such as PPE campaigns and vaccination drives could be seasonally focused to achieve maximum reduction in zoonotic spillover events.
4) Better quantifying the reduction in infectiousness afforded by immunity from previous infections and vaccination should be a priority for improving the reliability of mathematical models of the dynamics of MERS-CoV in dromedaries.
5) MERS-CoV vaccination could lead to large reductions in incidence in dromedaries, even if vaccines only reduce infectiousness rather than protecting individuals from infection, providing that high vaccination coverage is reached in calves.

As zoonotic disease continues to pose a major threat to public health globally, the development of reliable quantitative frameworks within which to study the dynamics of zoonotic infectious diseases in reservoir populations is only going to increase in importance. Dynamic models such as those developed in this thesis provide a framework in which to simulate vaccination strategies and, together with further empirical studies of vaccine efficacy, offer an important contribution to informing effective responses to the zoonotic transmission of MERS-CoV going forward.

Bibliography

[1] WHO, "WHO MERS-CoV Global Summary and Assessment of Risk, August 2018," Geneva, Aug. 2018.

[2] G. Dudas, L. M. Carvalho, A. Rambaut, and T. Bedford, "MERS-CoV spillover at the camel-human interface," *Elife*, vol. 7, Jan. 2018, doi: 10.7554/eLife.31257.

[3] E. I. Azhar *et al.*, "Evidence for Camel-to-Human Transmission of MERS Coronavirus," *N. Engl. J. Med.*, vol. 370, no. 26, pp. 2499–2505, Jun. 2014, doi: 10.1056/nejmoa1401505.

[4] M. A. Müller *et al.*, "Presence of Middle East respiratory syndrome coronavirus antibodies in Saudi Arabia: A nationwide, cross-sectional, serological study," *Lancet Infect. Dis.*, vol. 15, no. 5, pp. 559–564, May 2015, doi: 10.1016/S1473-3099(15)70090-3.

[5] FAO-OIE-WHO MERS Technical Working Group *et al.*, "MERS: Progress on the global response, remaining challenges and the way forward," *Antiviral Research*, vol. 159. Elsevier B.V., pp. 35–44, Nov. 01, 2018, doi: 10.1016/j.antiviral.2018.09.002.

[6] N. K. Alharbi *et al.*, "Humoral Immunogenicity and Efficacy of a Single Dose of ChAdOx1 MERS Vaccine Candidate in Dromedary Camels," *Sci. Rep.*, vol. 9, no. 1, Dec. 2019, doi: 10.1038/s41598-019-52730-4.

[7] N. K. Alharbi *et al.*, "ChAdOx1 and MVA based vaccine candidates against MERS-CoV elicit neutralising antibodies and cellular immune responses in mice," *Vaccine*, vol. 35, no. 30, pp. 3780–3788, Jun. 2017, doi: 10.1016/j.vaccine.2017.05.032.

[8] B. L. Haagmans *et al.*, "An orthopoxvirus-based vaccine reduces virus excretion after MERS-CoV infection in dromedary camels," *Science (80-.).*, vol. 351, no. 6268, pp. 77–81, Jan. 2016, doi: 10.1126/science.aad1283.

[9] K. A. M. Gaythorpe, C. L. Trotter, and A. J. K. Conlan, "Modelling norovirus transmission and vaccination," *Vaccine*, vol. 36, no. 37, pp. 5565–5571, Sep. 2018, doi: 10.1016/J.VACCINE.2018.07.053.

[10] K. M. Bubar *et al.*, "Model-informed COVID-19 vaccine prioritization strategies by age and serostatus," *Science (80-.).*, vol. 371, no. 6532, pp. 916–921, Feb. 2021, doi: 10.1126/SCIENCE.ABE6959/SUPPL_FILE/PAPV3.PDF.

[11] N. M. Ferguson, I. Rodríguez-Barraquer, I. Dorigatti, L. Mier-Y-Teran-Romero, D. J. Laydon, and D. A. T. Cummings, "Benefits and risks of the sanofi-pasteur dengue vaccine: Modeling optimal deployment," *Science (80-.).*, vol. 353, no. 6303, pp. 1033–1036, Sep. 2016, doi: 10.1126/SCIENCE.AAF9590/SUPPL_FILE/AAF9590_FERGUSON_SM.PDF.

[12] A. J. Kucharski, R. M. Eggo, C. H. Watson, A. Camacho, S. Funk, and W. J. Edmunds, "Effectiveness of Ring Vaccination as Control Strategy for Ebola Virus Disease," *Emerg. Infect. Dis.*, vol. 22, no. 1, p. 105, Jan. 2016, doi: 10.3201/EID2201.151410.

[13] A. Camacho *et al.*, "Real-time dynamic modelling for the design of a cluster-randomized phase 3 Ebola vaccine trial in Sierra Leone," *Vaccine*, vol. 35, no. 4, pp. 544–551, Jan. 2017, doi: 10.1016/J.VACCINE.2016.12.019.

[14] G. Chowell, C. Viboud, X. Wang, S. M. Bertozzi, and M. A. Miller, "Adaptive Vaccination Strategies to Mitigate Pandemic Influenza: Mexico as a Case Study," *PLoS One*, vol. 4, no. 12, p. e8164, 2009, doi: 10.1371/JOURNAL.PONE.0008164.

[15] D. A. J. Tyrrell and M. L. Bynoe, "Cultivation of a Novel Type of Common-cold Virus in

Organ Cultures," *Br. Med. J.*, vol. 1, no. 5448, pp. 1467–1470, Jun. 1965, doi: 10.1136/bmj.1.5448.1467.

[16] K. McIntosh, J. H. Dees, W. B. Becker, A. Z. Kapikian, and R. M. Chanock, "Recovery in tracheal organ cultures of novel viruses from patients with respiratory disease.," *Proc. Natl. Acad. Sci. U. S. A.*, vol. 57, no. 4, pp. 933–940, Apr. 1967, doi: 10.1073/pnas.57.4.933.

[17] "Virology: Coronaviruses," *Nature*, vol. 220, no. 5168. Nature Publishing Group, p. 650, 1968, doi: 10.1038/220650b0.

[18] C. C. Y. Yip *et al.*, "A six-year descriptive epidemiological study of human coronavirus infections in hospitalized patients in Hong Kong," *Virol. Sin.*, vol. 31, no. 1, pp. 41–48, Feb. 2016, doi: 10.1007/s12250-016-3714-8.

[19] D. Isaacs, D. Flowers, J. R. Clarke, H. B. Valman, and M. R. MacNaughton, "Epidemiology of coronavirus respiratory infections," *Arch. Dis. Child.*, vol. 58, no. 7, pp. 500–503, Jul. 1983, doi: 10.1136/adc.58.7.500.

[20] S. B. Greenberg, "Update on Human Rhinovirus and Coronavirus Infections," *Semin. Respir. Crit. Care Med.*, vol. 37, no. 4, pp. 555–571, Aug. 2016, doi: 10.1055/s-0036-1584797.

[21] S. Su *et al.*, "Epidemiology, Genetic Recombination, and Pathogenesis of Coronaviruses," *Trends in Microbiology*, vol. 24, no. 6. Elsevier Ltd, pp. 490–502, Jun. 01, 2016, doi: 10.1016/j.tim.2016.03.003.

[22] A. S. Monto, "Coronaviruses," *Yale Journal of Biology and Medicine*, vol. 47, no. 4. Yale Journal of Biology and Medicine, pp. 234–251, 1974, Accessed: Jan. 22, 2021. [Online]. Available: https://www.ncbi.nlm.nih.gov/pmc/articles/PMC2595130/.

[23] N. J. MacLachlan and E. J. Dubovi, "Coronaviridae," in *Fenner's Veterinary Virology (Fifth Edition)*, N. J. MacLachlan and E. J. Dubovi, Eds. Elsevier, 2017, pp. 435–461.

[24] Y. Guan *et al.*, "Isolation and characterization of viruses related to the SARS coronavirus from animals in Southern China," *Science (80-.).*, vol. 302, no. 5643, pp. 276–278, Oct. 2003, doi: 10.1126/science.1087139.

[25] WHO, "Consensus document on the epidemiology of severe acute respiratory syndrome (SARS)," 2003.

[26] H. D. Song *et al.*, "Cross-host evolution of severe acute respiratory syndrome coronavirus in palm civet and human," *Proc. Natl. Acad. Sci. U. S. A.*, vol. 102, no. 7, pp. 2430–2435, Feb. 2005, doi: 10.1073/PNAS.0409608102/SUPPL_FILE/09608TABLE4.PDF.

[27] WHO EMRO, "MERS situation update - December 2021," Nasr City Cairo, Dec. 2021. Accessed: Mar. 06, 2022. [Online]. Available: www.emro.who.int.

[28] Y. Liu, A. A. Gayle, A. Wilder-Smith, and J. Rocklöv, "The reproductive number of COVID-19 is higher compared to SARS coronavirus," *J. Travel Med.*, vol. 27, no. 2, pp. 1–4, Mar. 2020, doi: 10.1093/JTM/TAAA021.

[29] W. Yang and J. Shaman, "Development of a model-inference system for estimating epidemiological characteristics of SARS-CoV-2 variants of concern," *Nat. Commun. 2021 121*, vol. 12, no. 1, pp. 1–9, Sep. 2021, doi: 10.1038/s41467-021-25913-9.

[30] M. O'Driscoll *et al.*, "Age-specific mortality and immunity patterns of SARS-CoV-2," *Nat. 2020 5907844*, vol. 590, no. 7844, pp. 140–145, Nov. 2020, doi: 10.1038/s41586-020-2918-0.

[31] R. Verity *et al.*, "Estimates of the severity of coronavirus disease 2019: a model-based

analysis," *Lancet. Infect. Dis.*, vol. 20, no. 6, p. 669, Jun. 2020, doi: 10.1016/S1473-3099(20)30243-7.

[32] S. Lytras *et al.*, "Exploring the Natural Origins of SARS-CoV-2 in the Light of Recombination," *Genome Biol. Evol.*, vol. 14, no. 2, Feb. 2022, doi: 10.1093/GBE/EVAC018.

[33] V. S. Raj *et al.*, "Dipeptidyl peptidase 4 is a functional receptor for the emerging human coronavirus-EMC," *Nature*, vol. 495, no. 7440, pp. 251–254, Mar. 2013, doi: 10.1038/nature12005.

[34] W. Li *et al.*, "Angiotensin-converting enzyme 2 is a functional receptor for the SARS coronavirus," *Nat. 2003 4266965*, vol. 426, no. 6965, pp. 450–454, Nov. 2003, doi: 10.1038/nature02145.

[35] R. Yan, Y. Zhang, Y. Li, L. Xia, Y. Guo, and Q. Zhou, "Structural basis for the recognition of SARS-CoV-2 by full-length human ACE2," *Science (80-.).*, vol. 367, no. 6485, pp. 1444–1448, Mar. 2020, doi: 10.1126/SCIENCE.ABB2762/SUPPL_FILE/ABB2762S1.MP4.

[36] A. Banerjee, K. Kulcsar, V. Misra, M. Frieman, and K. Mossman, "Bats and coronaviruses," *Viruses*, vol. 11, no. 1. MDPI AG, Jan. 01, 2019, doi: 10.3390/v11010041.

[37] P. C. Y. Woo, S. K. P. Lau, K. S. M. Li, A. K. L. Tsang, and K. Y. Yuen, "Genetic relatedness of the novel human group C betacoronavirus to Tylonycteris bat coronavirus HKU4 and Pipistrellus bat coronavirus HKU5," *Emerging Microbes and Infections*, vol. 1, no. 11. Emerg Microbes Infect, 2012, doi: 10.1038/emi.2012.45.

[38] V. M. Corman *et al.*, "Rooting the Phylogenetic Tree of Middle East Respiratory Syndrome Coronavirus by Characterization of a Conspecific Virus from an African Bat," *J. Virol.*, vol. 88, no. 19, pp. 11297–11303, Oct. 2014, doi: 10.1128/jvi.01498-14.

[39] S. K. P. Lau *et al.*, "Severe acute respiratory syndrome coronavirus-like virus in Chinese horseshoe bats," *Proc. Natl. Acad. Sci. U. S. A.*, vol. 102, no. 39, pp. 14040–14045, Sep. 2005, doi: 10.1073/pnas.0506735102.

[40] X. Y. Ge *et al.*, "Isolation and characterization of a bat SARS-like coronavirus that uses the ACE2 receptor," *Nature*, vol. 503, no. 7477, pp. 535–538, 2013, doi: 10.1038/nature12711.

[41] J. E. Pekar *et al.*, "SARS-CoV-2 emergence very likely resulted from at least two zoonotic events," *preprint*. Feb. 26, 2022, doi: 10.5281/ZENODO.6291628.

[42] M. A. Müller *et al.*, "Mers coronavirus neutralizing antibodies in camels, eastern Africa, 1983–1997," *Emerg. Infect. Dis.*, vol. 20, no. 12, pp. 2093–2095, Dec. 2014, doi: 10.3201/eid2012.141026.

[43] Z. A. Memish *et al.*, "Middle East respiratory syndrome coronavirus in Bats, Saudi Arabia," *Emerg. Infect. Dis.*, vol. 19, no. 11, pp. 1819–1823, Nov. 2013, doi: 10.3201/eid1911.131172.

[44] S. Cauchemez, M. D. Van Kerkhove, S. Riley, C. A. Donnelly, C. Fraser, and N. M. Ferguson, "Transmission scenarios for middle east respiratory syndrome coronavirus (MERS-CoV) and how to tell them apart," *Eurosurveillance*, vol. 18, no. 24, Jun. 2013, doi: 10.2807/ese.18.24.20503-en.

[45] S. Cauchemez *et al.*, "Unraveling the drivers of MERS-CoV transmission," *Proc. Natl. Acad. Sci. U. S. A.*, vol. 113, no. 32, pp. 9081–9086, Aug. 2016, doi: 10.1073/pnas.1519235113.

[46] M. E. Killerby, H. M. Biggs, C. M. Midgley, S. I. Gerber, and J. T. Watson, "Middle east respiratory syndrome coronavirus transmission," *Emerg. Infect. Dis.*, vol. 26, no. 2, pp.

191–198, 2020, doi: 10.3201/eid2602.190697.

[47] Z. A. Memish, A. I. Zumla, R. F. Al-Hakeem, A. A. Al-Rabeeah, and G. M. Stephens, "Family Cluster of Middle East Respiratory Syndrome Coronavirus Infections," *N. Engl. J. Med.*, vol. 368, no. 26, pp. 2487–2494, Jun. 2013, doi: 10.1056/nejmoa1303729.

[48] J. C. Hunter *et al.*, "Transmission of middle east respiratory syndrome coronavirus infections in healthcare settings, abu dhabi," *Emerg. Infect. Dis.*, vol. 22, no. 4, pp. 647–656, Apr. 2016, doi: 10.3201/eid2204.151615.

[49] S. H. Park *et al.*, "Outbreaks of middle east respiratory syndrome in two hospitals initiated by a single patient in Daejeon, South Korea," *Infect. Chemother.*, vol. 48, no. 2, pp. 99–107, 2016, doi: 10.3947/ic.2016.48.2.99.

[50] M. M. Al-Abdallat *et al.*, "Hospital-associated outbreak of middle east respiratory syndrome coronavirus: A serologic, epidemiologic, and clinical description," *Clin. Infect. Dis.*, vol. 59, no. 9, pp. 1225–1233, Nov. 2014, doi: 10.1093/cid/ciu359.

[51] A. J. Kucharski and C. L. Althaus, "The role of superspreading in middle east respiratory syndrome coronavirus (MERS-CoV) transmission," *Eurosurveillance*, vol. 20, no. 25, pp. 14–18, Jun. 2015, doi: 10.2807/1560-7917.ES2015.20.25.21167/CITE/PLAINTEXT.

[52] A. M. Zaki, S. van Boheemen, T. M. Bestebroer, A. D. M. E. Osterhaus, and R. A. M. Fouchier, "Isolation of a Novel Coronavirus from a Man with Pneumonia in Saudi Arabia," *N. Engl. J. Med.*, vol. 367, no. 19, pp. 1814–1820, Nov. 2012, doi: 10.1056/nejmoa1211721.

[53] B. Hijawi *et al.*, "Supplement 1 2013 Eastern Mediterranean Health Journal La Revue de Santé de la Méditerranée orientale S12 Country experience."

[54] D. S. Hui, E. I. Azhar, Y. J. Kim, Z. A. Memish, M. don Oh, and A. Zumla, "Middle East respiratory syndrome coronavirus: risk factors and determinants of primary, household, and nosocomial transmission," *The Lancet Infectious Diseases*, vol. 18, no. 8. Lancet Publishing Group, pp. e217–e227, Aug. 01, 2018, doi: 10.1016/S1473-3099(18)30127-0.

[55] A. Abbad *et al.*, "Middle East respiratory syndrome coronavirus (MERS-CoV) neutralising antibodies in a high-risk human population, Morocco, November 2017 to January 2018," *Eurosurveillance*, vol. 24, no. 48, pp. 1–8, Nov. 2019, doi: 10.2807/1560-7917.ES.2019.24.48.1900244.

[56] C. K. P. Mok *et al.*, "T-cell responses to MERS coronavirus infection in people with occupational exposure to dromedary camels in Nigeria: an observational cohort study," *Lancet Infect. Dis.*, vol. 0, no. 0, 2020, doi: 10.1016/S1473-3099(20)30599-5.

[57] A. S. M. Sayed, S. S. Malek, and M. F. N. Abushahba, "Seroprevalence of Middle East Respiratory Syndrome Corona Virus in dromedaries and their traders in upper Egypt," *J. Infect. Dev. Ctries.*, vol. 14, no. 2, pp. 191–198, 2020, doi: 10.3855/jidc.10862.

[58] J. Zheng *et al.*, "Middle East respiratory syndrome coronavirus seropositivity in camel handlers and their families, Pakistan," *Emerg. Infect. Dis.*, vol. 25, no. 12, pp. 2307–2309, 2019, doi: 10.3201/eid2512.191169.

[59] A. N. Kiyong'a *et al.*, "Middle East respiratory syndrome coronavirus (MERS-CoV) seropositive camel handlers in Kenya," *Viruses*, vol. 12, no. 4, Apr. 2020, doi: 10.3390/v12040396.

[60] C. Gossner *et al.*, "Human-Dromedary Camel Interactions and the Risk of Acquiring Zoonotic Middle East Respiratory Syndrome Coronavirus Infection," *Zoonoses Public Health*, vol. 63, no. 1, pp. 1–9, Feb. 2016, doi: 10.1111/zph.12171.

[61] A. A. Degnah *et al.*, "Seroprevalence of MERS-CoV in healthy adults in western Saudi Arabia, 2011–2016," *J. Infect. Public Health*, vol. 13, no. 5, pp. 697–703, May 2020, doi: 10.1016/j.jiph.2020.01.001.

[62] C. A. Donnelly, M. R. Malik, A. Elkholy, S. Cauchemez, and M. D. Van Kerkhove, "Worldwide reduction in MERS cases and deaths since 2016," *Emerg. Infect. Dis.*, vol. 25, no. 9, pp. 1758–1760, 2019, doi: 10.3201/eid2509.190143.

[63] Kandeil *et al.*, "Middle East Respiratory Syndrome Coronavirus (MERS-CoV) in Dromedary Camels in Africa and Middle East," *Viruses*, vol. 11, no. 8, p. 717, Aug. 2019, doi: 10.3390/v11080717.

[64] M. G. Hemida, M. Waheed, A. M. Ali, and A. Alnaeem, "Detection of the Middle East respiratory syndrome coronavirus in dromedary camel's seminal plasma in Saudi Arabia 2015–2017," *Transbound. Emerg. Dis.*, 2020, doi: 10.1111/tbed.13610.

[65] M. F. Yusof *et al.*, "Diversity of Middle East respiratory syndrome coronaviruses in 109 dromedary camels based on full-genome sequencing, Abu Dhabi, United Arab Emirates," *Emerg. Microbes Infect.*, vol. 6, no. 11, p. e101, Nov. 2017, doi: 10.1038/emi.2017.89.

[66] S. Kasem *et al.*, "The prevalence of Middle East respiratory Syndrome coronavirus (MERS-CoV) infection in livestock and temporal relation to locations and seasons," *J. Infect. Public Health*, vol. 11, no. 6, pp. 884–888, Nov. 2018, doi: 10.1016/j.jiph.2018.01.004.

[67] S. Ommeh *et al.*, "Genetic Evidence of Middle East Respiratory Syndrome Coronavirus (MERS-Cov) and Widespread Seroprevalence among Camels in Kenya," *Virol. Sin.*, vol. 33, no. 6, pp. 484–492, Dec. 2018, doi: 10.1007/s12250-018-0076-4.

[68] D. K. W. Chu *et al.*, "MERS coronaviruses from camels in Africa exhibit region-dependent genetic diversity," *Proc. Natl. Acad. Sci. U. S. A.*, vol. 115, no. 12, pp. 3144–3149, Mar. 2018, doi: 10.1073/pnas.1718769115.

[69] A. Zohaib *et al.*, "Countrywide Survey for MERS-Coronavirus Antibodies in Dromedaries and Humans in Pakistan," *Virol. Sin.*, vol. 33, no. 5, pp. 410–417, Oct. 2018, doi: 10.1007/s12250-018-0051-0.

[70] S. Kasem *et al.*, "Cross-sectional study of MERS-CoV-specific RNA and antibodies in animals that have had contact with MERS patients in Saudi Arabia," *J. Infect. Public Health*, vol. 11, no. 3, pp. 331–338, May 2018, doi: 10.1016/j.jiph.2017.09.022.

[71] M. G. Hemida *et al.*, "Seroepidemiology of middle east respiratory syndrome (MERS) coronavirus in Saudi Arabia (1993) and Australia (2014) and characterisation of assay specificity," *Eurosurveillance*, vol. 19, no. 23, Jun. 2014, doi: 10.2807/1560-7917.ES2014.19.23.20828.

[72] M. A. Ali *et al.*, "Systematic, active surveillance for Middle East respiratory syndrome coronavirus in camels in Egypt," *Emerg. Microbes Infect.*, vol. 6, no. 1, Jan. 2017, doi: 10.1038/emi.2016.130.

[73] A. N. Alagaili *et al.*, "Middle east respiratory syndrome coronavirus infection in dromedary camels in Saudi Arabia," *MBio*, vol. 5, no. 2, Feb. 2014, doi: 10.1128/mBio.00884-14.

[74] B. Meyer *et al.*, "Antibodies against MERS coronavirus in dromedaries, United Arab Emirates, 2003 and 2013," *Emerg. Infect. Dis.*, vol. 20, no. 4, pp. 552–559, 2014, doi: 10.3201/eid2004.131746.

[75] S. K. P. Lau *et al.*, "Middle East Respiratory Syndrome Coronavirus Antibodies in Bactrian

and Hybrid Camels from Dubai," *mSphere*, vol. 5, no. 1, Jan. 2020, doi: 10.1128/msphere.00898-19.

[76] D. David *et al.*, "Middle East respiratory syndrome coronavirus specific antibodies in naturally exposed Israeli llamas, alpacas and camels," *One Heal.*, vol. 5, pp. 65–68, Jun. 2018, doi: 10.1016/j.onehlt.2018.05.002.

[77] E. I. Azhar *et al.*, "Detection of the middle east respiratory syndrome coronavirus genome in an air sample originating from a camel barn owned by an infected patient," *MBio*, vol. 5, no. 4, Jul. 2014, doi: 10.1128/mBio.01450-14.

[78] V. Stalin Raj *et al.*, "Isolation of MERS coronavirus from dromedary camel, Qatar, 2014," *Emerg. Infect. Dis.*, vol. 20, no. 8, pp. 1339–1342, 2014, doi: 10.3201/eid2008.140663.

[79] B. L. Haagmans *et al.*, "Middle East respiratory syndrome coronavirus in dromedary camels: An outbreak investigation," *Lancet Infect. Dis.*, vol. 14, no. 2, pp. 140–145, Feb. 2014, doi: 10.1016/S1473-3099(13)70690-X.

[80] B. M. Alraddadi *et al.*, "Risk factors for primary middle east respiratory syndrome coronavirus illness in humans, Saudi Arabia, 2014," *Emerg. Infect. Dis.*, vol. 22, no. 1, pp. 49–55, Jan. 2016, doi: 10.3201/eid2201.151340.

[81] A. N. Alshukairi *et al.*, "High Prevalence of MERS-CoV Infection in Camel Workers in Saudi Arabia," *MBio*, vol. 9, no. 5, Oct. 2018, doi: 10.1128/mBio.01985-18.

[82] C. B. E. M. Reusken *et al.*, "Occupational exposure to dromedaries and risk for MERS-CoV infection, Qatar, 2013–2014," *Emerg. Infect. Dis.*, vol. 21, no. 8, pp. 1422–1425, Jul. 2015, doi: 10.3201/eid2108.150481.

[83] A. Khudhair *et al.*, "Risk factors for MERS-CoV seropositivity among animal market and slaughterhouse workers, Abu Dhabi, United Arab Emirates, 2014–2017," *Emerg. Infect. Dis.*, vol. 25, no. 5, May 2019, doi: 10.3201/eid2505.181728.

[84] T. Y. So Ray *et al.*, "Lack of serological evidence of middle east respiratory syndrome coronavirus infection in virus exposed camel abattoir workers in Nigeria, 2016," *Eurosurveillance*, vol. 23, no. 32, Aug. 2018, doi: 10.2807/1560-7917.ES.2018.23.32.1800175.

[85] M. G. Hemida, A. Al-Naeem, R. A. P. M. Perera, A. W. H. Chin, L. L. M. Poon, and M. Peiris, "Lack of middle east respiratory syndrome coronavirus transmission from infected camels," *Emerg. Infect. Dis.*, vol. 21, no. 4, pp. 699–701, 2015, doi: 10.3201/eid2104.141949.

[86] A. S. Aburizaiza *et al.*, "Investigation of anti-middle east respiratory syndrome antibodies in blood donors and slaughterhouse workers in Jeddah and Makkah, Saudi Arabia, Fall 2012," *J. Infect. Dis.*, vol. 209, no. 2, pp. 243–246, Jan. 2014, doi: 10.1093/infdis/jit589.

[87] Z. A. Memish *et al.*, "Sparse evidence of <scp>MERS</scp> - <scp>C</scp> o <scp>V</scp> infection among animal workers living in <scp>S</scp> outhern <scp>S</scp> audi <scp>A</scp> rabia during 2012," *Influenza Other Respi. Viruses*, vol. 9, no. 2, pp. 64–67, Mar. 2015, doi: 10.1111/irv.12287.

[88] P. Munyua *et al.*, "No serologic evidence of middle east respiratory syndrome coronavirus infection among camel farmers exposed to highly seropositive camel herds: A household linked study, Kenya, 2013," *Am. J. Trop. Med. Hyg.*, vol. 96, no. 6, pp. 1318–1324, 2017, doi: 10.4269/ajtmh.16-0880.

[89] R. Conzade *et al.*, "Reported direct and indirect contact with dromedary camels among laboratory-confirmed MERS-CoV cases," *Viruses*, vol. 10, no. 8, Aug. 2018, doi:

10.3390/v10080425.

[90] M. G. Hemida, A. M. Al, M. Alhammadi, and A. Alnaeem, "The Middle East respiratory syndrome coronavirus in the breath of some infected dromedary camels (Camelus dromedarius)," *Epidemiol. Infect.*, vol. 148, 2020, doi: 10.1017/S0950268820002459.

[91] C. B. E. M. Reusken *et al.*, "Middle east respiratory syndrome coronavirus (MERS-CoV) RNA and neutralising antibodies in milk collected according to local customs from dromedary camels, Qatar, April 2014," *Eurosurveillance*, vol. 19, no. 23, Jun. 2014, doi: 10.2807/1560-7917.ES2014.19.23.20829.

[92] S. Bornstein and M. Younan, "Significant veterinary research on the dromedary camels of Kenya: Past and Present," *Bornstein/ J. Camelid Sci.*, vol. 6, pp. 1–48, 2013, Accessed: Mar. 15, 2022. [Online]. Available: http://www.isocard.org.

[93] FAOSTAT, "FAOSTAT [database]," 2020. https://www.fao.org/faostat/en/#data/QA (accessed Mar. 15, 2022).

[94] B. Faye, "How many large camelids in the world? A synthetic analysis of the world camel demographic changes," *Pastoralism*, vol. 10, no. 1, pp. 1–20, Dec. 2020, doi: 10.1186/S13570-020-00176-Z/FIGURES/23.

[95] H. R. Abdallah and B. Faye, "Typology of camel farming system in Saudi Arabia," *Emirates J. Food Agric.*, vol. 25, no. 4, pp. 250–260, Apr. 2013, doi: 10.9755/ejfa.v25i4.15491.

[96] B. Faye, "The camel, new challenges for a sustainable development," *Tropical Animal Health and Production*, vol. 48, no. 4. Springer Netherlands, pp. 689–692, Apr. 01, 2016, doi: 10.1007/s11250-016-0995-8.

[97] I. Ngere *et al.*, "High MERS-CoV seropositivity associated with camel herd profile, husbandry practices and household socio-demographic characteristics in Northern Kenya," *Epidemiol. Infect.*, vol. 148, 2020, doi: 10.1017/S0950268820002939.

[98] E. Miguel *et al.*, "Risk factors for MERS coronavirus infection in dromedary camels in Burkina Faso, Ethiopia, and Morocco, 2015," *Eurosurveillance*, vol. 22, no. 13, Mar. 2017, doi: 10.2807/1560-7917.ES.2017.22.13.30498.

[99] C. B. E. M. Reusken *et al.*, "Geographic distribution of MERS coronavirus among dromedary camels, Africa," *Emerg. Infect. Dis.*, vol. 20, no. 8, pp. 1370–1374, 2014, doi: 10.3201/eid2008.140590.

[100] W. K. Saalfeld and G. P. Edwards, "Distribution and abundance of the feral camel (Camelus dromedarius) in Australia," *Rangel. J.*, vol. 32, no. 1, p. 1, Apr. 2010, doi: 10.1071/RJ09058.

[101] R. Al Jassim and A. Lisle, "Prediction and management of the feral camel population in Australia," 2016, Accessed: Mar. 15, 2022. [Online]. Available: https://www.researchgate.net/publication/280038591_Prediction_of_camel_population_in_Australia.

[102] M. Saqib *et al.*, "Serologic evidence for MERS-CoV infection in Dromedary Camels, Punjab, Pakistan, 2012–2015," *Emerging Infectious Diseases*, vol. 23, no. 3. Centers for Disease Control and Prevention (CDC), pp. 550–551, Mar. 01, 2017, doi: 10.3201/eid2303.161285.

[103] S. Alexandersen, G. P. Kobinger, G. Soule, and U. Wernery, "Middle east respiratory syndrome coronavirus antibody reactors among camels in Dubai, United Arab Emirates, in 2005," *Transbound. Emerg. Dis.*, vol. 61, no. 2, pp. 105–108, Apr. 2014, doi: 10.1111/tbed.12212.

[104] G. Crameri *et al.*, "Absence of MERS-CoV antibodies in feral camels in Australia: Implications for the pathogen's origin and spread," *One Heal.*, vol. 1, pp. 76–82, Dec. 2015, doi: 10.1016/j.onehlt.2015.10.003.

[105] E. M. Fèvre, B. M. D. C. Bronsvoort, K. A. Hamilton, and S. Cleaveland, "Animal movements and the spread of infectious diseases," *Trends Microbiol.*, vol. 14, no. 3, p. 125, Mar. 2006, doi: 10.1016/J.TIM.2006.01.004.

[106] B. Faye, "TADs in the Dromedary," *Transbound. Anim. Dis. Sahel. Africa Connect. Reg.*, pp. 91–103, Jan. 2019, doi: 10.1007/978-3-030-25385-1_6.

[107] M. Younan, S. Bornstein, and I. V. Gluecks, "MERS and the dromedary camel trade between Africa and the Middle East," *Trop. Anim. Health Prod.*, vol. 48, no. 6, pp. 1277–1282, Aug. 2016, doi: 10.1007/s11250-016-1089-3.

[108] M. G. Hemida *et al.*, "Phylogenetic Analysis of MERS-CoV in a Camel Abattoir, Saudi Arabia, 2016–2018," *Emerg. Infect. Dis.*, vol. 26, no. 12, pp. 3089–3091, Dec. 2020, doi: 10.3201/eid2612.191094.

[109] Z. Zhou *et al.*, "Phenotypic and genetic characterization of MERS coronaviruses from Africa to understand their zoonotic potential," *Proc. Natl. Acad. Sci. U. S. A.*, vol. 118, no. 25, Jun. 2021, doi: 10.1073/PNAS.2103984118/SUPPL_FILE/PNAS.2103984118.SD01.XLSX.

[110] G. Fournié *et al.*, "Investigating poultry trade patterns to guide avian influenza surveillance and control: A case study in Vietnam," *Sci. Rep.*, vol. 6, Jul. 2016, doi: 10.1038/srep29463.

[111] B. Faye, H. Madani, and S. A. H El-Rouili, "Camel milk value chain in Northern Saudi Arabia," vol. 26, no. 4, pp. 359–365, 2014, doi: 10.9755/ejfa.v26i4.17278.

[112] S. Gikonyo *et al.*, "Mapping Potential Amplification and Transmission Hotspots for MERS-CoV, Kenya," *Ecohealth*, vol. 15, no. 2, pp. 372–387, Jun. 2018, doi: 10.1007/s10393-018-1317-6.

[113] T. Mirkena, E. Walelign, N. Tewolde, G. Gari, G. Abebe, and S. Newman, "Camel production systems in Ethiopia: a review of literature with notes on MERS-CoV risk factors," *Pastoralism*, vol. 8, no. 1, pp. 1–17, Dec. 2018, doi: 10.1186/S13570-018-0135-3/TABLES/4.

[114] B. Abbas, A. A. Al Qarawi, and A. Al Hawas, "Survey on camel husbandry in Qassim region, Saudi Arabia: Herding strategies, productivity and mortality," *Rev. Élev. Méd. vét. Pays trop*, vol. 53, no. 3, pp. 293–298, 2000.

[115] Z. Farah, M. Mollet, M. Younan, and R. Dahir, "Camel dairy in Somalia: Limiting factors and development potential," *Livest. Sci.*, vol. 110, no. 1–2, pp. 187–191, Jun. 2007, doi: 10.1016/J.LIVSCI.2006.12.010.

[116] U. Wernery *et al.*, "Acute middle east respiratory syndrome coronavirus infection in livestock dromedaries, Dubai, 2014," *Emerg. Infect. Dis.*, vol. 21, no. 6, pp. 1019–1022, 2015, doi: 10.3201/eid2106.150038.

[117] S. E. Almutairi, I. Boujenane, A. Musaad, and F. Awad-Acharari, "Non-genetic factors influencing reproductive traits and calving weight in Saudi camels," *Trop. Anim. Health Prod.*, vol. 42, no. 6, pp. 1087–1092, 2010, doi: 10.1007/s11250-010-9529-y.

[118] M. G. Hemida *et al.*, "Dromedary Camels and the Transmission of Middle East Respiratory Syndrome Coronavirus (MERS-CoV)," *Transboundary and Emerging Diseases*, vol. 64, no. 2. Blackwell Publishing Ltd, pp. 344–353, Apr. 01, 2017, doi: 10.1111/tbed.12401.

[119] A. M. Abdussamad, W. Holtz, M. Gauly, M. S. Sulieman, and M. B. Bello, "Reproduction and breeding in dromedary camels: insights from pastoralists in some selected villages of the Nigeria-Niger corridor," *Livest. Res. Rural Dev.*, vol. 23, no. 8, 2011, Accessed: Mar. 07, 2022. [Online]. Available: http://www.lrrd.org/lrrd23/8/abdu23178.htm.

[120] A. Ali *et al.*, "Factors affecting reproductive performance in dromedary camel herds in Saudi Arabia," *Trop. Anim. Health Prod.*, vol. 50, no. 5, pp. 1155–1160, Jun. 2018, doi: 10.1007/s11250-018-1545-3.

[121] M. S. M. Zaky, A. E. Abdel-Khalek, T. H. Mostafa, S. A. Gabr, and M. E. Hammad, "Productive and Reproductive Characterization, Breeding Season and Calving Season in Reference with the Effect of Parity Order on Milk Production of Camel in Egypt," *J. Anim. Poult. Prod.*, vol. 11, no. 12, pp. 573–581, Dec. 2020, doi: 10.21608/JAPPMU.2020.161201.

[122] B. Faye, M. Bengoumi, and A. Barkat, "The development of peri-urban dairy camel systems in Africa - Les Publications du Cirad," *Publ. du CIRAD*, 2003, Accessed: Mar. 16, 2022. [Online]. Available: http://publications.cirad.fr/une_notice.php?dk=525459.

[123] W. Widagdo, S. S. Na Ayudhya, G. B. Hundie, and B. L. Haagmans, "Host determinants of mers-CoV transmission and pathogenesis," *Viruses*, vol. 11, no. 3. MDPI AG, Mar. 01, 2019, doi: 10.3390/v11030280.

[124] N. Van Doremalen *et al.*, "High prevalence of middle east respiratory coronavirus in young dromedary camels in Jordan," *Vector-Borne Zoonotic Dis.*, vol. 17, no. 2, pp. 155–159, Feb. 2017, doi: 10.1089/vbz.2016.2062.

[125] A. Islam *et al.*, "Middle east respiratory syndrome Coronavirus antibodies in dromedary camels, Bangladesh, 2015," *Emerging Infectious Diseases*, vol. 24, no. 5. Centers for Disease Control and Prevention (CDC), pp. 926–928, May 01, 2018, doi: 10.3201/eid2405.171192.

[126] E. G. Gardner *et al.*, "Force of infection of Middle East respiratory syndrome in dromedary camels in Kenya," *Epidemiol. Infect.*, vol. 147, p. e275, Sep. 2019, doi: 10.1017/S0950268819001663.

[127] J. Rui *et al.*, "The transmission dynamics of Middle East Respiratory Syndrome coronavirus," *Travel Med. Infect. Dis.*, vol. 45, p. 102243, Jan. 2022, doi: 10.1016/J.TMAID.2021.102243.

[128] Q. Lin, A. P. Y. Chiu, S. Zhao, and D. He, "Modeling the spread of Middle East respiratory syndrome coronavirus in Saudi Arabia," *Stat. Methods Med. Res.*, vol. 27, no. 7, pp. 1968–1978, Jul. 2018, doi: 10.1177/0962280217746442.

[129] S. Al Muhairi *et al.*, "Epidemiological investigation of Middle East respiratory syndrome coronavirus in dromedary camel farms linked with human infection in Abu Dhabi Emirate, United Arab Emirates," *Virus Genes*, vol. 52, no. 6, pp. 848–854, Dec. 2016, doi: 10.1007/s11262-016-1367-1.

[130] D. R. Adney *et al.*, "Replication and shedding of MERS-CoV in upper respiratory tract of inoculated dromedary camels," *Emerg. Infect. Dis.*, vol. 20, no. 12, pp. 1999–2005, Dec. 2014, doi: 10.3201/eid2012.141280.

[131] B. Meyer *et al.*, "Time course of MERS-CoV infection and immunity in dromedary camels," *Emerg. Infect. Dis.*, vol. 22, no. 12, pp. 2171–2173, Dec. 2016, doi: 10.3201/eid2212.160382.

[132] D. Falzarano *et al.*, "Dromedary camels in northern Mali have high seropositivity to MERS-CoV," *One Heal.*, vol. 3, pp. 41–43, Jun. 2017, doi: 10.1016/j.onehlt.2017.03.003.

[133] S. L. Deem *et al.*, "Serological evidence of MERS-CoV antibodies in dromedary camels (camelus dromedaries) in laikipia county, Kenya," *PLoS One*, vol. 10, no. 10, Oct. 2015, doi: 10.1371/journal.pone.0140125.

[134] M. F. Yusof *et al.*, "Prevalence of Middle East respiratory syndrome coronavirus (MERS-CoV) in dromedary camels in Abu Dhabi Emirate, United Arab Emirates," *Virus Genes*, vol. 50, no. 3, pp. 509–513, Jun. 2015, doi: 10.1007/s11262-015-1174-0.

[135] J. S. M. Sabir *et al.*, "Co-circulation of three camel coronavirus species and recombination of MERS-CoVs in Saudi Arabia," *Science (80-.).*, vol. 351, no. 6268, pp. 81–84, Jan. 2016, doi: 10.1126/science.aac8608.

[136] K. Muthumani *et al.*, "A synthetic consensus anti–spike protein DNA vaccine induces protective immunity against Middle East respiratory syndrome coronavirus in nonhuman primates," *Sci. Transl. Med.*, vol. 7, no. 301, p. 301ra132, Aug. 2015, doi: 10.1126/SCITRANSLMED.AAC7462.

[137] H. Mou, V. S. Raj, F. J. M. van Kuppeveld, P. J. M. Rottier, B. L. Haagmans, and B. J. Bosch, "The receptor binding domain of the new Middle East respiratory syndrome coronavirus maps to a 231-residue region in the spike protein that efficiently elicits neutralizing antibodies," *J. Virol.*, vol. 87, no. 16, pp. 9379–9383, Aug. 2013, doi: 10.1128/JVI.01277-13.

[138] T. P. Monath, "Vaccines against diseases transmitted from animals to humans: a one health paradigm," *Vaccine*, vol. 31, no. 46, pp. 5321–5338, Nov. 2013, doi: 10.1016/J.VACCINE.2013.09.029.

[139] L. Busani *et al.*, "Vaccination reduced the incidence of outbreaks of low pathogenicity avian influenza in northern Italy," *Vaccine*, vol. 27, no. 27, pp. 3655–3661, Jun. 2009, doi: 10.1016/j.vaccine.2009.03.033.

[140] D. A. Halvorson, "Prevention and management of avian influenza outbreaks: Experiences from the United States of America," *OIE Rev. Sci. Tech.*, vol. 28, no. 1, pp. 359–369, 2009, doi: 10.20506/rst.28.1.1866.

[141] C. C. Broder *et al.*, "A treatment for and vaccine against the deadly Hendra and Nipah viruses," *Antiviral Research*, vol. 100, no. 1. pp. 8–13, 2013, doi: 10.1016/j.antiviral.2013.06.012.

[142] R. P. Lavan, A. I. M. G. King, D. J. Sutton, and K. Tunceli, "Rationale and support for a One Health program for canine vaccination as the most cost-effective means of controlling zoonotic rabies in endemic settings," *Vaccine*, vol. 35, no. 13. Elsevier Ltd, pp. 1668–1674, Mar. 23, 2017, doi: 10.1016/j.vaccine.2017.02.014.

[143] M. Baguelin, A. J. Van Hoek, M. Jit, S. Flasche, P. J. White, and W. J. Edmunds, "Vaccination against pandemic influenza A/H1N1v in England: A real-time economic evaluation," *Vaccine*, vol. 28, no. 12, pp. 2370–2384, Mar. 2010, doi: 10.1016/J.VACCINE.2010.01.002.

[144] C. E. Wagner, C. M. Saad-Roy, and B. T. Grenfell, "Modelling vaccination strategies for COVID-19," *Nat. Rev. Immunol. 2022 223*, vol. 22, no. 3, pp. 139–141, Feb. 2022, doi: 10.1038/s41577-022-00687-3.

[145] C. J. E. Metcalf, W. J. Edmunds, and J. Lessler, "Six challenges in modelling for public health policy," *Epidemics*, vol. 10, pp. 93–96, Mar. 2015, doi: 10.1016/J.EPIDEM.2014.08.008.

[146] L. Bradley, D. Bernoulli, and J. L. R. d'Alembert, "Smallpox inoculation : an eighteenth century mathematical controversy," p. 72, 1971.

[147] F. Brauer, "Mathematical epidemiology: Past, present, and future," *Infect. Dis. Model.*, vol.

2, no. 2, pp. 113–127, May 2017, doi: 10.1016/J.IDM.2017.02.001.

[148] R. Ross, “The evidence of variability and of persistency of type,” 1906.

[149] G. Macdonald, *The Epidemiology and Control of Malaria.* London, Oxford Univ. Pr., 1957.

[150] L. A. Meyers, B. Pourbohloul, M. E. J. Newman, D. M. Skowronski, and R. C. Brunham, “Network theory and SARS: predicting outbreak diversity,” *J. Theor. Biol.*, vol. 232, no. 1, p. 71, Jan. 2005, doi: 10.1016/J.JTBI.2004.07.026.

[151] M. J. Keeling *et al.*, “Dynamics of the 2001 UK foot and mouth epidemic: Stochastic dispersal in a heterogeneous landscape,” *Science (80-.).*, vol. 294, no. 5543, pp. 813–817, Oct. 2001, doi: 10.1126/SCIENCE.1065973.

[152] N. M. Ferguson, C. A. Donnelly, and R. M. Anderson, “The Foot-and-Mouth Epidemic in Great Britain: Pattern of Spread and Impact of Interventions,” *Science (80-.).*, vol. 292, no. 5519, pp. 1155–1160, May 2001, doi: 10.1126/SCIENCE.1061020.

[153] M. Lipsitch *et al.*, “Transmission dynamics and control of severe acute respiratory syndrome,” *Science*, vol. 300, no. 5627, pp. 1966–1970, Jun. 2003, doi: 10.1126/SCIENCE.1086616.

[154] C. A. Donnelly *et al.*, “Epidemiological determinants of spread of causal agent of severe acute respiratory syndrome in Hong Kong,” *Lancet (London, England)*, vol. 361, no. 9371, pp. 1761–1766, May 2003, doi: 10.1016/S0140-6736(03)13410-1.

[155] M. D. Van Kerkhove and N. M. Ferguson, “Epidemic and intervention modelling: a scientific rationale for policy decisions? Lessons from the 2009 influenza pandemic,” *Bull. World Health Organ.*, vol. 90, pp. 306–310, 2012, doi: 10.1590/S0042-96862012000400015.

[156] I. Ghosh, S. S. Nadim, and J. Chattopadhyay, “Zoonotic MERS-CoV transmission: modeling, backward bifurcation and optimal control analysis,” *Nonlinear Dyn.*, vol. 103, no. 3, pp. 2973–2992, Feb. 2021, doi: 10.1007/s11071-021-06266-w.

[157] K. Murphy and C. Weaver, “Principles of adaptive immunity. Janeway’s Immunobiology.,” in *Janeway’s Immunobiology. Ninth Edition.*, Ninth Edit., New York, NY: Garland Science, Taylor and Francis Group, 2017, pp. 12–24.

[158] H. Muench, “Derivation of Rates from Summation Data by the Catalytic Curve,” *J. Am. Stat. Assoc.*, vol. 29, no. 185, pp. 25–38, 1934, doi: 10.1080/01621459.1934.10502684.

[159] N. Imai, I. Dorigatti, S. Cauchemez, and N. M. Ferguson, “Estimating Dengue Transmission Intensity from Case-Notification Data from Multiple Countries,” *PLoS Negl. Trop. Dis.*, vol. 10, no. 7, p. e0004833, Jul. 2016, doi: 10.1371/journal.pntd.0004833.

[160] Z. M. Cucunubá *et al.*, “Modelling historical changes in the force-of-infection of Chagas disease to inform control and elimination programmes: application in Colombia,” *BMJ Glob. Heal.*, vol. 2, no. 3, p. e000345, Sep. 2017, doi: 10.1136/BMJGH-2017-000345.

[161] D. A. Griffiths, “A Catalytic Model of Infection for Measles,” *J. R. Stat. Soc. Ser. C (Applied Stat.*, vol. 23, no. 3, pp. 330–339, Nov. 1974, doi: 10.2307/2347126.

[162] C. Reusken *et al.*, “Specific serology for emerging human coronaviruses by protein microarray,” *Eurosurveillance*, vol. 18, no. 14, pp. 2–7, Apr. 2013, doi: 10.2807/1560-7917.ES2013.18.14.20441/CITE/PLAINTEXT.

[163] G. Zhao *et al.*, “A safe and convenient pseudovirus-based inhibition assay to detect neutralizing antibodies and screen for viral entry inhibitors against the novel human coronavirus MERS-CoV,” *Virol. J.*, vol. 10, 2013, doi: 10.1186/1743-422X-10-266.

[164] R. A. Perera *et al.*, "Seroepidemiology for MERS coronavirus using microneutralisation and pseudoparticle virus neutralisation assays reveal a high prevalence of antibody in dromedary camels in Egypt, june 2013," *Eurosurveillance*, vol. 18, no. 36, Sep. 2013, doi: 10.2807/1560-7917.ES2013.18.36.20574.

[165] C. B. E. M. Reusken *et al.*, "Middle East respiratory syndrome coronavirus neutralising serum antibodies in dromedary camels: A comparative serological study," *Lancet Infect. Dis.*, vol. 13, no. 10, pp. 859–866, Oct. 2013, doi: 10.1016/S1473-3099(13)70164-6.

[166] K. Mullis, F. Faloona, S. Scharf, R. Saiki, G. Horn, and H. Erlich, "Specific enzymatic amplification of DNA in vitro: the polymerase chain reaction," *Cold Spring Harb. Symp. Quant. Biol.*, vol. 51 Pt 1, no. 1, pp. 263–273, 1986, doi: 10.1101/SQB.1986.051.01.032.

[167] C. Y. Ou *et al.*, "DNA Amplification for Direct Detection of HIV-1 in DNA of Peripheral Blood Mononuclear Cells," *Science (80-.).*, vol. 239, no. 4837, pp. 295–297, 1988, doi: 10.1126/SCIENCE.3336784.

[168] R. Higuchi, C. Fockler, G. Dollinger, and R. Watson, "Kinetic PCR analysis: real-time monitoring of DNA amplification reactions," *Biotechnology. (N. Y).*, vol. 11, no. 9, pp. 1026–1030, 1993, doi: 10.1038/NBT0993-1026.

[169] M. Becker-André and K. Hahlbrock, "Absolute mRNA quantification using the polymerase chain reaction (PCR). A novel approach by a PCR aided transcript titration assay (PATTY).," *Nucleic Acids Res.*, vol. 17, no. 22, p. 9437, Nov. 1989, doi: 10.1093/NAR/17.22.9437.

[170] V. M. Corman *et al.*, "Detection of a novel human coronavirus by real-time reverse-transcription polymerase chain reaction," *Eurosurveillance*, vol. 17, no. 39, 2012, doi: 10.2807/ese.17.39.20285-en.

[171] OIE, "Chapter 3.5.2 Middle East Respiratory Syndrome (Infection of Dromedary camels with Middle East Respiratory Syndrome Coronavirus)," *OIE Terrestrial Manual* , 2021. https://www.oie.int/fileadmin/Home/eng/Health_standards/tahm/3.05.02_MERS-CoV.pdf (accessed Feb. 25, 2022).

[172] WHO, "Laboratory Testing for Middle East Respiratory Syndrome Coronavirus," 2018. Accessed: Feb. 25, 2022. [Online]. Available: http://www.who.int/csr/resources/publications/surveillance/CDS_EPR_AR.

[173] R. S. Sikkema *et al.*, "Global status of middle east respiratory syndrome coronavirus in dromedary camels: A systematic review," *Epidemiology and Infection*, vol. 147. Cambridge University Press, 2019, doi: 10.1017/S095026881800345X.

[174] Elsevier, "Embase Classic + Embase [Database] (accessed via Ovid)." Ovid Wolters Kluwer, 2018, Accessed: Mar. 08, 2022. [Online]. Available: https://ovidsp.ovid.com/.

[175] National Library of Medicine, "MEDLINE [Database] (accessed via Ovid)." Ovid Wolters Kluwer, 2018, Accessed: Mar. 08, 2022. [Online]. Available: https://ovidsp.dc1.ovid.com/ovid-b/ovidweb.cgi.

[176] Clarivate Analytics, "Web of Science [Database]," *Clarivate Analytics*. 2018.

[177] K. A. Mohran *et al.*, "The sample of choice for detecting Middle East respiratory syndrome coronavirus in asymptomatic dromedary camels using real-time reverse-transcription polymerase chain reaction," *OIE Rev. Sci. Tech.*, vol. 35, no. 3, pp. 905–911, Dec. 2016, doi: 10.20506/rst.35.3.2578.

[178] Clarivate Analytics, "EndNote X8.2." Clarivate Analytics, 2018.

[179] C. Gutiérrez, M. T. Tejedor-Junco, M. González, E. Lattwein, and S. Renneker, "Presence of antibodies but no evidence for circulation of MERS-CoV in dromedaries on the Canary Islands, 2015," *Eurosurveillance*, vol. 20, no. 37, Sep. 2015, doi: 10.2807/1560-7917.ES.2015.20.37.30019.

[180] D. K. W. Chu *et al.*, "MERS coronaviruses in dromedary camels, Egypt," *Emerg. Infect. Dis.*, vol. 20, no. 6, pp. 1049–1053, 2014, doi: 10.3201/eid2006.140299.

[181] M. A. Ali *et al.*, "Cross-sectional surveillance of middle east respiratory syndrome coronavirus (MERS-CoV) in dromedary camels and other mammals in Egypt, August 2015 to January 2016," *Eurosurveillance*, vol. 22, no. 11, Mar. 2017, doi: 10.2807/1560-7917.ES.2017.22.11.30487.

[182] S. Fukushi *et al.*, "Characterization of novel monoclonal antibodies against the MERS-coronavirus spike protein and their application in species-independent antibody detection by competitive ELISA," *J. Virol. Methods*, vol. 251, pp. 22–29, Jan. 2018, doi: 10.1016/j.jviromet.2017.10.008.

[183] H. T. Thwiny, T. A. Al Hamed, and A. R. Nazzal, "Seroepidemiological study of Middle East respiratory syndrome (MERS) virus infection in Iraqi dromedary camels," *Vet. Arh.*, vol. 88, no. 2, pp. 191–200, 2018, doi: 10.24099/vet.arhiv.161224.

[184] S. F. Al Salihi and M. A. Alrodhan, "Phylogenetic Analysis of MERSCoV in Human and Camels in Iraq," *AL-Qadisiyah Med. J.*, vol. 13, no. 23, 2017.

[185] J. L. Harcourt *et al.*, "The prevalence of Middle East respiratory syndrome coronavirus (MERS-CoV) antibodies in dromedary camels in Israel," *Zoonoses Public Health*, vol. 65, no. 6, pp. 749–754, Sep. 2018, doi: 10.1111/zph.12482.

[186] K. Shirato *et al.*, "Middle east respiratory syndrome coronavirus infection not found in camels in Japan," *Japanese Journal of Infectious Diseases*, vol. 68, no. 3. National Institute of Health, pp. 256–258, 2015, doi: 10.7883/yoken.JJID.2015.094.

[187] C. B. Reusken *et al.*, "Middle east respiratory syndrome coronavirus (MERS-CoV) serology in major livestock species in an affected region in Jordan, june to September 2013," *Eurosurveillance*, vol. 18, no. 50, 2013, doi: 10.2807/1560-7917.ES2013.18.50.20662.

[188] E. Miguel *et al.*, "Absence of Middle East respiratory syndrome coronavirus in camelids, Kazakhstan, 2015," *Emerging Infectious Diseases*, vol. 22, no. 3. Centers for Disease Control and Prevention (CDC), pp. 555–557, Mar. 01, 2016, doi: 10.3201/eid2203.151284.

[189] V. M. Corman *et al.*, "Antibodies against MERS coronavirus in dromedary camels, Kenya, 1992-2013," *Emerg. Infect. Dis.*, vol. 20, no. 8, pp. 1319–1322, 2014, doi: 10.3201/eid2008.140596.

[190] S. Kiambi *et al.*, "Detection of distinct MERS-Coronavirus strains in dromedary camels from Kenya, 2017," *Emerg. Microbes Infect.*, vol. 7, no. 1, pp. 1–4, Dec. 2018, doi: 10.1038/s41426-018-0193-z.

[191] M. Alfuwaires, A. Altaher, A. Alhafufi, and M. Kandeel, "Middle east respiratory syndrome coronavirus in healthy and diseased dromedaries," in *Journal of Camel Practice and Research*, Dec. 2017, vol. 24, no. 3, pp. 217–220, doi: 10.5958/2277-8934.2017.00036.4.

[192] R. Harrath and F. M. Abu Duhier, "Sero-prevalence of Middle East respiratory syndrome coronavirus (MERS-CoV) specific antibodies in dromedary camels in Tabuk, Saudi Arabia," *J. Med. Virol.*, vol. 90, no. 8, pp. 1285–1289, Aug. 2018, doi: 10.1002/jmv.25186.

[193] M. G. Hemida *et al.*, "Middle east respiratory syndrome (MERS) coronavirus

seroprevalence in domestic livestock in Saudi Arabia, 2010 to 2013," *Eurosurveillance*, vol. 18, no. 50, 2013, doi: 10.2807/1560-7917.ES2013.18.50.20659.

[194] A. I. Khalafalla, X. Lu, A. I. A. Al-Mubarak, A. H. S. Dalab, K. A. S. Al-Busadah, and D. D. Erdman, "MERS-CoV in upper respiratory tract and lungs of dromedary camels, Saudi Arabia, 2013–2014," *Emerg. Infect. Dis.*, vol. 21, no. 7, pp. 1153–1158, 2015, doi: 10.3201/eid2107.150070.

[195] D. K. Chu *et al.*, "Middle east respiratory syndrome coronavirus (MERSCoV) in dromedary camels in nigeria, 2015," *Eurosurveillance*, vol. 20, no. 49, pp. 1–7, Dec. 2015, doi: 10.2807/1560-7917.ES.2015.20.49.30086.

[196] N. Nowotny and J. Kolodziejek, "Middle East Respiratory Syndrome coronavirus (MERS-CoV) in dromedary camels, Oman, 2013," *Eurosurveillance*, vol. 19, no. 16, 2014, doi: 10.2807/1560-7917.ES2014.19.16.20781.

[197] U. Wernery *et al.*, "A phylogenetically distinct Middle East respiratory syndrome coronavirus detected in a dromedary calf from a closed dairy herd in Dubai with rising seroprevalence with age," *Emerg. Microbes Infect.*, vol. 4, Dec. 2015, doi: 10.1038/emi.2015.74.

[198] Y. Li *et al.*, "Identification of diverse viruses in upper respiratory samples in dromedary camels from United Arab Emirates," *PLoS One*, vol. 12, no. 9, Sep. 2017, doi: 10.1371/journal.pone.0184718.

[199] C. R. Paden *et al.*, "Zoonotic origin and transmission of Middle East respiratory syndrome coronavirus in the UAE," *Zoonoses Public Health*, vol. 65, no. 3, pp. 322–333, May 2018, doi: 10.1111/zph.12435.

[200] Z. M. Al Hammadi *et al.*, "Asymptomatic MERS-CoV infection in humans possibly linked to infected dromedaries imported from Oman to United Arab Emirates, May 2015," *Emerg. Infect. Dis.*, vol. 21, no. 12, pp. 2197–2200, Dec. 2015, doi: 10.3201/eid2112.151132.

[201] E. A. B. A. Farag *et al.*, "High proportion of MERS-CoV shedding dromedaries at slaughterhouse with a potential epidemiological link to human cases, Qatar 2014," *Infect. Ecol. Epidemiol.*, vol. 5, no. 1, p. 28305, Jan. 2015, doi: 10.3402/iee.v5.28305.

[202] S. M. S. Chan *et al.*, "Absence of MERS-Coronavirus in bactrian camels, Southern Mongolia, November 2014," *Emerging Infectious Diseases*, vol. 21, no. 7. Centers for Disease Control and Prevention (CDC), pp. 1269–1271, 2015, doi: 10.3201/eid2107.150178.

[203] R. Liu, Z. Wen, J. Wang, J. Ge, H. Chen, and Z. Bu, "Absence of Middle East respiratory syndrome coronavirus in Bactrian camels in the West Inner Mongolia Autonomous Region of China: Surveillance study results from July 2015," *Emerging Microbes and Infections*, vol. 4. Nature Publishing Group, Dec. 01, 2015, doi: 10.1038/emi.2015.73.

[204] FAOSTAT, "FAOSTAT [database]," 2016. https://www.fao.org/faostat/en/#data (accessed Apr. 14, 2022).

[205] The World Bank, "The World Bank: Land area," 2016. https://data.worldbank.org/indicator/AG.LND.TOTL.K2. (accessed Apr. 14, 2022).

[206] M. G. Hemida *et al.*, "Mers coronavirus in dromedary camel herd, Saudi Arabia," *Emerg. Infect. Dis.*, vol. 20, no. 7, pp. 1231–1234, 2014, doi: 10.3201/eid2007.140571.

[207] Z. A. Memish *et al.*, "Human Infection with MERS coronavirus after exposure to infected camels, Saudi Arabia, 2013," *Emerg. Infect. Dis.*, vol. 20, no. 6, pp. 1012–1015, 2014, doi: 10.3201/eid2006.140402.

[208] M. G. Hemida *et al.*, "Longitudinal study of Middle East Respiratory Syndrome coronavirus infection in dromedary camel herds in Saudi Arabia, 2014-2015," *Emerg. Microbes Infect.*, vol. 6, no. 6, p. e56, Jun. 2017, doi: 10.1038/emi.2017.44.

[209] M. Gilbert *et al.*, "Predicting the risk of avian influenza A H7N9 infection in live-poultry markets across Asia," *Nat. Commun.*, vol. 5, Jun. 2014, doi: 10.1038/ncomms5116.

[210] E. G. Gardner, D. Kelton, Z. Poljak, M. Van Kerkhove, S. Von Dobschuetz, and A. L. Greer, "A case-crossover analysis of the impact of weather on primary cases of Middle East respiratory syndrome," *BMC Infect. Dis.*, vol. 19, no. 1, Feb. 2019, doi: 10.1186/s12879-019-3729-5.

[211] J. A. Al-Tawfiq and Z. A. Memish, "Lack of seasonal variation of Middle East Respiratory Syndrome Coronavirus (MERS-CoV)," *Travel Med. Infect. Dis.*, vol. 27, pp. 125–126, Jan. 2019, doi: 10.1016/J.TMAID.2018.09.002.

[212] OIE-WAHIS [Database], "World Animal Health Information System (OIE-WAHIS)." https://wahis.oie.int/#/events?viewAll=true (accessed Mar. 05, 2022).

[213] N. Hens *et al.*, "Seventy-five years of estimating the force of infection from current status data," *Epidemiol. Infect.*, vol. 138, no. 6, pp. 802–812, Jun. 2010, doi: 10.1017/S0950268809990781.

[214] J. C. Kleinman, "Proportions with extraneous variance: Single and independent samples," *J. Am. Stat. Assoc.*, vol. 68, no. 341, pp. 46–54, 1973, doi: 10.1080/01621459.1973.10481332.

[215] R Core Team, "R: A Language and Environment for Statistical Computing." Vienna, Austria, 2021, [Online]. Available: https://www.r-project.org/.

[216] B. Carpenter *et al.*, "Stan: A probabilistic programming language," *J. Stat. Softw.*, vol. 76, no. 1, pp. 1–32, Jan. 2017, doi: 10.18637/jss.v076.i01.

[217] Stan Development Team, "RStan: the R interface to Stan," *R package version 2.17.3.* Accessed: Oct. 28, 2020. [Online]. Available: https://mc-stan.org/.

[218] R. M. Neal, "MCMC using Hamiltonian dynamics," *Handb. Markov Chain Monte Carlo*, pp. 1–592, Jun. 2012, doi: 10.1201/b10905.

[219] M. Betancourt, "A Conceptual Introduction to Hamiltonian Monte Carlo," Jan. 2017, Accessed: Nov. 03, 2021. [Online]. Available: https://arxiv.org/abs/1701.02434v2.

[220] B. Lambert, "The intuition behind the Hamiltonian Monte Carlo algorithm - YouTube," *YouTube*, 2018. https://www.youtube.com/watch?v=a-wydhEuAm0 (accessed Mar. 09, 2022).

[221] Stan Development Team, "9 MCMC Sampling using Hamiltonian Monte Carlo | CmdStan User's Guide," 2019. https://mc-stan.org/docs/2_24/cmdstan-guide/mcmc-config.html (accessed Mar. 26, 2022).

[222] J. Gabry and T. Mahr, "bayesplot: Plotting for Bayesian Models." 2022, Accessed: Apr. 01, 2022. [Online]. Available: https://mc-stan.org/bayesplot/.

[223] J. Gabry, D. Simpson, A. Vehtari, M. Betancourt, and A. Gelman, "Visualization in Bayesian workflow," *J. R. Stat. Soc. Ser. A Stat. Soc.*, vol. 182, no. 2, pp. 389–402, Feb. 2019, doi: 10.1111/RSSA.12378.

[224] D. J. Spiegelhalter, N. G. Best, B. P. Carlin, and A. Van Der Linde, "Bayesian measures of model complexity and fit," *J. R. Stat. Soc. Ser. B (Statistical Methodol.*, vol. 64, no. 4, pp. 583–639, Oct. 2002, doi: 10.1111/1467-9868.00353.

[225] M. S. Bartlett, “The Critical Community Size for Measles in the United States,” *J. R. Stat. Soc. Ser. A*, vol. 123, no. 1, pp. 37–44, Jan. 1960, doi: 10.2307/2343186.

[226] M. S. Bartlett, “Measles Periodicity and Community Size,” *J. R. Stat. Soc. Ser. A*, vol. 120, no. 1, p. 48, 1957, doi: 10.2307/2342553.

[227] F. L. Black, “Measles endemicity in insular populations: critical community size and its evolutionary implication,” *J. Theor. Biol.*, vol. 11, no. 2, pp. 207–211, 1966, doi: 10.1016/0022-5193(66)90161-5.

[228] M. J. Keeling and B. T. Grenfell, “Disease extinction and community size: modeling the persistence of measles,” *Science*, vol. 275, no. 5296, pp. 65–67, Jan. 1997, doi: 10.1126/SCIENCE.275.5296.65.

[229] R. FitzJohn and T. Fischer, “odin: ODE generation and Integration.” 2022, Accessed: Mar. 20, 2022. [Online]. Available: https://github.com/mrc-ide/odin.

[230] R. FitzJohn and J. Lees, “odin.dust: Compile Odin to Dust.” 2022, Accessed: Mar. 20, 2022. [Online]. Available: https://github.com/mrc-ide/odin.dust.

[231] J. A. Lees *et al.*, “Reproducible parallel inference and simulation of stochastic state space models using odin, dust, and mcstate,” *Wellcome open Res.*, vol. 5, 2021, doi: 10.12688/WELLCOMEOPENRES.16466.2.

[232] PlotDigitizer, “PlotDigitizer: Extract Data from Graph Image Online.” 2022, Accessed: Feb. 28, 2022. [Online]. Available: https://plotdigitizer.com/.

[233] F. Gascuel, M. Choisy, J. M. Duplantier, F. Débarre, and C. Brouat, “Host Resistance, Population Structure and the Long-Term Persistence of Bubonic Plague: Contributions of a Modelling Approach in the Malagasy Focus,” *PLOS Comput. Biol.*, vol. 9, no. 5, p. e1003039, May 2013, doi: 10.1371/JOURNAL.PCBI.1003039.

[234] H. L. Beyer, K. Hampson, T. Lembo, S. Cleaveland, M. Kaare, and D. T. Haydon, “The implications of metapopulation dynamics on the design of vaccination campaigns,” *Vaccine*, vol. 30, no. 6, pp. 1014–1022, Feb. 2012, doi: 10.1016/J.VACCINE.2011.12.052.

[235] S. Bansal, B. T. Grenfell, and L. A. Meyers, “When individual behaviour matters: homogeneous and network models in epidemiology,” *J. R. Soc. Interface*, vol. 4, no. 16, p. 879, Oct. 2007, doi: 10.1098/RSIF.2007.1100.

[236] M. J. Keeling, “Metapopulation moments: coupling, stochasticity and persistence,” *J. Anim. Ecol.*, vol. 69, no. 5, pp. 725–736, Sep. 2000, doi: 10.1046/J.1365-2656.2000.00430.X.

[237] B. H. Hayes, M. Andraud, L. G. Salazar, N. Rose, and T. Vergne, “Hayes et al. | ASF mechanistic modeling-systematic review Mechanistic modeling of African swine fever: A systematic review.”

[238] F. I. Korennoy, V. M. Gulenkin, A. E. Gogin, T. Vergne, and A. K. Karaulov, “Estimating the Basic Reproductive Number for African Swine Fever Using the Ukrainian Historical Epidemic of 1977,” *Transbound. Emerg. Dis.*, vol. 64, no. 6, pp. 1858–1866, Dec. 2017, doi: 10.1111/TBED.12583.

[239] Saudi Press Agency, “‘Microchip won’t break the camels neck.’” 2018.

[240] M. G. Hemida and A. Alnaeem, “Some One Health based control strategies for the Middle East respiratory syndrome coronavirus,” *One Heal.*, vol. 8, p. 100102, Dec. 2019, doi: 10.1016/J.ONEHLT.2019.100102.

[241] D. Bold, N. Van Doremalen, O. Myagmarsuren, B. Zayat, V. J. Munster, and J. A. Richt, “Middle East Respiratory Syndrome-Coronavirus Seropositive Bactrian Camels,

Mongolia," *Vector-Borne Zoonotic Dis.*, vol. 21, no. 2, pp. 128–131, Feb. 2021, doi: 10.1089/vbz.2020.2669.

Appendix Chapter 2

Contents

A2.1 – Search Terms 191
A2.2 – PRISMA 2009 flowchart 192
A2.3 – PRISMA 2009 Checklist 200

A2.1. Search Terms

MEDLINE search

MERS-CoV (mp†) **OR** Middle East Respiratory Syndrome Coronavirus (mp) **OR** MERS Coronavirus (mp) **OR** hCoV-EMC (mp) **OR** Middle East Respiratory Syndrome Coronavirus (subject heading‡)

AND

Seroprevalence (mp) **OR** sero prevalence (mp) **OR** serology (mp) **OR** seropositiv* (mp) **OR** sero positiv* (mp) **OR** Antibod* (mp) **OR** Seroepidemiolog* (mp) **OR** Sero epidemiolog* (mp) **OR** prevalence (mp) **OR** infection (mp) **OR** RNA (mp) **OR** shedding (mp) **OR** RT-PCR (mp) **OR** seroepidemiologic studies (subject heading)

AND

Camels (mp) **OR** camel (mp) **OR** dromedary* (mp) **OR** Camelus (subject heading)

EMBASE search

MERS-CoV (mp) **OR** Middle East Respiratory Syndrome Coronavirus (mp) **OR** MERS Coronavirus (mp) **OR** hCoV-EMC (mp) **OR** Middle East respiratory syndrome coronavirus (subject heading)

AND

Seroprevalence (mp) **OR** sero prevalence (mp) **OR** serology (mp) **OR** seropositiv* (mp) **OR** sero positiv* (mp) **OR** Antibod* (mp) **OR** Seroepidemiolog* (mp) **OR** Sero epidemiolog* (mp) **OR** prevalence (mp) **OR** infection (mp) **OR** RNA (mp) **OR** shedding (mp) **OR** RT-PCR (mp) **OR** seroprevalence (subject heading)

AND

Camels (mp) **OR** camel (mp) **OR** dromedary* (mp) **OR** camel (subject heading)

Web of Science search (DocType=All document types; Language=All languages). All terms used to search both TS (topic) and TI (title).

MERS-CoV (TS,TI) **OR** Middle East Respiratory Syndrome Coronavirus (TS,TI) **OR** MERS Coronavirus (TS,TI) **OR** hCoV-EMC

AND

Seroprevalence (TS,TI) **OR** sero prevalence (TS,TI) **OR** serology (TS,TI) **OR** seropositiv* (TS,TI) **OR** sero positiv* (TS,TI) **OR** Antibod* (TS,TI) **OR** Seroepidemiolog* (TS,TI) **OR** Sero epidemiolog* (TS,TI) **OR** prevalence (TS,TI) **OR** infection (TS,TI) **OR** RNA (TS,TI) **OR** shedding (TS,TI) **OR** RT-PCR (TS,TI)

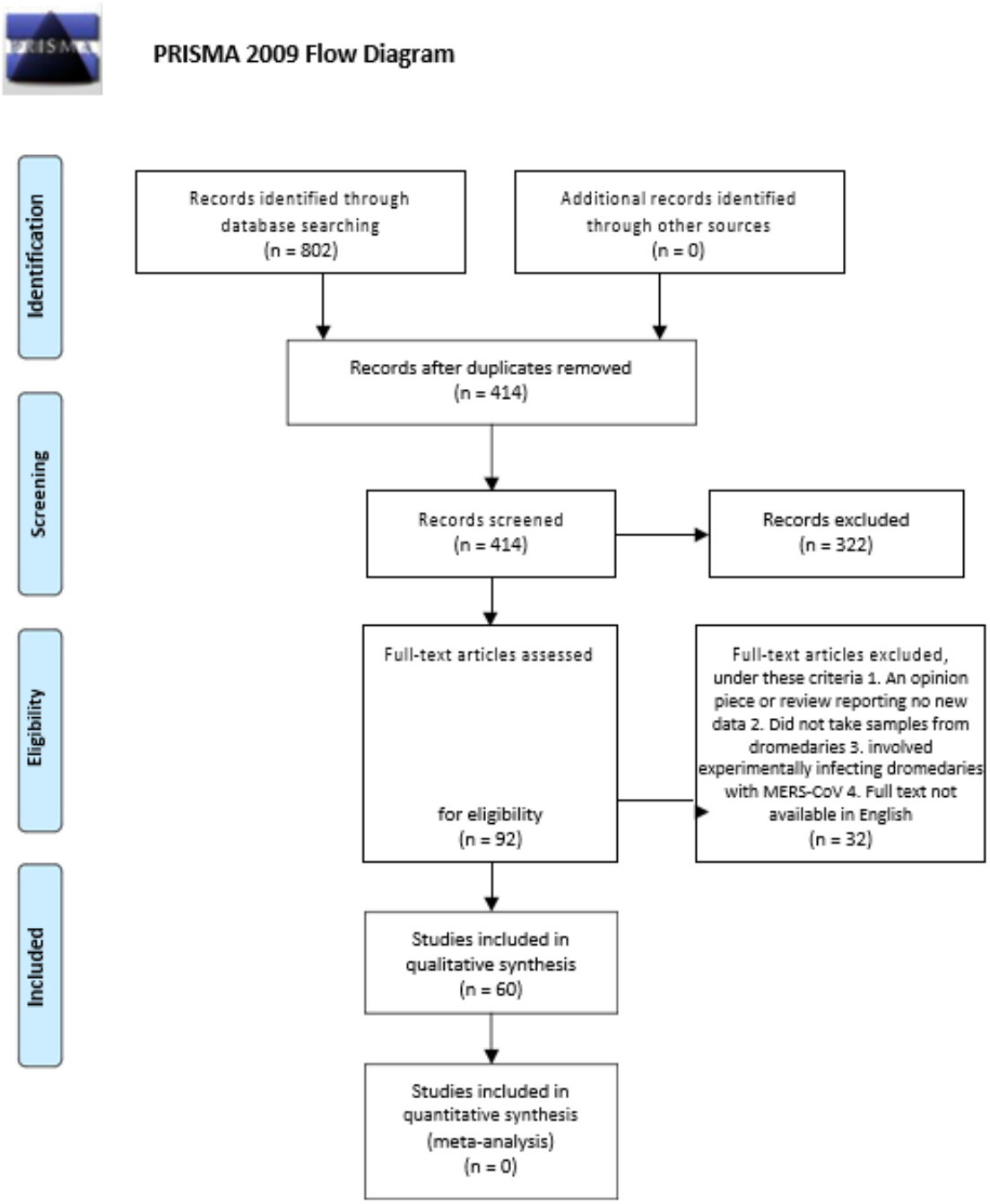
AND

Camels (TS,TI) **OR** camel (TS,TI) **OR** dromedary* (TS,TI)

† *mp = title, abstract, original title, name of substance word, subject heading word, floating sub-heading word, keyword heading word, protocol supplementary concept word, rare disease supplementary concept word, unique identifier, synonyms*

‡ *subject heading = database specific classification of article subjects*

A2.2. PRISMA 2009 Flow Diagram



From: Moher D, Liberati A, Tetzlaff J, Altman DG, The PRISMA Group (2009). *P*referred *R*eporting *I*tems for *S*ystematic Reviews and *M*eta-*A*nalyses: The PRISMA Statement. PLoS Med 6(7): e1000097. doi:10.1371/journal.pmed1000097

For more information, visit www.prisma-statement.org.

PRISMA 2009 Checklist (Adapted for KIN 4400)

A2.3. PRISMA 2009 Checklist

Section/topic	#	Checklist item	Reported on page #
TITLE			
Title	1	Identify the report as a literature review.	1
ABSTRACT			
Structured summary	2	Provide a structured summary including, as applicable: background; objectives; data sources; study eligibility criteria, participants, and interventions; study appraisal and synthesis methods; results; limitations; conclusions and implications of key findings;	2
INTRODUCTION			
Rationale	3	Describe the rationale for the review in the context of what is already known about your topic.	3 & 4
Objectives	4	Provide an explicit statement of questions being addressed with reference to participants, interventions, comparisons, outcomes, and study design (PICOS).	4
METHODS			
Eligibility criteria	5	Specify study characteristics (e.g., PICOS, length of follow-up) and report characteristics (e.g., years considered, language, publication status) used as criteria for eligibility, giving rationale.	4
Information sources	6	Describe all information sources (e.g., databases with dates of coverage) in the search and date last searched.	4
Search	7	Present full electronic search strategy for at least one database, including any limits used, such that it could be repeated.	S2
Study selection	8	State the process for selecting studies (i.e., screening, eligibility).	5
Risk of bias in individual studies	9	Describe methods used for assessing risk of bias of individual studies (including specification of whether this was done at the study or outcome level).	Not done at the individual level

Section/topic	#	Checklist item	Reported on page #
Risk of bias across studies	10	Specify any assessment of risk of bias that may affect the cumulative evidence (e.g., publication bias, selective reporting within studies).	5
RESULTS			
Study selection	11	Give numbers of studies screened, assessed for eligibility, and included in the review, with reasons for exclusions at each stage, ideally with a flow diagram.	6
Study characteristics	12	For each study, present characteristics for which data were extracted (e.g., study size, PICOS, follow-up period) and provide the citations.	7 & 8
Synthesis of results of individual studies	13	For all outcomes considered (benefits or harms), present, for each study: (a) summary of results and (b) relationship to other studies under review (e.g. agreements or disagreements in methods, sampling, data collection or findings).	6-17
DISCUSSION			
Summary of evidence	14	Summarize the main findings including the strength of evidence for each main outcome; consider their relevance to key groups (e.g., healthcare providers, users, and policy makers).	18-20
Limitations	15	Discuss limitations at study and outcome level (e.g., risk of bias), and at review-level (e.g., incomplete retrieval of identified research, reporting bias).	20-21 (At review level only)
CONCLUSION			
Conclusions	16	Provide a general interpretation of the results in the context of other evidence, and implications for future research.	21

Adapted from: Moher D, Liberati A, Tetzlaff J, Altman DG, The PRISMA Group (2009). Preferred Reporting Items for Systematic Reviews and Meta-Analyses: The PRISMA statement. *PLoS Medicine*, 6(6), e1000097. doi:10.1371/journal.pmed1000097

For more information, visit: **www.prisma-statement.org**.

Appendix Chapter 3

Contents

A3.1 – Rules followed for interpreting age classes in serological studies....191
A3.2 – Catalytic model solutions....192
A3.3 – Model validation – recovery of true parameters when fitting to simulated data....200
A3.4 – Model validation – Influence of each individual dataset....204
A3.5 – DIC when alternative fixed test-specific sensitivity and specificity is used....211
A3.6 – Catalytic model fits for all models....211
A3.7 – Parameter correlation....220

A3.1 – Rules followed for interpreting age classes in serological studies

1. If the study gives no lower age bound for the lowest age class this is assumed to be zero

2. If the study gives no upper age bound of the highest age class this is assumed to be 20 years

3. If the study describes an age class as >X years, its lower boundary is regarded as X years + 0.01 years if the previous age classes upper bound is X years.

4. If the study describes an age class as <X years, its upper boundary is regarded as X years - 0.01 years if the following age classes upper bound is X years.

5. If the study describes an age class as X-Y years, its upper boundary is considered to be Y years exactly, unless the other age classes indicate that it should reflect the whole year of life following the Yth birthday, in which case the upper boundary is regarded as Y + 0.99 years.
    i. E.g., If age class 1 is </=2yrs, and age class 2 is 3-5yrs, age class 2 is considered to be bounded by 3 years and 5.99 years. If instead age class 1 is <2 yrs and age class 2 is 2-5 years we would consider age class 2 to be bounded by 2 and 5 years exactly.

6. If the study describes an age class to be upper bound by <X years and the subsequent age class to be bound by >X years, we consider the upper bound of the 1st to be the Xth birthday (X years exactly) and the lower bound of the subsequent age class to be X + 0.01 years.

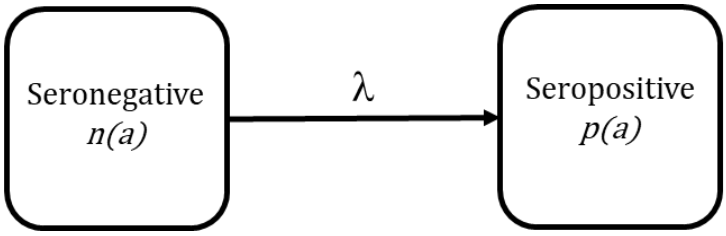
7. For studies that have age classes at the month scale rather than the year, the equivalent interpretations are made, with the smallest unit of age being 0.01 years as above.

8. If the study has described age classes as e.g. 0-2years, 2.1-3 years, 3.1-7 years, we have taken these boundaries (effectively 0.1 used instead of 0.01 as the smallest unit).

A3.2 – Catalytic model solutions

I) Model 1 the simplest catalytic model:

Where *a* is time/age, and λ is the force of infection (constant with age).

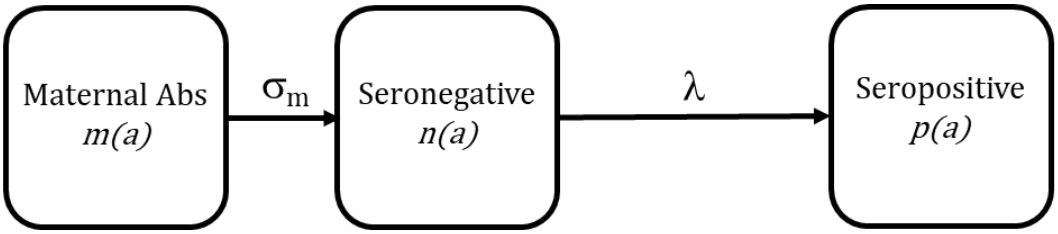


The proportion of individuals that are seropositive at age A is given by:

$$p(A) = \int_0^A \lambda e^{-\lambda a}\, da \; = 1 - \; e^{-\lambda A}$$

$$\boldsymbol{p(a) = 1 - \; e^{-\lambda a}}$$

II) Model 2 with maternal antibodies that wane at rate ω:



$$m(a) = m_0 e^{-\omega a}$$

$$n(a) = m_0 \left(\frac{\omega}{\lambda - \omega} \left(e^{-\omega a} - \; e^{-\lambda a} \right) \right) + \; e^{-\lambda a}(1 - m_0)$$

$$p(a) = 1 - m(a) - s(a)$$

<u>Workings</u>

Step one –the differential equations that represent our model

Since:

$$\frac{dm(a)}{da} = -\omega m(a)$$

We know that:

$$m(a) = m_0 e^{-\omega a}$$

If we substitute this into our differential equation for the rate of change of seronegative individuals n(a), which is:

$$\frac{dn(a)}{da} = \omega m(a) - \lambda n(a)$$

We get:

$$\frac{dn(a)}{da} = \omega m_0 e^{-\omega a} - \lambda n(a)$$

Step two – rearrangement to standard form

$$\frac{dn(a)}{da} + \lambda n(a) = \omega m_0 e^{-\omega a}$$

Step three – prep to solve using integrating factors

The necessary integrating factor is $IF = e^{\lambda a}$

(because $IF = e^{\int p(a)da}$ where p(a) in this case is $\lambda n(a)$)

By multiplying each side by the integrating factor, we get:

$$\frac{dn(a)}{da} e^{\lambda a} + \lambda n(a) e^{\lambda a} = \omega m_0 e^{-\omega a} e^{\lambda a}$$

Using the product rule, we see that the left-hand side it equivalent to the differential of the product of $n(a)$ and $e^{\lambda a}$. So, substituting this in we get:

$$\frac{d(n(a)e^{\lambda a})}{da} = \omega m_0 e^{-\omega a} e^{\lambda a}$$

Step four – solve using integration

$$\int_0^A \frac{d(n(a)e^{\lambda a})}{da} da = \int_0^A \omega m_0 e^{-\omega a}\, e^{\lambda a}\, da$$

So:

$$n(a)e^{\lambda a} - n(0) = m_0 \left[\frac{\omega}{\lambda - \omega} e^{\lambda a - \omega a}\right]_0^A$$

And since the initial proportion of the population that is susceptible will be 1 – the proportion born with maternally acquired immunity this is:

$$n(a)e^{\lambda a} - (1 - m_0) = m_0 \left[\frac{\omega}{\lambda - \omega} e^{\lambda a - \omega a}\right]_0^A$$

If we solve this, it becomes:

$$n(a)e^{\lambda a} - (1 - m_0) = m_0 \left(\frac{\omega e^{(\lambda-\omega)a}}{\lambda - \omega} - \frac{\omega}{\lambda - \omega}\right)$$

$$n(a) = m_0 \left(\frac{\omega}{\lambda - \omega}\left(e^{-\omega a} - e^{-\lambda a}\right)\right) + e^{-\lambda a}(1 - m_0)$$

And so, since p(a) = 1 – (n(a) + m(a))

$$\boldsymbol{p(a) = 1 - e^{-\lambda a} - m_0 \left(\frac{\omega}{\lambda - \omega}\left(e^{-\omega a} - e^{-\lambda a}\right)\right) + m_0(e^{-\lambda a} - e^{-\omega a})}$$

We can see that when m_0 is equal to zero, Model 2 simplifies to Model 1

$$p(a) = 1 - e^{-\lambda a} \cancel{- m_0 \left(\frac{\omega}{\lambda - \omega}\left(e^{-\omega a} - e^{-\lambda a}\right)\right) + m_0(e^{-\lambda a} - e^{-\omega a}}$$

$$p(a) = 1 - e^{-\lambda a}$$

Rather than using the solution of n(a) to solve p(a), we can also directly solve p(a):

$$\frac{dp(a)}{da} = \lambda n(a) = \lambda\left(1 - \left(p(a) + m(a)\right)\right)$$

$$= \lambda - \lambda p(a) - \lambda m_0 e^{-\omega a}$$

$$\frac{dp(a)}{da} + \lambda p(a) = \lambda(1 - m_0 e^{-\omega a})$$

Using $e^{\lambda a}$as an integrating factor (since IF = $e^{\int q a}$ where q = λ in this case), and according to the product rule, when we multiply both sides by IF, the left-hand side becomes equivalent to the differential of p(a)*IF.

$$e^{\lambda a}\left(\frac{dp(a)}{da} + \lambda p(a)\right) =$$

$$\frac{dp(a)e^{\lambda a}}{da} = \lambda e^{\lambda a}(1 - m_0 e^{-\omega a})$$

So $p(a)e^{\lambda a} = \int \lambda e^{\lambda a} - \lambda m_0 e^{-\omega a} da = \left[e^{\lambda a} - \frac{\lambda}{\lambda-\omega} m_0 e^{(\lambda-\omega)a}\right]_0^A$

$= e^{\lambda a} - \frac{\lambda}{\lambda-\omega} m_0 e^{(\lambda-\omega)a} - \left(1 - \frac{\lambda}{\lambda-\omega} m_0\right)$

If we divide through by the integrating factor to get p(a), we get:

$$\boldsymbol{p(a) = 1 - e^{-\lambda a} - m_0\left(\frac{\lambda}{\lambda-\omega}\left(e^{-\omega a} - e^{-\lambda a}\right)\right)}$$

These solutions for p(a) are equivalent. I show this below:

(1) $p(a) = 1 - e^{-\lambda a} - m_0\left(\frac{\omega}{\lambda-\omega}\left(e^{-\omega a} - e^{-\lambda a}\right)\right) + m_0(e^{-\lambda a} - e^{-\omega a})$

(2) $p(a) = 1 - e^{-\lambda a} - m_0\left(\frac{\lambda}{\lambda-\omega}\left(e^{-\omega a} - e^{-\lambda a}\right)\right)$

Let's say $x = m_0\left(\frac{1}{\lambda-\omega}\left(e^{-\omega a} - e^{-\lambda a}\right)\right)$

(1) $1 - e^{-\lambda a} - \omega x + m_0\left(e^{-\lambda a} - e^{-\omega a}\right)$

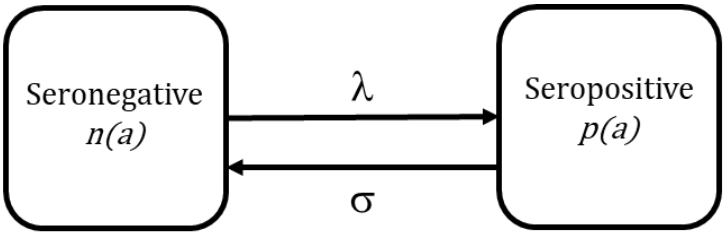
$= 1 - e^{-\lambda a} - \omega x - x(\lambda - \omega)$

(2) $1 - e^{-\lambda a} - \lambda x$

And we can see that ωx cancels out and (1) = (2).

Choosing a prior for ω. Longitudinal studies find that antibodies (assumed maternal) seem to last around 4-5 months. We use a lognormal distribution with a mean of 1 and a standard deviation of 0.2.

III) Model 3 with seroreversion at rate σ:



1. $\frac{dp}{da} = \lambda - (\lambda + \sigma)p$
2. $p = xe^{-(\lambda+\sigma)a}$

Substituting 2 into 1 and using the product rule:

$$\frac{d\left(xe^{-(\lambda+\sigma)a}\right)}{da} =$$

$$e^{-(\lambda+\sigma)a}\left[\frac{dx}{da} - (\lambda+\sigma)x\right] = \lambda - (\lambda+\sigma)xe^{-(\lambda+\sigma)a}$$

Dividing through by $e^{-(\lambda+\sigma)a}$ gives:

$$\frac{dx}{da} - (\lambda+\sigma)x = \lambda e^{(\lambda+\sigma)a} - (\lambda+\sigma)x$$

Cancelling out $(\lambda+\sigma)x$ leaves us with:

$$\frac{dx}{da} = \lambda e^{(\lambda+\sigma)a}$$

Integrating $\frac{dx}{da}$ gives us:

$$x(a) = \int \lambda e^{(\lambda+\sigma)a}\, da$$

$$= \left[\frac{\lambda}{\lambda+\sigma} e^{(\lambda+\sigma)a}\right]_0^A$$

$$= \frac{\lambda}{\lambda+\sigma}\left[e^{(\lambda+\sigma)a} - 1\right]$$

Substituting this back into equation 2 gives:

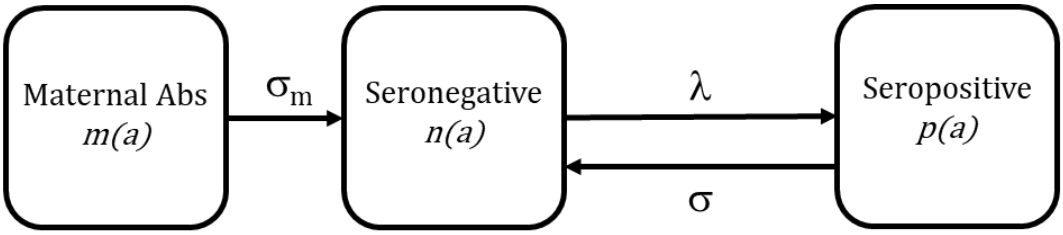
$$p(a) = \frac{\lambda}{\lambda+\sigma}\left(e^{(\lambda+\sigma)a} - 1\right) e^{-(\lambda+\sigma)a}$$

$$= \frac{\boldsymbol{\lambda}}{\boldsymbol{\lambda+\sigma}}\left(\mathbf{1} - \boldsymbol{e}^{-(\boldsymbol{\lambda+\sigma})\boldsymbol{a}}\right)$$

We see that when σ is equal to zero, Model 3 simplifies to Model 1.

$$p(a) = \frac{\cancel{\lambda}}{\cancel{\lambda+\sigma}}\left(1 - e^{-(\lambda+\cancel{\sigma})a}\right)$$

IV) Model 4 with maternal antibodies and seroreversion:



$$\frac{dp}{da} = \lambda n - \sigma p$$

$$= \lambda\big(1 - (p + m)\big) - \sigma p$$

$$= \lambda\big(1 - (p + m_0 e^{-\omega a})\big) - \sigma p$$

$$= \lambda(1 - m_0 e^{-\omega a}) - (\lambda + \sigma)p$$

If we say:

$$p = xe^{-(\lambda+\sigma)a}$$

Then substituting that into equation one and using the product rule we have:

$$\frac{d\big(xe^{-(\lambda+\sigma)a}\big)}{da} =$$

$$e^{-(\lambda+\sigma)a}\left[\frac{dx}{da} - (\lambda + \sigma)x\right] = \lambda(1 - m_0 e^{-\omega a}) - (\lambda + \sigma)xe^{-(\lambda+\sigma)a}$$

Dividing through by $e^{-(\lambda+\sigma)a}$ and rearranging gives us:

$$\frac{dx}{da} = \lambda e^{(\lambda+\sigma)a} - \lambda m_0 e^{(\lambda+\sigma-\omega)a}$$

Integrating this gives:

$$x(a) = \int \lambda e^{(\lambda+\sigma)a} - \lambda m_0 e^{(\lambda+\sigma-\omega)a}\, da$$

$$= \left[\frac{\lambda}{\lambda + \sigma} e^{(\lambda+\sigma)a} - \frac{\lambda m_0}{\lambda + \sigma - \omega} e^{(\lambda+\sigma-\omega)a}\right]_0^A$$

$$= \frac{\lambda}{\lambda + \sigma}\big(e^{(\lambda+\sigma)a} - 1\big) - \frac{\lambda m_0}{\lambda + \sigma - \omega}(e^{(\lambda+\sigma-\omega)a} - 1)$$

Since:

$$p(a) = e^{-(\lambda+\sigma)a}x(a)$$

$$\boldsymbol{p(a) = \frac{\lambda}{\lambda+\sigma}\left(1 - e^{-(\lambda+\sigma)a}\right) - m_0 \frac{\lambda}{\lambda+\sigma-\omega}\left(e^{-\omega a} - e^{-(\lambda+\sigma)a}\right)}$$

As a sanity check, when m_0 is equal to zero, Model 4 simplifies to Model 3.

$$p(a) = \frac{\lambda}{\lambda+\sigma}\left(1 - e^{-(\lambda+\sigma)a}\right) \cancel{- m_0 \frac{\lambda}{\lambda+\sigma-\omega}\left(e^{-\omega a} - e^{-(\lambda+\sigma)a}\right)}$$

$$p(a) = \frac{\lambda}{\lambda+\sigma}\left(1 - e^{-(\lambda+\sigma)a}\right)$$

Similarly, when σ is equal to zero, Model 4 simplifies to Model 2.

$$p(a) = \frac{\cancel{\lambda}}{\cancel{\lambda+\sigma}}\left(1 - e^{-(\lambda+\cancel{\sigma})a}\right) - \frac{\lambda m_0}{\lambda+\cancel{\sigma}-\omega}\left(e^{-\omega a} - e^{-(\lambda+\cancel{\sigma})a}\right)$$

$$p(a) = 1 - e^{-\lambda a} - m_0\left(\frac{\lambda}{\lambda-\omega}\left(e^{-\omega a} - e^{-\lambda a}\right)\right)$$

Model 4 seroprevalence in an age class (rather than prevalence at a point age)

Starting point is point prevalence at age = a

$$p(a) = \frac{\lambda}{\lambda+\sigma}\left(1 - e^{-(\lambda+\sigma)a}\right) - m_0 \frac{\lambda}{\lambda+\sigma-\omega}\left(e^{-\omega a} - e^{-(\lambda+\sigma)a}\right)$$

To get the average prevalence in an age class bounded by $a_1 and\ a_2$, we need to integrate the above between $a_1 and\ a_2$:

$$p(\overline{a_1 \rightarrow a_2}) = \int_{a1}^{a2} \frac{\lambda}{\lambda+\sigma}\left(1 - e^{-(\lambda+\sigma)a}\right) - m_0 \frac{\lambda}{\lambda+\sigma-\omega}\left(e^{-\omega a} - e^{-(\lambda+\sigma)a}\right)da$$

$$= \frac{1}{a_2 - a_1}\left[\frac{\lambda}{\lambda+\sigma}\left(a + \frac{1}{\lambda+\sigma}e^{-(\lambda+\sigma)a}\right) - m_0 \frac{\lambda}{\lambda+\sigma-\omega}\left(\frac{1}{\lambda+\sigma}e^{-(\lambda+\sigma)a} - \frac{1}{\omega}e^{-\omega a}\right)\right]_{a1}^{a2}$$

$$= \frac{1}{a_2 - a_1}\left(\frac{\lambda}{\lambda+\sigma}\left((a_2 - a_1) + \frac{1}{\lambda+\sigma}\left(e^{-(\lambda+\sigma)a_2} - e^{-(\lambda+\sigma)a_1}\right)\right)\right.$$
$$\left. - m_0 \frac{\lambda}{\lambda+\sigma-\omega}\left(\frac{1}{\lambda+\sigma}\left(e^{-(\lambda+\sigma)a_2} - e^{-(\lambda+\sigma)a_1}\right) - \frac{1}{\omega}\left(e^{-\omega a_2} - e^{-\omega a_1}\right)\right)\right)$$

Reduced to model 1 this is:

$$= \frac{1}{a_2 - a_1}\left(a_2 - a_1 + \frac{1}{\lambda}\left(e^{-\lambda a_2} - e^{-\lambda a_1}\right)\right)$$

Reduced to model 3 this is:

$$= \frac{1}{a_2 - a_1}\left(\left(a_2 - a_1 + \frac{1}{\lambda}\left(e^{-\lambda a_2} - e^{-\lambda a_1}\right)\right)\right.$$
$$\left. - m_0 \frac{\lambda}{\lambda-\omega}\left(\frac{1}{\lambda}\left(e^{-\lambda a_2} - e^{-\lambda a_1}\right) - \frac{1}{\omega}\left(e^{-\omega a_2} - e^{-\omega a_1}\right)\right)\right)$$

A3.3 – Model validation – recovery of true parameters when fitting to simulated data

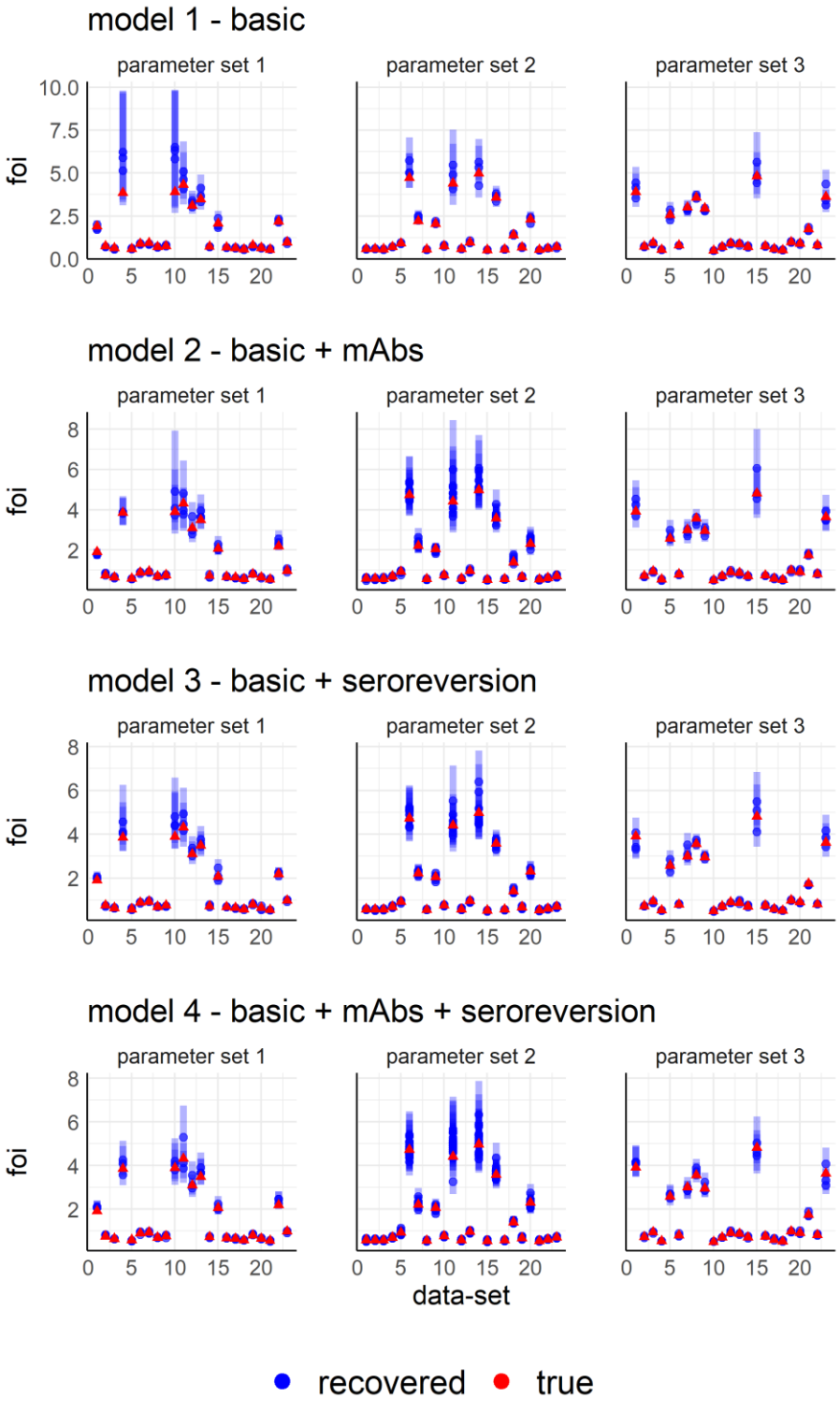


Figure A3.3.1. Comparison of true FoI values used in binomially distributed data simulation and recovered estimates for all four catalytic models of infection. *Red represents true values, blue dots are central estimates and bars are 95% CrIs from model fitting to multiple simulations for each set of parameters.*

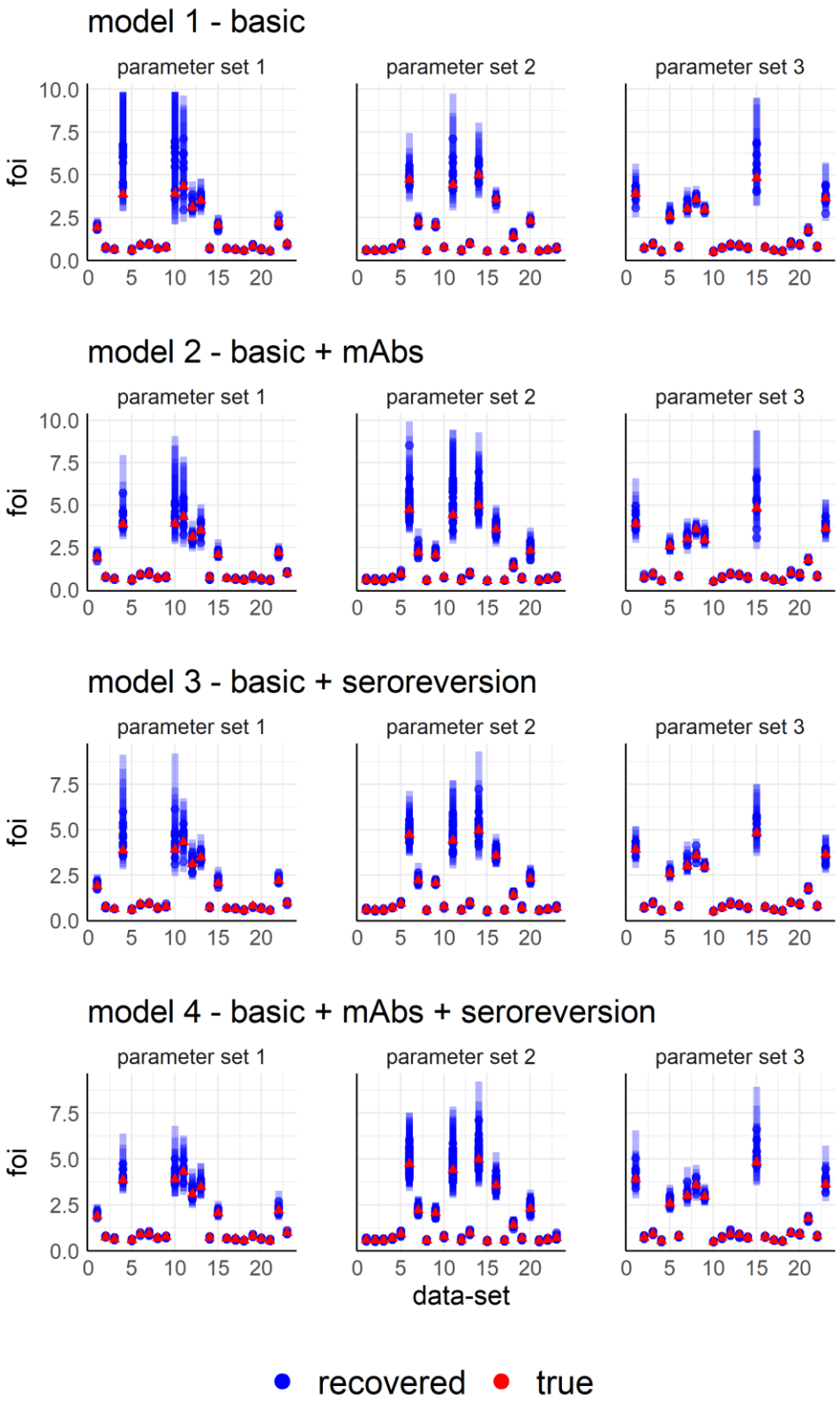


Figure A3.3.2. Comparison of true FoI values used in overdispersed data simulation and recovered estimates for all four catalytic models of infection*. Red represents true values, blue dots are central estimates and bars are 95% CrIs from model fitting to multiple simulations for each set of parameters.*

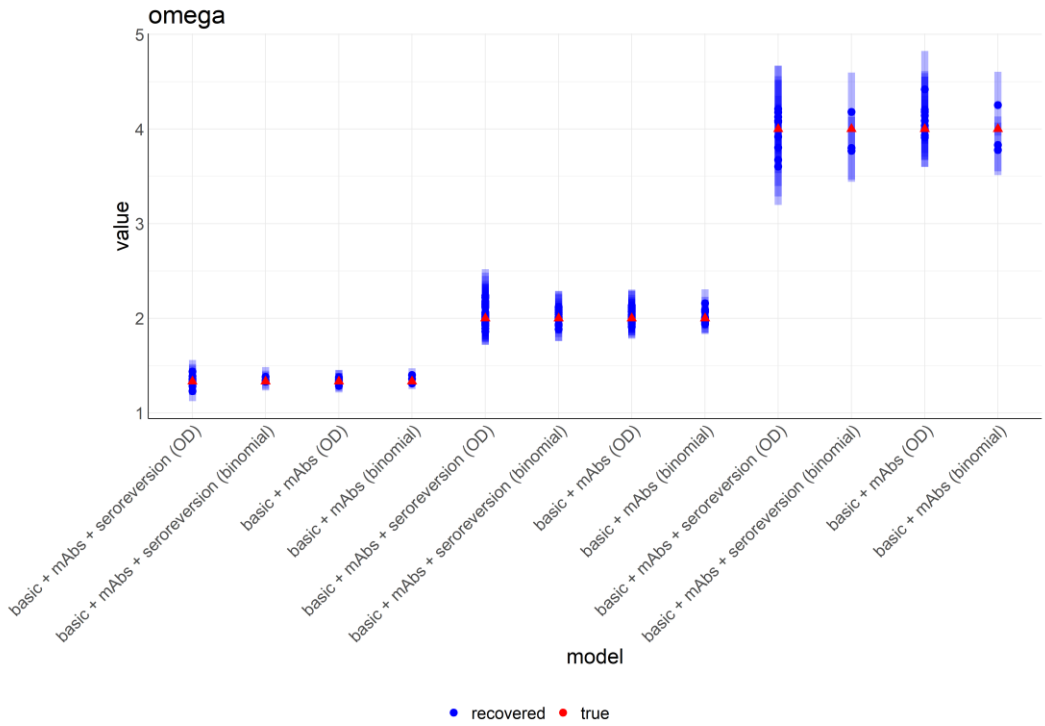


Figure A3.3.3. Comparison of true and recovered estimates for the rate of waning of mAbs, ω. *Red represents true values and blue represents recovered estimates (blue 95% CrI for fitting to multiple simulated datasets). The value of ω is recovered well.*

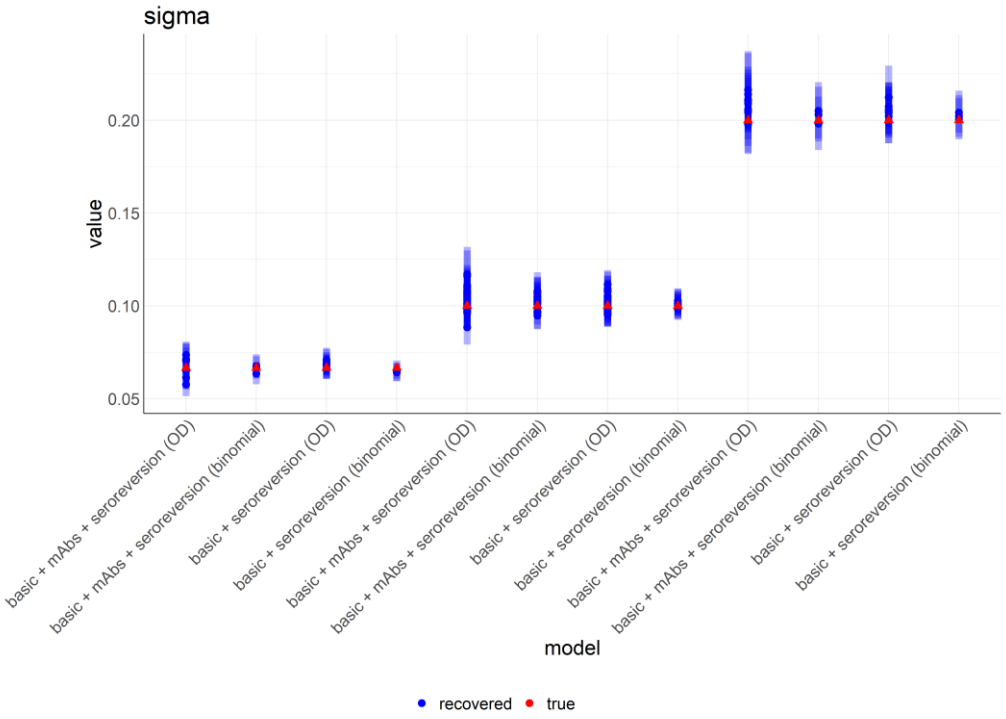


Figure A3.3.4. Comparison of true and recovered estimates for the rate of waning of Abs following infection, σ. *Red represents true values and blue represents recovered estimates (blue 95% CrI for fitting to multiple simulated datasets). The value of σ is recovered well.*

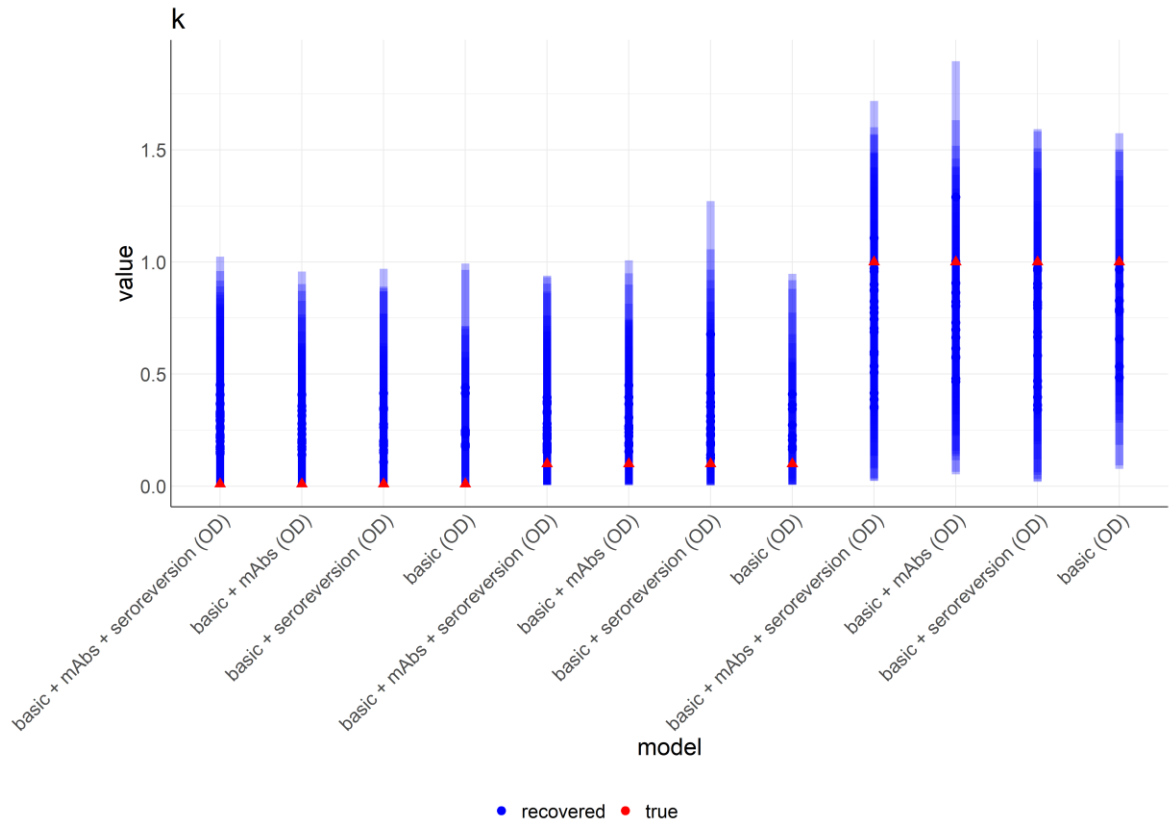


Figure A3.3.5. Comparison of the true and recovered estimates of the overdispersion parameter, k. *Red represents true values, and blue represents recovered values (blue 95% CrI are shown for fitting to multiple simulated datasets). When the true value of k is small, k is often over-estimated.*

A3.4 – Model validation – Influence of each individual dataset

To check the influence of each real data set on the global parameters, each data set was removed in turn and the parameters were re-estimated. The ranking of model 4 as the best fitting model was not affected by the exclusion of any dataset (***Figure A3.4A***). The parameter estimates were relatively consistent when each of the 23 datasets were removed (***Figures A3.4B-E***), with two notable exceptions. Firstly, for model 4 (***Figure A3.4E***), omitting the dataset measuring seroprevalence in Kenya [88] increased estimates for ω and σ when the seroprevalence data was assumed to be binomially distributed. This effect was lessened when the data was assumed to be over dispersed. Secondly, the removal of the seroprevalence in dromedaries in Egypt described in [63] decreased the rate of waning of mAbs considerably in both model 2 (***Figure A3.4C***) and model 4, and decreased the estimated overdispersion parameter. Removal of the dataset had little effect on the estimated rate of antibody waning following infection (σ) when mAbs were included in the model, but for model 3 – in which mAbs are absent – its omission led to an increase in the estimate of σ. The study in question measured a much lower seroprevalence measure for young calves compared to the other studies included in model fitting. This difference likely explains the dataset's effect on ω and on the overdispersion parameter.

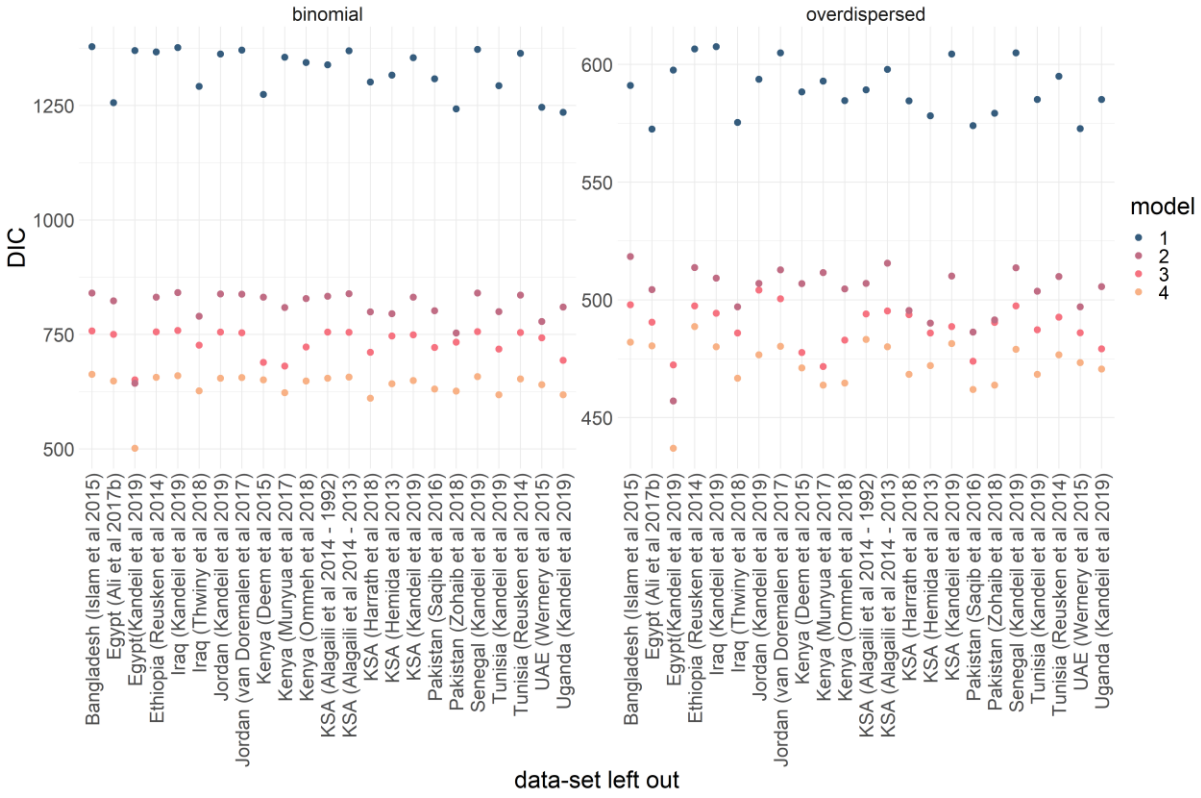


Figure A3.4.1 Comparison of the DIC across models when each dataset is left out in turn *(model 1: seroconversion, model 2: seroconversion + mAbs, model 3: seroconversion + seroreversion, model 4: seroconversion + mAbs + seroreversion). The best fitting model is model 4 in all cases. Adding seroreversion alone to the model improves fit by more than adding mAbs alone except when Egypt (Kandeil et al 2019) is excluded in which case there is a reversal in model rank.*

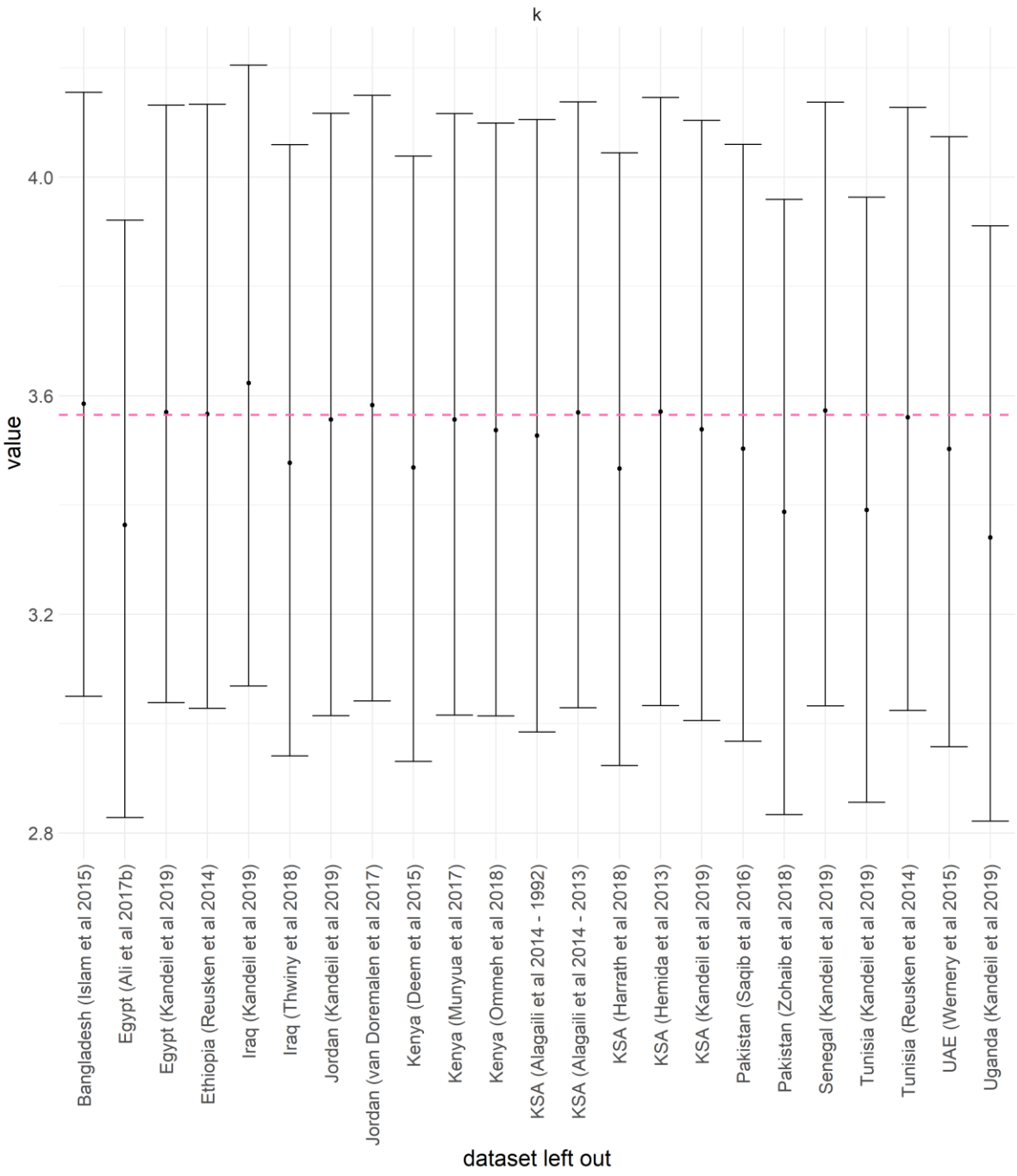


Figure A3.4.2 Comparison of the model 1 estimate of the overdispersion parameter, k, when each dataset is left out in turn. *Error bars represent 95% CrIs. The pink dotted line represents the central estimates when all datasets are included.*

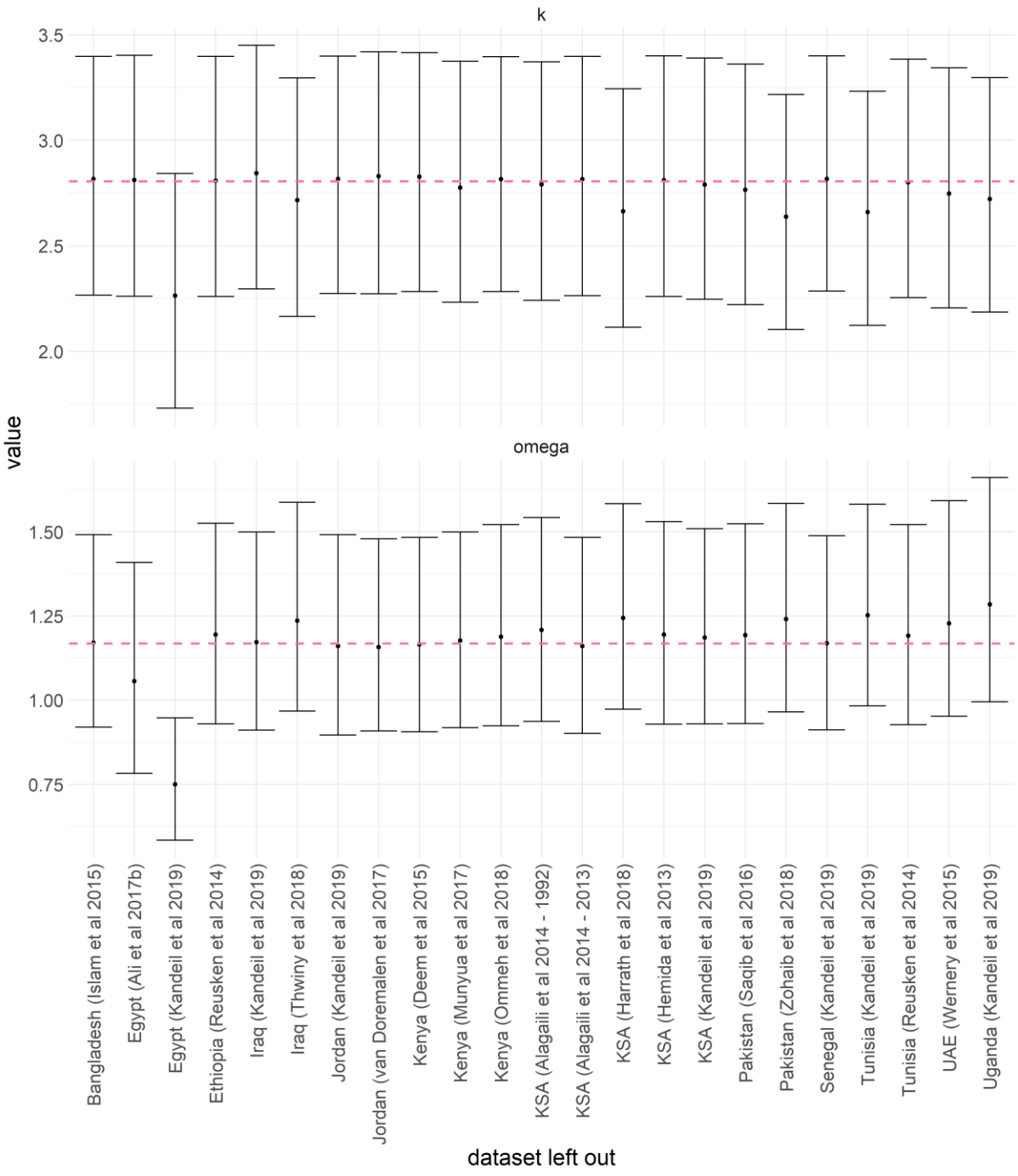


Figure A3.4.3. Comparison of the model 2 estimates of the overdispersion parameter, k, and the rate of waning of mAbs, ω, when each dataset is left out in turn. *Error bars represent 95% CrIs. The pink dotted line represents the central estimates when all datasets are included.*

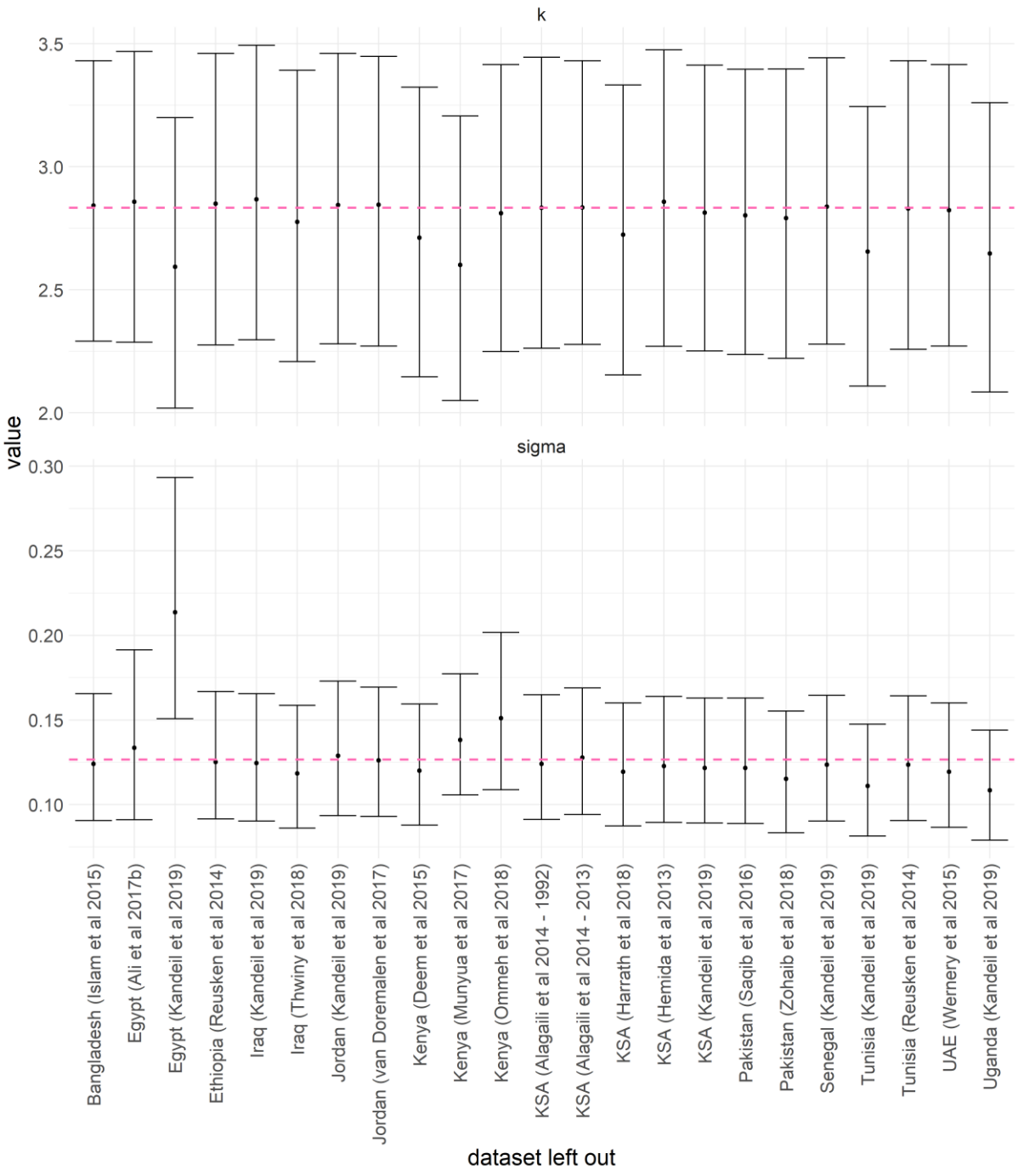


Figure A3.4.4. Comparison of the model 3 estimates of the overdispersion parameter, k, and the rate of waning of Abs following infection, σ, when each dataset is left out in turn. *Error bars represent 95% CrIs. The pink dotted line represents the central estimates when all datasets are included.*

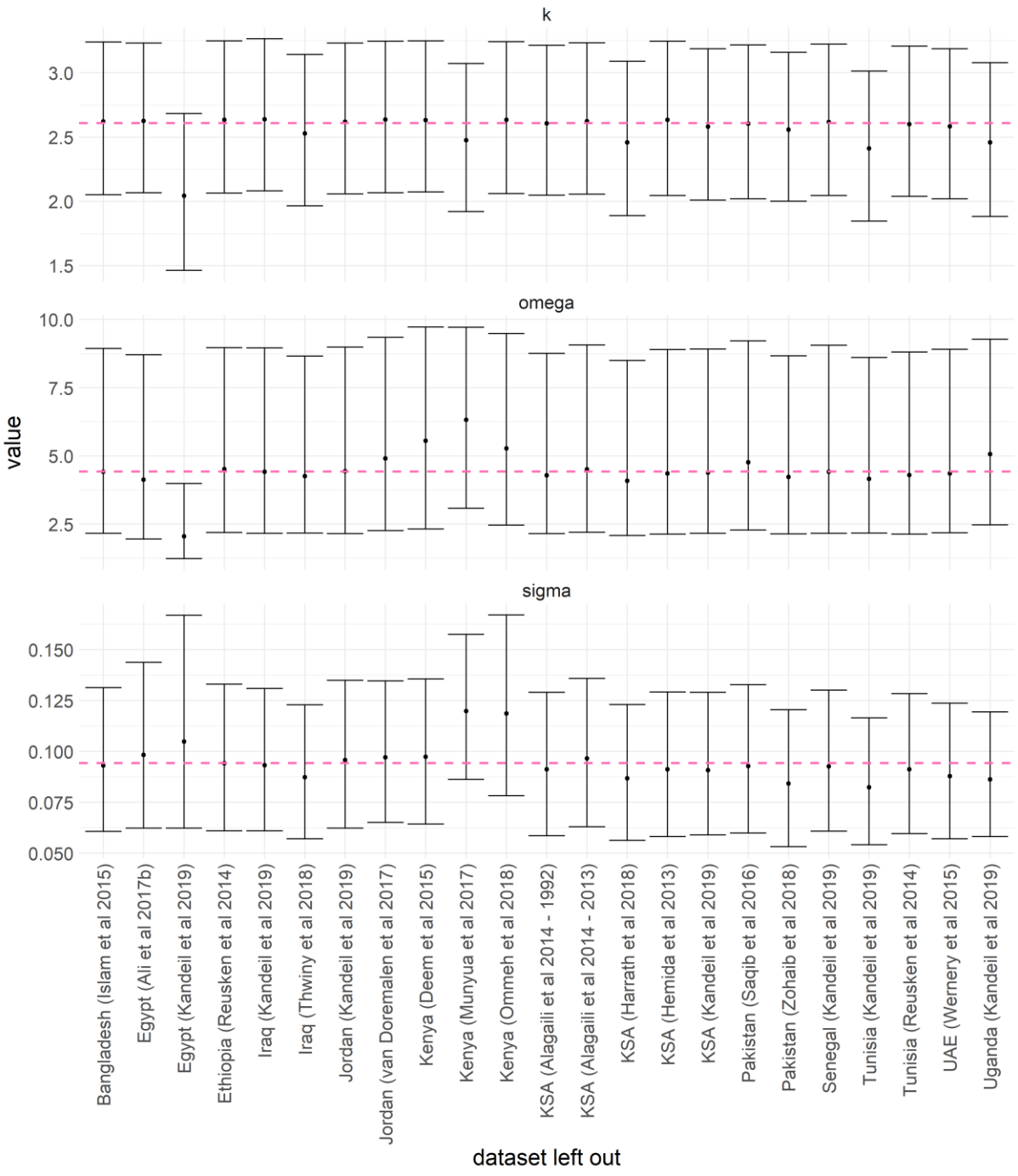


Figure A3.4.5 Comparison of the model 4 estimates of the overdispersion parameter, k, the rate of waning of mAbs, ω, and the rate of waning of Abs following infection, σ, when each dataset is left out in turn. *Error bars represent 95% CrIs. The pink dotted line represents the central estimates when all datasets are included.*

A3.5 – DIC models when alternative fixed test-specific sensitivity and specificity is used

Table A3.5.1 Comparison of model fit for alternative fixed values of test-type specific sensitivity and specificity - *when test-specific sensitivity is reduced from 99% to 85% for neutralisation tests, and specificity is reduced from 100% to 85% for ELISAs*

		DIC	*Effective number of parameters*
Over dispersed	seroconversion	513	17
	seroconversion + seroreversion	504	20
	seroconversion + mAbs	494	18
	seroconversion + mAbs + seroreversion	490	19

A3.6 – Catalytic model fits for all models

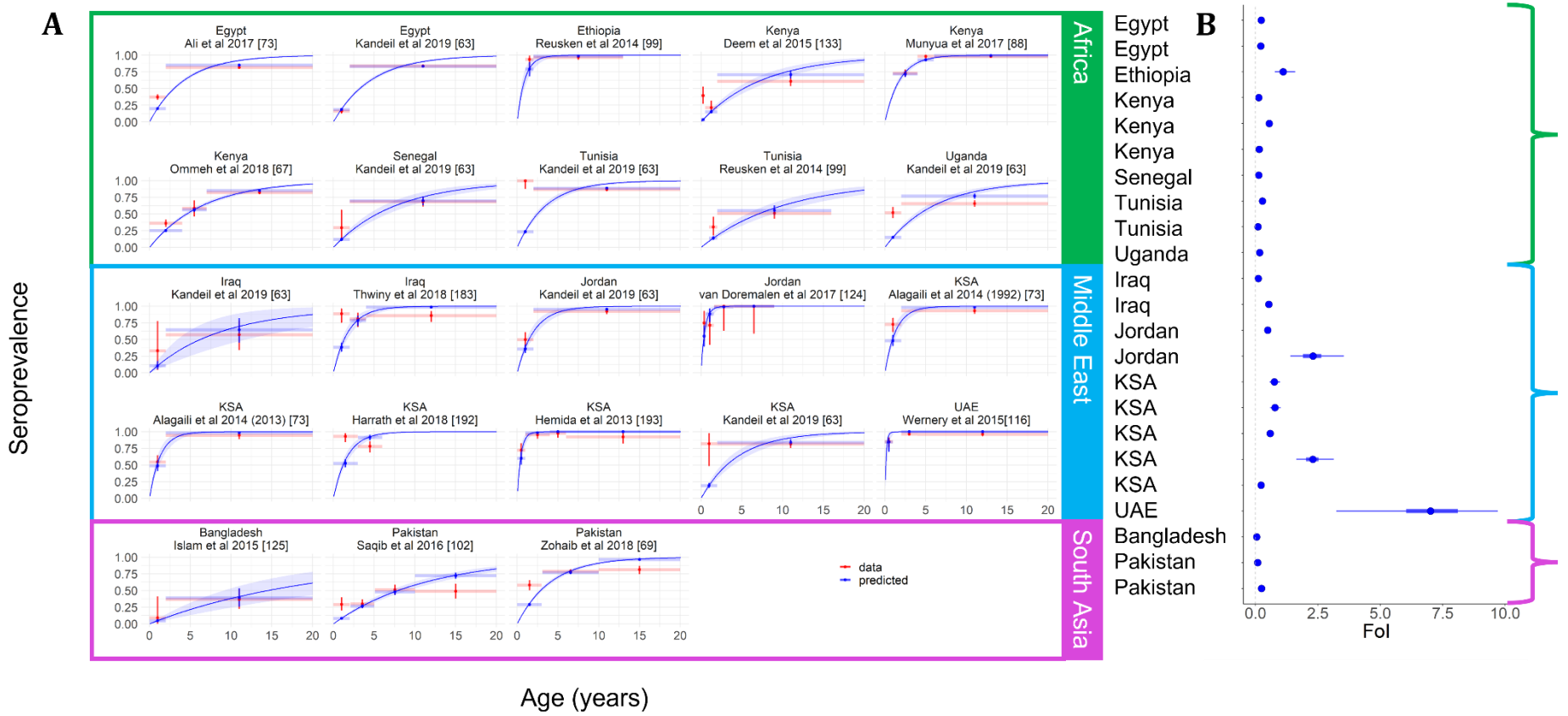


Figure A3.6.1. Predicted seroprevalence and FoI estimates using Model 1a (binomial). A. *Predicted seroprevalence by age (blue) with vertical 95% credible intervals, fitted to age-stratified seroprevalence shown with vertical 95% confidence intervals (red). Horizontal bars show age class width* ***B.*** *Posterior estimates for the FoI for each study, where the point represents the mean, the thicker line represents the 25th-75th percentiles and the thinner line represents the range of samples falling between the 2.5th and 97.5th percentiles.*

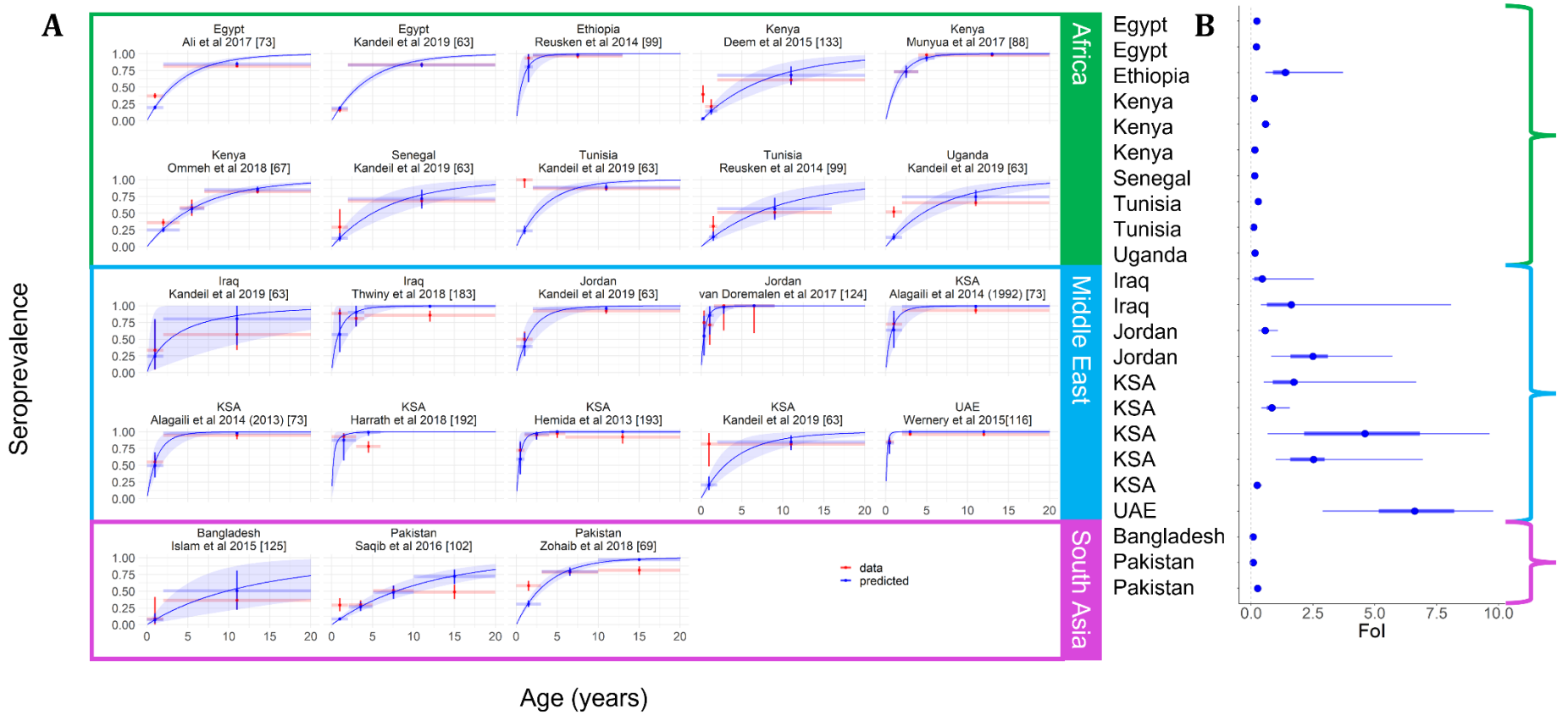


Figure A3.6.2. Predicted seroprevalence and FoI estimates using Model 1b (overdispersed) A. *Predicted seroprevalence by age (blue) with vertical 95% credible intervals, fitted to age-stratified seroprevalence shown with vertical 95% confidence intervals (red). Horizontal bars show age class width* ***B.*** *Posterior estimates for the FoI for each study, where the point represents the mean, the thicker line represents the 25th-75th percentiles and the thinner line represents the range of samples falling between the 2.5th and 97.5th percentiles.*

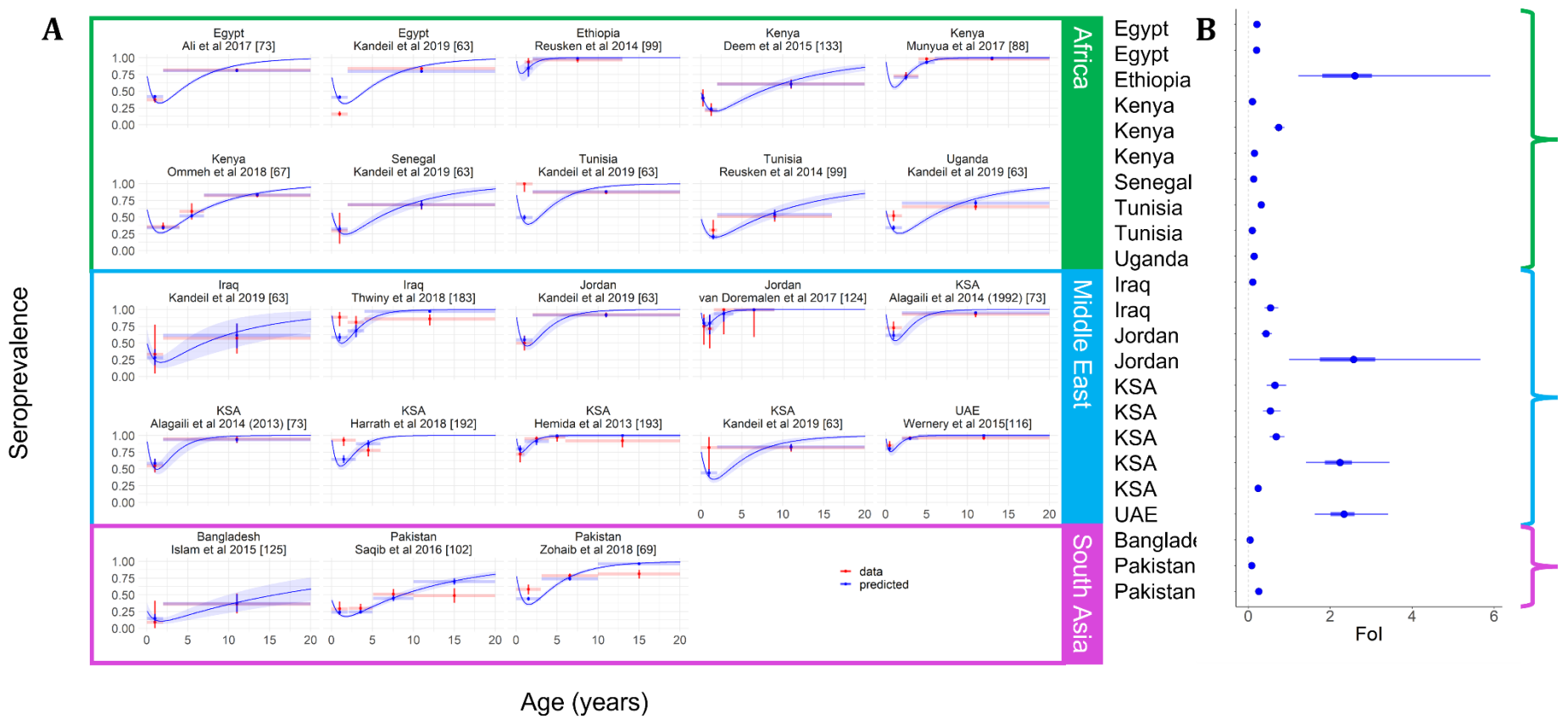


Figure A3.6.3. Predicted seroprevalence and FoI estimates using Model 2a (binomial). A. *Predicted seroprevalence by age (blue) with vertical 95% credible intervals, fitted to age-stratified seroprevalence shown with vertical 95% confidence intervals (red). Horizontal bars show age class width* ***B.*** *Posterior estimates for the FoI for each study, where the point represents the mean, the thicker line represents the 25th-75th percentiles and the thinner line represents the range of samples falling between the 2.5th and 97.5th percentiles.*

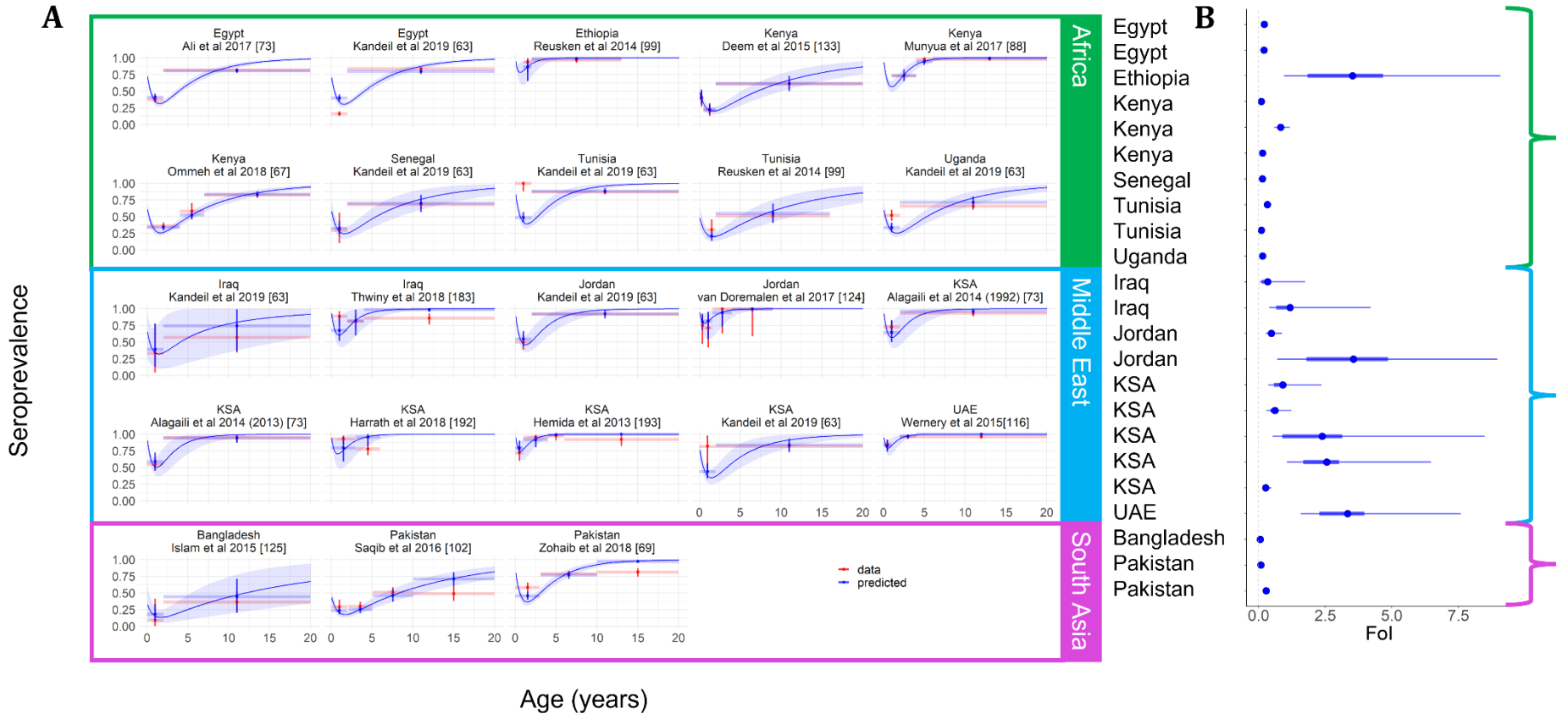


Figure A3.6.4. Predicted seroprevalence and FoI estimates using Model 2b (overdispersed). A. *Predicted seroprevalence by age (blue) with vertical 95% credible intervals, fitted to age-stratified seroprevalence shown with vertical 95% confidence intervals (red). Horizontal bars show age class width* ***B.*** *Posterior estimates for the FoI for each study, where the point represents the mean, the thicker line represents the 25th-75th percentiles and the thinner line represents the range of samples falling between the 2.5th and 97.5th percentiles.*

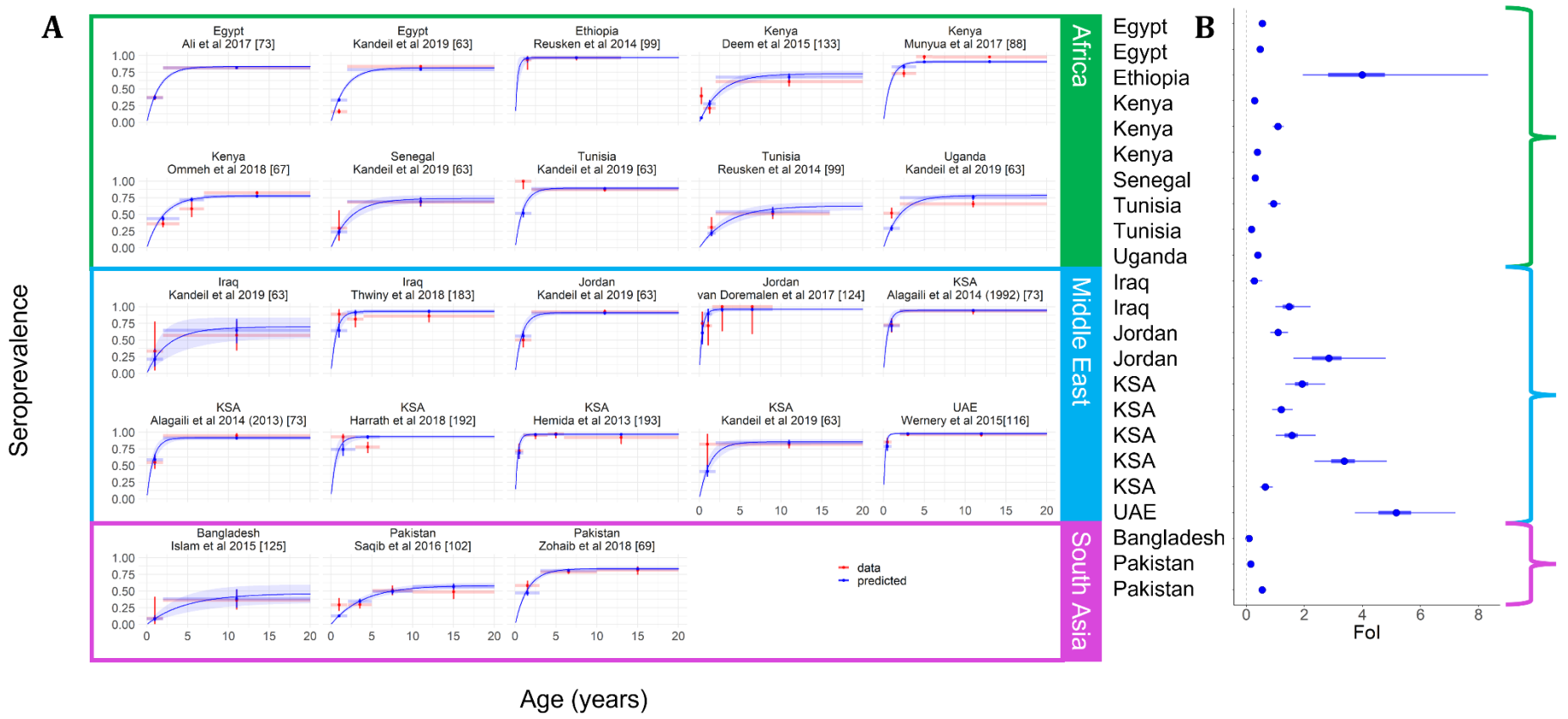


Figure A3.6.5. Predicted seroprevalence and FoI estimates using Model 3a (binomial).) A. *Predicted seroprevalence by age (blue) with vertical 95% credible intervals, fitted to age-stratified seroprevalence shown with vertical 95% confidence intervals (red). Horizontal bars show age class width* ***B.*** *Posterior estimates for the FoI for each study, where the point represents the mean, the thicker line represents the 25th-75th percentiles and the thinner line represents the range of samples falling between the 2.5th and 97.5th percentiles.*

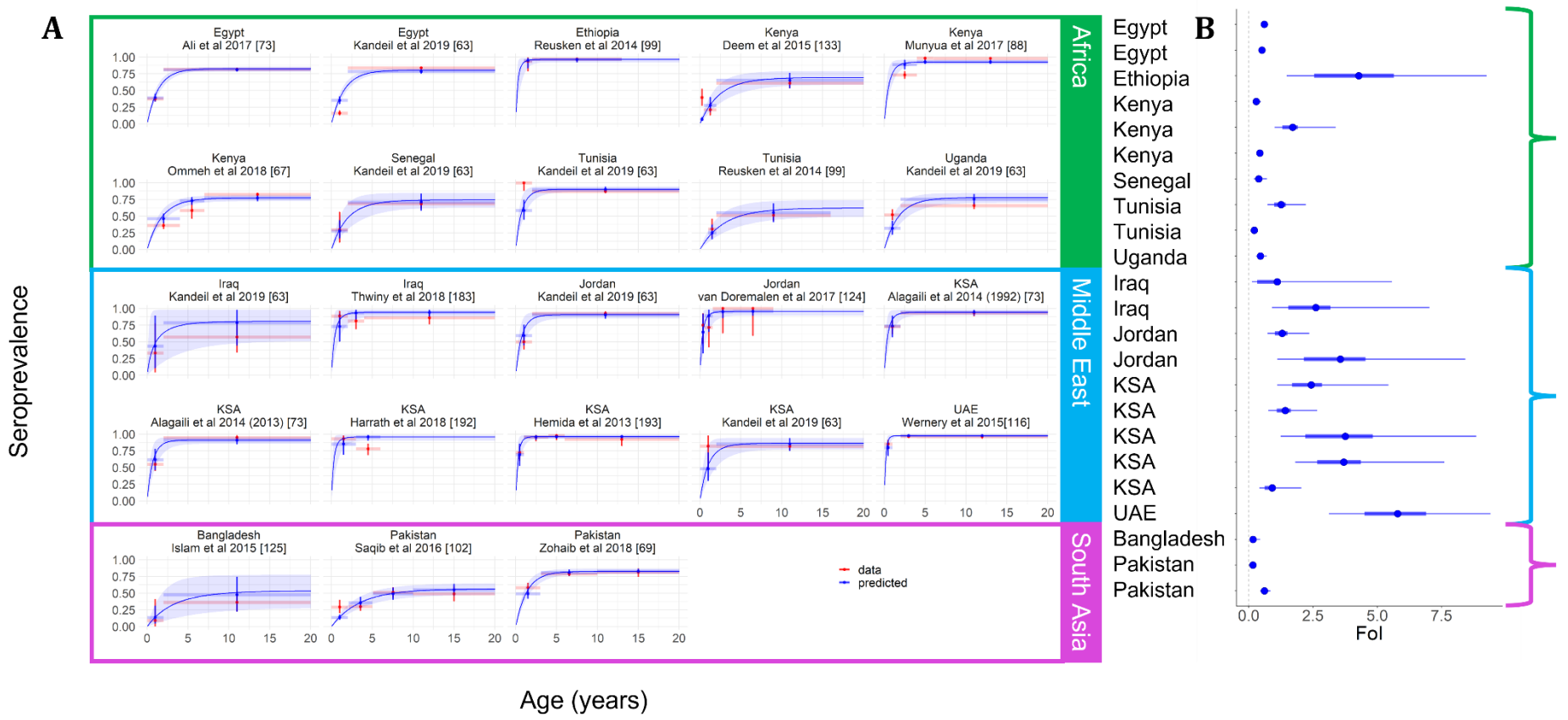


Figure A3.6.6. Predicted seroprevalence and FoI estimates using Model 3b (overdispersed). A. *Predicted seroprevalence by age (blue) with vertical 95% credible intervals, fitted to age-stratified seroprevalence shown with vertical 95% confidence intervals (red). Horizontal bars show age class width* ***B.*** *Posterior estimates for the FoI for each study, where the point represents the mean, the thicker line represents the 25th-75th percentiles and the thinner line represents the range of samples falling between the 2.5th and 97.5th percentiles.*

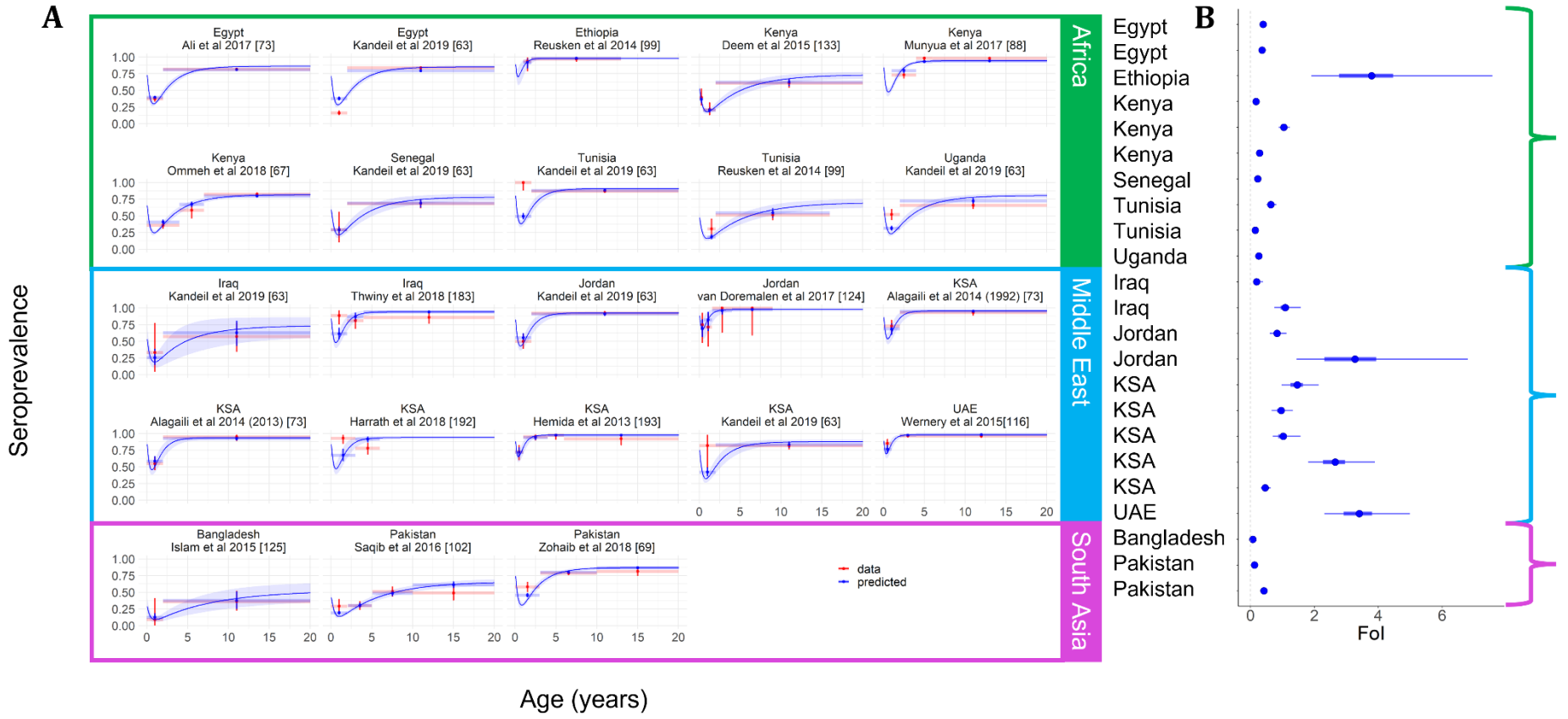


Figure A3.6.7. Predicted seroprevalence and FoI estimates using Model 4a (binomial). A. *Predicted seroprevalence by age (blue) with vertical 95% credible intervals, fitted to age-stratified seroprevalence shown with vertical 95% confidence intervals (red). Horizontal bars show age class width* ***B.*** *Posterior estimates for the FoI for each study, where the point represents the mean, the thicker line represents the 25th-75th percentiles and the thinner line represents the range of samples falling between the 2.5th and 97.5th percentiles.*

Table A3.6.1*. *Parameter estimates for core catalytic models (with test sensitivity fixed at 99% when not fitted, and test specificity fixed at 100%).

parameter	region	country	study	1. basic		2. basic + mAbs		3. basic + seroreversion		4. basic + mAbs + seroreversion	
				binomial	over-dispersed	binomial	over-dispersed	binomial	over-dispersed	binomial	over-dispersed
FoI, λ	Africa	Egypt	[72]	0.23 (0.22, 0.25)	0.23 (0.20, 0.27)	0.21 (0.2, 0.23)	0.22 (0.19, 0.25)	0.55 (0.49, 0.62)	0.61 (0.48, 0.76)	0.40 (0.34, 0.46)	0.50 (0.38, 0.64)
			[63]	0.21 (0.20, 0.23)	0.22 (0.18, 0.25)	0.20 (0.19, 0.22)	0.20 (0.17, 0.24)	0.48 (0.43, 0.54)	0.52 (0.41, 0.66)	0.36 (0.31, 0.42)	0.44 (0.34, 0.56)
		Ethiopia	[99]	1.11 (0.78, 1.59)	1.38 (0.58, 3.71)	2.60 (1.22, 5.91)	3.53 (0.96, 9.07)	3.99 (1.94, 8.33)	4.28 (1.48, 9.25)	3.79 (1.91, 7.57)	4.01 (1.46, 9.17)
		Kenya	[133]	0.13 (0.11, 0.16)	0.13 (0.08, 0.20)	0.10 (0.08, 0.12)	0.11 (0.07, 0.15)	0.29 (0.23, 0.36)	0.30 (0.18, 0.47)	0.18 (0.14, 0.22)	0.24 (0.14, 0.37)
			[97]	0.55 (0.48, 0.63)	0.58 (0.44, 0.78)	0.75 (0.63, 0.89)	0.83 (0.59, 1.18)	1.09 (0.92, 1.29)	1.71 (1.01, 3.39)	1.04 (0.88, 1.23)	1.36 (0.91, 2.16)
			[67]	0.15 (0.14, 0.17)	0.15 (0.13, 0.19)	0.15 (0.14, 0.17)	0.15 (0.13, 0.18)	0.38 (0.33, 0.44)	0.43 (0.32, 0.58)	0.28 (0.24, 0.34)	0.36 (0.26, 0.48)
		Senegal	[63]	0.13 (0.10, 0.16)	0.14 (0.09, 0.23)	0.13 (0.1, 0.17)	0.14 (0.09, 0.23)	0.31 (0.23, 0.41)	0.39 (0.21, 0.72)	0.23 (0.17, 0.30)	0.32 (0.17, 0.55)
		Tunisia	[63]	0.28 (0.25, 0.32)	0.29 (0.22, 0.40)	0.32 (0.27, 0.37)	0.33 (0.24, 0.46)	0.94 (0.75, 1.18)	1.26 (0.73, 2.22)	0.64 (0.50, 0.81)	0.95 (0.56, 1.63)
			[99]	0.10 (0.08, 0.12)	0.11 (0.06, 0.17)	0.10 (0.08, 0.13)	0.11 (0.06, 0.17)	0.18 (0.14, 0.24)	0.22 (0.12, 0.36)	0.15 (0.11, 0.19)	0.19 (0.11, 0.31)
		Uganda	[63]	0.17 (0.14, 0.19)	0.16 (0.10, 0.23)	0.14 (0.12, 0.17)	0.15 (0.11, 0.21)	0.40 (0.33, 0.48)	0.46 (0.29, 0.7)	0.26 (0.21, 0.33)	0.35 (0.22, 0.54)
	Middle East	Iraq	[63]	0.12 (0.06, 0.2)	0.45 (0.05, 2.54)	0.11 (0.05, 0.2)	0.34 (0.04, 1.74)	0.28 (0.12, 0.55)	1.11 (0.13, 5.58)	0.20 (0.09, 0.39)	0.86 (0.09, 4.74)
			[183]	0.53 (0.42, 0.67)	1.63 (0.4, 8.09)	0.54 (0.40, 0.73)	1.18 (0.40, 4.21)	1.48 (1.00, 2.22)	2.61 (0.91, 7.03)	1.09 (0.75, 1.57)	2.14 (0.76, 5.96)
		Jordan	[63]	0.49 (0.38, 0.62)	0.57 (0.30, 1.08)	0.43 (0.32, 0.58)	0.48 (0.27, 0.87)	1.10 (0.83, 1.44)	1.31 (0.73, 2.36)	0.83 (0.60, 1.13)	1.11 (0.61, 1.95)
			[124]	2.30 (1.40, 3.55)	2.50 (0.81, 5.71)	2.57 (1.00, 5.67)	3.56 (0.70, 8.96)	2.84 (1.62, 4.80)	3.57 (1.12, 8.43)	3.27 (1.45, 6.8)	4.16 (1.14, 9.28)
		KSA	[73] year 1992	0.76 (0.57, 0.99)	1.73 (0.51, 6.67)	0.65 (0.45, 0.93)	0.91 (0.37, 2.36)	1.93 (1.35, 2.71)	2.43 (1.11, 5.44)	1.46 (0.97, 2.13)	2.10 (0.93, 4.81)
			[73] year 2013	0.78 (0.58, 1.02)	0.84 (0.41, 1.57)	0.54 (0.36, 0.79)	0.62 (0.30, 1.23)	1.21 (0.90, 1.60)	1.43 (0.77, 2.67)	0.96 (0.66, 1.33)	1.23 (0.65, 2.24)
			[192]	0.59 (0.47, 0.71)	4.61 (0.67, 9.65)	0.68 (0.52, 0.88)	2.39 (0.53, 8.48)	1.57 (1.02, 2.39)	3.76 (1.24, 8.85)	1.03 (0.70, 1.56)	3.61 (1.08, 8.95)
			[193]	2.30 (1.64, 3.14)	2.53 (0.99, 6.94)	2.24 (1.41, 3.45)	2.56 (1.07, 6.47)	3.38 (2.35, 4.84)	3.7 (1.82, 7.61)	2.65 (1.80, 3.89)	3.21 (1.57, 6.86)
			[63]	0.22 (0.18, 0.28)	0.24 (0.14, 0.44)	0.24 (0.19, 0.31)	0.27 (0.15, 0.48)	0.66 (0.47, 0.91)	0.91 (0.41, 2.05)	0.46 (0.33, 0.63)	0.70 (0.33, 1.54)
		UAE	[116]	7.01 (3.24, 9.71)	6.62 (2.89, 9.79)	2.34 (1.62, 3.41)	3.34 (1.58, 7.59)	5.17 (3.74, 7.20)	5.79 (3.12, 9.41)	3.41 (2.31, 4.99)	4.96 (2.46, 8.93)
	South Asia	Bangladesh	[125]	0.05 (0.03, 0.08)	0.08 (0.02, 0.19)	0.05 (0.03, 0.07)	0.06 (0.02, 0.14)	0.10 (0.05, 0.16)	0.17 (0.05, 0.44)	0.07 (0.04, 0.12)	0.13 (0.04, 0.33)
		Pakistan	[102]	0.09 (0.08, 0.10)	0.09 (0.06, 0.12)	0.09 (0.07, 0.10)	0.09 (0.06, 0.12)	0.15 (0.13, 0.18)	0.16 (0.12, 0.23)	0.12 (0.10, 0.15)	0.14 (0.10, 0.20)
			[69]	0.24 (0.22, 0.26)	0.26 (0.21, 0.33)	0.26 (0.23, 0.28)	0.29 (0.23, 0.35)	0.55 (0.47, 0.64)	0.61 (0.45, 0.84)	0.42 (0.36, 0.49)	0.51 (0.38, 0.70)
ω^{*}	Global		across all studies	NA	NA	1.09 (0.96, 1.24)	1.17 (0.91, 1.48)	NA	NA	2.40 (1.84, 3.24)	4.42 (2.18, 9.00)
σ^{**}				NA	NA	NA	NA	0.11 (0.09, 0.12)	0.13 (0.09, 0.17)	0.06 (0.05, 0.08)	0.09 (0.06, 0.13)
k^{***}				NA	3.56 (3.04, 4.13)	NA	2.81 (2.27, 3.38)	NA	2.83 (2.28, 3.43)	NA	2.60 (2.04, 3.21)

*(*rate of waning of maternally acquired antibodies, **rate of waning of antibodies following infection, ***overdispersion parameter)*

Table A3.6.2*. *Parameter estimates for overdispersed catalytic models whilst using alternative test-type specific sensitivity *and specificity (sensitivity 99% ELISA & PM, 85% MN & ppNT, and specificity 85% ELISA, 100% PM, MN, ppNT)*

parameter	region	country	study	1. basic over-dispersed	2. basic + mAbs over-dispersed	3. basic + seroprevalence over-dispersed	4. basic + mAbs + seroreversion over-dispersed
FoI, l	Africa	Egypt	[72]	0.64 (0.47, 0.85)	0.75 (0.57, 0.99)	0.54 (0.4, 0.74)	0.69 (0.51, 0.92)
		Ethiopia	[63]	0.39 (0.31, 0.50)	0.51 (0.39, 0.65)	0.38 (0.3, 0.48)	0.48 (0.37, 0.63)
			[99]	3.63 (0.82, 9.54)	3.77 (1.03, 9.46)	4.53 (1.14, 9.60)	4.11 (1.17, 9.48)
		Kenya	[133]	0.13 (0.08, 0.19)	0.18 (0.11, 0.28)	0.12 (0.08, 0.18)	0.16 (0.10, 0.25)
			[97]	0.59 (0.43, 0.80)	0.75 (0.54, 1.07)	0.71 (0.50, 1.00)	0.80 (0.57, 1.13)
			[67]	0.13 (0.11, 0.16)	0.19 (0.14, 0.26)	0.13 (0.11, 0.16)	0.18 (0.14, 0.24)
		Senegal	[63]	1.18 (0.14, 8.07)	1.07 (0.19, 6.99)	0.92 (0.14, 7.37)	0.91 (0.18, 6.39)
		Tunisia	[63]	6.98 (2.71, 9.87)	7.15 (3.00, 9.89)	6.98 (2.68, 9.87)	7.16 (2.98, 9.89)
		Uganda	[99]	0.11 (0.06, 0.16)	0.13 (0.08, 0.22)	0.11 (0.06, 0.17)	0.13 (0.08, 0.21)
			[63]	1.24 (0.41, 3.00)	1.00 (0.42, 2.17)	0.67 (0.20, 1.98)	0.78 (0.30, 1.79)
	Middle East	Iraq	[63]	4.23 (0.18, 9.65)	4.01 (0.2, 9.64)	4.03 (0.14, 9.63)	3.88 (0.17, 9.62)
			[183]	4.05 (0.50, 9.57)	2.79 (0.54, 8.86)	2.75 (0.41, 9.12)	2.32 (0.48, 8.44)
		Jordan	[63]	2.17 (0.70, 7.55)	2.72 (0.87, 8.35)	2.11 (0.66, 7.30)	2.60 (0.82, 8.28)
			[124]	2.68 (0.71, 7.80)	2.88 (0.77, 7.95)	3.55 (0.71, 9.10)	3.60 (0.80, 9.10)
		KSA	[73] 1992	2.06 (0.50, 6.96)	1.81 (0.64, 5.11)	1.48 (0.38, 5.47)	1.62 (0.55, 4.66)
			[73] 2013	0.76 (0.34, 1.55)	0.90 (0.43, 1.75)	0.65 (0.28, 1.38)	0.81 (0.37, 1.62)
			[192]	6.83 (2.64, 9.86)	6.86 (2.67, 9.86)	6.87 (2.65, 9.87)	6.89 (2.67, 9.87)
			[193]	6.50 (2.74, 9.80)	6.78 (3.01, 9.84)	6.50 (2.64, 9.83)	6.73 (2.94, 9.83)
		UAE	[63]	0.24 (0.12, 0.39)	0.37 (0.17, 0.83)	0.23 (0.13, 0.39)	0.33 (0.17, 0.68)
			[116]	6.41 (2.95, 9.76)	5.75 (2.56, 9.61)	5.24 (1.68, 9.61)	5.27 (1.94, 9.51)
	South Asia	Bangladesh	[125]	0.37 (0.03, 4.02)	0.31 (0.04, 2.14)	0.21 (0.03, 1.00)	0.26 (0.04, 1.37)
		Pakistan	[102]	0.12 (0.09, 0.17)	0.15 (0.10, 0.21)	0.13 (0.09, 0.17)	0.15 (0.10, 0.20)
			[69]	0.23 (0.18, 0.29)	0.30 (0.23, 0.40)	0.24 (0.19, 0.30)	0.29 (0.23, 0.38)
ω^{*}	Global		across all studies	NA	2.67 (1.56, 4.57)	NA	4.54 (2.13, 9.04)
σ^{**}				NA	NA	0.03 (0.01, 0.06)	0.03 (0.01, 0.05)
k^{***}				2.84 (2.29, 3.44)	2.64 (2.09, 3.23)	2.78 (2.22, 3.38)	2.62 (2.06, 3.23)

*(*rate of waning of maternally acquired antibodies, **rate of waning of antibodies following infection, ***overdispersion parameter*

A3.7 – Parameter correlation

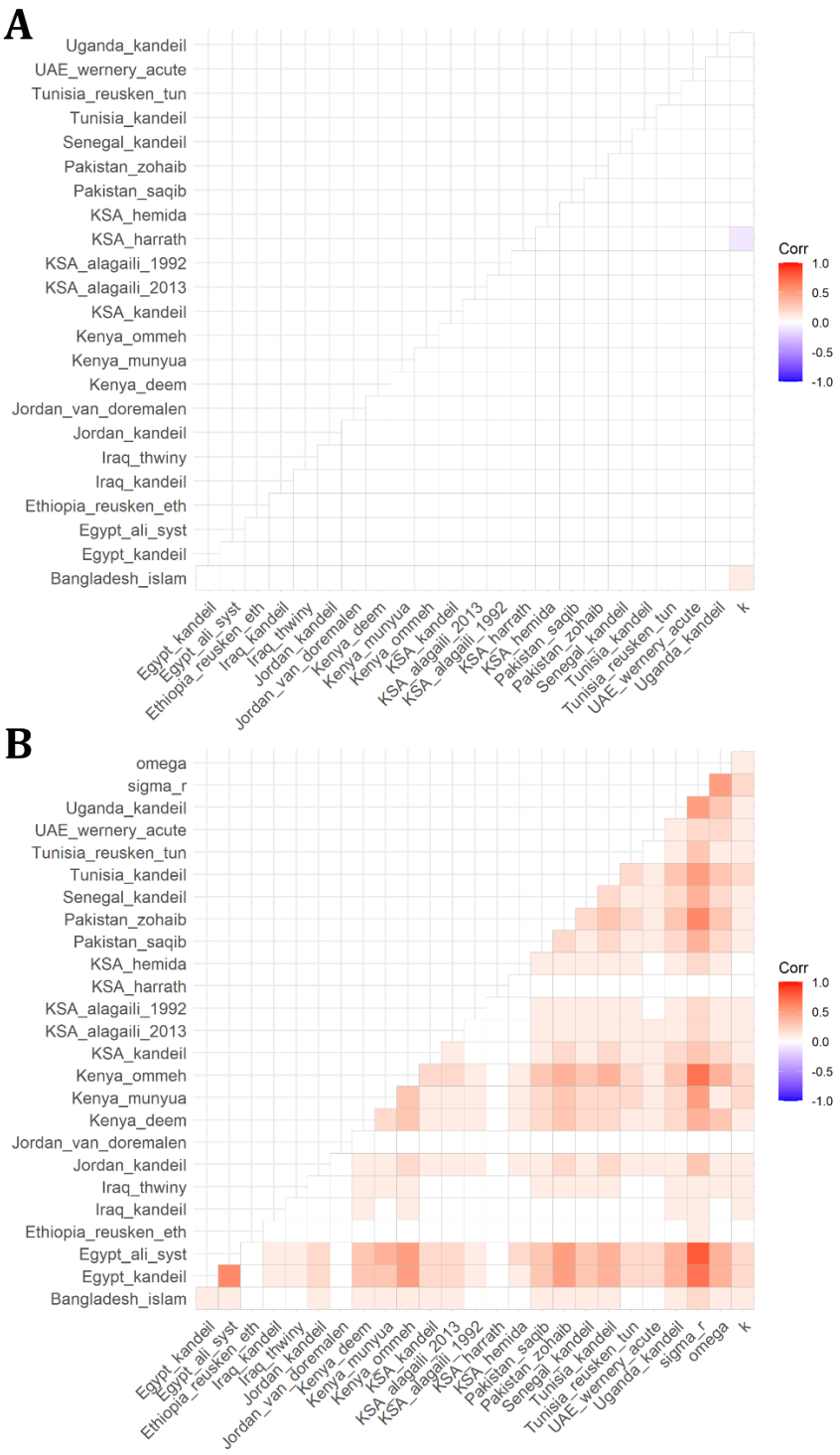


Figure 3.7.1 Correlation between posterior samples when seroprevalence is assumed to be overdispersed. ***A****. Model 1. seroconversion: very little correlation as expected for study-specific FoI estimates.* ***B.*** *Model 4. seroconversion + mAbs + seroreversion: correlation between FoI and seroreversion parameter (and therefore correlation between FoI values indirectly).*

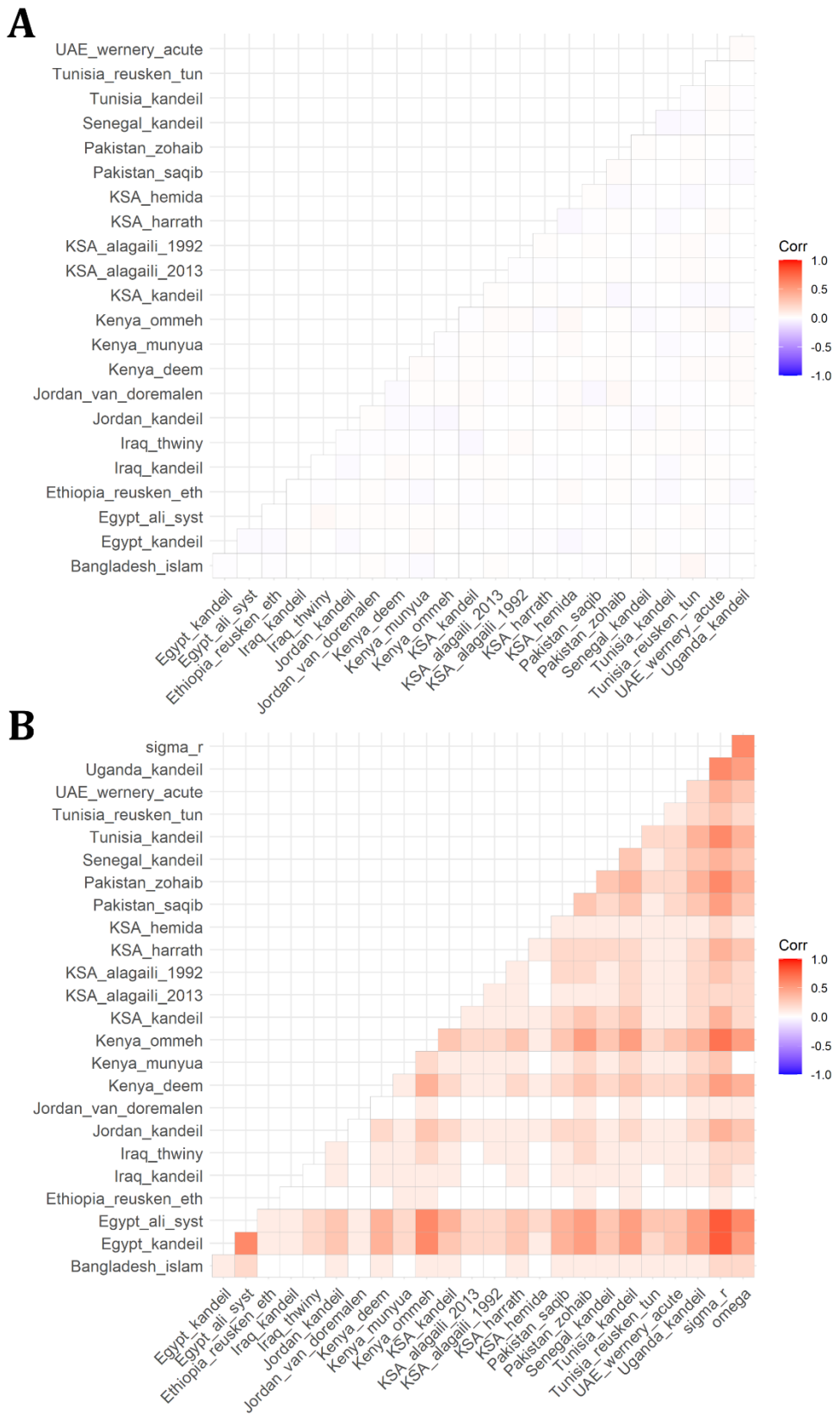


Figure 3.7.2 Correlation between posterior samples when seroprevalence is assumed to be binomially distributed. A*. Model 1. seroconversion: very little correlation as expected for study-specific FoI estimates.* ***B.*** *Model 4. seroconversion + mAbs + seroreversion: correlation between FoI and seroreversion parameter (and therefore correlation between FoI values indirectly)*

Appendix Chapter 4

Contents

A4.1 – R_0 estimates across all scenarios.....191
A4.2 – Mean R_e values are close to unity at endemic equilibrium.....1923
A4.3 – Choosing representative R_0 values.....200
A4.4 – Persistence of transmission in homogeneous and structured populations. 204
A4.5 – CCS estimates as determined using different cut-offs for defining persistence. 211
A4.6 – Periodicity when births are moderately seasonal. .....**Error! Bookmark not defined.**

A4.1 R_0 estimates across all scenarios

Table A4.1. *R_0 estimates across all scenarios*. See separate file "A4.1.xlsx"

A4.2 Mean R_e values are close to unity at endemic equilibrium

Table A4.2. *Mean R_e values are close to unity at endemic equilibrium.*

		R_e relative infectiousness of reinfections		
Region	Study population	1%	25%	50%
Africa	Egypt, Kandeil *et al.,* 2019 [63]	0.97 (0.96, 0.97)	0.97 (0.97, 0.97)	0.97 (0.97, 0.98)
	Egypt, Ali *et al.,* 2017 [72]	0.97 (0.96, 0.97)	0.97 (0.97, 0.98)	0.98 (0.97, 0.98)
	Ethiopia, Reusken *et al.,* 2014 [99]	1.00 (0.98, 1.01)	0.99 (0.98, 0.99)	0.98 (0.98, 0.99)
	Kenya, Deem *et al.,* 2015 [133]	0.96 (0.96, 0.96)	0.97 (0.96, 0.97)	0.97 (0.97, 0.97)
	Kenya., Munyua *et al.,* 2017 [88]	0.98 (0.98, 0.99)	0.98 (0.98, 0.98)	0.98 (0.98, 0.98)
	Kenya, Ommeh *et al.,* 2018 [67]	0.96 (0.96, 0.97)	0.97 (0.97, 0.97)	0.97 (0.97, 0.98)
	Senegal, Kandeil *et al.,* 2019 [63]	0.96 (0.96, 0.97)	0.97 (0.97, 0.97)	0.97 (0.97, 0.98)
	Tunisia, Kandeil *et al.,* 2019 [63]	0.98 (0.97, 0.99)	0.98 (0.97, 0.98)	0.98 (0.98, 0.98)
	Tunisia, Reusken *et al.,* 2014 [99]	0.96 (0.96, 0.96)	0.97 (0.96, 0.97)	0.97 (0.97, 0.97)
	Uganda, Kandeil *et al.,* 2019 [63]	0.96 (0.96, 0.97)	0.97 (0.97, 0.97)	0.97 (0.97, 0.98)
Middle East	Iraq, Kandeil *et al.,* 2019 [63]	0.98 (0.96, 1.00)	0.98 (0.96, 0.99)	0.98 (0.97, 0.98)
	Iraq, Thwiny *et al.*,2018 [183]	0.99 (0.97, 1.00)	0.98 (0.98, 0.99)	0.98 (0.98, 0.99)
	Jordan, Kandeil *et al.,* 2019 [63]	0.98 (0.97, 0.99)	0.98 (0.97, 0.98)	0.98 (0.98, 0.98)
	Jordan, van Doremalen *et al.,* 2017 [124]	1.00 (0.98, 1.01)	0.99 (0.98, 0.99)	0.98 (0.98, 0.99)
	KSA, Kandeil *et al.,* 2019 [63]	0.97 (0.96, 0.99)	0.98 (0.97, 0.98)	0.98 (0.97, 0.98)
	KSA, (2013) Alagaili *et al.,* 2014 [73]	0.98 (0.97, 0.99)	0.98 (0.98, 0.98)	0.98 (0.98, 0.98)
	KSA (1992) Alagaili *et al.,* 2014 [73]	0.99 (0.98, 1.00)	0.98 (0.98, 0.99)	0.98 (0.98, 0.98)
	KSA, Harrath *et al.,* 2018 [192]	0.99 (0.98, 1.01)	0.98 (0.98, 0.99)	0.98 (0.98, 0.99)
	KSA, Hemida *et al.,* 2013 [193]	0.99 (0.99, 1.00)	0.98 (0.98, 0.99)	0.98 (0.98, 0.99)
	UAE, Wernery *et al.,* 2015 [116]	1.00 (0.99, 1.01)	0.99 (0.98, 0.99)	0.98 (0.98, 0.99)
South Asia	Bangladesh, Islam *et al.,* 2018 [125]	0.96 (0.95, 0.96)	0.96 (0.96, 0.97)	0.97 (0.96, 0.97)
	Pakistan, Saqib *et al.,* 2017 [102]	0.96 (0.96, 0.96)	0.97 (0.96, 0.97)	0.97 (0.97, 0.97)
	Pakistan, Zohaib *et al.,* 2018 [69]	0.97 (0.96, 0.97)	0.97 (0.97, 0.98)	0.98 (0.97, 0.98)

A4.3. Choosing representative R_0 values

The relationship between the inferred force of infection, and the estimated R_0 is highly dependent on the assumed relative infectiousness of reinfections. Throughout the analysis I explore three different infectiousness scenarios (where reinfected animals are either 1%, 25% or 50% as infectious as first-time infected animals). For each of the three infectiousness scenarios I have selected 4 R_0 values (Low, medium, High, and Very High) to span the transmissibility inferred across the 23 age-stratified seroprevalence studies. Figure A4.1 shows the values chosen for each infectiousness scenario, and how they compare to the estimated R_0 values across the studies.

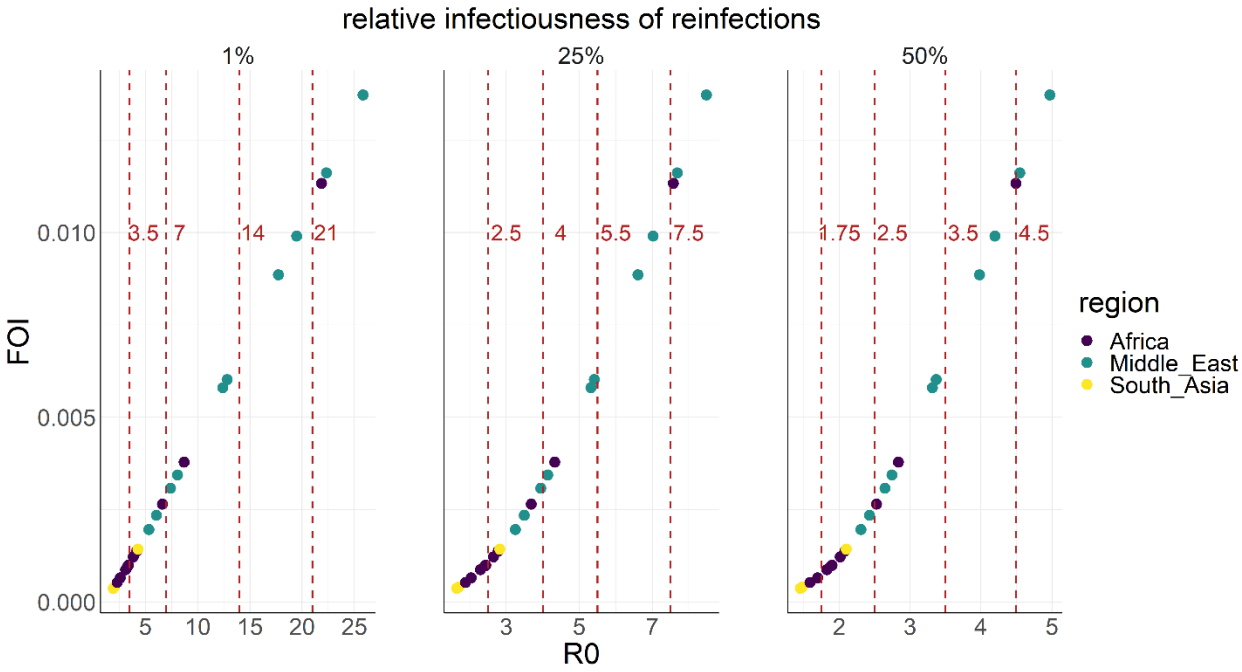


Figure A4.3.1 Choosing representative R_0 values. The R_0 values for use in analysis represent the full span of inferred transmissibility across the 23 studies of age-stratified seroprevalence

A4.4 Persistence of transmission in homogeneous and structured populations

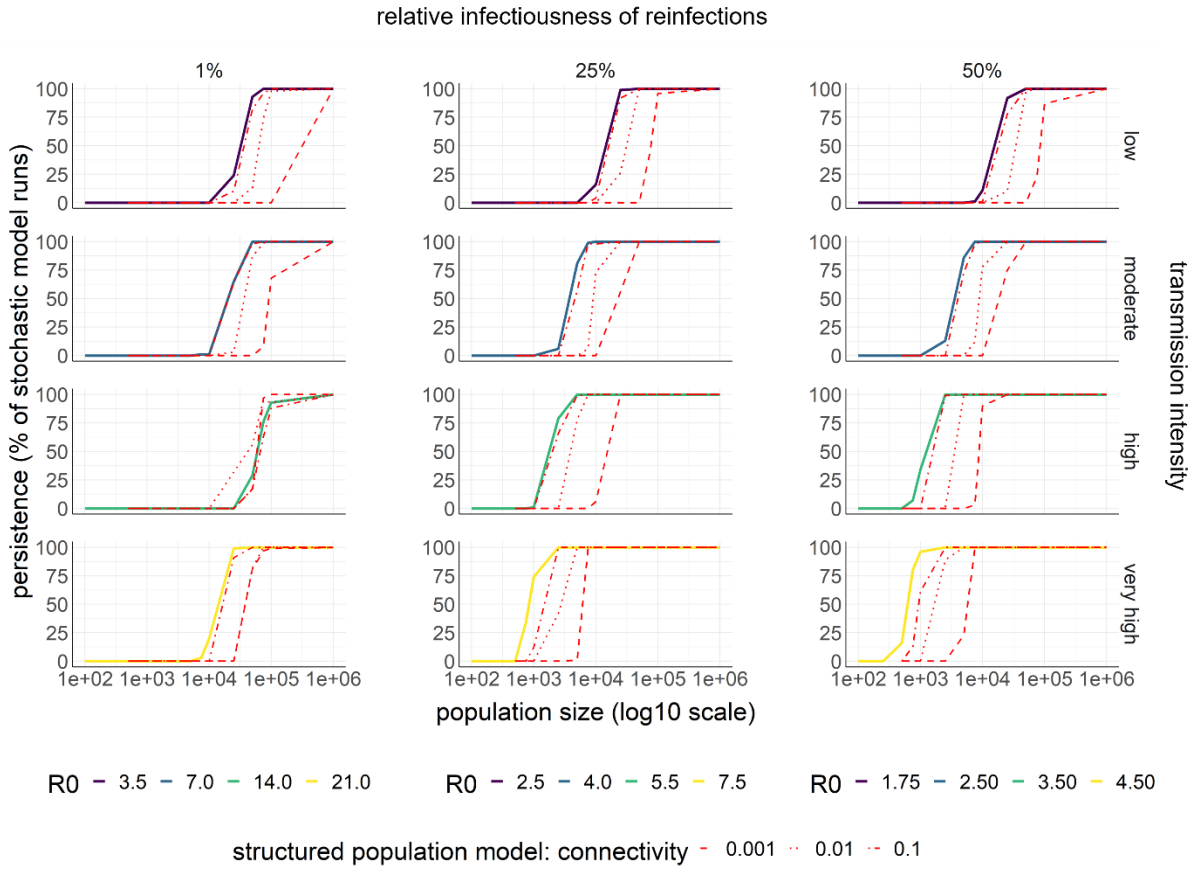


Figure A4.4.1 Persistence of transmission in homogeneous and structured populations. *The persistence of transmission for 25 years after background FoI is turned off is shown for the model assuming a homogeneous population (solid lines), and for a structured population where the sub populations are connected to increasing degrees (dotted and dashed lines). Results are shown for different assumed levels of infectiousness of reinfections (panels from right to left) and for different transmission settings (panels top to bottom, with Ro values shown in the colour key for each reinfection assumption).*

A4.5 CCS estimates as determined using different cut-offs for defining persistence

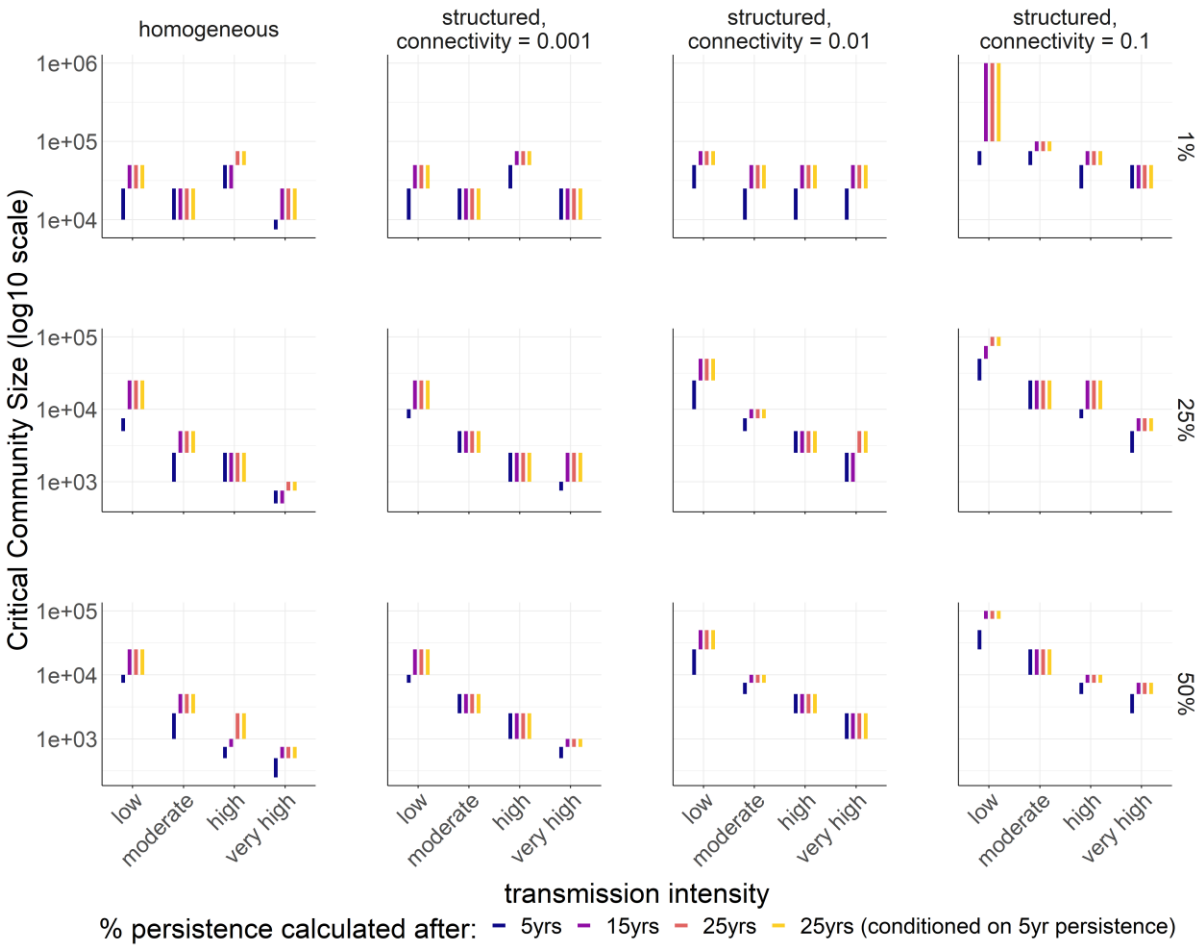


Figure A4.5.1 CCS estimates as determined using different cut-offs for defining persistence. *CCS estimates are presented as the window of population sizes between which transmission persists in a closed population in >50% of stochastic model runs. The CCS estimates are relatively robust to different cut-offs for measuring of persistence if they are taken >5 years after background FoI is switched off. Colours represent CCS estimates calculated using the four different measures of persistence. Results are shown for different levels of relative infectiousness of reinfected individuals (panel rows), and for different population structures (panel columns). In the structured models, a connectivity of 0.01, for example, means that 1% of an individual's contacts are individuals from each of the 2-4 neighbouring herds outside their own herd (making up a total of 2-4% of their contacts), and the remainder of their contacts are within their own herd.*

A4.6 Periodicity when births are moderately seasonal

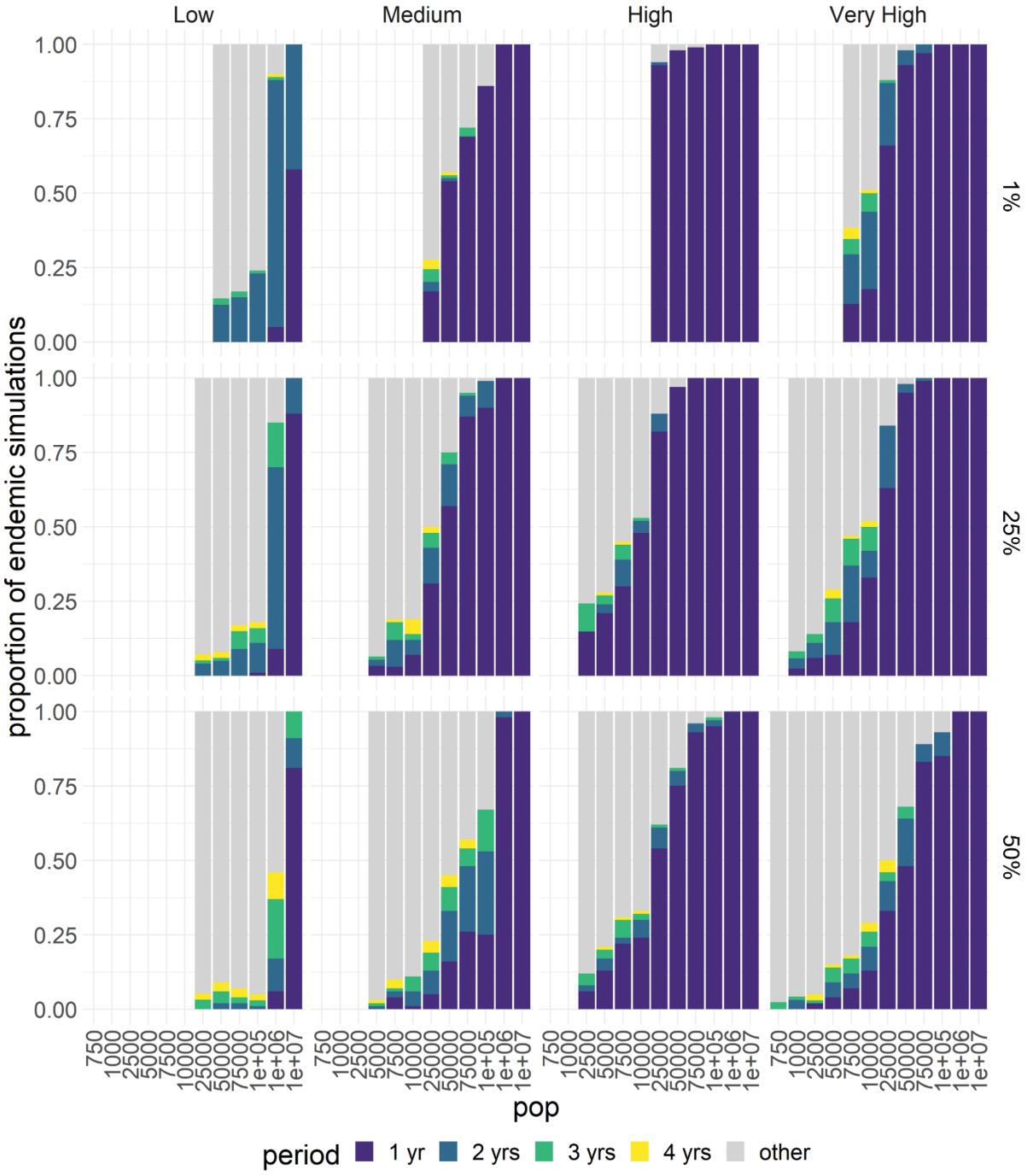


Figure A4.6.1 Periodicity when births are moderately seasonal ($\delta = 0.5$) *as opposed to fully seasonal. The proportion of stochastic simulations of persistent transmission in which periodicity was annual (purple), biennial (blue), triennial (green), quadrennial (yellow) and other (grey) for increasing population sizes along the x-axis. Each panel shows the results for a particular transmission intensity (columns) and for different assumed level of infectiousness of reinfected animals relative to first-time infections (rows).*

Appendix Chapter 5

Contents

A5.1 – The effect of target age of vaccination on incidence of infection when mAbs last 6 months 191

A5.2 – The percentage of stochastic model runs in which a patch experienced infection when infectiousness was proprotional to the log(viral shedding) 192

A5.1 The effect of target age of vaccination on incidence of infection when mAbs last 6 months

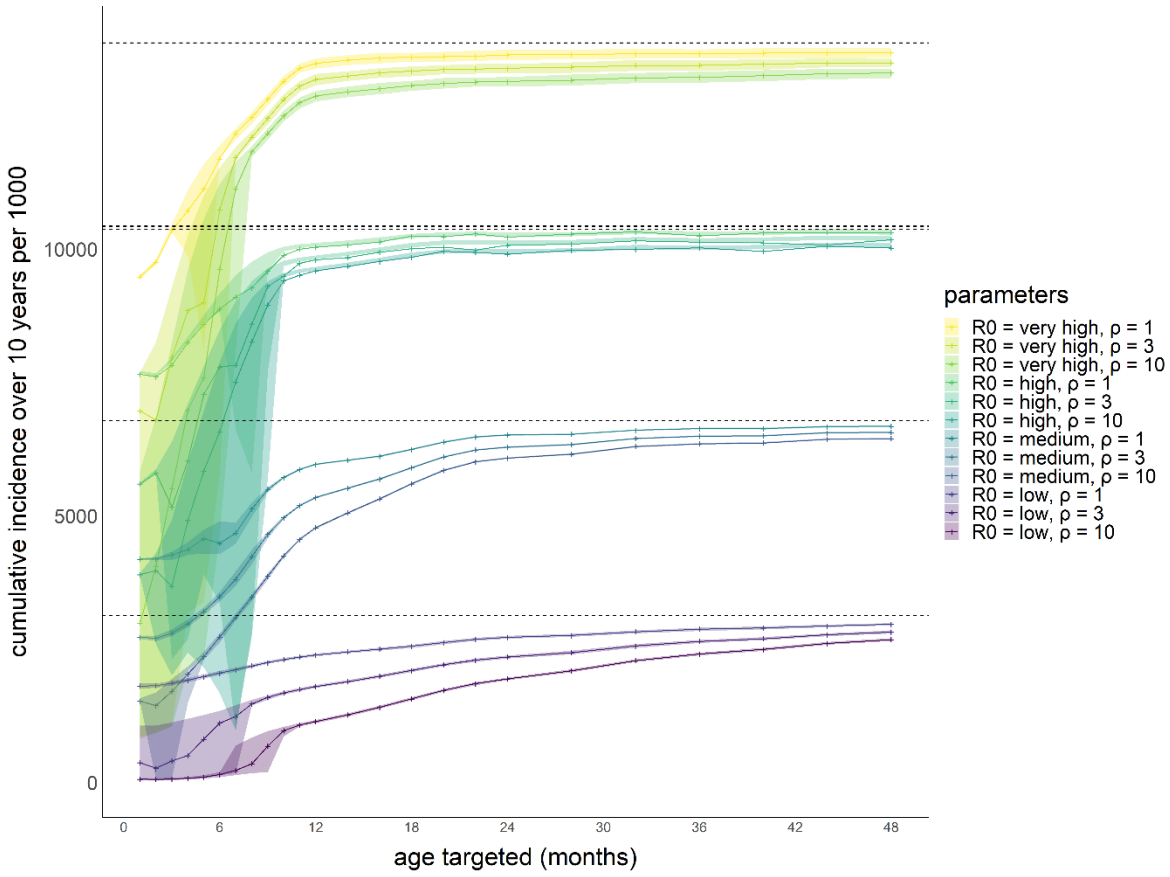


Figure A5.1.1 The effect of target age on the cumulative incidence of infection in the ten years following vaccine introduction, when mAbs were assumed to last six months, *rather than 3 months. Incidence is measured as the cumulative incidence per 1000 animals. Colours indicate different combinations of R_0 and duration of vaccine-induced effects, ρ. Dotted lines show the incidence in the absence of vaccination for each R_0 value. Assumptions: vaccination reduced infectiousness and susceptibility (scenario 1) and infectiousness was proportional to viral RNA shedding. Points show mean values over 100 stochastic runs, and transparent ribbons represent 95% quantiles.*

A5.2. The percentage of stochastic model runs in which a patch experienced infection when infectiousness was proportional to the log(viral shedding)

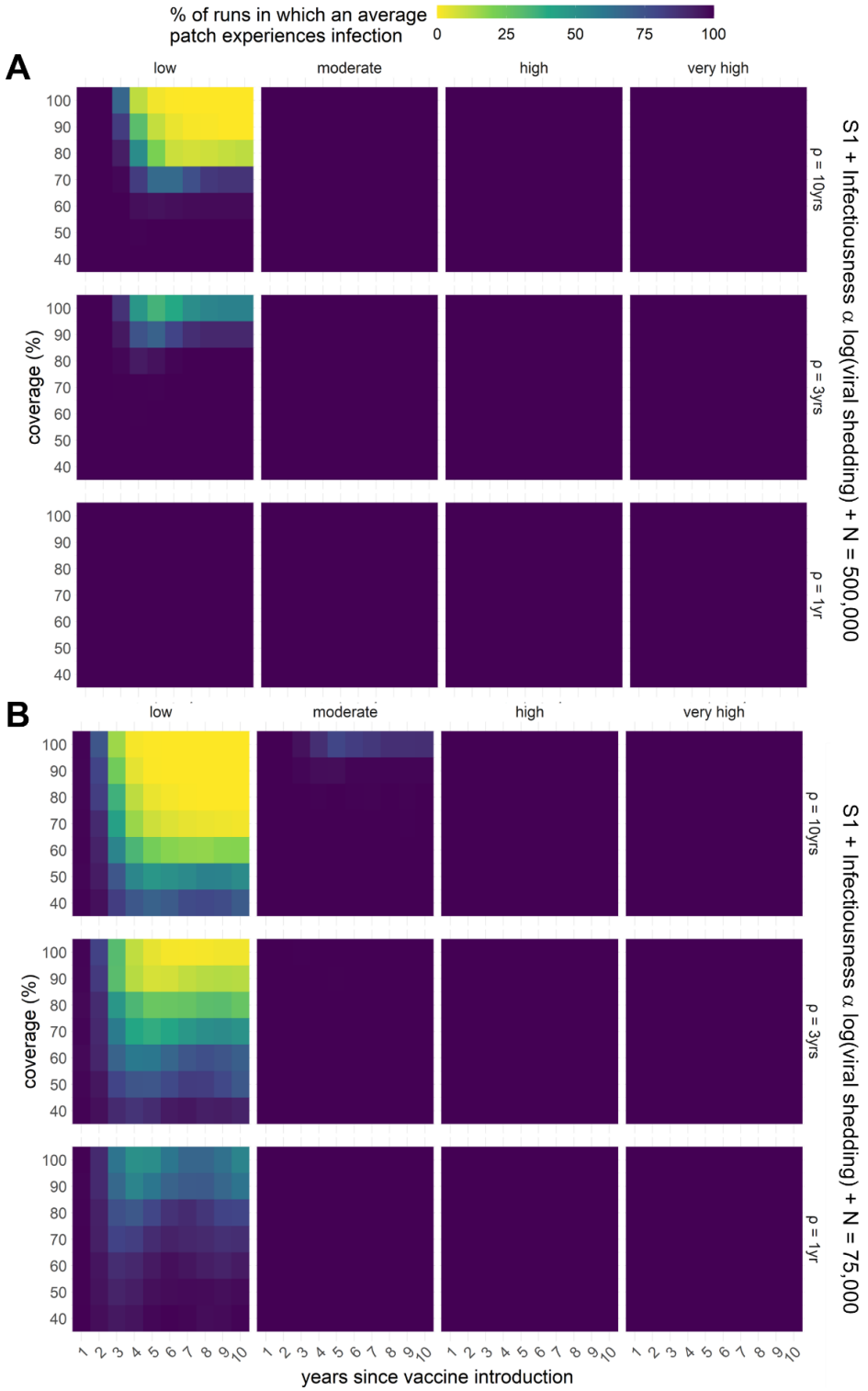


Figure A5.2.1 The percentage of stochastic model runs in which a patch experienced infection in scenario 1, when infectiousness was proportional to log(viral RNA shedding) *for each year following vaccine introduction. Results are shown in different transmission settings (columns), and for different durations of vaccine induced effects (rows), for* ***A****. a population of 500,000 dromedaries and* ***B****. a population of 75,000 dromedaries.*

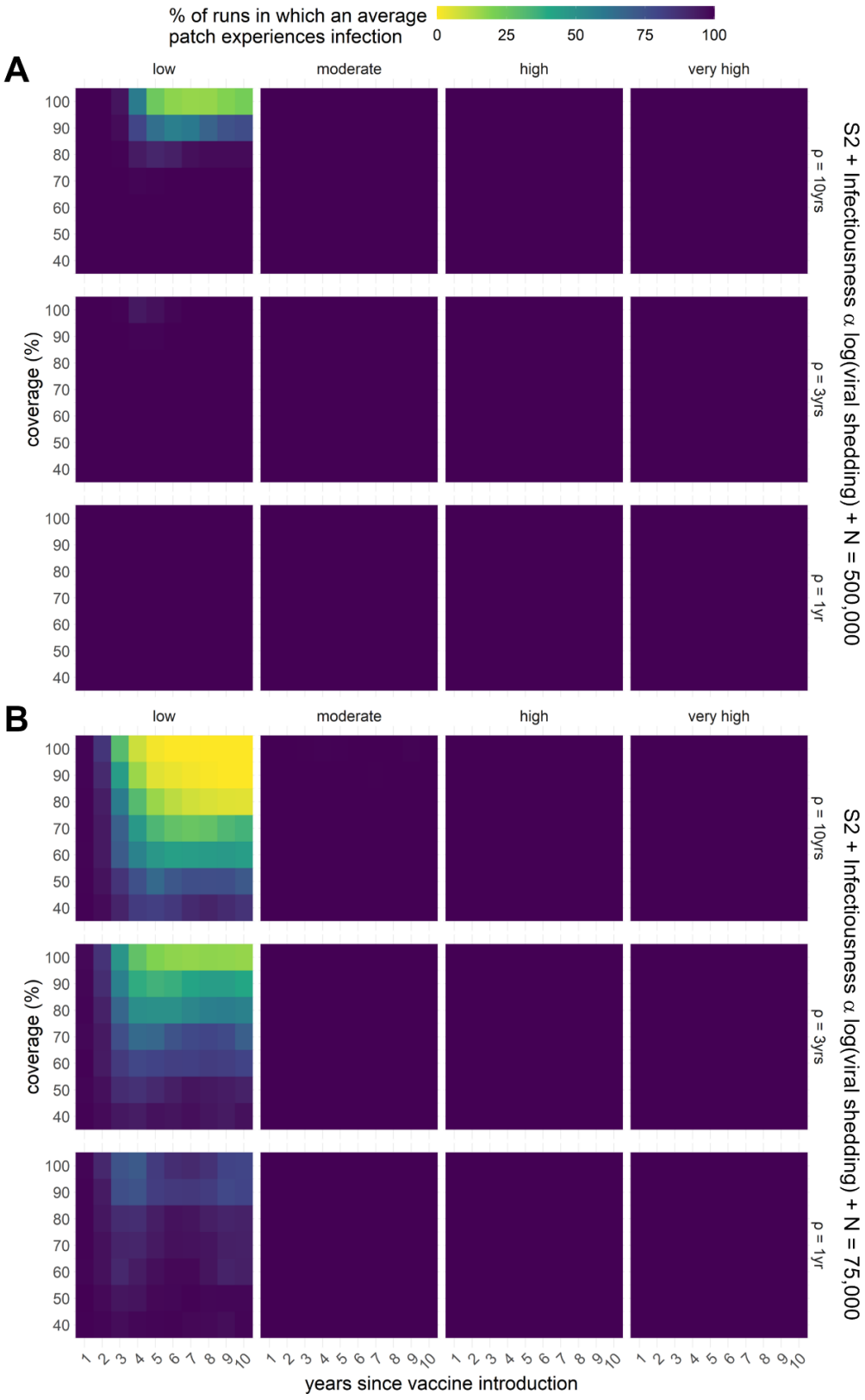


Figure A5.2.2 The percentage of stochastic model runs in which a patch experienced infection in scenario 2, when infectiousness was proportional to log(viral RNA shedding), *for each year following vaccine introduction. Results are shown in different transmission settings (columns), and for different durations of vaccine induced effects (rows), for* ***A****. a population of 500,000 dromedaries and* ***B****. a population of 75,000 dromedaries.*

Appendix 6

A6.1 Assuming a constant mortality rate, μ_0, for camels <2 years, and μ for camels ≥2 years rather than a uniform age distribution within each class

In the core results presented in ***Chapter 3***, the FoI estimates produced by fitting catalytic models to age-stratified seroprevalence data are based on predicted seroprevalence which assumed a uniform distribution of age within each age class sampled. On the other hand, in the dynamic model animals are assumed to die at a constant rate of μ_0 for animals <2 years, and μ ≥2 years, meaning survival and the resultant age distribution is exponential. In order to assess how FoI estimates are affected by the assumed age distribution within each age class, alternative solutions for the predicted seroprevalence in each age class were used to refit the catalytic models assuming constant rates of mortality of μ_0 for animals <2 years, and μ ≥2 years rather than assuming a uniform age distribution. This appendix details how the alternative solutions were reached, before describing the effect of changing the assumed age distribution on the parameter estimates.

Solutions

In the most complex model of seroconversion, the predicted seroprevalence at age a is given by:

$$p(a) = \frac{\lambda}{\lambda+\sigma}\left(1 - e^{-(\lambda+\sigma)a}\right) - m_0 \frac{\lambda}{\lambda+\sigma-\omega}\left(e^{-\omega a} - e^{-(\lambda+\sigma)a}\right) \qquad A6.1.1$$

Where λ is the rate at which animals become seropositive (the FoI), σ is the rate at which seropositivity wanes, m_0 is the proportion of calves born with maternally acquired antibodies (mAbs) and ω is the rate at which these mAbs wane.

With a constant mortality rate of μ_0 for animals <2 years, and μ ≥2 years, survival at age a is:

$$s(a) = e^{-\mu_0 a} \qquad a < 2 \qquad A6.1.2$$

$$s(a) = e^{-\left(2\mu_0 + \mu(a-2)\right)} \qquad a \geq 2$$

$$= e^{-\mu a} e^{2(\mu-\mu_0)} \qquad A6.1.3$$

The age distribution is $f(a) = cs(a)$ where c is the normalising constant:

$$c = \frac{1}{\int_0^\infty s(a)\,da}$$

$$\frac{1}{c} = \int_0^\infty s(a)\,da$$

$$= \int_0^2 e^{-\mu_0 a}\,da + e^{2(\mu-\mu_0)}\int_2^\infty e^{-\mu a}\,da$$

$$= \left[-\frac{e^{-\mu_0 a}}{\mu_0}\right]_0^2 + e^{2(\mu-\mu_0)}\left[-\frac{e^{-\mu a}}{\mu}\right]_2^\infty$$

$$= \frac{1-e^{-2\mu_0}}{\mu_0} + \frac{e^{-2\mu_0}}{\mu}$$

$$= \frac{\mu + (\mu_0 - \mu)e^{-2\mu_0}}{\mu_0\mu}$$

Meaning that:

$$f(a) = \frac{s(a)\mu_0\mu}{\mu + (\mu_0 - \mu)e^{-2\mu_0}} \qquad A6.1.4$$

The predicted seroprevalence in a representatively sampled age class ranging from a_1 to a_2 is:

$$p(a_1 \rightarrow a_2) = \frac{\int_{a1}^{a2} p(a)f(a)\,da}{\int_{a1}^{a2} f(a)\,da} \qquad A6.1.5$$

Taking the predicted seroprevalence at age a (***equation A6.1.1***) and the age distribution (***equation A6.1.4*** and *A**6.1.5***) becomes:

1. When $a_1 < 2$ and $a_2 < 2$, $f(a) \propto \mu_0 e^{-\mu_0 a}$

$$p(a_1 \rightarrow a_2) = \frac{\left[\frac{\lambda}{\lambda+\sigma}\left(-e^{-\mu_0 a} + \frac{\mu_0 e^{-(\lambda+\sigma+\mu_0)a}}{\lambda+\sigma+\mu_0}\right) - \frac{m_0\,\lambda\mu_0}{\lambda+\sigma-\omega}\left(\frac{e^{-(\omega+\mu_0)a}}{\omega+\mu_0} - \frac{e^{-(\lambda+\sigma+\mu_0)a}}{\lambda+\sigma+\mu_0}\right)\right]_{a_1}^{a_2}}{[e^{-\mu_0 a}]_{a_1}^{a_2}}$$

$$= \frac{\mu_0}{e^{-\mu_0 a_1} - e^{-\mu_0 a_2}} \left[\frac{\lambda}{\lambda + \sigma} \left(\frac{e^{-\mu_0 a_1} - e^{-\mu_0 a_2}}{\mu_0} - \frac{e^{-(\lambda+\sigma+\mu_0)a_1} - e^{-(\lambda+\sigma+\mu_0)a_2}}{\lambda + \sigma + \mu_0} \right) \right.$$

$$\left. - \frac{m_0 \lambda}{\lambda + \sigma - \omega} \left(\frac{e^{-(\omega+\mu_0)a_1} - e^{-(\omega+\mu_0)a_2}}{\omega + \mu_0} - \frac{e^{-(\lambda+\sigma+\mu_0)a_1} - e^{-(\lambda+\sigma+\mu_0)a_2}}{\lambda + \sigma + \mu_0} \right) \right] \quad A6.1.6$$

2. When $a_1 \geq 2$ and $a_2 \geq 2$, $f(a) \propto \mu e^{-\mu a}$ so $p(a_1 \rightarrow a_2)$ is the same as for ***equation A6.1.6***, substituting μ replacing μ_0

3. When $a_1 < 2$ and $a_2 \geq 2$, the age class is split into two and each band is dealt with separately before averaging the predicted seroprevalence across the whole age class whilst considering the age distribution:

First the age band is split into $a_1 \rightarrow a_2'$ and $a_1' \rightarrow a_2$ where:

$$a_1' = a_2' = 2$$

Then $p(a_1 \rightarrow 2)$ and $p(2 \rightarrow a_2)$ must be calculated, and average appropriately to get $p(a_1 \rightarrow a_2)$ as follows:

$$p(a_1 \rightarrow a_2) = \frac{F_1 p(a_1 \rightarrow 2) + F_2 p(2 \rightarrow a_2)}{F_1 + F_2}$$

where:

$$F_1 = \int_{a_1}^{2} f(a)da = \frac{c}{\mu_0}[e^{-\mu_0 a_1} - e^{-2\mu_0}]$$

$$F_2 = \int_{2}^{a_2} f(a)da = \frac{ce^{-2\mu_0}}{\mu}\left[1 - e^{-\mu(a_2-2)}\right]$$

So:

$$p(a_1 \rightarrow a_2) = \frac{\mu[e^{-\mu_0 a_1} - e^{-2\mu_0}]p(a_1 \rightarrow 2) + \mu_0 e^{-2\mu_0}\left[1 - e^{-\mu(a_2-2)}\right]p(2 \rightarrow a_2)}{\mu[e^{-\mu_0 a_1} - e^{-2\mu_0}] + \mu_0 e^{-2\mu_0}[1 - e^{-\mu(a_2-2)}]} \quad A6.7$$

Similarly, the proportion of animals with maternally acquired antibodies, when constant mortality rates are considered, is as follows:

When $a_1 < 2$, $a_2 < 2$:

$$m(a_1 \to a_2) = \frac{\mu_0 m_0 (e^{-(\omega+\mu_0)a_1} - e^{-(\omega+\mu_0)a_2})}{(\omega+\mu_0)(e^{-\mu_0 a_1} - e^{-\mu_0 a_2})}$$

When $a_1 \geq 2$, $a_2 \geq 2$:

$$m(a_1 \to a_2) = \frac{\mu m_0 (e^{-(\omega+\mu)a_1} - e^{-(\omega+\mu)a_2})}{(\omega+\mu)(e^{-\mu a_1} - e^{-\mu a_2})}$$

And when $a_1 < 2$, $a_2 \geq 2$:

$$m(a_1 \to a_2) = \frac{F_1 m(a_1 \to 2) + F_2 m(2 \to a_2)}{F_1 + F_2}$$

The effect of the assumed age distribution on parameter estimation

Assuming an exponential age distribution within the age classes, with a constant mortality rate of μ_0 for animals <2 years, and μ for animals ≥2 years, led to small increases in some of the FoI estimates (displayed in ***Table A6.1.1*** alongside the core estimates for the best fitting model presented in ***Chapter 3***). This slight increase is likely to be because when a constant mortality rate is considered, animals are exponentially distributed within the age class meaning more of the animals in the class are towards the younger age boundary as compared to when the age distribution is assumed to be uniform in the core results in ***Chapter 3***. The rate of waning of mAbs, ω, also increased when age distribution was assumed to be exponential, giving an average duration of 2 months of maternally acquired protection as opposed to the 3 months estimated when the age distribution is assumed to be uniform. The rate of waning of antibodies following infections, σ, and the overdispersion parameter, k, were not affected by the change in assumed age distribution.

Table A6.1.1 *Comparing parameter estimates when individuals are assumed to be distributed uniformly versus exponentially as a result of considering mortality rates within each age class*

	Dataset	*Model 4b: Uniform age mean (95% CrI)*	*Model 4b: Exponential age mean (95% CrI)*
FoI, λ	***Africa***		
	Egypt [72]	0.49 (0.37, 0.65)	0.59 (0.46, 0.75)
	Egypt [63]	0.44 (0.34, 0.57)	0.53 (0.42, 0.67)
	Ethiopia [99]	4.08 (1.44, 9.13)	4.00 (1.44, 9.27)
	Kenya [133]	0.24 (0.14, 0.37)	0.29 (0.18, 0.44)
	Kenya [88]	1.36 (0.91, 2.17)	1.37 (0.85, 2.46)
	Kenya [67]	0.36 (0.26, 0.49)	0.37 (0.27, 0.50)
	Senegal [63]	0.32 (0.17, 0.56)	0.38 (0.22, 0.65)
	Tunisia [63]	0.95 (0.56, 1.64)	1.04 (0.65, 1.74)
	Tunisia [99]	0.19 (0.11, 0.31)	0.22 (0.13, 0.35)
	Uganda [63]	0.35 (0.22, 0.55)	0.41 (0.27, 0.62)
	Middle East		
	Iraq [63]	0.84 (0.10, 4.63)	0.97 (0.12, 5.42)
	Iraq [183]	2.17 (0.76, 6.20)	2.53 (0.79, 7.31)
	Jordan [63]	1.11 (0.61, 2.00)	1.27 (0.72, 2.31)
	Jordan [124]	4.18 (1.12, 9.29)	4.12 (1.14, 9.14)
	KSA, 1992-2010 [73]	2.09 (0.93, 4.70)	2.45 (1.06, 5.78)
	KSA, 2013 [73]	1.24 (0.64, 2.28)	1.45 (0.77, 2.73)
	KSA [192]	3.57 (1.13, 8.84)	2.98 (0.97, 7.79)
	KSA [193]	3.19 (1.59, 6.56)	3.33 (1.53, 7.08)
	KSA [63]	0.71 (0.33, 1.58)	0.80 (0.40, 1.70)
	UAE [116]	4.94 (2.43, 8.95)	5.41 (2.71, 9.25)
	Asia		
	Bangladesh [125]	0.13 (0.04, 0.34)	0.17 (0.05, 0.40)
	Pakistan [102]	0.14 (0.10, 0.20)	0.15 (0.11, 0.21)
	Pakistan [69]	0.52 (0.38, 0.71)	0.53 (0.39, 0.73)
	Global		
rate of waning of mAbs, ω	Across all datasets	4.42 (2.17, 8.96)	6.30 (3.23, 9.74)
rate of waning of Abs, σ	Across all datasets	0.09 (0.06, 0.13)	0.10 (0.06, 0.15)
Overdispersion, k	Across all datasets	2.61 (2.03, 3.23)	2.68 (2.11, 3.29)

The small increases in FoI and ω had little effect on simulated dynamics. When mAbs were modelled to last for 2 months and the dynamic model was calibrated to the alternative FoI estimates assuming exponential age distribution, R_0 was estimated to be slightly higher for most populations compared to in the core results in ***Chapter 3*** (***Table A6.1.2***). However, the range of transmissibility estimates across the study populations did not meaningfully change, and the general trend of higher transmissibility estimates for populations sampled in the Middle East remained.

Table A6.1.2 *Comparing R_0 estimates when individuals are assumed to be distributed uniformly versus exponentially as a result of considering mortality rates within each age class*

		R_0 relative infectiousness of reinfections:					
		1%		25%		50%	
	Study	uniform*	exponential*	uniform*	exponential*	uniform*	exponential*
Africa	Egypt [63]	3.8 (3.2, 4.6)	4.3 (3.7, 5)	2.6 (2.4, 2.9)	2.8 (2.6, 3.1)	2.0 (1.9, 2.2)	2.1 (2.0, 2.2)
	Egypt [72]	4.2 (3.4, 5.0)	4.6 (3.9, 5.4)	2.8 (2.5, 3.1)	2.9 (2.7, 3.3)	2.1 (1.9, 2.3)	2.2 (2.0, 2.3)
	Ethiopia [99]	21.9 (9.1, 44.9)	21.1 (8.9, 44.7)	7.6 (4.4, 12.7)	7.4 (4.4, 12.7)	4.5 (2.9, 7.3)	4.4 (2.9, 7.3)
	Kenya [133]	2.6 (2.0, 3.4)	2.9 (2.2, 3.8)	2.0 (1.7, 2.5)	2.2 (1.8, 2.6)	1.7 (1.5, 1.9)	1.8 (1.5, 2.0)
	Kenya [88]	8.7 (6.4, 12.8)	8.6 (6.0, 14)	4.3 (3.6, 5.4)	4.3 (3.5, 5.7)	2.8 (2.5, 3.4)	2.8 (2.4, 3.5)
	Kenya [67]	3.4 (2.7, 4.1)	3.3 (2.7, 4.1)	2.4 (2.1, 2.8)	2.4 (2.1, 2.8)	1.9 (1.7, 2.1)	1.9 (1.7, 2.1)
	Senegal [63]	3.1 (2.2, 4.5)	3.4 (2.4, 4.9)	2.3 (1.8, 2.9)	2.5 (1.9, 3.1)	1.8 (1.5, 2.2)	1.9 (1.6, 2.2)
	Tunisia [63]	6.6 (4.5, 10.1)	6.9 (4.9, 10.4)	3.7 (2.9, 4.7)	3.8 (3.1, 4.8)	2.5 (2.2, 3.0)	2.6 (2.2, 3.1)
	Tunisia [99]	2.3 (1.7, 3.1)	2.5 (1.9, 3.3)	1.9 (1.5, 2.3)	2.0 (1.6, 2.4)	1.6 (1.4, 1.8)	1.6 (1.4, 1.9)
	Uganda [63]	3.3 (2.5, 4.5)	3.6 (2.8, 4.8)	2.4 (2.0, 2.9)	2.6 (2.1, 3.0)	1.9 (1.7, 2.1)	2.0 (1.7, 2.2)
Middle East	Iraq [63]	6.0 (1.7, 24.4)	6.6 (1.8, 27.6)	3.5 (1.5, 8.2)	3.7 (1.5, 8.9)	2.4 (1.3, 4.8)	2.5 (1.4, 5.2)
	Iraq [183]	12.8 (5.6, 31.6)	14.4 (5.7, 36)	5.4 (3.3, 9.8)	5.8 (3.4, 10.8)	3.4 (2.3, 5.7)	3.5 (2.4, 6.2)
	Jordan [63]	7.4 (4.8, 11.8)	8.1 (5.3, 13.3)	3.9 (3.0, 5.2)	4.1 (3.2, 5.5)	2.6 (2.2, 3.2)	2.7 (2.3, 3.4)
	Jordan [124]	22.3 (7.5, 45.6)	21.7 (7.5, 44.2)	7.7 (4.0, 12.9)	7.5 (3.9, 12.6)	4.5 (2.7, 7.4)	4.5 (2.6, 7.2)
	KSA [63]	5.3 (3.2, 9.8)	5.7 (3.5, 10.2)	3.2 (2.4, 4.6)	3.4 (2.5, 4.7)	2.3 (1.9, 3.0)	2.4 (1.9, 3.0)
	KSA 2013 [73]	8.1 (4.9, 13.4)	9.0 (5.6, 15.3)	4.1 (3.1, 5.5)	4.4 (3.3, 6.0)	2.7 (2.2, 3.4)	2.9 (2.3, 3.7)
	KSA 1992 [73]	12.4 (6.5, 24.7)	14.0 (7.0, 29.2)	5.3 (3.6, 8.2)	5.7 (3.8, 9.2)	3.3 (2.5, 4.8)	3.5 (2.6, 5.4)
	KSA [192]	19.5 (7.5, 43.6)	16.5 (6.6, 38.2)	7.0 (4.0, 12.5)	6.3 (3.7, 11.3)	4.2 (2.7, 7.1)	3.8 (2.5, 6.5)
	KSA [193]	17.7 (9.9, 33.2)	18.1 (9.4, 35.0)	6.6 (4.7, 10.2)	6.7 (4.5, 10.6)	4.0 (3.0, 5.9)	4.0 (2.9, 6.1)
	UAE [116]	25.8 (14.2, 44.1)	27.5 (15.3, 44.7)	8.5 (5.7, 12.6)	8.9 (6.0, 12.7)	5.0 (3.5, 7.2)	5.2 (3.7, 7.3)
South Asia	Bangladesh [125]	1.9 (1.3, 3.2)	2.1 (1.3, 3.5)	1.6 (1.2, 2.4)	1.8 (1.2, 2.5)	1.4 (1.1, 1.9)	1.5 (1.2, 1.9)
	Pakistan [102]	2.0 (1.7, 2.3)	2.0 (1.7, 2.4)	1.7 (1.5, 1.9)	1.7 (1.5, 1.9)	1.5 (1.4, 1.6)	1.5 (1.4, 1.6)
	Pakistan [69]	4.3 (3.5, 5.3)	4.3 (3.5, 5.3)	2.8 (2.5, 3.3)	2.8 (2.5, 3.2)	2.1 (1.9, 2.3)	2.1 (1.9, 2.3)

** assumed distribution of individuals within each age-class when estimating FoI and ω from age-stratified seroprevalence data*

Without having access to the precise ages of dromedaries sampled by the studies, it is not known whether the true age distribution within the age classes is closer to an exponential distribution reflecting the mortality rates within the population, or closer to a uniform distribution. However, this sensitivity analysis suggests that the assumed age distribution within an age class does not have a considerable effect on the parameter estimates and does not alter any of the main conclusions drawn from ***Chapter 3***.